Transcriptional variation in human malaria parasites and its association with drug resistance

Mok, Sachel

2013

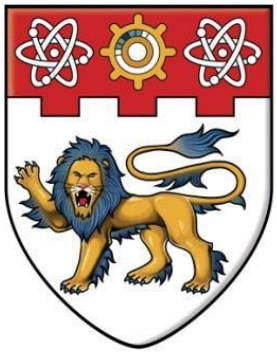

NANYANG TECHNOLOGICAL UNIVERSITY

TRANSCRIPTIONAL VARIATION IN HUMAN MALARIA PARASITES AND ITS ASSOCIATION WITH DRUG RESISTANCE

SACHEL MOK

SCHOOL OF BIOLOGICAL SCIENCES

2013

TRANSCRIPTIONAL VARIATION IN HUMAN MALARIA PARASITES AND ITS ASSOCIATION WITH DRUG RESISTANCE

SACHEL MOK

SCHOOL OF BIOLOGICAL SCIENCES

A thesis submitted to the Nanyang Technological University in partial fulfillment of the requirement for the degree of Doctor of Philosophy

2013

Acknowledgements

I am truly indebted to my supervisor, ZB, for being the channel of blessings and for his patience and kindness to me throughout the seven years in his lab since I was an undergraduate student. His creativity, openness and support towards any new research idea has given me endless opportunities to work on different projects and present at a number of important conferences. Both of which have equipped me with necessary skills and character to accomplish all these.

I am filled with much gratitude towards my family, especially my mum who selflessly provided for my brother and I in countless ways and imparted a sense of purpose and shown me the importance of faith ever since I was a child. I am thankful to my parents for not asking me to start earning my first pay check immediately after graduation 6 years ago but having much patience to see me through graduate school. I am grateful to my dad for supporting the family over the years while I am still a student. I greatly appreciate Kek for her optimism and Zhaoting for her perseverance and their enthusiasm in spirit that keeps me going an extra mile further. I am grateful to my "mentees" (FYP students) who have taught me how to teach and lead others. My thanks to Guangan, who gave me both words of wisdom and counsel in scientific discussions; Bernardo, for many hours of discussion on statistics and to both for providing scripts which helped make analysis easier; Sabna for giving a hug on the lowest of days; Archna for her calming presence and clarity of thought in her advice. And the rest of the lab members, who have made the life of the lab guinea pig a whole lot more enjoyable and exciting! No end would be without a start. His Grace is more than sufficient. I thank God for His faithfulness to me in my research explorations these years and more ahead to come in my pursuit of a career in science.

Table of Contents

Table of Abbreviations

ABBREVIATION	***EXTENDED FORM***
ART	Artemisinin
ACTs	Artemisinin-based combination therapies
BSA	Bovine Serum Albumin
cDNA	complementary DNA
CGH	Comparative Genomic Hybridization
CMM	Cell-medium-mixture
CNV	Copy Number Variants
CQ	Chloroquine
CSP	Circumsporozoite protein
DMSO	Dimethyl Sulfoxide
DDT	Dichlorodiphenyltrichloroethane; Dicophane
DE	Differentially expressed
DHFR	Dihydrofolate reductase
DHFS	Dihydrofolate synthase
DHPS	Dihydropteroate synthase
DR	Drug-resistant
DS	Drug-sensitive
DTT	Dithiothreitol
eba	Erythrocyte binding antigen
EDTA	Ethylenediaminetetraacetic acid
etramp	Early transcribed membrane protein
FL	Firefly luciferase
FS	First-Strand
G6PD	Glucose-6-phosphate dehydrogenase
gbp	Glycophorin-binding protein
gDNA	Genomic DNA
GMAP	Global Malaria Action Plan
GO	Gene Ontology database
GPARC	Global Plan for Artemisinin Resistance Containment
GSEA	Gene set enrichment analysis
hdac	histone deacetylase 1 protein
hpi	hours post invasion
IC	Inhibitory concentration
IDC	Intraerythrocytic developmental cycle
IFA	Immuno-fluorescence Assay
iRBC	Infected Red Blood Cells
IRS	Indoor residual spraying
kahrp	Knob-associated histidine rich protein
KEGG	Kyoto Encyclopedia of Genes and Genomes
LLIN	Long-lasting insecticide-treated bed net
MC	Maurer's cleft
MEF	Mefloquine
mesa	Mature-parasite-infected erythrocyte surface antigen

MMuLV	Moloney murine leukemia virus
MPMP	Malaria metabolic pathway maps
mRNA	Messenger RNA
msp	Merozoite surface protein
Mut	Mutant
NES	Normalized enrichment score
OD	Optical density
PBS	Phosphate-Buffered Saline
PCC	Pearson correlation coefficient
PCR	Polymerase chain reaction
pct	Parasite clearance time
pfacs	*P. falciparum* acetyl co-A synthetase
PfCRT	*P. falciparum* chloroquine resistance transporter protein
PfEMP1	*P. falciparum* erythrocyte membrane protein 1
pfgch1	*P. falciparum* GTP cyclohydrolase I
PfMDR1	*P. falciparum* multi-drug resistant protein
PfMRP	multidrug resistance-associated protein
phist	*Plasmodium* helical interspersed subtelomeric family
pRBC	packed Red Blood Cells
RBC	Red blood cells
resa	Ring-infected expressed surface antigen
rex	ring-exported protein
RL	Renilla luciferase
RPMI	Roswell Park Memorial Institute
SD	Standard deviation
SDS	Sodium dodecyl sulphate
SNR	Signal to noise ratio
SNP	Single nucleotide polymorphism
SRCC	Spearman rank correlation coefficient
SS	Single strand
TCTP	Translationally controlled tumor protein
TP	Time point
UTR	Untranslated region
WHO	World Health Organization
WT	Wild-type

List of Figures

List of Tables

List of Publications

I. Bozdech Z, **Mok S**, Gupta AP: **DNA Microarray-based Genome-wide Analyses of Plasmodium Parasites.** In *Malaria - Methods and Protocols.* Edited by Ménard R: Humana Press; 2013: 189-211: *Methods in Molecular Biology*.

II. Claessens A, Adams Y, Ghumra A, Lindergard G, Buchan CC, Andisi C, Bull PC, **Mok S**, Gupta AP, Wang CW, et al: **A subset of group A-like var genes encodes the malaria parasite ligands for binding to human brain endothelial cells.** *Proc Natl Acad Sci U S A* 2012, **109:**E1772-1781.

III. Rovira-Graells N, Gupta AP, Planet E, Crowley VM, **Mok S**, Ribas de Pouplana L, Preiser PR, Bozdech Z, Cortes A: **Transcriptional variation in the malaria parasite Plasmodium falciparum**. *Genome Res* 2012.

IV. **Mok S**, Imwong M, Mackinnon MJ, Sim J, Ramadoss R, Yi P, Mayxay M, Chotivanich K, Liong KY, Russell B *et al*: **Artemisinin resistance in Plasmodium falciparum is associated with an altered temporal pattern of transcription**. *BMC Genomics* 2011, **12**:391.

V. Claessens A, Ghumra A, Gupta AP, **Mok S**, Bozdech Z, Rowe JA: **Design of a variant surface antigen-supplemented microarray chip for whole transcriptome analysis of multiple Plasmodium falciparum cytoadherent strains, and identification of strain-transcendent rif and stevor genes**. *Malar J* 2011, **10**:180.

VI. Hu G, Cabrera A, Kono M, **Mok S**, Chaal BK, Haase S, Engelberg K, Cheemadan S, Spielmann T, Preiser PR *et al*: **Transcriptional profiling of growth perturbations of the human malaria parasite Plasmodium falciparum**. *Nat Biotechnol* 2010, **28**(1):91-98.

VII. Mackinnon MJ, Li J, **Mok S**, Kortok MM, Marsh K, Preiser PR, Bozdech Z: **Comparative transcriptional and genomic analysis of Plasmodium falciparum field isolates**. *PLoS Pathog* 2009, **5**(10):e1000644.

VIII. Bozdech Z, **Mok S**, Hu G, Imwong M, Jaidee A, Russell B, Ginsburg H, Nosten F, Day NP, White NJ *et al*: **The transcriptome of Plasmodium vivax reveals divergence and diversity of transcriptional regulation in malaria parasites**. *Proc Natl Acad Sci U S A* 2008, **105**(42):16290-16295.

IX. Foth BJ, Zhang N, **Mok S**, Preiser PR, Bozdech Z: **Quantitative protein expression profiling reveals extensive post-transcriptional regulation and post-translational modifications in schizont-stage malaria parasites**. *Genome Biol* 2008, **9**(12):R177.

List of Conferences and Awards

Presentations at Conferences

- 61st American Society for Tropical Medicine and Hygiene Meeting, Atlanta, USA, 11th – 15th Nov '12. (Oral)
- Molecular Approaches to Malaria MAM 2012, Lorne, Australia, 19th – 23rd Feb '12. (Oral)
- Singapore Malaria Network Meeting 2012, Singapore, 16th – 17th Feb '12. (Oral)
- 60st American Society for Tropical Medicine and Hygiene Meeting, Philadelphia, USA, 3rd – 8th Dec '11.
- 7th Annual BioMalPar Conference 2011, EMBL Heidelberg, Germany, 16th – 18th May '11. (Poster)
- International Congress of Parasitology ICOPA XII 2010, Melbourne, Australia, 15th – 20th Aug '10. (Oral)
- International Conference on Materials for Advanced Technologies, GEM4/SMART Symposium on Infections Diseases, Singapore, 28th Jun – 3rd Jul '09. (Oral)
- Molecular Approaches to Malaria MAM 2008, Lorne, Australia, 3rd – 7th Feb '08.
- Singapore Malaria Network Meeting 2008, Singapore, 31st Jan & 1st Feb '08.
- Molecular Parasitology Meeting 2007 MPM XVII, Marine Biological Laboratory, Woods Hole, USA, 16th – 20th Sept '07. (Poster)

Awards

National Institutes of Health's Fogarty International Center and the United Nations Foundation (FIC-UNF) Travel Grant to attend the 60th ASTMH Meeting in Philadelphia, USA……Dec 2011

Research Summary

A number of studies have been carried out to study transcriptional variation *in P falciparum* ranging from *in vitro* profiling of culture-adapted strains to drug perturbation experiments. Transcriptional variation is largely stochastic and not a directed transcriptional response in clones. Yet in field isolates, transcriptional profiles associated with distinct metabolic states are observed, which may reflect diversifications in the physiology of the cell depending on individual host cell conditions such as nutrient availability and host immune responses. Hence, we propose that these metabolic states may be involved in drug resistance phenotype. Using microarray technology, we first established an infrastructure to investigate transcriptional changes between clones of a culture-adapted strain 3D7. Additionally, we aimed to identify transcriptional changes that occur in the process of adapting a field isolate to culture. In this respect, we utilized this infrastructure to determine cell-specific responses to *in vitro* culturing which represented a change in growth conditions. Surprisingly, we observed large and significant overlaps in genes showing transcriptional changes between clones and between generations of a culture adapted clone at the qualitative level. They mainly comprise of genes coding for host cell remodeling factors such as Maurer's cleft exported proteins, invasion-related, protein kinases and genes for sexual stage development. There was no particular pathway or gene that was selected for over the course of *in vitro* culturing, suggesting that these changes are not directed transcriptional responses to changing growth conditions. Whether this stochastic expression helps it to survive remain unanswered. More importantly, we observed that major transcriptional differences between isolates were maintained in culture throughout the generations which include the differential expression of two drug-resistance candidate genes belonging to the folate biosynthesis

pathway. Taken together, we have defined a set of genes known to be differentially expressed between any two parasite lines or between generations. On another note, using our microarray infrastructure, we established transcriptional profiles of *in vivo* isolates from South East Asia and identified key features associated with clinical artemisinin resistance which has emerged in Western Cambodia. In the ring and trophozoite stages, we observed reduced expression of many basic metabolic and cellular pathways which suggests a slower growth and maturation of these parasites during the first half of the asexual intraerythrocytic developmental cycle (IDC). In the schizont stage, an increased expression of essentially all functionalities associated with protein metabolism may indicate the increased capacity of protein synthesis during the second half of the resistant parasite IDC. This modulation of the *P. falciparum* intraerythrocytic transcriptome may result from differential expression of regulatory proteins such as transcription factors or chromatin remodeling associated proteins. In addition, there is a unique and uniform copy number variation pattern in the Cambodian parasites which may represent an underlying genetic background that contributes to the resistance phenotype. Our microarray analyses of the clones also revealed significant transcriptional variation of a drug transporter gene coding for multidrug resistance-associated protein (PfMRP2). Analysis proved the importance of a 4.1 kilo base pair sequence acting as a *cis* regulatory element controlling the timing of expression of the drug resistant gene. This gave rise to differential protein expression levels which associated with differential sensitivities of clones to antimalarial drugs - mefloquine and chloroquine. This is the first study in *Plasmodium* demonstrating the role of copy number polymorphisms in the intergenic promoters of drug resistant genes that result in drug-resistant phenotype and potentially can be used as a marker for mefloquine and chloroquine resistance in the field.

Chapter 1 : Introduction

1.1 Malaria as an infectious disease and Pathogenesis

With Malaria fevers described as early as 5000 BC in the ancient Sanskrit text of *Bhagavad Gitta*, in the Chinese book *Huang Di Nei Ching* in 2700 BC, by Hippocrates in his writings *Corpus Hippocratorum* in 400 BC Greece as well as in Egyptian, Arabian and Italian literature, it is apparent that Malaria has been a major and global human health burden throughout the centuries [1, 2]. Presently, it kills an average of 780,000 to 1 million people yearly, with another 200-250 million infected cases mostly in under-developed countries [3]. Globally, a total of 106 countries and areas are endemic for Malaria as of 2010 [3]. It is reported that approximately 20% of the world's population amounting to 1.2 billion live in areas with a high risk of malaria [3, 4]. Malaria which literally means 'bad air' in Italian is an infectious disease caused by the protozoan parasite *Plasmodium* species. Of the 5 *Plasmodium* species, *P. falciparum, P. vivax, P. malariae, P. ovale* and more recently reported *P. knowlesi*, which are able to establish infections in the human host, *Plasmodium falciparum* contributes to the highest mortality rates and the most severe symptoms in patients. The spread of *P. falciparum* is transmitted via the *Anopheles* mosquito vector where it resides in tropical and sub-tropical areas of Africa, South America and parts of South-East Asia. Till today, sub-Saharan Africa still bears the greatest brunt of the disease, not just the toll on human health and mortality (91% of deaths annually occur in Africans) but economically and socially. The disease predominantly affects young children with greater severity than patients of other age groups and in 2009, an estimated 85% of malaria-related deaths worldwide are of children below the age of five [3]. Patients suffering from malaria often develop recurring symptoms of high

fevers, headaches, chills, arthralgia, vomiting, respiratory distress and anemia due to increase in parasite burden through the cyclical multiplication, release and invasion of new progeny into other non-infected red blood cells during the asexual intraerythrocytic stage of the parasite which occurs every 48 hours. Often, complications may arise when parasite-infected red blood cells adhere to endothelium and obstruct capillaries that are important for supplying oxygen and nutrients to the brain and vital organs, resulting in organ damage and sometimes fatality. Pregnant women are at high risk to malaria. In cases where pregnant women are infected with malaria, adhesion in the placenta leads to low birth weight and high infant mortality rates. However, the degree of severity of the disease and clinical outcome is not solely correlated with parasitemia load in patients' blood as other factors play a role in determining survival, and symptoms usually vary from individual to individual or infection to infection across the lifetime of an individual [5].

1.2 Lifecycle of *Plasmodium falciparum*

The apicomplexan parasite's lifecycle is complex and comprises stages in both the mosquito vector as well as in the human host as shown in Figure 1-1. While the sporogonic stage occurs in the Anopheles mosquito, both the exoerythrocytic cycle and the intraerythrocytic cycle occur in the human host and take place in the liver and the red blood cells respectively. When a human host is bitten by an infected mosquito, sporozoites are released from the salivary glands and injected into the epidermal layer of the victim and remains there for up to 30 min. Thereafter, the sporozoites enter the victim's bloodstream and migrate to the liver where they invade hepatocyte cells. These liver-stage parasites remain there approximately for the next 6.5 to 14 days while continuously differentiating and undergoing asexual multiplication to give rise to thousands of merozoites stored in cysts which are subsequently released from the

hepatoctyes. The merozoites travel to the blood stream and invade host red blood cells, where it develops from rings to trophozoites to schizonts. In the ring stage, little metabolic activity occurs as the parasite establishes itself in the host. Most of the parasite's metabolic activities such as degradation of host cell hemoglobin, glycolysis, cytoplasmic translation machinery and DNA replication, are concentrated in the trophozoite phase during which the parasitophorous food vacuole is most prominent. Remodeling of host cell occurs and transport properties of the red cell membrane are altered during this stage and the infected erythrocyte becomes more rigid and less deformable. The expression of parasite's variant surface antigen proteins on the surface of the infected RBC allows for the adhesion to receptors on endothelial cells of the microvasculature, thereby enabling the iRBC to escape the host's immune detection and clearance by the spleen. Subsequently, DNA replication occurs in the parasite as it matures to schizont and segmentation takes place, forming 8- 32 daughter merozoites. During egress, the infected red blood cell membrane and parasitophorous vacuolar membrane lyse to release free merozoites which invade other uninfected red blood cells. This cycle is repeated approximately every 48 hours for *P. falciparum*. In conditions of nutrient starvation, the merozoites differentiate into either male or female sexual gametocyte forms which are taken up by a female Anopheles mosquito during her feeding. After fertilization of male and female gametes in the gut, the resulting ookinete matures to become an oocyst that ruptures, thereby releasing hundreds of sporozoites that travel from the gut wall via the hemolymph to the salivary glands, ready to be injected into the next victim.

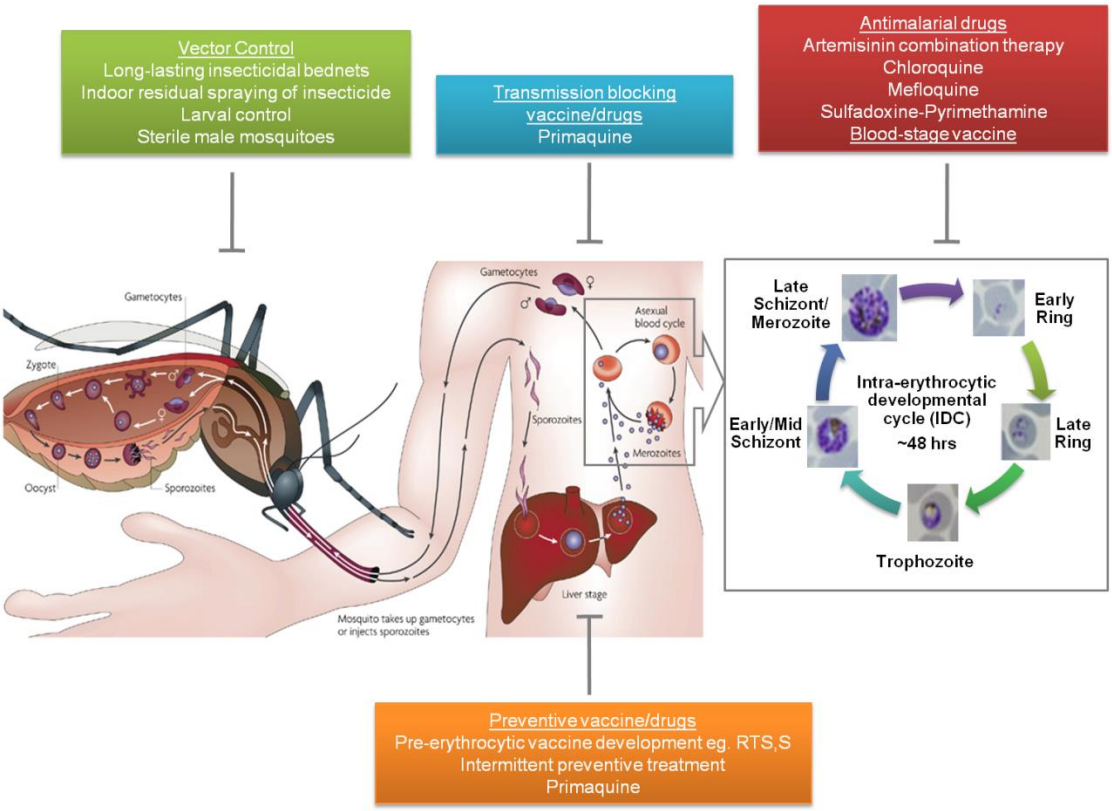

Figure 1-1. Overview of the developmental lifecycle of the *Plasmodium* parasite.
(Adapted from [6]) Giemsa-stained smears visualized under a bright-field microscope depict rings, trophozoites and schizont stages of the intraerythrocytic developmental cycle studied. Malaria control strategies targeting the various stages in the lifecycle are depicted in colored boxes.

1.3 Global Malaria Program: Roll-back Malaria Partnership and Global Malaria Action Plan (GMAP)

In 1998, the World Health Organization (WHO) introduced the Roll-back Malaria Partnership under the Global Malaria Programme [7]. Its aims were to achieve universal coverage for all populations at risk with locally appropriate interventions for prevention and case management by 2010. More specifically, the long term goals were to reduce the number of global malaria cases by 50% in 2010 and by 75% in 2015 from 2000 levels, to reduce global malaria deaths by 50% in 2010 from 2000 levels and to near zero preventable deaths in 2015, to eliminate malaria in 8-10 countries by 2015 and afterwards in all countries in the pre-elimination phase, and

ultimately, to eradicate malaria world-wide by reducing the global incidence to zero through progressive elimination in countries [8].

To achieve these targets, the GMAP has been implemented since 2005 with the contribution of now US$1.8 billion yearly to the program [8]. With this huge expenditure, it brings to mind the question of what results has it achieved so far? With GMAP implemented to contain and control the disease since 2005, an increase in the number of African families owning an insecticide-treated bed net (ITN) have been observed. In mid-2010, 42% of African families own bed nets compared to 3% in 2000 [3]. The number of cases have fallen from 244 million to 225 million (7.8%) in 2009 and number of deaths have reduced from 927,000 to 781,000 (15.7%) in 2009 [3]. Compared to 2000 levels, there has only been a slight reduction of 3.4% in cases from 233 million to 225 million [3]. This is far cry from the 50% reduction in Malaria cases hope to be met out by 2010. Looking at the numbers per country, 43 countries reported at least a 50% reduction in number of reported confirmed cases from 2000 to 2009 [3]. This is evidence of the effectiveness of the GMAP policies in these 43 countries and the reduction in cases in the other counties is mainly hindered by the accessibility of resources, which is often governed by a country's political instability and internal conflicts. Till now, only 2 countries have been given the status of having eliminated Malaria [3]. The results for GMAP have been encouraging so far but there is still room to improve upon in order to meet the targets set out.

1.4 Malaria Control measures

1.4.1 Preventing transmission by targeting mosquito host: IRS, LLIN

Current strategies to reduce risk of Malaria infections at the transmission level include the implementation of long-lasting insecticide-treated nets (LLINs), indoor residual

spraying (IRS) of long-acting insecticide, larval control through larvicides, using repellents as personal protection and fogging. The pesticide dicophane (DDT) was once the common and effective means to eradicate mosquito vectors but due to environmental damage and health concerns, use of DDT has been phased out for the past 30 years. As at 2006, WHO has once again advocated the use of DDT for indoor spraying in controlling malaria [9] and its use has resulted in a 60% reduction in malaria cases. Similarly, insecticide-treated bed nets have proved to be useful in the protection against mosquito bites and have reduced the number of malaria cases by 50% [10-12]. In 2010, 42% of African households own a LLIN due to the GMAP. The disadvantage of this method is that a LLIN is good for up to 3 years and needs to be replaced regularly, thus creating a continuous cost and resource burden. With the increased use of insecticides, there has also been increasing concerns of the emergence of pyrethroid resistance in the mosquito vector.

1.4.2 Preventing *Plasmodium* infection in humans through Vaccine development

The Holy Grail in preventing human malaria infections stems from a successful vaccine that is safe with minimal side effects or complications and efficacious in protection to the individual. However, research so far has only identified few antigens such as Circumsporozoite Protein (CSP), Merozoite Surface Protein 1 (MSP1) and Apical Membrane Antigen 1 as potential candidates for vaccine development and many of the vaccine trials gave disappointing results. The main obstacles in designing an ideal *Plasmodium* vaccine are the parasite's rapid alteration and huge variation in antigenic determinants and allelic diversity observed as well as individual to individual difference in host's immune response. The vaccine candidate that has advanced furthest clinically to phase 3 trials is RTS,S-AS01/AS02 produced by GlaxoSmithKline company together with PATH Malaria Vaccine Initiative, and

which is designed to target the pre-erythrocytic stage of *P. falciparum* [13]. RTS,S is a recombinant protein consisting of the tandem-repeat region of the CSP, $CD4^+$ and $CD8^+$ T-cell epitopes, in addition to the hepatitis B surface antigen to heighten the protein's immunogenicity while AS01/AS02 acts as an adjuvant system [14]. In phase IIb of clinical trials in Gambia completed in 2005, the vaccine efficacy of RTS,S/AS02A in young children was reported to be 57.7% against severe clinical malaria over an observation period of 6 months which declined to 48.6% for a total duration of 18.5 months [15, 16]. In the more recent concluded phase III trials, protective immunity (ie. prevention of the first clinical episode of *P. falciparum* malaria) to clinical and severe malaria was achieved with a vaccine efficacy of 55.8% and 47.3% respectively for the total 6000 children aged 5 to 17 months tested from 7 African countries [13]. So far, these results are remarkable as the % in reduction of cases for this vaccine is similar to that achieved in the adoption of LLINs and IRS. However, similar proportions of children died in both the vaccinated and control groups. Furthermore, the vaccine has so far only been proven to be effective up to 12 months. Cases of convulsive seizures were twice as frequent and meningitis was more frequent in the RTS,S/AS01 group than the control group of children [13] and should be looked into. The long-term effectiveness of it remains to be seen in this ongoing clinical study and results will be known in 2013. As this vaccine is still not yet ideal to be implemented in a large-scale vaccination program, further research is necessary to generate one that provides higher rates of long-lasting protective immunity across all age groups [17] and that will reduce the mortality rate. This will increase the cost-effectiveness of the vaccination program as a strategy to combat malaria and present it as an attractive choice to save lives.

1.4.3 Targeting *Plasmodium* using antimalarial drugs

On another note, eradicating this parasitic disease in infected humans is altogether a different challenge and antimalarial drugs, most of which target the asexual blood stage, serves as the mainstay treatment and prophylaxis (as intermittent preventive treatment, IPT during pregnancy and infancy) through the centuries. In the early 17th century, the Cinchona bark which is a source of quinine became the first effective drug therapy used to treat malaria. With the advent of world-war II and escalating number of deaths due to Malaria, a much cheaper and more effective synthetic antimalarial compound, chloroquine was thus created in 1934 by the US army, which became the most widely used drug over the next few decades. Besides chloroquine, other quinoline-containing antimalarial compounds such as amodiaquin and primaquine were later developed in the 1940s and 50s and mefloquine in 1975, also arising from another war (Vietnam War). Antifolate drugs: proguanil and pyrimethamine were also independently synthesized during that same period [18]. The combination of atovaquone with proguanil (malarone) proved to be an effective therapy in the late 1990s. However, with the implementation and wide-use of any new antimalarial drug, parasite's resistance to them also followed shortly. This was repeatedly observed throughout history, leaving artemisinin-based combination therapies (ACTs) as the only last hope against fighting the disease. Hence, in 2004, Malaria Foundation International and World Health Organization made a stand to support a major global switch to the use of ACTs and since 2006, WHO has called for a ban on the use of oral artemisinin monotherapy in the treatment of malaria [19]. Today, artemisinin continues to be as one of the few remaining effective antimalarial drugs [20]. Although antimalarials have been used for centuries, the mechanisms of cytotoxic action on the *Plasmodium* parasite for most of the drugs have not been fully

understood. Here is an overview of antimalarial compounds and known mechanisms of action till date:

Pyrimethamine/Sulfadoxine (Fansidar)

Pyrimethamine, like proguanil, exerts its anti-parasitic action through inhibition of the *Plasmodium*'s dihydrofolate reductase enzyme (DHFR), thus preventing the reduction of dihydrofolate to tetrahydrofolate, which is needed for biosynthesis of nucleotides such as thymidylate (dTMP). As sulfadoxine is a structural analogue of para-aminobenzoic acid, it competitively binds to dihydropteroate synthase (DHPS), an enzyme required for the de novo synthesis of folates. Reduction in folate levels results in less dTMP available. Hence, these events elicited by both drugs ultimately lead to an arrest in DNA synthesis and failure of nuclear division, resulting in parasite death. Taken together, this synergistic drug combination is effective in killing the parasite.

Chloroquine, Quinine and Mefloquine (Lariam)

All 3 drugs belong to the class of quinolines. However, quinine and mefloquine are methanol-quinoline compounds, bear characteristics of a much weaker base and is soluble in lipids at neutral pH whereas chloroquine is 4-aminoquinoline compound, showing characteristics of a weak base that becomes diprotonated and hydrophilic at neutral pH. Hence, chloroquine which enters the digestive food vacuole by simple diffusion becomes protonated and trapped, and overtime accumulates inside the acidic food vacuole of the parasite. Even though these 2 drugs interact with the same target in the parasitic cell, i.e. food vacuole, they are known to interact using different mechanisms [21]. The parasitic food vacuole is the organelle where hemoglobin, ingested from the host erythrocyte, is degraded to free heme (iron-prophyrin complex), which is subsequently polymerized to hemozoin (malaria pigment), a compound non-toxic to the parasite. Chloroquine has been shown to cause parasite death by slowing

the rate of β-hematin formation, thereby inhibiting biocrystallization of heme to hemozoin (Figure 1-2) [22]. The resulting accumulated free heme and heme-CQ complex destabilizes membranes and generates reactive oxygen intermediates (ROIs) that is highly toxic to the parasite [23]. Recently, it was also shown that chloroquine causes specific oxidative stress and damage to proteins which are important for the parasite's physiological processes [24]. The mechanisms of quinine and mefloquine are less well-understood but one of the ways in which they cause parasite death is likely to be mediated by a mechanism similar to that of chloroquine [25]. Nevertheless, the possibility that they may act on alternative targets in the parasite also exists [26].

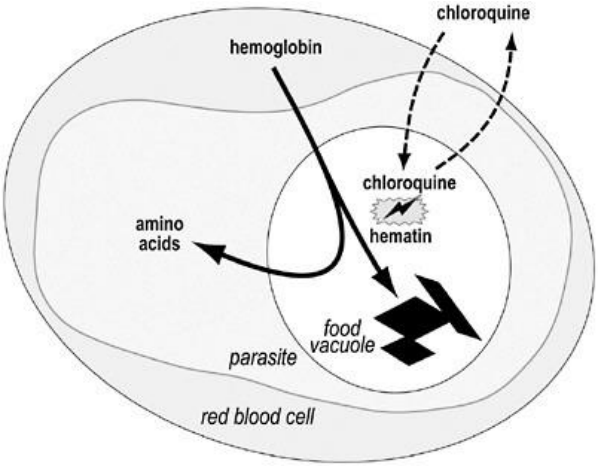

Figure 1-2. Schematic of the mechanism of action of chloroquine in the parasite. Chloroquine inhibits the β-hematin formation and polymerization of heme to hemozoin in the food vacuole, resulting in accumulation of toxic heme and death of the cell.

The association between chloroquine and gametocytogenesis was first documented by a study showing that the drug increased infectivity of *P. berghei* parasites to Anopheles mosquitos and much more so for drug-resistant parasites [27, 28]. Later from *in vitro* experiments, chloroquine was proven to induce gametocytes and at 5-fold higher than control untreated parasites [29]. While the quinolines (chloroquine,

quinine and mefloquine) act as schizonticidals meaning they are effective in killing trophozoite and schizont stages, artemisinin on the other hand, is effective in killing all the different forms of the asexual blood stage, as well as early gametocyte stages [30].

Artemisinin

Artemisinin is a traditional Chinese antimalarial drug first described in 340AD for treatment of fevers and is extracted from the plant *Artemisia annua*, also called sweet wormwood or 青蒿素. It is currently used as a first-line treatment for multi-drug resistant strains of *P. falciparum*. The activity of this compound was previously suggested to arise from the cleavage of its endoperoxide bridge by labile ferrous iron (Fe2+), found in the food vacuole [31, 32] thereby producing carbon-centered free radicals [33]. These alkylate heme [34], lipids and various other proteins including albumin, catalase, cytochrome b and the *Plasmodium*'s translationally controlled tumor protein (TCTP) homologue [35-38]. However, a recent study has shown otherwise, that artemisinin antimalarial activity is derived from the intrinsic reactivity of the peroxide and is neither dependent on the cleavage of the peroxide nor C radicals generated [39]. No matter which postulation is correct, both have come into agreement that PfATP6 protein is a target of artemisinin and is likely that the iron-dependent alkylation leads to inhibition of this calcium-dependent (SERCA) ATPase transporter found in the endoplasmic reticulum membranes of the parasite [40]. Interestingly, artemisinins form covalent adducts with four other major membrane-associated parasite proteins, which are yet to be characterized (Figure 1-3) [41, 42]. Other studies have suggested differing mechanisms of action such as the potential to interfere with mitochondria electron transport chain based on observations that

artemisinin depolarizes mitochondria inner membrane potential in yeast cells mediated by the generation of reactive oxygen species [43].

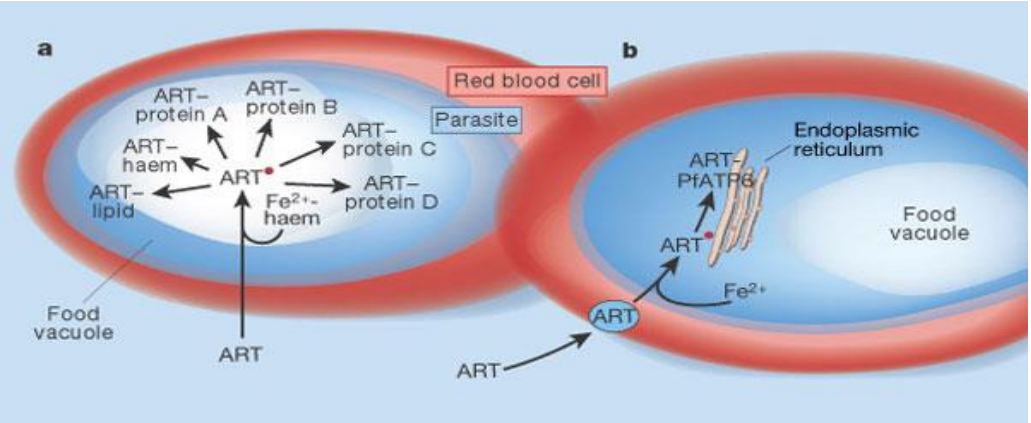

Figure 1-3. Possible targets and mechanism of action of artemisinin. Artemisinin is first activated by labile ferrous iron generated during the degradation of hemoglobin to heme in the food vacuole of the infected red blood cell. Thereafter, the reactive carbon-centered free radicals are proposed to cause alkylation of parasite proteins, heme and lipids. Alternatively, the activated drug may also target and inhibit the parasite's sarcoplasmic/endoplasmic reticulum calcium ATPase pump (SERCA or PfATP6). These lead to production of free radicals and downstream cytotoxic effects which kill the parasite.

1.5 Current Challenges in eradication of malaria: Drug resistance

Control and eradication of malaria are plagued by problems at the administrative and technical levels. Insufficient education given to high-risk malaria exposed people on how to prevent or seek treatment for the disease, poverty of victims keeping them from obtaining drugs and lack of proper health infrastructures in under-developed countries are some administrative and technical issues at hand. The increasing resistance of mosquitoes to insecticides and resistance of *Plasmodium* parasites to antimalarial drugs, requiring the use of alternate drugs that are often more expensive, only further hampers the control of the disease.

The definition of drug resistance as per WHO guidelines is "the ability of a parasite strain to survive and/or multiply despite the administration and absorption of a drug given in doses equal to or higher than those usually recommended but within

tolerance of the subject" [44]. And that "the form of the drug active against the parasite must be able to gain access to the parasite or the infected erythrocyte for the duration of the time necessary for its normal action." [45]. An updated definition of drug resistance by WHO is "Patients who are infected with resistant strains will fail to clear parasites and or resolve clinical symptoms despite correct and complete administration of treatment." [46].

It is of interest to note that *P. falciparum* resistance to the once most effective drug, chloroquine, was first observed in Thai-Cambodian border in 1957, just merely 12 years after it was first introduced and used world-wide. Within the span of the next 20 years, chloroquine resistance spread to Africa. Due to the loss of its effectiveness, chloroquine was replaced by sulfadoxine-pyrimethamine as a first-line drug in Thailand in 1967. This time resistance to this antifolate drug combination emerged even much more rapidly; in the same year as first implementation of its use. Hence, mefloquine was used next to treat Malaria. However, following the introduction of this drug in 1977, resistance appeared at the Thai-Cambodian border shortly in 1982 [47]. Throughout history, a similar recurring pattern is the emergence of drug resistance not long following the introduction of the drug in the field to treat malaria patients and even more shockingly, all the various *Plasmodium* resistant-types originate from the same geographical area at the Thai-Cambodian border (Figure 1-4A). As of 2005, resistance towards the commonly used antimalarials is found in almost every country where malaria is endemic (Figure 1-4B). Reports were later published suggesting the phenomenon of multi-drug resistance in parasites and the ARMD (accelerated resistance to multiple drugs) phenotype, which arises from continual exposure of malarial parasite populations to various drugs. This selects not only for resistance to individual drugs but more importantly, for genetic traits that

A.

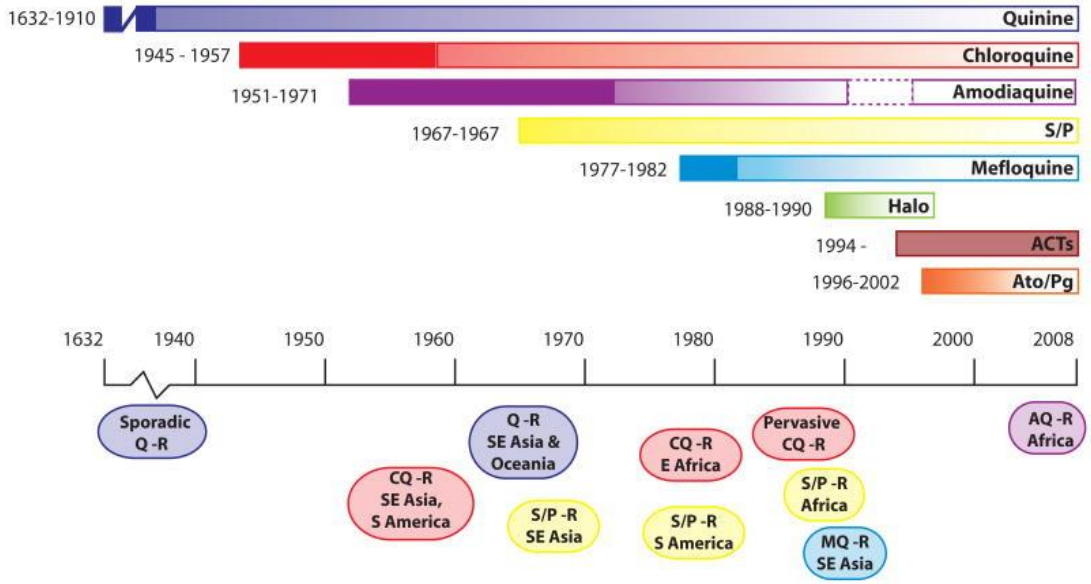

B.

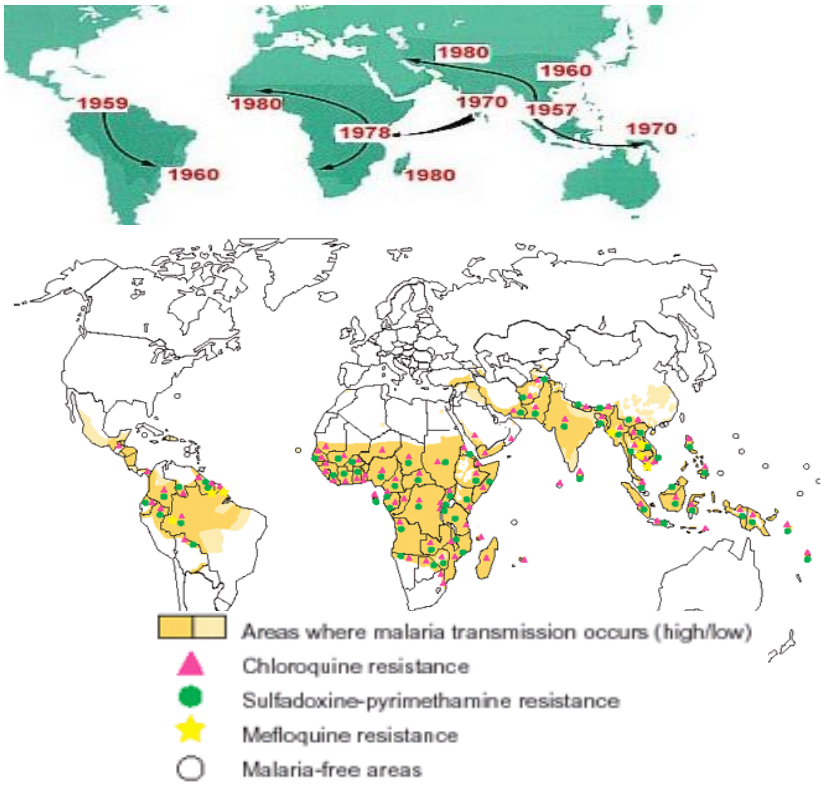

Figure 1-4. Onset and spread of parasite resistance to various antimalarial drugs. A. Diagram illustrating the time from introduction of each antimalarial drug to the first instance of drug-resistance reported. B. Distribution of drug-resistant *Plasmodium* world-wide (World Malaria Report, WHO 2005).

favor initiation of resistance to other novel unrelated antimalarials that have yet to be used in clinical treatments [48, 49]. This raises the concern that drug resistance which is a continuing problem, could threaten to render any newly discovered compounds ineffective over time.

Several studies have managed to uncover the genetics of resistance towards some of these antimalarials, however, due to differences between samples collected from different geographical locations as well as between *in vitro* and *in vivo* studies, there are still several controversies surrounding the mechanism of resistance, suggesting that resistance is a complex multi-gene trait.

1.6 Genetics of *Plasmodium* resistance to antimalarials:

Polymorphisms or gene duplication encoding drug targets or drug influx/efflux transporters

Chloroquine Resistance

Mutations, in particular, from lysine to threonine at amino acid residue position 76 in the *pfcrt* gene, which encodes for the chloroquine resistance transporter protein, located at the food vacuolar membranes, is found in all isolates of Asian, African, or South American origin associated with treatment failure and therefore, has been well-correlated to chloroquine resistance [50, 51]. Point mutations such as the Asn86Tyr mutation in PfMDR1 (multi-drug resistant protein) and gene amplification of *pfmdr1* has also been observed in some field isolates in Africa and chloroquine resistant reference clones, and thus associated with resistance to this compound [51, 52]. The *pfmdr1* gene is situated on chromosome 5 and codes for the P-glycoprotein homologue 1 which plays a role in mediating drug-resistance in certain cancer cell lines. Previously, there were 3 possible hypothesized mechanisms proposed for chloroquine resistance: efflux of chloroquine out of acidic food vacuole via an energy

coupled transporter, leakage of charged CQ out of vacuole and pH-dependent changes resulting in reduced accumulation of drug. It has been recently confirmed that chloroquine resistance in resistant parasites is due to leakage or increased efflux of the drug out of the parasite's food vacuole mediated by binding of the drug to mutant PfCRT with a change in a single amino acid [53, 54].

Mefloquine Resistance

Besides chloroquine, mefloquine resistance has also been linked to mutations in PfMDR1 protein or increase in *pfmdr1* gene copy number in numerous field studies [55]. Akin to the case in *Plasmodium falciparum*, an over expression of *pcmdr1*, the analogue of *pfmdr1*, has been shown to be an important determinant of mefloquine resistance in *P. chaubaudi*, a mouse malaria. Nevertheless, not all mefloquine-resistant progeny contained the duplicated gene, thus it is highly likely that at least one other gene is associated with Mefloquine resistance [56].

Pyrimethamine/Sulfadoxine Resistance

Of all the various antimalarials, the basis of resistance to this drug combination is the most clearly defined supported by the fact that their drug targets have already been known previously. Parasites possessing point mutations in the DHFR enzyme primarily at the Ser108Asn codon as well as Asn51Ile, Cys59Arg or Ile164Leu codons [57, 58] are highly resistant to pyrimethamine. Interestingly, the accumulation of mutations at these codons in the enzyme correlates positively with the level of resistance, meaning that parasites having quadruple mutations exhibit the highest level and most severe form of resistance to this drug combination [59]. Resistance to sulfadoxine is derived from mutations found in another enzyme involved in the anti-folate pathway - the DHPS gene at these sites: Ser436Ala/Phe, Ala437Gly, Lys540Glu, Ala581Gly and Ala613Thr/Ser codons [60, 61] and similar to DHFR,

sequential acquisition of mutations in DHPS leads to higher levels of sulfadoxine resistance [62]. The problem of widespread resistance of the asexual blood stage of the parasite to pyrimethamine/sulfadoxine could be driven by the fact that this drug combination increases transmission rates to mosquitoes [63]. It has been reported that the combination of pyrimethamine/sulfadoxine administered to patients has a much higher rate (56%) of post-gametocyte prevalence as compared to CQ (18.0%) [64]. Hence, administering sub-curative doses of this drug combination would be counterproductive short term and lead to both higher rates of malaria cases and higher chance of a single resistant parasite being transmitted in selective sweeps across the populations as observed.

Artemisinin Resistance

Artemisinin resistance has been confirmed in *Plasmodium falciparum* parasites in South East Asia, notably in Pailin, Western Cambodia. It is characterized by a significant increase in parasite clearance time (pct) independent of starting parasite densities and drug concentration levels in the blood. The parasite clearance time is the total duration (in hours) taken for the parasites to completely clear from the patient following administration of the antimalarial drug therapy (Figure 1-5). According to WHO's Global Plan for Artemisinin Resistance Containment (GPARC), the term 'artemisinin resistance' is a working definition used to refer to either of the 3 criteria being fulfilled: 1) an increase in parasite clearance time, as evidenced by 10% of cases with parasites detectable on day 3 (72 hours) after treatment with an ACT (suspected resistance); or 2) early treatment failure as evidenced by the persistence of parasites for 7 days (168 hours) after treatment with an oral artemisinin-based monotherapy with adequate blood plasma concentration of dihydroartemisinin, or 3) the presence of parasites at day 3 and recrudescence within 28 or 42 days after the

start of artemisinin-based monotherapy treatment (late treatment failure) (confirmed resistance). Other papers have proposed that reduced *in vitro* susceptibility to dihydroartemisinin with increased IC_{50} values combined with prolonged parasite clearance and treatment failure presents a case of confirmed artemisinin resistance [65]. However, in the study by Dondorp et al (2009), only a markedly prolonged parasite clearance time and without any increase in IC_{50} values was used to define artemisinin resistance [66]. Although the parasite clearance time has been the most widely-used clinical end-point to measure resistance to date, the parameter parasite clearance rate is now suggested to be more robust [67]. The clearance rate is the slope of the log linear of the parasitemia versus time graph (Figure 1-5) and is independent of the initial parasite density or the situation of lingering low levels of parasite counts at the tail phase which may arise from inaccurate or insufficient monitoring of parasite counts by microscopy [67]. On the other hand, the parasite reduction ratio (prr) is the fold change between the initial parasite count on admission and the parasite count at a particular time following drug administration to the patient.

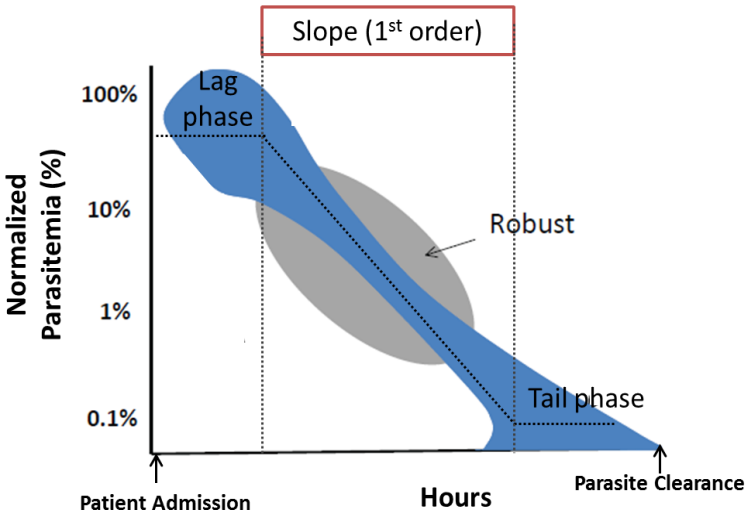

Figure 1-5. The normalized parasitemia versus time parasite clearance curve showing the slope of the log linear segment, known as the parasite clearance rate. The lag and tail phase contributing to sources of variation in pct values that may arise from asynchronous schizont rupture and/or extent of accuracy in detection of live parasites by microscopy is depicted. Adapted from source: [67]

Although artemisinin resistance was confirmed only two years ago, it is debatable as to when exactly did artemisinin resistant parasites first appeared. The first case of late treatment failure marked by parasite recrudescence appeared in 1998 at the Western border of Thailand [68], and later in India in 2000 [69] and Sierra Leone in 2001 [70]. However, in the first report, the *in vitro* tested IC_{50} did not differ between the cleared and recrudesced parasites. As for the latter two reports, it is not known if treatment failures were due to parasite recrudescence or if they were new cases of infection that were misdiagnosed since confirmation by PCR was never carried out. To build on the questionability of artemisinin resistance in these three reports, it is uncertain whether treatment failure occurred due to artemisinin monotherapy being administered for less than 7 days, (7 days is the minimum duration required ensuring the drug clears all parasites in the patient) or if the drug was of sub-standard quality and contained less than the normal amount of artemisinin compared to the authentic drug. Notwithstanding, other reports observed that in Vietnam, while the *in vitro* IC_{50} for artemisinin had remained constant between 1998 and 2001, the IC_{90} and IC_{99} had increased by 2-fold and 4-fold, respectively [71]. In Central African Republic, a study showed that at day 42 curative treatment rates were only 85%, after patients followed 7 days of artesunate monotherapy. Furthermore, the IC_{90} values were 5-fold higher in the recrudesced parasites even though the IC_{50} values did not differ significantly [72].

Of most concern, nevertheless, are findings in the recent report on the containment of artemisinin tolerance by WHO that the *Plasmodium* parasites in the Thai-Cambodian border may be developing resistance to artemisinin [46, 73]. Evidence from the interim results showed that out of 20 patients who were given artesunate monotherapy daily for 7 days, 7 of them (35%) had recurrences of *falciparum* infection, with a

median time to recurrence of 28 days. In addition, prolonged parasite clearance times were observed in all patients, with the median parasite clearance times of 87 hr (42–120 hr) for treatment with artesunate for 7 days and 78 hr (36–114 hr) for mefloquine and artesunate treatment for 3 days. Surprisingly, *in vitro* susceptibility tests observe that the parasites were not particularly resistant [73]. The huge disparity in the parasite clearance time ranging from approximately 2 days to 5 days presents a case where the degree of parasite sensitivity to artemisinin is quite variable in the population and there is a shift in the population to having reduced sensitivity towards the drug. Regardless of whether parasites are showing resistance or increased tolerance, both the phenomenon of increased parasite recurrence and longer parasite clearance time would only increase the chance of producing gametocytes in sufficient densities for transmission [63]. This is worsened further that it is these artemisinin-tolerated parasites that are given the opportunity to be transmitted in the human population. Hence, to control the spread of artemisinin resistance, parasite must be cleared from the patient's system early and effectively, to prevent recrudescence from happening. To minimize the likelihood of artemisinin tolerance and resistance emerging, WHO currently recommends any of these five artemisinin based combination therapies: artesunate + amodiaquine, artesunate + sulfadoxine–pyrimethamine, amodiaquine + sulfadoxine–pyrimethamine, artesunate + mefloquine and artemether–lumefantrine, on the basis that there is a diminishing chance from 1/109 to 1/1018 of a parasite resistant to two drugs with different modes of action as compared to a single drug emerging [74].

A few explanations were proposed for this worrying finding of parasite's increased tolerance to artemisinin which could be due to parasite or host factors. First possible

scenario is that of parasite having intrinsic resistance and the emergence or the selection of parasites with reduced ring-stage susceptibility. Secondly, parasites have unusual 'metabolism' states or the ability to become dormant. Thirdly, there may be lack of proper absorption or increased host metabolism of the drug, and lastly, splenic hypofunction or red blood cell abnormalities where artemisinin may be concentrated in uninfected RBCs or certain types of RBCs may break down the drug much more efficiently, thereby reducing the amount of drug that the parasite becomes exposed to [44, 73].

The exact mechanism behind reduced susceptibility towards artemisinin has yet to be elucidated whether in clinical field studies or in laboratory *in vitro* studies. However, evidence suggesting that PfATP6 and/or PfMDR1 may be implicated has been shown from *in vitro* experiments. Mutation of a single amino acid, in *P. falciparum* SERCA (PfATP6) decreases *in vitro* sensitivity to artemisinin dramatically when expressed in *Xenopus laevis* oocytes [75, 76]. In addition, field isolates showing elevated IC_{50} values and reduced *in vitro* sensitivity to artemether were found to possess a point mutation in the PfATP6 gene corresponding to a change in an amino acid from serine to arginine at the 769th position [76]. Other studies have attributed amplification of the *pfmdr1* or *pymdr1* gene to be involved in the mechanism of artemisinin resistance in various *Plasmodium* species [77] and in Thailand, higher copy number of *pfmdr1* gene modulates parasites' resistance to mefloquine as well as reduced sensitivity to artemisinin [55, 78]. In *Plasmodium yoelii*, artemisinin resistance is linked to decreased accumulation of the drug in the resistant parasite by 43% compared to artemisinin sensitive strains but was not associated with TCTP levels even though the resistant strain produced 2.5 times more TCTP protein than the sensitive strain [79].

In this case, TCTP is most likely a downstream target of artemisinin as it was previously shown to bind the drug [37]. Whether these parasites are truly resistant or merely exhibit increased tolerance to artemisinin is another question since resistance to the drug was transient and the parasites readily lost their resistance upon removal of drug pressure [80]. In genetically stable selected artemisinin and artesunate resistant *P. chabaudi* clones, resistance to artesunate as well as chloroquine has been correlated with the mutation of a gene encoding a deubiquitinating enzyme [81]. On the other hand, the genetic basis of the artemisinin resistant clone has yet to be established but it was earlier confirmed that it is not associated with polymorphisms or increased copy number in orthologues of molecular makers such as *pfatp6, pftctp, pfmdr1*, *pfcg10* and *pfubp1* which were previously believed to play a possible role in mediating artemisinin resistance [82]. Although all these *in vitro* studies are interesting in their own right and may point towards some basis of artemisinin resistance, there has yet to be any clinical relevance of these candidates to artemisinin resistance *in vivo*. Moreover, at present no *in vitro* correlates of clinical resistance exist. These studies using murine models to investigate the basis of artemisinin resistance in *Plasmodium* are also based on assumptions that the mechanisms will be similar to that in human *Plasmodium*. Henceforth, studies to elucidate and discover other genes or factors that give rise to artemisinin resistance is therefore now most crucial in monitoring the development and preventing the spread of drug resistance.

Anti-oxidant defense and redox regulation in the parasite

In the host, the *Plasmodium* parasite is subjected to oxidative stress generated from frequent assaults by the host immune response as well as to anti-malarial drugs upon drug administration to the patient. Moreover, the parasite has to degrade large

amounts of hemoglobin to heme as it develops within the host red blood cell. This process occurs in the parasite's digestive vacuole and produces ferriprotoporphyrin IX and large amounts of toxic reactive oxidative species (ROS) [83]. The parasite removes ROS through thioredoxin and glutathione redox processes which occur in various organelles ranging from cytosol, apicoplast, parasitophorous vacuole, mitochondria and nucleus [84, 85]. Interestingly, the parasite expresses enzymes involved in these pathways such as superoxide dismutase, thioredoxins, peroxiredoxins glutaredoxins, thio- or glutaredoxin reductases, plasmoredoxins but lacks catalase enzyme and endogenous glutathione peroxidases. To compensate, the parasite is able to recruit human detoxification enzymes including human peroxiredoxin 2, superoxide dismutase and catalase, by importing them into the parasite cytosol from the host RBC and utilize them for its own anti-oxidative functions [86, 87]. Over decades, the continuous administration of anti-malarial quinolones compounds such as chloroquine and mefloquine which induces oxidative damage has resulted in the selection of parasites that are able to withstand oxidative stress. This is either through 1) increased expression of metabolic enzymes directly involved in redox reactions (glutathione synthase) [88], or 2) regulation of transport processes i.e. higher rate of efflux of oxidized glutathione (GSSG) or glutathione-drug conjugates and increased import of reduced glutathione (GSH) into the parasite's digestive vacuole [89] or 3) elevated import of human enzymes, peroxiredoxin 2 into the parasite [87]. In contrast, the human genetic defect, X-chromosome-linked glucose-6-phosphate dehydrogenase (G6PD) deficiency in RBCs, manages to confer protection against severe malaria [90], due to lack of NADPH production and reduced glutathione levels (state of redox imbalance) [91]. This renders the parasite unable to infect or develop proficiently within these RBCs and leads to lesser fatalities [92].

However, there is a possibility that *Plasmodium* parasites may adapt to survive in such unfavorable host cell conditions given sufficient time and opportunity. Contrary to the report in 1969 that G6PD deficiency protects heterozygous females from malaria [93], there is new evidence from a controlled study in Mali that the same morbidity and mortality rates of *Plasmodium falciparum* infections occur in heterozygous females compared to non-deficient females [94]. There is also an unresolved controversy over whether hemizygous males are more susceptible to malaria compared to heterozygous deficient females [95], based on the theory that parasites can adapt to oxidatively stressful conditions over many generations. This raises the question of whether parasites that can proliferate in the presence of redox disequilibrium by modulating their redox "lifestyle" to fit a variety of host cell environments are slowly being selected for.

1.7 Transcriptome of the *Plasmodium falciparum* IDC

Transcriptional profiling studies of the 48-hour intraerythrocytic developmental cycle (IDC) of *Plasmodium* have shown that *Plasmodium* genes are tightly regulated in a highly coordinated and periodic fashion. Genes associated with a particular metabolic pathway are co-regulated and expressed during a particular stage in the lifecycle, just prior to the time when they are required, allowing for continued development of the cell [96]. For example, genes associated with surface antigen presentation on the host red blood cell membrane are most highly expressed in late ring stage whereas those involved in DNA replication and invasion machinery have their peak of expression in late trophozoite and late schizont stage respectively (Figure 1-6). Hence, the development of the *Plasmodium* parasite in the host erythrocyte cell is shown to be temporally regulated at the mRNA level.

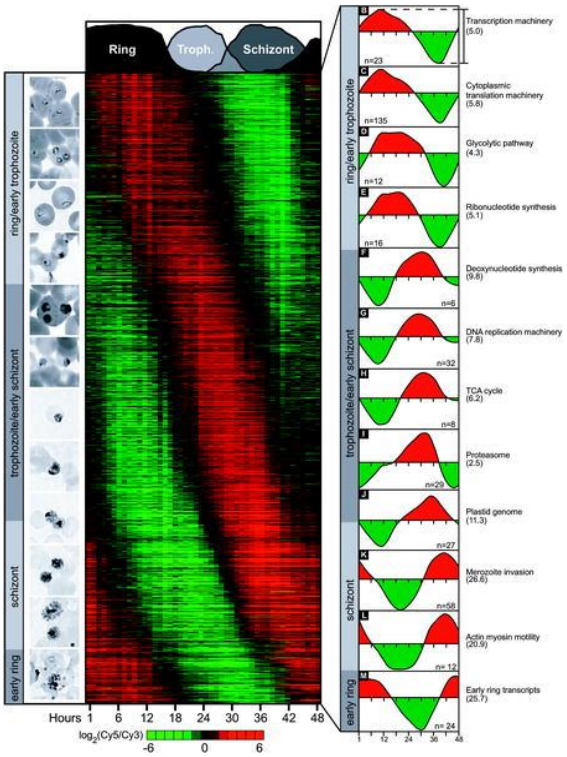

Figure 1-6. Established transcriptome of *P. falciparum* asexual lifecycle. Shown are the timing of expression of *P. falciparum* genes belonging to various metabolic pathways which are associated with development of the parasite across the 48 hr lifecycle [96].

Transcriptional variation underlying drug resistance in *Plasmodium*

The transcriptome is highly conserved between different lab strains and a report showed that there is little or no inter-strain differences in transcriptional levels that contribute to varying levels of drug sensitivities between Dd2, 3D7 and HB3 [97]. However, another study looking at expression QTLs reported contrasting results. They showed that changes in transcriptional levels between the progenies of the HB3 and Dd2 cross play a significant role as a source of phenotypic variation and strain-specific diversity in malaria parasites [98]. Most of the eQTLs act as *trans*-acting factors and most notably, amplification of PfMDR1 in the chromosome 5 amplicon coincided with changes in expression levels of 269 transcripts. However, these analyses which either support or contradict the link between drug sensitivity and

transcriptional profiles are indirect and subjected to different experimental and analysis approaches and no functional follow ups were done.

Transcriptional profiles associated with distinct physiological states of *P. falciparum*

On the other hand, microarray analyses study of African field isolates obtained fresh from patients revealed that distinct transcriptional states exist in the asexual stage of *Plasmodium* field isolates *in vivo* [99]. This suggests that natural variations in the metabolism of the parasite occur from host to host. The study observed that while some isolates exhibit a typical ring stage profile of active glycolysis, amino acid and nitrogen metabolism, nuclear transcription and cytoplasmic translation as expected (Figure 1-7 Cluster 2), other alternative metabolic states exist. Surprisingly, transcriptional profiles associated with up-regulation of genes coding for proteins in the mitochondria TCA cycle, FAS enzymes of the apicoplast, oxidative phosphorylation, respiration, mitochondrial biogenesis, and genes involved in the uptake and metabolism of glycerol were present, indicating a possibility of the parasite being "starved" and hence resulting in the parasite using alternative sources of carbon such as glycerol, lactic acid or lipids present in the patient's blood for energy production. This metabolic state also allows for high production of metabolites such as citric acid and acetyl-coA [99]. Acetyl-coA serves as an energy source as well as the primary substrate required to synthesize fatty acids via the FAS type II pathway in the plastid [100]. A study has suggested that this "starved" state of cluster 1 is due to the presence of a fraction of sexual-stage gametocytes present in the *in vivo* samples [101], hence presenting a confounder to the idea that alternative physiological states exist in the *P. falciparum* parasite. This claim has been refuted on several grounds, mainly because a high proportion of gametocytes has to be present to

give such high correlations, yet no sexual forms were seen in most parasite samples by microscopy [102]. Furthermore, no consistent up-regulation of early gametocytogenesis markers was observed. Daily et al also observed a third metabolic state of the parasite in a subset of *in vivo* samples which includes the up-regulation of molecular chaperones such as heat shock proteins, indicative of the parasite's stress response to environmental host inflammation markers [99]. A more recent study of transcriptional profiling of clinical samples from patients with cerebral malaria has found that a transcriptional state accompanied by an increased expression of a endoplasmic reticulum associated protein degradation enzyme, Hrd1, is associated with the level of parasitemia in the infected patient [103]. This affirms that the biology of *in vivo* parasites is unique and certainly worth further exploring and understanding in association with a clinical parameters/outcomes.

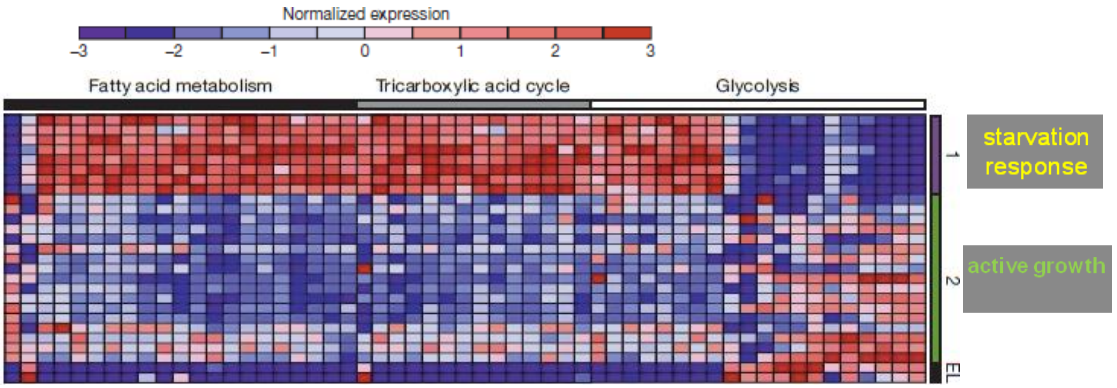

Figure 1-7. Expression profiles of parasites with distinct metabolic states. Heat map showing the expression ratios of the *in vivo* parasites with different physiological states – Cluster 1 ("starved" response) and Cluster 2 (typical ring-like glycolytic state). Source: Daily et al, 2007 [99].

1.8 Overall Aims of thesis

We propose that since field isolates exhibit transcriptionally different metabolic states which may be driven by host-related factors, this physiological variation may play a role in the variation in drug sensitivities. Hence, this formed the basis for dissecting

the transcriptional variation in *P. falciparum* parasites in the asexual stage of the lifecycle. My goal was to first establish an infrastructure to identify genome-wide gene expression differences between single clones of a culture adapted *P. falciparum* strain, 3D7, using microarray technology (Chapter 3). Next, utilizing this approach, we investigated gene expression changes in two Thai isolates obtained from patients which were subjected to culture adaptation (Chapter 3) in order to ascertain the effects of adapting an isolate to *in vitro* growth conditions and impact on the physiological state of the parasite. We sought to determine if transcriptional differences observed between parasites were maintained after undergoing culture adaptation. At the same time, we compared the diversity in transcription levels of single clones to *ex vivo* field isolates and using these general transcriptional changes as a backdrop, we aimed to characterize transcriptional profiles associated with the *in vivo* artemisinin resistant field isolates (Chapter 4). In addition, we characterize the fitness of the 3D7 clones in terms of their antimalarial drug sensitivities. Using genomics, cellular and molecular techniques, we relate the observed clones' phenotypic divergence to the level of *pfmrp2* mRNA abundance and characterize this protein of interest, the multidrug resistance-associated protein.

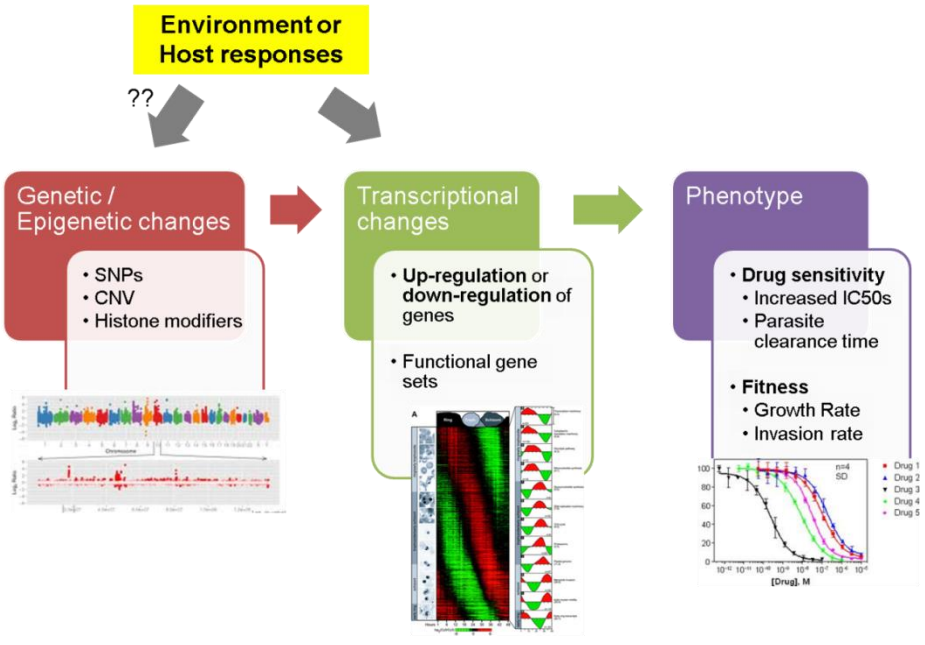

Chapter 2 : Materials and Methods

All solutions made were either sterilized by filtering or autoclaving, except organic solvents and solutions containing Sodium dodecyl sulphate (SDS). DNase-free and RNase-free sterile plastics were used and nitrile gloves were worn when preparing chemical solutions, handling biological samples and laboratory equipment.

2.1 *In vitro* tissue culture of *Plasmodium falciparum*

The *Plasmodium falciparum* lab strain 3D7 was cultured to generate a single common reference pool as our microarray probes were designed for 3D7 strain of *P. falciparum*. In addition, single clones were derived from this 3D7 strain. After thawing of cryopreserved stocks, parasites were maintained in human red blood cells (RBCs) and grown in HEPES (4-(2-hydroxyethyl)-1-piperazineethanesulfonic acid) - buffered RPMI 1640 medium (GIBCO, USA) supplemented with 0.25% Albumax II (GIBCO, USA), 0.2% sodium bicarbonate (SIGMA, Germany), 0.1 mM hypoxanthine (SIGMA, Germany) and 10 mg/l gentamycin (GIBCO, USA), at pH 7.4, in sterile cell culture flasks. The cell-medium mixture (CMM) was grown in a gas mixture of 5% CO_2, 3% O_2, and 92% N_2 in a 37°C incubator. Fresh RBCs was added into the CMM every cycle in the schizont stage and the CMM was kept at 1-2% hematocrit throughout. To obtain highly synchronized cultures, cultures were synchronized using 5% D-Sorbitol (SIGMA, USA) twice within the same cycle at the schizont-ring and ring-trophozoite transitions, 14-16 hours apart for at least 3 generations before the cultures were used for further experiments [104].

2.2 Large scale culture of *P. falciparum* in Bio-fermenter

Large scale culture in a Bio-fermenter was carried out in order to obtain sufficient amounts of total RNA to generate a single common reference pool of *P. falciparum*

that was used for all competitive microarray hybridizations against samples from the field and *in vitro* studies. The rationale being that it will allow for transcript expression levels to be compared directly across all samples. Briefly, the 3D7 strain of *P. falciparum* was grown in 10 large (175cm^3) flasks and kept at 8% hematocrit in late schizont stage prior to invasion for efficient invasion of uninfected RBCs. Following 6 hours after invasion, 78 ml of pRBC cultures containing majority of early rings at 10% parasitemia was resuspended in 4.8 L of culture medium and transferred to the 7L Bio-fermenter. The culture was kept at 1.0-1.6% hematocrit over 48 hours. Every 6 hours for a total of 8 time points (TPs), an adjusted volume of pRBC was harvested based on calculations of expected equal RNA amounts for each time point. About 8 times more pRBC and 3 times more pRBC were harvested in ring and trophozoite stage respectively compared to schizont stage. A total of 9.92 mg of RNA was obtained from the single Bio-fermenter run and was sufficient for more than 1000 hybridizations with *in vitro* samples (without RNA amplification) or more than 100,000 hybridizations with field samples (with RNA amplification).

2.2.1 Establishment of Reference pool for Microarray Hybridizations

After isolating the RNA from the 8 TPs of the Bio-fermenter run, a reference pool comprising of equal amounts of RNA from the different stages of the intraerythrocytic lifecycle of the 3D7 strain was used to generate a standard cDNA pool which was labeled with Cy5 and used for all microarray hybridizations pertaining to transcriptional profiling. For CGH, 3D7 was used as the reference strain and its genomic DNA was harvested from *in vitro* cultures in the lab. The klenow reaction DNA product was labeled with Cy5 and used in microarray hybridizations against all other gDNA samples.

2.3 Cloning by limiting dilution technique

Derivation of single isogenic clones from the 3D7 lab clone was carried out by the method of limiting dilution as previously described [105]. To rule out the possibility of getting multiply-infected RBCs, which is a hallmark of *P. falciparum* infections, the 3D7 cultures were placed on a shaker at least 12 hours prior to invasion and the parasitemia was checked on Giemsa-stained smears by light microscopy after invasion was completed. Only when at least 95% of iRBCs was infected with a single ring form parasite, the parasites were then serially diluted with fresh RBCs based on percent parasitemia count and calculations of expected parasite numbers in order to obtain a diluent consisting of 0.5 parasite per 0.1 ml of CMM. This volume of Diluent C was then transferred to total of 72 wells in 96-well plates as shown below (Figure 2-1A and B). Alongside, 3 wells of Diluents A and B each were set up on the same plate as controls. The plates were gassed and kept at 37°C. Culture medium was replaced every 48 hours, kept at 5% hematocrit and fresh RBCs were added only every 6 days to each well. On day 4 and day 6, control wells for diluents A and B were checked for parasites and the presence of parasites in these wells serve as the experiment's positive controls. On day 12, smears were made for all 72 wells to check for presence of parasites and the CMM from any positive wells were transferred to 24-well plates and kept at 1-2% hematocrit. All 23 clones were subsequently scaled up and cryopreserved as stocks in liquid N2. 5 of these clones, 1A, 5D, 6A, 8B and 11C were chosen randomly to be scaled up and their highly synchronized cultures were harvested subsequently in 8 hourly time courses for RNA to measure their transcriptional profiles.

A.

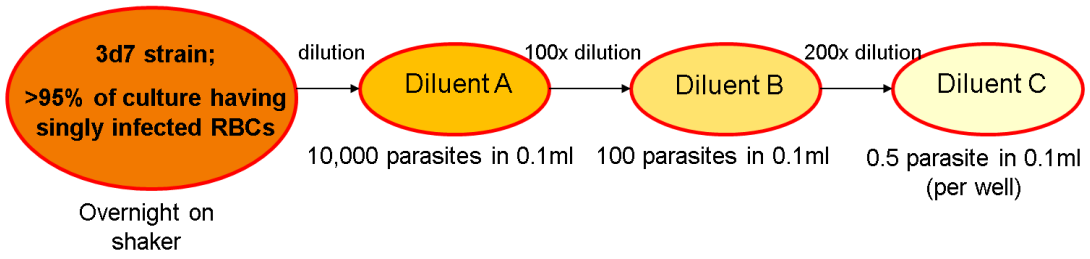

B.

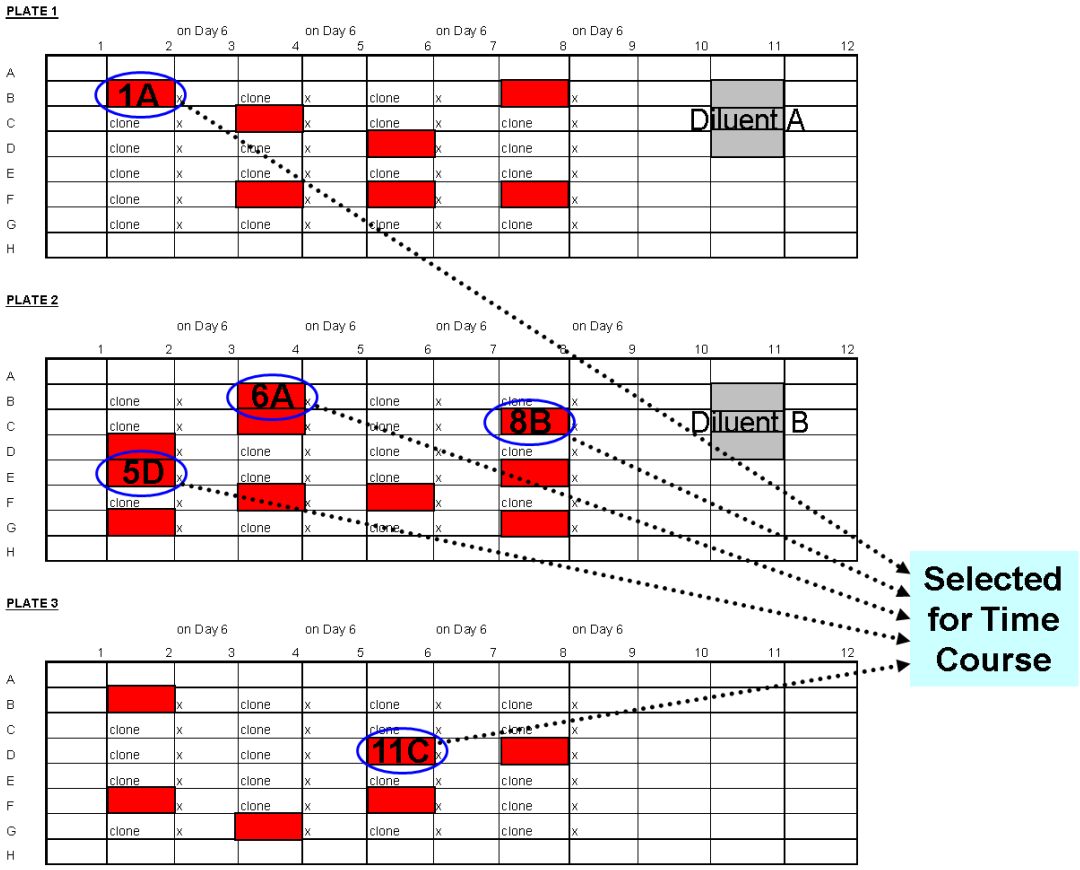

Figure 2-1. Outline of limiting dilution experiment. A. Schematic of serial dilution of parasitemia to obtain 0.5 parasite per well. B. Diagram of wells positive (red) for clones on day 12 post limiting dilution.

2.4 *In vitro* drug sensitivity assays (Modified Schizont Maturation Assay)

Chloroquine (CQ), artemisinin (ART), and mefloquine (MEF) drug sensitivity assays were carried out on 3D7 strain and the individual clones at the mid ring (14 hpi), mid trophozoite (24 hpi) and mid schizont (34 hpi) stages. Stock solutions (1 M) and their

subsequent serially diluted drug concentrations were prepared from artemisinin (Mr = 282.332) (CalbioChem, USA), mefloquine hydrochloride (Mr = 414.78) (SIGMA, Germany) in dimethyl sulfoxide (DMSO) (SIGMA, France) and chloroquine diphosphate (Mr = 515.87) (SIGMA, UK) in deionized water. Parasitized blood from the cultures was diluted with purified RBCs and media to obtain a final CMM of 1% hematocrit and 3% parasitemia, which was distributed into the wells of a standard 24-well microculture plate. Serial dilutions of the drug were carried out for a total of at least 8 different drug concentrations and done in duplicates for each assay. 2 positive drug-free controls were present, one with CMM only and the other consisting of CMM and DMSO (ART assay) or deionized water (CQ assay). The plates were then kept in a bag filled with 5% CO_2, 3% O_2 gas mixture in a 37°C incubator. Upon invasion of new rings in the control, thin smears were prepared from each well, stained with Giemsa (Fluka, USA) and the % of parasitemia for rings, trophozoites and schizonts were counted for at least 300 RBCs. The geometric mean of percentage rings was transformed to % growth which was then plotted against the base 10 logarithm of drug concentrations to calculate the inhibitory concentrations. The 50% and 90% inhibitory concentration, IC_{50} and IC_{90}, were determined by nonlinear regression analysis based on a polynomial regression mode using the software (HN-NonLin V1.1) from http://malaria.farch.net. The assays were repeated at least 2 times for each drug at the 3 stages.

2.5 Microarray-based Transcriptional Profiling

2.5.1Collection of Time Point samples across 48 hr asexual lifecycle

Highly synchronized cultures of the isogenic clones 1A, 5D, 6A, 8B, 11C and parent 3D7 were used to generate the time course of the IDC. Between 300 µl to 1 ml of

pRBC samples of cultures with 7-10% parasitemia were collected every 8 hr for a total of 6 TPs such that parasites from early ring to late schizont stages at approximately 8, 16, 24, 32, 40 and 48 hpi were obtained. Cells were harvested by washing the packed RBCs once in 10X volume of PBS, mix by inversion and spun down at 1,000g for 5 min (no brake) and supernatant was removed. Samples were flash frozen in liquid nitrogen and stored at -80°C till ready for RNA isolation. 1 ml of pRBC sample for each clone was harvested similarly for genomic DNA.

Sample collection from patient and during *ex vivo* IDC

On admission to the hospital and upon consent, 10 ml of total infected blood was taken from each adult *P. falciparum*-infected patient from the various field sites (Pailin, Cambodia; Xepon, Savannakhet Province, Laos; Mae Sot, Thailand) for a total of 11 isolates. For the *ex vivo* patient samples, it was crucial that human white blood cells were first depleted using CF11 columns or Plasmodipur filters immediately after blood sample collection from the patient. This was followed by several subsequent washes with RPMI medium or PBS to minimize the presence of all possible human white blood cells contamination. The cells were then pelleted down at 1,000g for 5 min and the resulting pRBC samples were either subjected to *in vitro* culture in malaria culture medium for 1 generation of the IDC over 48 hours or immediately flash frozen in liquid N2 and stored at -80°C. For every isolate, a total of 6 to 10 samples were harvested at regular intervals of 2 to 8 hours throughout the IDC. 100-500ul of packed red blood cells with 1% - 10% parasitemia was collected per time point sampling. (These steps were carried out by lab personnel in various field sites) The samples were stored at -80°C before shipping to Zbynek Bozdech Lab, Nanyang Technological University, Singapore.

2.5.2 Total RNA isolation from *Plasmodium* parasites

Great care was observed when isolating *Plasmodium* RNA due to its precarious nature. For all steps in RNA isolation, all materials were handled with gloves throughout and only clean and sterile glassware, plastic ware and pipette tips were used. Samples were kept on ice at all times. This prevented any RNases from entering the material which could lead to potential degradation of RNA.

2.5.3 RNA isolation for large sample volumes from *in vitro* cultures

RNA from the *P. falciparum* samples that were harvested from *in vitro* cultures (0.4 ml to 2 ml) were isolated as described previously (Bozdech et al, 2003a). Frozen samples were first thawed in a 65°C water bath for 1-2 min. TRIzol reagent (Invitrogen, USA), an acidic phenol, was added to the pRBC sample in a 10:1 ratio to lyse the infected RBCs. The sample was mixed well by pipetting up and down, ensuring that most of the clumps are dissociated and sample is homogenized. This was followed by addition of chloroform (Fisher Scientific, USA) in a 5:1 (TRIzol:chloroform) ratio and sample shaken hard to mix well. After keeping on ice for 5 min, the sample was spun at 3,900g (acceleration = 9, brake = 0) in a swing rotor centrifuge for 10 min at 4°C. A distinct separation of phases should be seen with DNA and proteins in the inter phase and bottom organic phase respectively and the top colorless aqueous phase containing RNA. The aqueous supernatant was transferred to a fresh tube and an equal volume of isopropanol (Fisher Scientific, USA) was added, mixed well and kept at -20°C overnight to allow for RNA precipitation. The next day, samples were spun at 10,400g for 1 hr at 4°C in a fixed angle rotor and a white translucent pellet was observed. The supernatant was removed with a pipette. An equal volume of 70% ethanol (Merck, USA) (to TRIzol volume used originally) was added to wash the pellet by gently dislodging it from the tube. The sample was

kept on ice for 10 min to remove any contaminating salts. After spinning for 10 min at 10,400g at 4°C, the supernatant was carefully removed by pipetting and the pellet was air-dried at room temperature. When no moisture droplets were seen on the tube, the pellet was resuspended in 30-80 µl of RNAse-free deionized water. The concentration and purity of the RNA samples were measured using NanoDrop ND-1000 Spectrophotometer (Thermoscientific, USA) by the absorbance levels (OD_{260} absorbance value of 1.0 corresponds to 40 ng/µl of RNA concentration) and A260/A280 and A260/A230 ratios for any protein or salts/phenol contamination. Clean and pure RNA gave A260/A280 ratio between 1.9 to 2.1 and A260/A230 ratio between 1.8 – 2.2 for *in vitro* samples and 0.2-2.1 for clinical samples. Integrity of the RNA was monitored by running 0.5 to 2 µg of the samples on a 1% denaturing gel at 7 V/cm for 2 hr. Visualization of 3 distinct ribosomal RNA bands at 3.8 kb (28s rRNA), 2.0 kb (18s rRNA) and 160 bp (5.8s rRNA) indicated good intact RNA (Figure 2-2) while a smear would indicate that the RNA had degraded to some extent. All RNA samples were stored at -80°C.

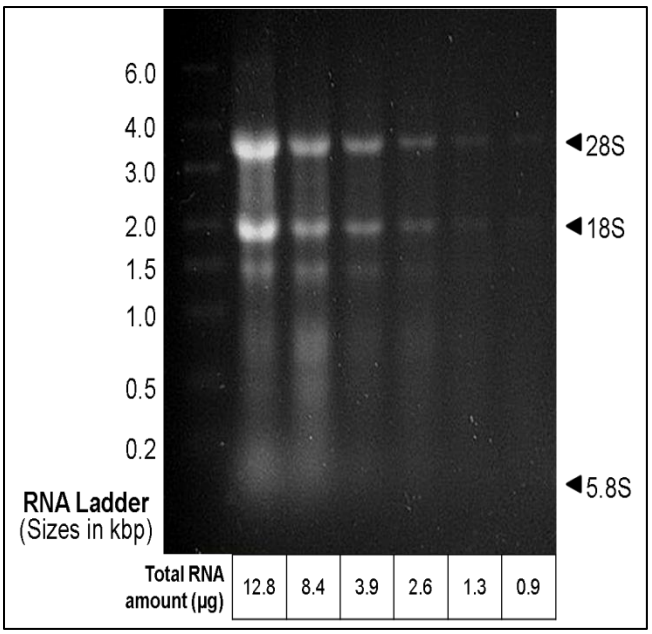

Figure 2-2. Gel picture of extracted RNA. Total RNA extracted from parasite samples ran on a denaturing gel show good quality intact RNA.

2.5.4 RNA isolation for small sample volumes from field isolates

RNA isolation of limited sample volumes ~100-300 µl with parasitemia around 1-2%, generally taken directly from patients was carried out for a total of 150 samples. The protocol is similar to the large volumes (see above) except that 1-2 µl of the glycogen carrier, GlycoBlue (Ambion, USA) was added together with isopropanol and stored at -20°C for at least overnight to enable more efficient precipitation and higher yields as well as easier visualization of the pellet after centrifugation. Importantly, after TRIzol was added to the pRBC sample, the tube was flicked hard instead of pipetting the sample up and down as the biological material would adhere to the pipette and result in substantial loss in RNA. 1.5 ml eppendorf tubes or 15 ml falcon tubes were used instead of 50 ml tubes for the smaller volumes. The amount of RNA yields for the various pRBC volumes were calculated as shown in Table 2-1.

Table 2-1. Total RNA yields expected from *P. falciparum* samples.
The yields calculated are based on starting % parasitemia and volumes of *P. falciparum* iRBC harvested from *in vitro* culture-adapted samples or from clinical samples of patients.

% Parasitemia*	Vol. of pRBC (µl)	Expected yield (µg)			Type of sample
		Ring (10-16hpi)	Trophozoite (22-28hpi)	Schizont (36-40hpi)	
10%	1000	**44.4**	**88.8**	**344.1**	*In vitro* cultures
5%	1000	**22.2**	**44.4**	**172.1**	
1%	1000	**4.44**	**8.88**	**34.4**	
10%	300	**13.3**	**26.6**	**103.1**	Clinical blood samples
5%	300	**6.7**	**13.4**	**51.9**	
1%	300	**1.3**	**2.6**	**10.1**	

* % parasitemia = (number of parasites / number of red blood cells) x 100% where a doubly-infected RBC is counted as 2 parasites.

2.5.5 cDNA synthesis by reverse transcription

For samples with at least 10 µg of starting total RNA, reverse transcription was performed to generate single strand cDNA that is reverse complement to the mRNA transcripts along with the incorporation of amino-allyl groups into the cDNA. Otherwise, amplification of the material was carried out (*see* Section 2.5.6). cDNA synthesis was performed as described by Bozdech et al, 2003a, with the following modifications: 10 µg total RNA in a volume of 28 µl was mixed with 2µl of 1:1 mixture of oligo-dT / random primer mix (2 µg/µl) (26.53 µl of 1000 µM oligo-dT (25-mer), 73.53 µl of 1000 µM random primer (9-mer)) and the mixture heated at 70°C for 10 min followed by placing the tube on ice for 10 min for initial priming. 1.5 µl of Amino-allyl dUTP-dNTP 30X stock (consisting of 34 µl of 100 mM dATP (30 mM), 17 µl of 100 mM dTTP (15 mM), 17 µl of 100 mM dCTP (15 mM), 17 µl of 100 mM dGTP (15 mM), 17 µl of 100 mM amino-allyl-dUTP (15 mM), 11.33 µl water to make total volume 113.33 µl), 4.5 µl of 100 mM DTT, 2.5 µl of deionized water, along with 300 units of RevertAid H Minus MMuLV (Moloney murine leukemia virus) Reverse transcriptase (Fermentas, USA) were added to the reaction mix to a total reaction volume of 50 µl. The tube was incubated at 42°C for 2 hr to synthesize the first strand cDNA. Subsequently, 10 µl of 0.5 M EDTA and 10 µl of 1 M NaOH were added and the mixture heated at 65°C for 15 min to hydrolyze the RNA template. Purification of the ss-cDNA product was carried out using the MinElute PCR purification kit (Qiagen, USA) (see Section 2.5.7). The cDNA was stored at -20ºC. The DNA concentration was measured using a spectrophotometer. An OD260 absorbance value of 1.0 corresponds to 33 ng/µl of ss-cDNA concentration. Typical yields ranged from 1.5 to 4 µg of cDNA product and the A260/A280 ratio ranged from 1.9-2.1 and A260/A230 ratio ranged from 1.8 – 2.1. 500 ng – 1 µg of the

purified product was run on a 1% agarose gel at 6 V/cm to monitor the quality of the cDNA. A smear up to 3 kilo base pair (kb) in size indicated good quality first strand product (FS-cDNA). 1.5 – 2 µg was labeled with Cy fluorophore (see Section 2.7).

2.5.6 cDNA Synthesis and Amplification by SMART-PCR

For samples with minute amounts of starting total RNA (<10 µg), amplification of total RNA was required to generate sufficient target DNA for microarray hybridization. The SMART PCR method which uses the template-switching mechanism of the reverse transcriptase enzyme at the 5' end of the mRNA template, was utilized in this respect, thus ensuring the synthesis of full length FS-cDNA products from both 5' and 3' ends of the mRNA template [106]. The full length FS-cDNA is then used as template to generate products exponentially in the PCR step and with the incorporation of the amino-allyl group. Using this method, transcriptome analysis of clinical isolates and where starting biological material is limited could be accomplished.

To 500 ng of total RNA in a total volume of 6 µl, 2 µl of SMART primer mix (50 µl of 100 µM TS-Oligo (50 µM), 25 µl of 100 µM SMART-Oligo-d(T) (25 µM), 25 µl of 100 µM SMART-N(9) (25 µM)) was added and mixed. Sequences for the primers are as follows: TS-Oligo - AAGCAGTGGTATCAACGCAGAGTACGCrGrGrG; SMART-Oligo-d(T) - AAGCAGTGGTATCAACGCAGAGTAC(T)30VN (N = A/C/G/T; V = A/G/C); SMART-N9 - AAGCAGTGGTATCAACGCAGAGT(N)9. The tube was incubated at 65ºC for 5 min and placed on ice for 10 min to initiate the priming reaction. To each tube, 4 µl of 5X First Strand reverse transcription buffer, 2 µl of 3 mM dNTP mix (300 µM), 2 µl of 100 mM DTT, 40 U of RNaseOUT Recombinant Ribonuclease Inhibitor enzyme (Invitrogen, USA) which removes any

residual RNases that may degrade the RNA template, and 2 µl of deionized water were added to total reaction volume of 19 µl and the tube kept at 25ºC for 2 min. Following which, 1 µl (200U) of SuperScript™ II reverse transcriptase enzyme (Invitrogen, USA) which has terminal transferase activity and adds extra bases at the 3' end of the newly synthesized cDNA strand was added to the reaction mix, mixed well and incubated at 42ºC for 50 min. 5 µl of the reaction mixture was run on a 1% agarose gel at 6 V/cm to monitor the quality of cDNA and a smear varying up to 3,000 base pair (bp) in length was observed. PCR was carried out next to exponentially amplify the cDNA products. To 2.5 µl (12.5%) of cDNA product mix, 10 µl of 10X reaction buffer, 1.5 µl of Amino-allyl dUTP-dNTP 30X stock, 6 µl of 100 mM Primer IIa (AAGCAGTGGTATCAACGCAGAGT), 2 µl (10U) of *Taq* DNA polymerase (New England Biolabs, USA) and 78 µl of deionized water were added for a total reaction volume of 100 µl. The reaction was run in a thermal cycler at 95ºC for 5 min, 60ºC for 1 min, 68ºC for 10 min, followed by 19 cycles of 95ºC for 30s, 60ºC for 30s, 68ºC for 5 min and a final extension step at 72ºC for 5 min. The amplified double-stranded DNA product was purified using MinElute PCR purification kit (Qiagen, USA) (see Section 2.5.7). The DNA was stored at -20ºC. The DNA concentration was measured using a spectrophotometer. An OD260 absorbance value of 1.0 corresponds to 50 ng/µl of DNA concentration. Typical yields ranged from 7 µg to 14 µg of total DNA product for a single PCR and up to a total of 100 µg of DNA can be synthesized from the starting 500 ng of total RNA. The A260/A280 ratio ranged from 1.9-2.1 and A260/A230 ratio ranged from 1.8 – 2.1. 1 µg of the DNA was run on a 1% agarose gel at 6 V/cm. The amplified products varied up to 1,500 bp in length. 4 µg of the DNA was used for fluorescent labeling with Cy dye (see Section 2.7).

2.5.7 DNA purification from PCR reaction using MinElute PCR purification kit (Qiagen, USA)

10 µl of 3 M sodium acetate, pH 5.0 was added to the reaction mixture prior to purification of DNA using the kit. This ensured the pH is optimal for DNA binding to the MinElute column. To purify the DNA, 700 µl PB binding buffer was added to the reaction mix, mixed well and transferred into the MinElute column. The mixture was spun at 13,200 rpm for 1 min in a table top centrifuge. The flow-through was removed and 750 µl of PE wash buffer was added into the column and spun twice at 13,200 rpm for 1 min to dryness. The column was placed in a clean 1.5 ml tube and the DNA was eluted by adding 15 µl of EB buffer, let sit for 2 min, and then spun at 13,200 rpm for 1 min. The DNA was stored at -20°C.

2.6 Microarray-based Comparative Genomic Hybridization (CGH)

2.6.1 Genomic DNA extraction from infected RBCs

Between 0.5 ml to 1 ml of pRBCs was harvested and washed once with 10 ml of 1X PBS. The pRBCs were resuspended and split into 1.5 ml tubes so that each tube contained 0.2 ml of pRBC and flash frozen and stored at -80°C till ready for extraction. Genomic DNA extraction by phenol-chloroform method was carried out as described [107]. After thawing, the pRBCs in each tube was resuspended with 1 ml of PBS. 10 µl of freshly made 5% saponin (for a final concentration of 0.05%) was added and gently mixed. After RBC lysis was observed, the tube was immediately centrifuged at 6,000g for 5 min and the supernatant was removed. 25 µl of lysis buffer (40 mM Tris–HCl, pH 8.0, 80 mM EDTA, pH 8.0, 2% SDS) and 75 µl of deionized water were added to the pellet and mixed well. The tube was incubated at 37°C for 2 hr. Next, 100 µl of deionized water and 200 µl of phenol (equilibrated with 0.1 M

Tris-HCl, pH 7.0) were added, mixed well and centrifuged at 2,000g for 8 min. The top clear aqueous layer was collected into a fresh tube and 200 µl of chloroform was added, mixed well and centrifuged at 2,000g for 8 min. Again, the top aqueous layer was collected and transferred to a fresh tube. Extraction with chloroform was repeated again as above. Finally, after the top layer was transferred to a fresh tube, the genomic DNA was precipitated by adding one-tenth volume of 3 M sodium acetate, pH5.0 and 2.5 volumes of absolute ethanol and the tube was kept overnight at −20°C. The DNA was further precipitated at13,200 rpm for 30 min at 4°C and washed once with 70% ethanol. After the spin, the DNA was air-dried at room temperature in a hood, and gently resuspended in 50 to 500 µl of deionized water, depending on size and expected yields. 200 µl of RBC at 10% parasitemia yields ~10-20 µg of gDNA The DNA was stored at -20°C. The DNA concentration was measured and 0.5 µg was run on and visualized on a 0.8% agarose gel to see that the gDNA runs as a high-molecular weight and free of RNA.

2.6.2 Amino-allyl-dUTP labeled DNA synthesis by klenow reaction

For *in vitro* culture adapted clones and lab strains with sufficient amounts of genomic DNA available (>10 µg), synthesis of genomic DNA coupled with amino-allyl-dUTP by klenow enzyme was done as previously described (Bozdech et al, 2003a).To 4 µg of gDNA, top up with deionized water to 30 µl total volume. 3.7 µl of random N9 primer (2.72 mg/ml) was added to the gDNA and mixed well. The tube was boiled for 5 min at 99°C, then cool on ice for 5 min. 5 µl of NEBuffer 2, 5 µl of 10X amino-allyl-dUTP/dNTP (stock: dATP 0.75 mM, dTTP 0.15 mM, amino-allyl-dUTP 0.60 mM, dGTP 0.15 mM, dCTP 0.15 mM), 4 µl of Klenow Fragment (3'→5'exo$^-$) enzyme (New England Biolabs, USA, 5U/µl) and 2.3 µl of deionized water were added for a final total volume of 50 µl, mixed well and incubated at 37°C for 2-3 hr.

Next, an additional 1 µl of Klenow Fragment (3'→5'exo$^-$) enzyme was added, mixed well and incubated at 37°C for a further 2-3 hr. The DNA product from the klenow reaction was purified using MinElute PCR Purification Kit (see Section 2.5.7). The DNA was stored at -20°C. The DNA concentration was measured using a spectrophotometer. An OD260 absorbance value of 1.0 corresponds to 50 ng/µl of DNA concentration. Typical yields ranged from 7 µg to 15 µg of total DNA product. The A260/A280 ratio ranged from 1.9-2.1 and A260/A230 ratio ranged from 1.8 – 2.1. 500 ng – 1 µg was run on a 1% agarose gel at 6 V/cm and the DNA appeared as a smear of up to ~1,500 bp. 2 µg was used for fluorescent labeling (see Section 2.7).

2.6.3 Amino-allyl-dUTP labeled DNA synthesis by klenow reaction and SMART-PCR amplification

This procedure to amplify the genomic DNA was carried out when the gDNA was limited and in sub microgram quantities. To 50 ng of genomic DNA, deionized water was added to make a total volume of 4 µl in a PCR tube. 1 µl of SMART-N9 primer (10 µM) was added and mixed by pipetting. The tube was incubated at 95ºC for 6 min and placed on ice for 4 min. To each tube, 1 µl of 10X Klenow NEBuffer, 1 µl of 3 mM dNTP mix (300 µM), 0.5 µl (2.5 U) of Klenow Fragment (3'→5'exo$^-$) enzyme (New England Biolabs, USA), and 2.5 µl of deionized water were added and mixed well to a total reaction volume of 10 µl. The tube was incubated at 25ºC for 10 min, 37ºC for 1 hr, and 75ºC for 20 min to synthesize the complementary strand of DNA. PCR amplification was carried out next. To the reaction tube, 10 µl of 10X reaction buffer, 1.5 µl of Amino-allyl dUTP-dNTP 30X stock, 6 µl of 100 mM Primer IIa (6 mM), 2 µl (10 U) of *Taq* DNA polymerase (New England Biolabs, USA) and 70.5 µl of deionized water were added for a total reaction volume of 100 µl. The reaction was run in a thermal cycler at 95ºC for 5 min, 60ºC for 1 min, 68ºC for 10 min, followed

by 19 cycles of 95ºC for 30s, 60ºC for 30s, 68ºC for 5 min and final extension step at 72ºC for 5 min. The amplified double-stranded DNA product was purified using MinElute PCR purification kit (Qiagen, USA) (see Section 2.5.7). The DNA was stored at -20ºC. The DNA concentration was measured using a spectrophotometer. An OD260 absorbance value of 1.0 corresponds to 50 ng/µl of DNA concentration. Typical yields ranged from 7 µg to 15 µg of total DNA product. The A260/A280 ratio ranged from 1.9-2.1 and A260/A230 ratio ranged from 1.8 – 2.1. 500 ng – 1 µg was run on a 1% agarose gel at 6 V/cm and the amplified product appeared as a smear reaching up to ~1,500 bp. 4 µg was used for fluorescent labeling (see Section 2.7).

2.7 DNA labeling and microarray hybridization

DNA samples (cDNA, amplified DNA/gDNA) were labeled with fluorophores, Cy3 or Cy5, via the coupling reaction between the Cyanine groups of Cy fluorophore molecules and amino-allyl groups incorporated into the DNA. To each DNA sample, 0.5 M sodium bicarbonate buffer, pH 9.0, was added and mixed well to give final concentration of 0.1 M. It was ensured that the total volume for labeling did not exceed 10 µl as labeling efficiency significantly decreased when the volume was larger than 10 µl. Each Cy3 or Cy5 pellet (40 nmol, GE Amersham Biosciences, USA) was thoroughly resuspended in 15 µl of DMSO. 2µl of Cy5 or Cy3 mixture was added to each sample and mixed well by pipetting. For transcriptional profiling, the cDNA/amplified DNA for reference pool was labeled with Cy3 while the cDNA/amplified DNA for all target samples (time course, treatment etc.) was labeled with Cy5 molecules. For comparative genomic hybridization, gDNA of 3D7 reference parental strain was labeled with Cy3 while sample gDNA was labeled with Cy5. The samples were kept in the dark for 1-4 hr at room temperature. The labeled DNA was

purified using MinElute PCR purification kit (Qiagen, USA) (see Section 2.5.7) in order to remove excess unincorporated Cy molecules.

After purification, the Cy3-labeled reference pool DNA were then pooled together and divided equally among the target samples. 15 µl of each Cy5-labeled sample was mixed with 15 µl of Cy3-labeled pool. 6 µl of 20X SSC, 2.14 µl deionized water, 0.98 µl 1 M HEPES and 0.88 µl of 10% SDS were added and mixed well. The hybridization mixture was boiled at 100°C for 3 min and cooled at room temperature for 5 min. The MAUI® mixer coverslips (BioMicro Systems, USA) were assembled on the array slides to create a hybridization chamber and placed onto the pre-warmed MAUI machine. The mixture was then loaded onto the array slide and the DNA was allowed to hybridize efficiently to the probes for 16-18 hr at 65°C using the MAUI® microfluidics hybridization system (BioMicro Systems, USA) which circulated the solution periodically throughout the slide. After hybridization, the MAUI mixers were removed individually from the arrays and the arrays were washed sequentially in glass dishes containing 0.6X SSC/0.03% SDS and then 0.06X SSC by plunging the slide rack up and down 10 times followed by an incubation of 5 min for each wash. The arrays were spun dry in a swing rotor table top centrifuge at 600g for 5 min and placed in a box to reduce exposure to light. The arrays were immediately scanned using the GenePix 4000B Dual Channel Microarray scanner (Axon Laboratory, USA) as Cy molecules degrade and quench differentially and delays could result in biased and inaccurate representations of fluorescence signal intensities.

2.8 Manufacture of custom-made long oligonucleotide microarray chip

2.8.1 *P. falciparum* oligonucleotide design

To profile genome-wide RNA transcript expression, 10,265 70-mer oligonucleotides representing 5,343 *Plasmodium falciparum* coding genes were designed based on the completed sequence of the 3D7 genome (PlasmoDB 7.4) using the OligoRankPick program [108]. An average of 1 oligonucleotide for every 2.2 kb segment of the coding sequence for each gene was designed. 5,402 50-mer oligonucleotides mapping to the upstream promoter regions (at 500th to 1,500th distance from translation start site) of the coding genes were additionally designed. This chip with total 15,667 probes having a wider coverage of the entire *P. falciparum* genome (average distance between probes of 1.5 kb) was used in CGH for CNV analysis. Information of these probes have been deposited in NCBI's Gene Expression Omnibus [109] and are accessible through GEO Platform accession numbers GPL11248 and GPL11250. (https://www.ncbi.nlm.nih.gov/geo/query/acc.cgi?acc=GPL11248; https://www.ncbi.nlm.nih.gov/geo/query/acc.cgi?acc=GPL11250).

These oligonucleotides were synthesized by Invitrogen Life Technologies, USA.

2.8.2 Preparing slides for Printing of long oligonucleotides onto chip

To manufacture in-house cDNA microarray chips, poly-l-lysine (Sigma, USA) coated gold-seal slides were first prepared. Briefly, gold seal microscope slides (Gerhard Menzel GmbH, Germany) placed on slide racks were washed in a solution of 2.5 M Sodium Hydroxide/60% ethanol in large beakers for 2 hours on a shaker to remove any residual dirt and then rinsed thoroughly with 5 washes of double distilled water. Next, a solution (180 ml poly-l-lysine, 210 ml 1X PBS, 1710 ml deionized water) was prepared and added to the glass slides in plastic beakers and placed on a shaker for 1

hr to coat the slides. Excess poly-l-lysine was removed by rinsing the slides with deionized water and the slides were spun dry at 600 rpm for 5 min in a centrifuge. After heating the slides for 20 min at 50°C in an incubator, the slides were transferred to a plastic slide box and stored at room temperature. These coated slides were aged for 2 weeks before spotting of the oligonucleotides was carried out. The 15,886 custom oligonucleotides synthesized in 384-well plate format (Invitrogen, USA) was first resuspended in 3X SSC (made from 20X SSC stock of 3 M Sodium Chloride, 0.3 M Sodium Citrate, pH 7.0), kept on a shaker at 4°C for 2 days and subsequently dried down in a SpeedVac Concentrator system (Thermo Scientific, USA) to lysophilize the oligonucleotides. Just prior to spotting, the oligonucleotides were rehydrated with 27 µl of deionized water to obtain a final DNA concentration of 20 µM and kept on a shaker at 4°C overnight to ensure complete dissolution. All liquid handling and transferring procedures were done automatically using the Gilson 940 Workstation Robotic system that we programmed. Oligonucleotide spotting on the microarray chip was then carried out using pre-cleaned microspotting pins (Arrayit Corp., USA) that delivered 600pl of oligonucleotide on every slide and produced spots of 100um diameter with 120um spacing in the VersArray ChipWriter Pro Systems (Biorad, USA). The grid for the microarray chip probe/spot identities was created using Array List Generator software in Genepix Pro 6.0 (Axon Laboratory, USA). The printed slides were stored in plastic slide boxes till ready to be used.

2.8.3 Preparation of microarray chip for hybridization

To prepare the chips for hybridization, they have to be first post-processed. Spots on the microarray chips were rehydrated by placing the slides with the array side faced down in a hydration chamber of 3X SSC solution on a slide warmer at 42°C for 1.5 min and quickly snapped dry over 3-5 s on a 100°C heat block. This ensured that all

the spots were big and uniform in size. Next, the DNA oligonucleotides were crosslinked to the glass surface of the slide in a UV crosslinker at 80mJ energy. Lastly, blocking of the free amines of the lysine groups over the slide surface (to prevent unspecific binding to DNA samples and reduce background fluorescence) was done by incubating the slides in a solution of BSA (12.5 ml 20X SSC, 0.5 ml 10% SDS, 0.5 g Bovine Serum Albumin (Sigma, USA) and 37 ml deionized water) on a rocker at 42°C for 45 min. The slides were then rinsed thoroughly in 5 washes of deionized water and spun dry at 600 rpm for 5 min in a centrifuge. They were now ready to be used in microarray hybridization experiments.

2.9 Statistical analysis of microarray data

The microarray slides were scanned with a GenePix 4000B scanner and the images analyzed using GenePix Pro 6.0 program (Axon Instruments, USA). Manual flagging was performed to filter off individual bad hybridization spots or areas with local high background fluorescence. Following that, the signal intensities for all probes across each array were Lowess Normalized and subsequently filtered for quality control in Acuity 4.0 software (Axon Instruments, United States). For all array features, only "spots" with at least 95% pixels median intensity above the local background intensity plus 2 standard deviations for either Cy channel were included for downstream analysis. Microarray data obtained from the Dd2 time course arrays were processed as follows to create the reference transcriptome used for all analyses.

The assembly of the IDC transcriptome for the reference Dd2 strain and all other clones/isolates was carried out using Fast Fourier Transform as previously described [96] with the following modifications; the expression $\log_2$ ratio value for each gene is represented by the averaged $\log_2$ ratios of the oligonucleotide probes representing

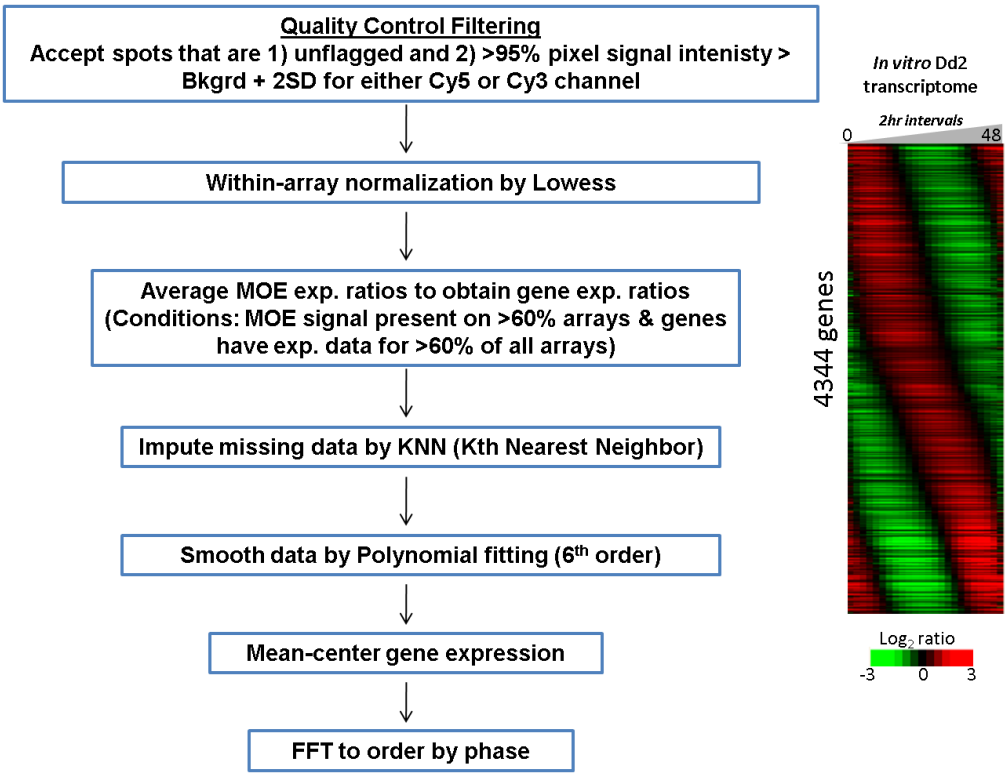

Figure 2-3. Outline of microarray data processing. Flow chart outlines the steps in processing the microarray data of the Dd2 transcriptome (24 TP arrays) to generate the reference *in vitro* transcriptome used to estimate cell stage. MOE: Molecular elements; KNN of K=10 was used.

each transcript/gene. To construct the phaseogram of reference IDC transcriptome for further comparisons, only genes with expression data in at least 19 out of 24 (80%) time points were extracted, any missing values were imputed and polynomial fit of order 6 was applied to generate smoothed data. This was then analyzed by Fast Fourier Transform method and all 4,634 genes with the mean-centered gene expression $\log_2$ ratios were sorted according to phase from $-\pi$ to π. The phaseogram of each isolate contains mean-centered gene expression data ordered according to the phase value. For each isolate's time course, only genes having at least 80% of data present were extracted and any missing data values (<20%) were imputed by KNN (K^{th} nearest neighbor) method using R version 2.10.1 package and *impute* function.

2.9.1 Mapping parasite's sample age to the reference IDC using MicroCorrel – Age Estimator of Cell Stage

For all time course experiments, the age of each isolate/clone time point sample relative to the progression of *in vitro* lab strain IDC was estimated using a best fit spearman rank correlation (SRCC) [86]. Spearman rank correlation coefficient (SRCC) values between global mRNA profiles (without data smoothing or mean-centering) for each isolate/clone time point and time points in the reference IDC transcriptome [86] (every 2 hour sample time point of the *in vitro* Dd2 lifecycle) were calculated. The stage (in terms of hours post invasion; hpi) corresponding to the peak SRCC value was assigned as the best estimate of the age of the parasite for that sample collection. This was performed automatically with a package and perl script "MicroCorrel". Only samples which had SRCC above a value of 0.35 were considered in the following analysis. To select time points for downstream differential analysis, we calculated the frequency distribution of isolate time points found within a window of three consecutive hpi and selected three windows based on the highest representation of isolates/clones with at least one sampling time point found within that window.

2.9.2 Identifying Differentially Expressed Genes of field isolates

Z scores were calculated by correlating the average gene expression to noise ratio (SNR) of the mRNA expression ratios to the ART-treatment clearance phenotype (ie. resistant - CP025, CP037, CP040 vs. sensitive – CP022, BMT061, BMT077, BMT076, XPN003, NHP2094, NHP4459, NHP4460) and normalized to sample size.

$$Z = \sqrt[3]{N} \cdot \frac{\mu_a - \mu_b}{\sigma_a + \sigma_b}$$

Where μ_a and μ_b are the mean expression $\log_2$ ratio of resistant and sensitive parasites respectively and σ_a and σ_b are the standard deviations of resistant and sensitive group respectively. Differentially expressed genes were defined with p-value cut-off < 0.01 from Student t- distribution of the z-scores carried out for the 3 stages. Gene set enrichment analysis [110] was carried out on the resistant vs. sensitive parasites using SNR. A total of 1261 gene sets comprising of KEGG pathways [111], MPMP and functional groups based on previous studies [96, 112-114] were included. Nominal p-value and False Discovery Rate (FDR) were calculated for each gene set from the observed normalized enrichment score (NES) against a null distribution using a gene set-based permutation test. Gene sets with p-value < 0.05 and FDR< 25% were considered to be statistically significant.

2.9.3 Other methods to identify differentially expressed genes

Cluster analysis was done using hierarchical average linkage clustering of genes using *Gene Cluster program version 2.11* and visualized with *TreeView version 1.60* software (http://rana.lbl.gov/EisenSoftware.htm). Further analyses were carried out using windows of time interval for each stage, standard deviations and fold-change in total relative abundance ie. "Sums" (area of each gene profile). In short, *sums* using $\log_2$ transformed values for each gene was calculated across each isolates' lifecycle and the difference in *sums* was determined by subtracting *sums* for one isolate from another for each gene. Pearson and Spearman rank correlation analysis was used to calculate the strength of associations.

2.9.4 Calculate Timing of Peak mRNA abundance of genes

The time of peak expression for each gene (represented by hpi) is derived from the phase of the Fourier transformation of the *in vitro* reference transcriptome using the

formula: $Peak\ Abundance\ Time\ (hpi) = 2 + [\frac{46(\theta+\pi)}{2\pi}]$ Where θ is the phase value of the gene.

2.9.5 Calculation of Rank Product Score

Using the z scores (see above) of each gene, we sorted the genes according to descending order and assigned a numerical rank score for every gene at each of the three stages. In order to generate a list of genes consistently up/down-regulated in the three stages, we calculate the geometric mean of the rank score to determine the rank product (RP) score of each gene using the formula:

$$RP_g = [rank_g^{14hpi} \times rank_g^{26hpi} \times rank_g^{34hpi}]/N^3$$

Where the $rank_g^{14hpi}$, $rank_g^{26hpi}$, $rank_g^{34hpi}$ corresponds to the rank score of the gene at 14 hpi, 26 hpi or 34 hpi respectively.

2.9.6 CNV analysis using Genomic Alteration Detection Analysis (GADA)

To identify significant CNVs among the 6 isolates, we performed comparative genomic hybridization using genomic DNA extracted from the isolates (CP022, CP025, CP037, CP040, BMT077, XPN003) against genomic DNA of the reference lab strain of 3D7 as previously described [115]. We carried out subtraction analysis between any 2 isolates in multiple pair-wise comparisons and considered only segments that have at least 1.7-fold change in mean amplitude and T-coefficient greater than 3.5 in minimum 2 consecutive gene probes between any 2 isolates as significant. CNV analysis of the 5 3D7 clones were carried out with the criteria that at least 1.7-fold change in mean amplitude and T-coefficient greater than 3.5 in minimum 2 consecutive gene probes between any 2 clones were observed. These

analysis were performed using the Genomic Alteration Detection Analysis (GADA) v0.8 program in R package [116].

2.10 Characterization of MRP2 Protein Expression in single clones of 3D7

2.10.1 Peptide synthesis and Polyclonal Antibody Generation in mouse

The Bcell Parker Hydrophilicity Prediction software was used to determine the best epitope for raising an antibody against the protein of interest. It was crucial that the epitope was not found within the transmembrane domains of PfMRP2 protein and would be spatially accessible for the antibody to bind. The amino acid sequence KNHTNKFHKRKKE, between positions 101th to 113th near the N-terminal of the protein was used. This 13 amino acid sequence was synthesized by Biosciences Peptide Synthesis Facility, School of Biological Sciences, Nanyang Technological University. The peptide or hapten was then covalently conjugated to a large carrier protein which helped to stimulate an immune response and generate antibodies specific for the hapten upon injection of the immunogen into the host animal. As the Keyhole limpet hemocyanin (KLH) elicits a stronger immune response than other carrier proteins like BSA and ovalbumin, it was used and conjugated to the peptide via the Imject KLH Carrier Protein and EDC Conjugation Kit (Pierce, ThermoScientific, USA). The purified mcKLH solution was mixed with the peptide hapten to create an immunogen through carboxyl and amine crosslinking (EDC Conjugation). The unreacted peptide was then separated from the immunogen by gel filtration. After mixing the immunogen (antigen) with complete adjuvant (to enhance the immunogenicity) in a 1:1 ratio, 4 individual BALB/c mice were immunized on day one (Figure 2-4). Three weeks later, the mice were injected with the 1st boost of antigen mixed with incomplete adjuvant. A week later, whole blood was collected

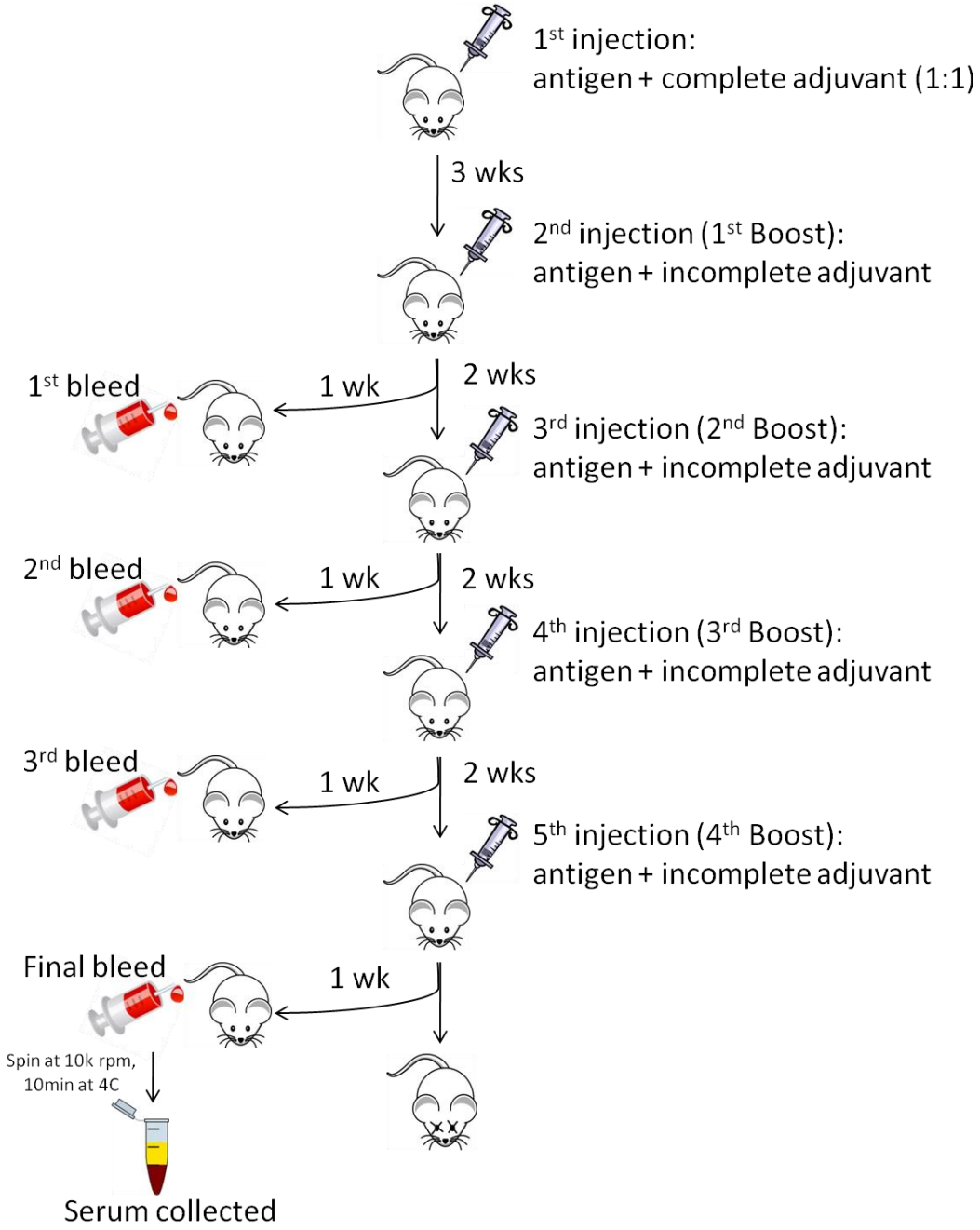

Figure 2-4. Outline of PfMRP2 antibody generation. Steps involved in immunizing mice with PfMRP2 peptide antigen and obtaining polyclonal antibodies specific for PfMRP2 protein.

from tail bleeding the mice. The mice were immunized every two weeks for a total of 4 booster jabs and always tail bled one week after the injection. A total of 4 bleeds were obtained from each mouse. The blood collected was allowed to clot on ice, then spun down at 10,000 rpm for 10 min at 4°C, and the serum was collected. Only the

serum from the final bled of the 4 mice were tested and used in all Western blot and IFA experiments. (Immunization in mouse work was performed by Huang Xi Mei, Peter Preiser's lab, SBS, NTU).

2.10.2 Harvesting of Protein samples by Saponin-lysis

To measure PfMRP2 protein expression levels between the clones 6A and 11C (showing the 2 different gene transcript profiles), 1 ml of pRBC was harvested every 6-8 hours over the 48 hour lifecycle from the highly-synchronized *in vitro* cultures of the clones (at 5-10% parasitemia) in a 50 ml falcon tube. The tube was spun at 2,500 rpm for 3 min (acc=9, brake = 2) and the supernatant was removed. 20 ml of PBS (at room temperature) was added to resuspend the RBCs and spun again. After removal of the supernatant, 10 volumes (ie. 10 ml) of freshly made 0.1% saponin in PBS was added to the pRBC, mixed gently by inverting the tube a several times, and incubated at room temperature for exactly 3 min. PBS was added to top up the mixture to 50 ml, mixed and spun at 4,500 rpm for 5 min (acc=9, brake=5). The supernatant was removed and the pellet (~50ul) was washed with 20 ml of PBS and spun at 4,500 rpm for 5 min (acc=9, brake=5). After removing the supernatant, 1 ml of PBS (pre-chilled to 4°C) was added and resuspended well and then transferred to a fresh 1.5 ml eppendorf tube. The tube was spun in a table-top centrifuge at 13,200 rpm, the supernatant was removed and the pellet was quickly flash frozen in liquid nitrogen. The pellets (~50 µl each) were stored at -80°C till ready to be used in SDS-PAGE.

2.10.3 Protein Quantification by Bradford Protein Assay (Bio-Rad, USA)

The samples were thawed by keeping the tubes in a 65°C waterbath for 1-2 min. 2 volumes (ie. 50 µl) of 2X loading buffer (containing 0.125 M Tris-HCl pH 6.8, 4% SDS, 20% glycerol and 10% beta-mercaptoethanol but without bromophenol blue)

was added to the pellet and boiled at 100°C in a heat block for 10 min to lyse the parasites. The sample was spun down for 10 min at 13,200 rpm and the supernatant containing parasite protein extract was quantified in the Bradford assay (Biorad protein assay Microassay procedure). 1 µl of the protein extract was added to 799 µl of PBS and 200 µl of dye reagent concentrate (BioRad, USA) for a total volume of 1 ml and mixed well. A standard curve was generated by making 5 BSA protein standards, S0: 0 µg protein (blank), S1: 0.5 µg protein, S2: 2.0 µg protein, S3: 3.5 µg protein and S4: 5.0 µg protein, which covers the linear range of the assay.1 µl of the 2X loading buffer was added to the tubes with the protein standards to ensure uniformity. The volume in each tube was topped up with PBS to 800 µl and 200 µl of dye reagent concentrate was added to each and mixed well. 200 µl of mixture from each tube (samples and protein standards) was transferred to a 96-well plate in duplicates and incubated at room temperature for 5 min. Absorbance readings was measured at 595 nm in a spectrophotometer for all the wells. The averaged optical density (OD) reading for blanks were subtracted from all readings of samples and "standards" (S1 to S5). A standard curve was generated by plotting the averaged OD readings for S2 to S5 against the protein concentrations (µg/ml) using and fitting a best fit line with a linear equation ($Y = aX + b$) through the points. Thus, the protein concentrations (x) in the samples were calculated from the blank subtracted OD readings of the samples (y) and multiplying by a dilution factor of 1000. The total protein yield was determined by multiplying the protein concentration (µg/ml) with the total volume of protein extract supernatant available.

2.10.4 SDS-PAGE of protein samples and Western Blotting

As PfMRP2 is a large protein of predicted 250 kDa in size, the protein samples were run on a pre-cast 4% stacking/6% resolving polyacrylamide gel. A speck of

Bromophenol blue was added to each sample and mixed for easier visualization of the loading front during the run.

To make the 6% resolving gel, 5 ml of 4X lower buffer (1.5 M Tris-Cl, pH8.8; 0.4% SDS), 3 ml of 40% Acrylamide/Bis, 12 ml of deionized water, 100 µl of 10% APS and 20 µl of TEMED was mixed in a 50 ml falcon tube and poured into 4 X 1mm gel casting plates. ~1 ml of isopropanol was added to 'straighten' the gel line. Once the gel set, the isopropanol was poured away before casting the stacking gel. To make the 4% stacking gel, 2.5 ml of 4X upper buffer (0.5 M Tris-Cl, pH6.8; 0.4% SDS), 1 ml of 40% Acrylamide/Bis, 6.5 ml of deionized water, 100 µl of 10%APS and 20 µl of TEMED was mixed in a falcon tube and poured over the resolving gel. The 15-well plastic combs were quickly placed into the stacking gel solution and ensuring no bubbles were present. When the gel was hardened, the comb was removed and the gel plates were transferred into the SDS-PAGE electrophoresis tank containing 1X SDS Electrophoresis Buffer (3.03 g Trizma-base, 14.4 g Glycine, 1 g SDS in 1 L of deionized water). Samples of equal protein amounts (25 µg) were loaded into the wells using a 10 µl pipette, along with a 250 kDa protein ladder and run at 100 V for 1-2 hr till the blue dye of the loading front reached the end of the gel. After which, the gel plates were carefully taken out of the tank and the stacking gel was removed. The resolving gel was then overlaid with a nitrocellulose membrane and tightly placed between filter papers and sponge in a cassette, which was put into a tank filled with western transfer buffer specifically for high molecular weight proteins (6 g Tris, 28.8 g Glycine, 0.1 g SDS, 200 ml Methanol and 800 ml of deionized water). The resolved protein was transferred onto the membrane at 4°C overnight at 40 V.

After the Western transfer, the membrane was rinsed with 5 ml of TBS-T buffer (20 ml of 1 M Tris-HCl, pH8.0, 8 g of NaCl, 10 ml of 10% Tween-20 in 970 ml of

deionized water) and Red Indian Dye was added to the membrane to visualize the protein bands and check if transfer was complete. Then the membrane was rinsed 3 times with TBS-T and blocking was done with 5% non-fat milk (BioRad, USA) in TBS-T on a shaker for 1 hr. The membrane was probed with PfMRP2 polyclonal mouse serum antibody in a 1:1000 dilution with 3% blocking solution for 3-4 hr on a shaker with gentle rocking and then washed 3X with TBS-T – 5 min twice and 15 min in the last wash. Anti-mouse Horseradish Peroxidase (HRP) conjugated secondary IgG antibody was added in a 1:3000 dilution to the membrane and kept on a shaker for 45 min with gentle rocking. The membrane was washed 3 times with TBS-T as before. Chemiluminescent western blotting substrate (Santa Cruz, USA) was added onto the membrane and incubated at room temperature in the dark for 5 min before the x-ray film was placed over the membrane for 5 min and then developed in the x-ray developing machine. The protein levels reflected by the intensity of the protein bands were analyzed using GS-800™ Calibrated Densitometer and the Quantity One® 1-D Analysis Software (Biorad, USA). Actin was used as the loading control for the protein samples. The membrane was washed with TBS-T and reprobed with Actin-specific antibodies the next day.

2.10.5 Immunofluorescence Assay (IFA) of MRP2 protein

To determine the cellular localization of PfMRP2 protein in the *Plasmodium* parasite, immunofluorescence assays using the four PfMRP2 serum antibodies obtained from the four mice were carried out. The iRBCs at different stages of *P. falciparum* were harvested and multiple smears were made on microscope slides and air-dried. One slide was Giemsa-stained. The rest were stored at -80°C with desiccants till ready for carrying out IFA. After thawing the slides at room temperature for 5 min, the cells were fixed in a solution of 4% paraformaldehyde and 0.0075% glutaraldehyde for 30

min at room temperature. The slides were then washed in PBS three times for 5 min each on a rocker. Next, the cells were permeabilized by incubating the slides in 0.1% Triton-X 100/PBS on a rocker for 10 min. After another three washes in PBS for 5 min each on a rocker to remove excess detergent, the slides were quenched in 0.001% Sodium Borohydride (Sigma Aldrich) three times for 15 min each. The slides were washed again three times for 5 min each. Blocking of the slide surface to prevent unspecific antibody binding was carried out in 3% BSA for 1 hr on a rocker at room temperature and the slides were washed with PBS three times for 5 min each. The cells were then incubated with 1:200 dilution of anti-PfMRP2 serum at 4°C for 16-18 hr. Alongside, cells were also incubated with the negative control of 1:200 dilution of mouse pre-immune serum. After primary antibody incubation, the slides were washed thoroughly with PBS three times for 5 min each. The next few steps were carried out in the dark as much as possible to prevent photobleaching of dyes. Incubation with secondary antibody of 1:800 dilution of Alexa Fluor® 488 or 594 goat anti-mouse monoclonal antibody was performed in the dark for 1 hr at room temperature. The slide were washed with PBS three times for 5 min each, incubated in DAPI solution for 30 s and washed with PBS for 5 min. Subsequently, the slide was air-dried and a drop of VECTASHIELD® Mounting Medium (Vector Labs, USA) was added. A cover slip was placed over the slide and the edges sealed with nail polish. Fluorescence images were immediately taken using Zeiss LSM 510 Meta confocal microscope (Carl Zeiss, Switzerland). Image processing was done using Zeiss LSM 510 software and ImageJ software v1.43.

2.11 Investigating structural polymorphisms within *pfmrp2* promoter

2.11.1 Polymerase Chain Reaction (PCR) – High Fidelity and Long-Range

PCR was carried out to amplify specific gene products using specifically-designed primers targeting the gene or region of interest and using DNA isolated from the single clones of 3D7 which showed the two different expression profiles of *pfmrp2* gene transcript. 20 primer pairs were designed for various sites within the 15 kb upstream region from the ATG translation start site of the *pfmrp2* (PFL1410c) gene. 3 additional primer pairs were designed spanning the ORF sequence of the gene.

PCR protocol for <2 kb product size

A master mix consisting of 2 µl of 10X reaction buffer (with $MgCl_2$), 0.5 µl of dNTP mix (10 mM of each dNTP), , 0.2 µl of *Taq* DNA Polymerase(5U/µl; New England Biolabs, USA) and 15.3 µl of RNase and DNase-free deionized water was made for the total number of PCR reactions carried out. 18 µl of master mix was aliquoted into 0.2 ml PCR tubes. 1 µl of each set of forward + reverse primer mix (5 µM of each primer) and 1 µl (corresponding to 15-50 ng) of template DNA was added to each tube and mixed thoroughly by pipetting. Thermocycling was carried out at 95°C for 5 min followed by 30 cycles of 95°C for 30s (DNA template denaturation step), 45°C to 55°C[1] for 40s (annealing of primers to single strand DNA template), 60°C for 1min[2] (extension step) and a final extension step at 72°C for 5 min or 10 min for colony PCR and a final hold at 4°C. To generate sufficient amounts of accurately amplified DNA for DNA sequencing, high fidelity PCR was performed using the High Fidelity DNA polymerase (Roche, Switzerland) which has reduced error rates.

[1] Annealing temperature depends on the primer size and GC content. It is 2-3C lower than the melting temperature, Tm.
[2] Extension time depends on size of DNA product. 1min is approximately required for every 1 kb size of the DNA product.

PCR protocol for >2 kb product size

Long-range PCR using the Expand Long Template PCR system 3 (Roche, Switzerland) was used to generate DNA products larger than 2 kb and up to 15 kb.

A master mix consisting of 2 µl of 10X Expand Long Template buffer 3 (with $MgCl_2$), 1 µl of dNTP mix (10 mM of each dNTP), 0.3 µl of Expand Enzyme Mix (5U/µl; Roche) and 14.5 µl of RNase and DNase-free deionized water was made for the total number of PCR reactions carried out. 17.8 µl of master mix was aliquoted into 0.2 ml PCR tubes. 1.2 µl of each set of forward + reverse primer mix (5 µM of each primer) and 1 µl (corresponding to 15-50 ng) of template DNA was added to each tube and mixed thoroughly by pipetting. Thermocycling was carried out at 94°C for 5 min (initial denaturation) followed by 10 cycles of 94°C for 30s (denaturation step), 50°C to 55°C[3] for 40s (annealing step), 60°C for 10min[4] (elongation step) and 20 cycles of 94°C for 30s (denaturation step), 50°C to 55°C[5] for 40s (annealing step), 60°C for 10min[6] with +20s elongation time for each successive cycle (elongation step) a final elongation step at 72°C for 10 min. The list of all primer sequences designed is in Chapter 9: Appendix Table 1. The PCR products were analyzed by agarose gel electrophoresis of a 5 µl aliquot from the total reaction. Generally, 1% agarose TAE gel was used for products less than 2kb and 0.7% gel was used for products greater than 2 kb in size. The products were visualized by UV transillumination of the ethidium bromide-stained gel. For DNA sequencing reactions, the PCR products were then further purified using the PCR gel extraction kit (Qiagen, USA).

[3] Annealing temperature depends on the primer size and GC content. It is 2-3C lower than the melting temperature, Tm.
[4] Extension time depends on size of DNA product. 1min is approximately required for every 1 kb size of the DNA product.
[5] Annealing temperature depends on the primer size and GC content. It is 2-3C lower than the melting temperature, Tm.
[6] Extension time depends on size of DNA product. 1min is approximately required for every 1 kb size of the DNA product.

2.11.2 Agarose gel electrophoresis

1% agarose gel was freshly made to run the samples. Briefly, 1 g of agarose powder was added to 100 ml of 1X TAE buffer and boiled in a microwave oven for 1 min to dissolve the powder. When the mixture had cooled to 50°C, 3 µl of ethidium bromide solution was added and mixed by swirling. The mixture was poured into a plastic tray with a 25-well comb and sit at room temperature for at least 30 min to set the gel. The comb was removed and the samples pre-mixed with 6X loading dye in a 5:1 ratio were loaded into the wells. After running the samples, the gel was placed in UV transilluminator equipment and exposed to UV to visualize the bands.

2.11.3 Purification of PCR products from agarose gel extraction (Qiagen, USA) and DNA sequencing

The gel fragment containing the band of interest was cut out with a sterile razor blade under UV light and weighed in a 1.5 ml eppendorf tube. The gel pieces were mixed with 3 gel volumes of QG buffer and incubated at 50°C in a heat block for 15 min to dissolve the gel. Next, 1 gel volume of isopropanol was added and the mixture was transferred to a MinElute spin column and spun for 1 min at 13,200 rpm. The flow through was discarded. 500 µl of QG buffer was added to the column and spun again. The flow through was discarded. To wash the column, 750 µl of PE buffer was added and spun as before. The flow through was discarded and the column spun once more to dryness. The column was placed in a fresh 1.5 ml eppendorf tube and 10 µl of EB buffer was added to the column to elute the DNA. After 2 min, it was spun for 1 min at 13,200 rpm. The purified PCR products along with the relevant primers were sent for DNA sequencing using BigDye® Terminator v3.1 cycle sequencing method (1st BASE, Singapore). The sequencing results were analyzed by BLAST search to the

3D7 genome (PlasmoDB database) and multiple sequence alignment using BioEdit Sequence Alignment Editor software V7.9.0 [117].

2.11.4 Restriction enzyme digestion of PCR products and Ligation of digested fragments into vector

2 different plasmid vectors: pPf86-5'UTR-WTmrp2-FL and pPf86-5'UTR-MTmrp2-FL were generated. PCR of the 2 kb upstream sequence of PFL1410c (*pfmrp2*) gene using clone 11C and 6A genomic DNA was carried out to obtain the constructs together with the *Xho*I and *Nco*I restriction sites. The Pf86 plasmid and the insert constructs were digested separately with restriction enzymes *Xho*I and *Nco*I. The digested construct (Mutant and Wild type *pfmrp2* promoters) were then added to each tube of digested PF86 plasmid and mixed well for the ligation step. Hence, the 5' hsp86 promoter in the plasmid was replaced with the mrp2 promoter, controlling the luciferin gene expression.

2.11.5 Transformation of plasmid DNA into E. coli

The E. coli competent cells (-80°C) were thawed on ice and incubated at 42°C on a heat block for 2 min. 1 µl of plasmid DNA (~100 ng) was mixed with 100 µl of competent cells. A negative control of water replacing plasmid was set up. The tubes were kept on ice for 20-30 min and then heat shocked by placing tubes on 42°C heat block for 60-90s. The tubes were placed on ice for 5 min to reduce damage to cells. 1 ml LB (Luria-Bertani) broth (without antibiotics) was added and mixed. The tubes were agitated at 220 rpm for 40 min to 1 hr at 37°C. After the tubes were spun at 13,200 rpm for 1min, the supernatant was removed. The pellet was resuspended in 100 µl of LB and spread onto LB agar plates with the following conditions: A) LB agar plain: untransformed competent cells (test competent cells r ok!) B) LB agar +

Ampicillin: untransformed competent cells (negative control) C) LB agar + Ampicillin: competent cells + original Pf86 plasmid (positive control) D) LB agar + Ampicillin: competent cells + Pf86 plasmid/insert (100ng). The plates were incubated overnight at 37°C for less than 16 hr. The plates were checked the next day and it was observed that conditions: A) a lot of colonies, B) no colony, C) some colonies and D) some colonies. The plates were sealed with parafilm and kept at 4°C. The competency of cells were calculated based on Competency of cells = no. of colonies/amount of plasmid DNA (µg). A total of 10 colonies were each placed into 5 ml LB broth (with 100 µg/ml Amp) in 50 ml tube and incubated at 37°C with shaking at 220 rpm for 16 hr. Next day, 1 ml culture was stored at 4°C as stock. The remaining 4 ml of culture was screened for inserts in the plasmid.

2.11.6 Plasmid extraction and purification (Miniprep and Maxiprep)

The plasmid DNA was extracted using QIAprep Spin Miniprep kit (Qiagen, USA) from the E. coli culture as this kit can purify up to 20 µg of high-copy plasmid DNA from up to 5 ml cultures of E. coli in LB medium The 4 ml overnight E. coli culture was split into 2 tubes and spun down to remove supernatant The E. coli cell pellet was thoroughly resuspended in 250 µl of Buffer P1and transferred to a microcentrifuge tube.250 µl of Buffer P2 was added and mixed by gentle inversion 4-6 times. 350 µl of Buffer N3 was added and immediately mixed by gentle inversion of the tube 4–6 times. The tube was spun at 13,200 rpm for 10 min, resulting in a white pellet. The supernatant was transferred to the QIAprep spin column by pipetting. The column was spun at 13,200 rpm for 1 min and the flow through was discarded. 0.5 ml of Buffer PB was added to wash the column and spun again for 1 min. The QIAprep spin column was then washed by adding 750 µl of Buffer PE and spun twice at 13,200 rpm for 1 min to remove residual wash buffer. The column was transferred to a clean 1.5

ml eppendorf tube and the DNA was eluted by adding 50 µl of water to the center of the column, let stand for 5 min, and centrifuged for 1 min at 13,200 rpm.

The plasmid DNA concentration was measured on Nanodrop spectrophotometer and stored at -20°C until it was used in restriction enzyme digestion, products ran on a gel and purified using Qiagen Gel extraction kit (see Section 2.11.3) and 1 µg of the digested fragments was sent for DNA sequencing. Only for products with good sequencing result, the 1 ml stock (stored at 4°C) was added to 2 L of LB media (with 100 µg/ml Ampicillin) and grown overnight at 37°C on a 220 rpm shaker. Plasmid extraction was carried out using the Plasmid Maxi-prep kit (Qiagen, USA) to obtain a larger amount of plasmid (up to 500 µg). The culture broth was transferred into 50 ml falcon tubes and spun for 15 min at 6,000 rpm at 4°C. After pouring off the supernatant the pellet was resuspended in 10 ml of Buffer P1 and mixed well. 10 ml of Buffer P2 was added, mixed well by gentle inversion 4-6 times and kept at room temperature for 5 min. 10 ml of chilled Buffer P3 was then added, mixed immediately by gentle inversion and kept on ice for 20 min. The tube was spun at 6,000 rpm at 4°C for 30 min. Meanwhile, the Qiagen-tip column was equilibrated by adding 10 ml of Buffer QBT and allowing the solution to drain through the column by gravity. The supernatant from the cell lysis was decanted into 50 ml tubes twice. Following which, the supernatant was added to the Qiagen -tip column and allowed to flow through by gravity. The column was washed twice with 30 ml of Buffer QC. Finally the DNA was eluted into a clean, fresh 50 ml falcon tube by adding 15 ml of Buffer QF into the column twice. The DNA was precipitated with 10.5 ml of isopropanol and spun at 12,000 rpm for 30 min at 4°C. The supernatant was removed and the DNA pellet was washed with 5 ml of 70% ethanol. The tube was spun at 12,000 rpm for 10 min at 4°C and the supernatant was discarded. The pellet was air-dried for 5-10 min and

resuspended in 500 µl of deionized water. The DNA was then verified to be correct size by restriction digestion and running the digested products on a 1% agarose gel.

2.11.7 Transient transfection of *P. falciparum* parasites with Firefly and Renilla Luciferase vectors containing the mrp2 promoter

Highly synchronized 3D7 parasites of 10-15% parasitemia of early rings (<6 hpi) were used for transient transfection by electroporation. The culture media was changed 2-3 hr before the transfection experiment. A total of 4 transfections were set up for each plasmid DNA type: 1) pPf86-5'UTR-MTmrp2-FL (Mutant MRP2 insert/Pf86 plasmid), 2) pPf86-5'UTR-WTmrp2-FL (Wild type MRP2 insert/Pf86 plasmid), 3) Pf86 plasmid (positive control) and 4) No plasmid (negative control) in order to monitor luciferase activity in each stage (ring/trophozoite/schizont) of the IDC. All parasite samples were also transfected with 50 µg of Renilla plasmid each, which was used as reference for normalizing firefly luciferase activity so as to reduce differences caused by transfection efficiency.

100 µg of total plasmid DNA (50 µg FL vector and 50 µg RL vector), in 100 µl volume, was dissolved in 300 µl of 2X Cytomix solution. 250 µl of washed uninfected pRBC in 48 ml of media were prepared in 175cm3 flasks, gassed and kept in 37°C incubator. 250 µl of infected pRBC (10-15% early rings) was mixed with 400 µl of DNA/2X cytomix solution in 1.5 ml eppendorf tube and transferred to a pre-chilled (4°C) 0.2 cm cuvette. The mixture was electroporated at 0.31 KV and 950 uF using the BioRad gene pulsar. The time constants and voltage were recorded. After the pulse, 2 ml of media was immediately added to it, mixed and transferred to the 175 cm^3 flask containing the CMM of total 50 ml (1% hematocrit). The transfected parasite cultures from the 4 flasks for each type of plasmid DNA was mixed together

and split to reduce any variability in transfection efficiency. The flasks were gassed and kept at 37°C in incubator. After 2-3 hr, the media was replaced for each flask.

2.11.8 Screening of Luciferase activity

The cells were harvested at each of the 3 stages: rings, trophozoites and schizonts and screened for level of luciferase activity for cells transfected with 1) either insert/Pf86 plasmid (target of interest), 2) the original Pf86 plasmid (positive control), 3) without plasmid (negative control) and against the reference renilla luciferase plasmid. The Dual Luciferase Reporter Assay system (Promega,. USA) was used as it can determine both firefly (target expression) and renilla (reference expression) luciferase activity from luciferin protein simultaneously from the same transfected sample. The stage of parasite was checked by Giemsa stained smears. At the time of harvest, the cells were spun at 1,500 rpm for 5 min (acc=9, brake= 2) and the supernatant was removed. 1 ml of freshly made 0.15% saponin was added to the pRBC pellet to lyse the RBCs, mixed well and kept on ice for 10 min. The pellet was washed with 5 ml of PBS, spun at 2,800 rpm for 5 min and the supernatant removed. The pellet was washed once more with PBS to remove any traces of ghost RBCs. The resulting pellet was resuspended with 1 ml of PBS and transferred into 1.5 ml eppendorf tubes. After spinning at 2,800 rpm for 5 min the supernatant was removed and 100 µl of lysis reagent (1X Passive Lysis Buffer, Promega, USA) was added and vortexed thoroughly. The mixture kept for 10 min on ice with vortexing at 3 min intervals to lyse the parasites. The tube was spun at 13,200 rpm for 1 min. The following steps were carried out in the dark. 80 µl of cell lysate was added to a tube of 100 µl LAR II aliquot (Promega, USA), and mixed by pipetting up and down exactly 3 times. The firefly luciferase activity was immediately measured twice using a luminometer (GloMax-Multi Jr, Promega, USA). 100 µl of Stop and Glow reagent (Renilla

Luciferase assay reagent, Promega, USA) was added and mixed well by pipetting 5 times. The renilla luciferase reading was again immediately taken twice. The transfection experiment was carried out in triplicates across different cell generations and the averaged luciferase activities were determined. The LUC readings for the negative control (without plasmid) were taken as the background LUC levels. Firefly LUC activity was measured in relative light units (RLUs) and the normalized LUC was calculated by the following formulas.

$FLuc_{(normalized\ to\ RLuc)}$ = (Actual FLuc – Background FLuc) / (Actual RLuc - Background RLuc)

where FLuc is Firefly Luciferase and RLuc is Renilla Luciferase activity

$FLuc_{(normalized\ to\ Pf86\ FLuc)}$ = 100% x [$FLuc_{(normalized\ to\ RLuc)}$ of Insert of interest / $FLuc_{(normalized\ to\ RLuc)}$ of Positive control Pf86 plasmid]

2.12 Genotyping of *msp1, msp2* and *glurp* to differentiate *P. falciparum* strains

To confirm and validate the identities of parental 3D7 and single clones of 3D7 as being of 3D7 origin, as well as identifying clonal populations within field isolates, the standard method of genotyping using the highly polymorphic surface antigens genes *msp1* (merozoite surface protein 1), *msp2* (merozoite surface protein 2) and *glurp* (glutamate rich protein) by nested PCR was carried out as previously described [118, 119]. The chloroquine-sensitive lab clone 3D7 was previously cloned from the NF54 isolate which had been sampled in the 1970s from an individual living near Schipol Airport, Amsterdam, The Netherlands and adapted to *in vitro* culture conditions [105, 120-122]. The isolate's origin is unknown although it is thought to be likely African in origin. However, it is known that 3D7 clone harbors the K1-type *msp1* allele and the 3D7-type *msp2* allele. In the first round of PCR, one reaction each for *msp1*

(primer set M1–OF/M1–OR), *msp2* (M2-OF/M2-OR) and *glurp* (G-OF/G-OR) were performed using sequence-specific primers to conserved sequences and template gDNA. In the secondary nested PCR, a single semi-nested PCR reaction for *glurp* RII repeat region (G-NF/G-OR), 3 reactions for *msp1* block 2 (M1–KF/M1–KR; M1–MF/M1–MR; M1–RF/M1–RR) to distinguish the K1, MAD20 and RO33 allelic families and 2 reactions for *msp2* block 3 (M2–FCF/M2–FCR; M2–ICF/M2–ICR) to distinguish FC27 and 3D7/IC allelic families were carried out using the reaction mix of the primary reaction as the template. The primer sequences used are listed in the table in Section 9: Appendix.

To carry out the primary PCR reaction, reaction mixtures of 1X buffer, $MgCl_2$ (1.5 mM final concentration), dNTP (125 μM final concentration), primer sets (250 nM final concentration), 0.4U of *Taq* DNA polymerase and deionized water to make up the total volume to 20 μl were set up in each 0.2 ml PCR tube. 1 μl of gDNA template (isolated from each clone/field isolate) was added to each tube. Negative controls of water substituting for DNA template were included. The PCR reaction was ran in a thermal cycler with the following steps: 95°C for 5 min, 25 cycles (Primary reaction) or 30 cycles (Nested reaction) of 94°C for 1 min (Denaturation), X°C for 2 min (Annealing) and 72°C for 2 min (Extension), followed by X°C for 2 min (Final annealing) and 72°C for 5 min (Final extension) and hold at 4°C. X is the annealing temperature used for each individual primer set as stated in the table in Chapter 9: Appendix. After the first amplification reaction was completed, 1 μl from the reaction tube was added to the prepared second amplification reaction tube containing the 50 μl reaction mix (same components as first PCR mix except primer sets and template DNA) and appropriate primer set. The PCR was run with the same cycling

parameters.15 µl of sample from each tube was ran on a 2.5% agarose gel and visualized in a UV transilluminator.

2.12.2 Sequencing of *pfmdr1* and *pfdhps* genes of field isolates

Nested PCR reactions were performed as previously described [123] to generate fragments of *mdr1* and *dhps* genes containing commonly found SNPs and products were sequenced with corresponding forward and reverse primers using ABI Big Dye Terminator cycle sequencing method.

2.13 Quantitative Real-time PCR

qRT-PCR was carried out to validate the microarray expression ratios for several genes using gene-specific primers designed. Real time PCR and the relative quantification of gene expression was performed in at least triplicates using the comparative CT method of calculating -ΔΔCt values and taking PFC0965w as a reference control gene, as previously described [108]. The DNA products ranged between 200-500 bp in size. 1 µl of DNA template (10-15 ng/µl) was pipetted into each well of the 96-well plate (Roche, Switzerland). Next, 2 µl of Forward + Reverse primer mix (5 µM of each primer) was pipetted into the well. A master mix of 7 µl of DNase and RNase free deionized water and 10 µl of 2X SYBR Green PCR Mix (Roche, Switzerland) per reaction was made accounting for the number of reactions to be run. 17 µl of this master mix was added to each well and the reaction mixture was mixed thoroughly by pipetting. The plate was sealed and spun down at 1000 rpm for 3 min to remove any bubbles in the wells. Negative controls with the DNA template substituted for deionized water was included to verify the absence of primer-dimer amplification and unspecific DNA contamination. The reactions were run with the following thermal cycling parameters: 50°C for 2 min (Hot start incubation), 94°C for

5 min (*Taq* Activation), 40 cycles of 95°C for 30s (Denaturation), 50-55°C for 40s (Annealing), 60°C for 50s (Extension and detection). The dissociation and melting curves were also measured.

To ensure that there was no unspecific amplification of secondary DNA products, 5-8 µl of the PCR product was run on a 1.5% agarose gel and a single band corresponding to the expected size of the DNA product was observed. The melting curves also showed a single peak for a single DNA product.

Chapter 3 : Genome-wide transcriptional variation in *P. falciparum* clones and during adaptation to *in vitro* culture conditions

3.1 Introduction

Clonally variant gene expression in *Plasmodium*

The most well-known gene family in *P. falciparum* showing clonally variant expression is the family of variant surface antigens, comprising of *var*, *rif* and *stevor* genes [124], which are highly polymorphic genes belonging to large multi-gene families and involved in mediating host-parasite interactions. There are a total of 60 *var*, 152 *rif* and 30 *stevor* genes identified so far in the 3D7 strain of *P. falciparum*. Most of the *vars* are found at the telomeric and sub-telomeric ends of the chromosomes (ups A and ups B) and the rest at centromeric regions (ups C) ([125], with 2 intermediate groups (B/A) and (B/C) classified [125, 126]. *var* genes are important to the parasite's survival as the *P. falciparum* erythrocyte membrane protein (PfEMP1) expressed on the surface of the iRBC is necessary for the cytoadhesion of the parasite-infected red blood cell to the host cell receptors in the microvasculature, thereby allowing the parasite to escape clearance by the spleen. By having 60 members and a single parasite expressing only 1 member per generation (based on the mutual exclusion theory), the 3D7 parasite is able to switch expression of its dominant *var*, thus enabling it to escape acquired host immune responses and remain in the blood circulation.

Transcriptional variation of non-VSA genes between parasites

Several studies have investigated variation in transcriptional levels between isogenic clones selected for various adhesive phenotypes [127, 128] and found that besides changes in variant surface antigen (VSA) gene expression for these cytoadherent

phenotype, there was also variation in the transcription of other non-VSA genes. 377 genes, representing 6.9% of the genome, and whose functionalities range from merozoite invasion, host cell remodeling and protein export (Maurer's cleft associated proteins), fatty acid metabolism, mitochondrial transporters, and protein kinases was found to vary by more than 3-fold change between rosetting and non-rosetting isogenic clones in a stage-specific manner [127]. Another study which compared the transcriptome of 2 isogenic clones, rosetting versus CD36-adhesive 3D7 parasites, observed that 262 genes (4.9% of genome) were differentially expressed by more than 2 fold in ring, trophozoites and schizont stages [128]. Of which, 6 genes were most highly differentially expressed by more than 5-fold and encode for invasion related such as *gbph2* (glycophorin-binding protein family), gbp-related antigen, regulators of cell cycle (histone deacetylase 1 protein; *hdac*) and DNA/RNA processing (*sera-5*, RNA-methylase). Genes belonging to the multi-gene family of *phist-a* (*Plasmodium* helical interspersed subtelomeric family) coding for exported proteins also displayed clonal variation [128]. A recent study which investigated transcriptional variation among isogenic lab lines found that transcriptional heterogeneity occurs in lab clones despite growing under similar *in vitro* conditions [129]. A total of 176 genes (~3.3%) were transcribed differently between single clones independent of genetic differences (specifically copy number variation). Furthermore, the findings showed that no two single parasite lines analyzed were identical in transcriptional levels. Genes which are transcribed differently between single parasite lines include those involved in immune evasion (PfEMP1 proteins), lipid metabolism (*pfacs*), protein folding, erythrocyte remodeling (exportome: *phist, hyp, gbp*), transcriptional regulation (containing ApiAP2 domains), transmission-related and merozoite invasion (*eba-140*). However,

var gene expression of these clones was not determined and no verification that single clones were derived.

Epigenetic regulation of transcription in *P. falciparum*

What controls clonal variation and causes variegated gene expression in the parasite in the absence of any genetic differences? From studies on *in vitro* cultured parasites, it has been shown that epigenetic plasticity can contribute to the observed variation in expression levels of invasion genes such as *rh4, eba-140, clag3.2* and clag3*.1* [129-133]. Post-translational modifications of histones can modify the chromatin structure and compactness, hence leading to changes in the accessibility of transcription factors to the promoters of genes on the DNA strand. The presence of histone modification marks such as histone 3 lysine 9 trimethylation (H3K9me3), histone 3 lysine 4 di- and tri-methylation (H3K4me2, H3K4me3) have been found to be highly associated with clonally variant surface antigens of *var*, *rif* and *stevor* families, along with several other gene families including *pfmc-2tm*, *clag*, *pfacs*, *surfins* and other exported protein families such as *hyp*, *dnaj*, *gbp130*, and *phist* genes by chromatin immunoprecipitation (ChIP) on chip approaches [131, 134]. While genetic loci having the heterochromatic H3K9me3 marks are linked to gene silencing specifically of VSA genes, acetylation of this same lysine on histone 3 (H3K9ac) correlates positively with the genome-wide transcription state [135]. The *var* gene family is most well-studied in terms of transcriptional control and regulation. Not only are broad ranged epigenetic mechanisms involved, but other factors such as promoters at the individual gene levels are also required for the regulation of transcription of a single *var* member in the allelic exclusion mechanism. Besides having H3K4me3 and H3K9ac epigenetic marks present in the promoter of the active *var* gene [136], the *cis* promoter element of the active *var* gene has to be activated for its expression [137, 138]. At the same

time to maintain the silencing in all other members of the *var* gene family, each individual *var* gene intron has to associate with the upstream *var* promoter [139, 140], along with gene silencing by a histone deacetylase, PfSIR2 [141]. The presence of the *var* gene intron also allows for the *var* gene to be retained at distinct perinuclear sites [142]. Expression of the active *var* gene is mediated by the sub-nuclear repositioning of telomeric clusters so that when a *var* gene is relocated from these transcriptionally silent sites to a transcriptionally permissible euchromatic site on the nuclear periphery via filamentous actin, active gene expression then occurs [142, 143]. Another epigenetic marker controlling active *var* gene expression is the occupancy of PfH2A.Z on the active *var* gene promoter, and absence on silent *var* genes found within the subtelomeric heterochromatin sites [144]. Recently it is reported that the epigenetic mark of H3K4me3 is likely established on the promoter of the active *var* gene by a methyltransferase, PfSET10 [145] and thus maintains the transcriptionally permissive chromatin environment of the active *var* promoter. The *P. falciparum* heterochromatin protein 1 (PfHP1) has been shown to be physically associated with H3K9me3 heterochromatin clusters at the sub-telomeric ends of chromosomes and associates with the clonally variant genes of *var, rif* and *stevor* multi-gene families along with 177 other genes [146, 147]. Although expression of *var* gene is highly linked to epigenetic factors, there is no study carried out that gives direct evidence of histone modifications contributing to differential expression of genes other than VSAs and invasion-related functionalities between clones. In the study by Rovira-Graells et al (2012), epigenetic plasticity is concluded to be the factor behind transcriptional variation in clones as the clones are assumed to be genetically homogenous based on looking at gene copy number polymorphisms and without considering nucleotide polymorphisms. We cannot exclude the possibility that *cis*-acting elements such as

SNPs or structural polymorphisms present in the non-coding regulatory region of the genome have a role in regulating transcriptional levels or pattern of expression either directly changing the expression of the gene downstream or modifying the expression of primary cell cycle regulators that act as *trans*-acting factors which may in turn affect other genes.

Transcriptional variation in the adaptation of an isolate to *in vitro* culture

Despite the fact that quite a number of transcriptional profiling studies on *P. falciparum* have so far been carried out, these have been limited to stage-specific profiling of *in vitro Plasmodium* cultures [96, 113, 148-150], profiling of the effect of drug exposure [151-155], association with clinical response [103, 156], field isolates [99, 115, 157] or association with *in vitro* phenotypes such as cytoadherence [127, 128]. Till date, studies on adaptation of a field isolate to *in vitro* culture conditions are very few and focused largely on *var* gene expression levels and antigenic switching during the adaptation process [158-160]. Little is known with regards to genome-wide transcriptional changes that occur during the course of adaptation and if culture adaptation has an impact on the parasite's transcriptional profile over time. A disproportionately large number of studies on *P. falciparum* transcriptomics involves long-term culture adapted clones rather than fresh isolates often because of the difficulty in obtaining such samples or the limitation of small sample amounts. Hence, gene expression changes, if any, as a consequence of the culture adaptation process may confound the results of previous comparative transcriptomics studies.

Challenges in analysis of transcription variation in *Plasmodium*

The major challenges in measuring transcriptional differences of *in vitro* cultures and especially field isolates stem from the highly periodic nature of gene expression,

variability in field isolate progression rates and changes in synchronicity over time. These lead to difficulty in separating true differential expression from cell-cycle dependent expression and false positives arising [101]. Hence, in the analysis of transcriptomes, estimation of cell cycle progression is necessary prior to downstream determination of transcriptional variability between cell lines.

To address these issues, our goal was to use microarrays to investigate genome-wide transcriptional variation among parasite lines and to incorporate estimation of parasite age in the analysis of differential expression. The first part of the study encompasses identifying differentially expressed genes between single clones of *P. falciparum* 3D7 strain over the intraerythrocytic cycle. To verify that clones were indeed single clones, we looked at expression of *var* gene family in each of the clones and explored the expression of other known clonally variant gene family of *rif* and *stevor*. Alongside, we carried out comparative genomic hybridizations to ascertain gene copy number changes within these single clones. In the second part of the study, we aimed to investigate whether differential expression of genes occurs during the process of culture adaptation. In addition, we wanted to determine whether the transcriptional changes that occur during culture adaptation of any field isolate consistently involved the same sets of genes or same functional groups as this would suggest the importance of such genes in the parasite's ability to adapt to fluctuating environments. Hence, using 2 isolates from Thailand, we investigated the transcriptional changes between an isolate freshly obtained from a patient and of that same isolate following short-term culture adaptation over 30 generations. Lastly, the diversity in transcription levels of single clones and changes in gene expression upon short-term culture adaptation was compared.

3.2 Results

To investigate the effect of long term culture adaptation on *P. falciparum* field isolates, two Thai isolates, MS6 and MS9 were taken from an infected patient and culture adapted to *in vitro* growth conditions. The parasites obtained directly from infected patients' blood are highly (>90%) synchronous early/mid ring stage due to the fact that later asexual stages cytoadhere to the microvasculature and are not in circulation. Hence, except for the *ex vivo* culture at generation 0, the cultures were synchronized at least twice before the harvest cycle to reduce any transcriptional differences due to population staging effects. The parasites were harvested at generations 0 (*ex vivo*), 14 and 30 at 6 hour intervals and a total of 8 time points across the 48 hour IDC were collected for each generation (Figure 3-1). To investigate differences in global gene expression levels between single clones, a total of 23 single clones were derived from 3D7 strain using limiting dilution method. Five healthy growing clones were grown continuously in culture with tight synchronizations and harvested regularly every 8 hours over the 48 hour IDC at the 15^{th}- 20^{th} generation (Figure 3-1B), shortly after the limiting dilution procedure was carried out to ensure that the clones remained homogenous in population. Microarray hybridizations were then carried out of these samples against the same reference pool and analyzed for transcriptional differences.

3.2.1 Genotyping of the 3D7 single clones by *msp1* and *msp2* genes

Genotyping by *msp1* and *msp2* of the clones was first carried out after limiting dilution experiment to verify that the clones were of 3D7 origin. Only DNA products of ~250 base pairs (bp) for the K1 primers were observed from the nested PCR

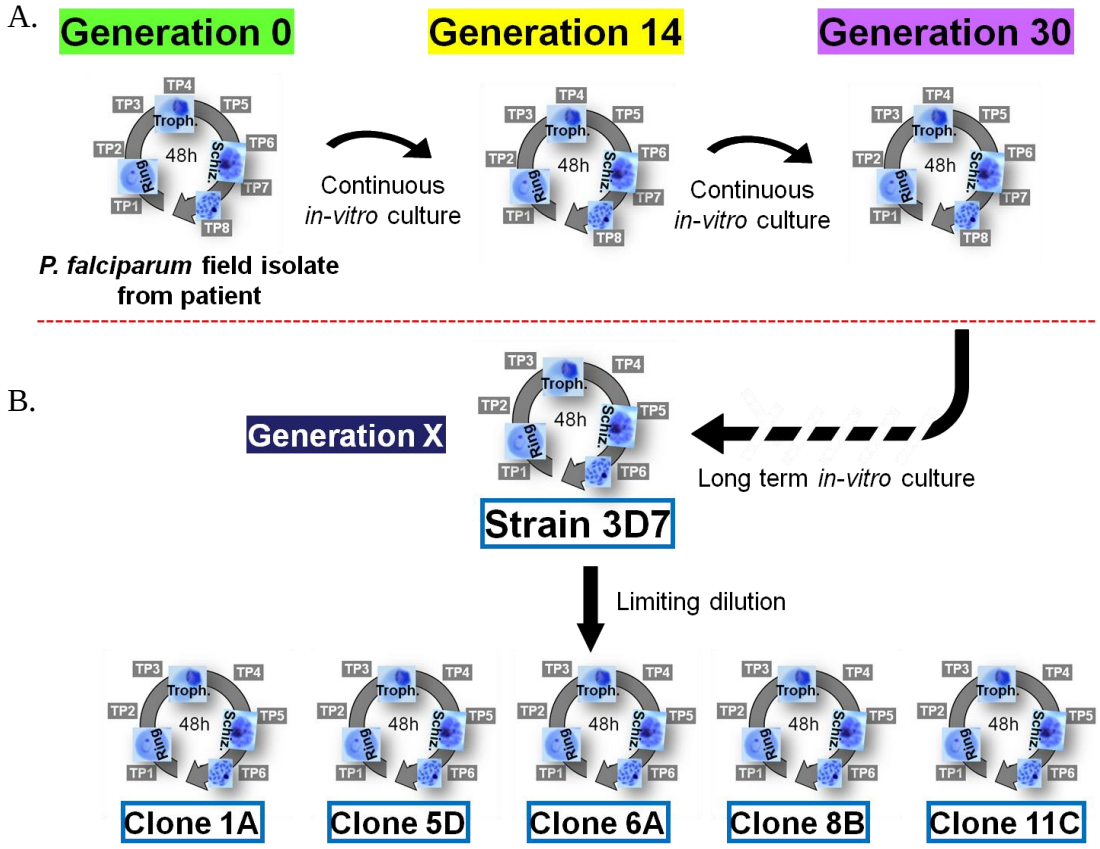

Figure 3-1. Schematic of experiment in investigation of transcriptional variation. Outline of experimental study looking at transcriptional changes during culture adaptation of a field isolate taken fresh from a patient (A) and at transcriptional variation among single clones derived by limiting dilution from the long-term culture adapted 3D7 strain (B). To generate each transcriptome, parasites were harvested from highly synchronized cultures at 6 or 8 hr regular intervals across 48 hr representing the time of development across the IDC and hybridized against a common 3D7 reference pool to allow for direct comparisons of transcriptional levels between time point samples.

reactions and no PCR product was obtained with primers for MAD20 and RO33 allelic families for all 5 clones along with the parent 3D7 as expected for the 3D7 strain (Figure 3-2). In addition, the msp2 nested PCR reaction gave identical bands of ~300 bp size for only the 3D7/IC allelic block for all the 5 clones and parent 3D7 (Figure 3-2). Thus, confirming that the clones are indeed of 3D7 origin.

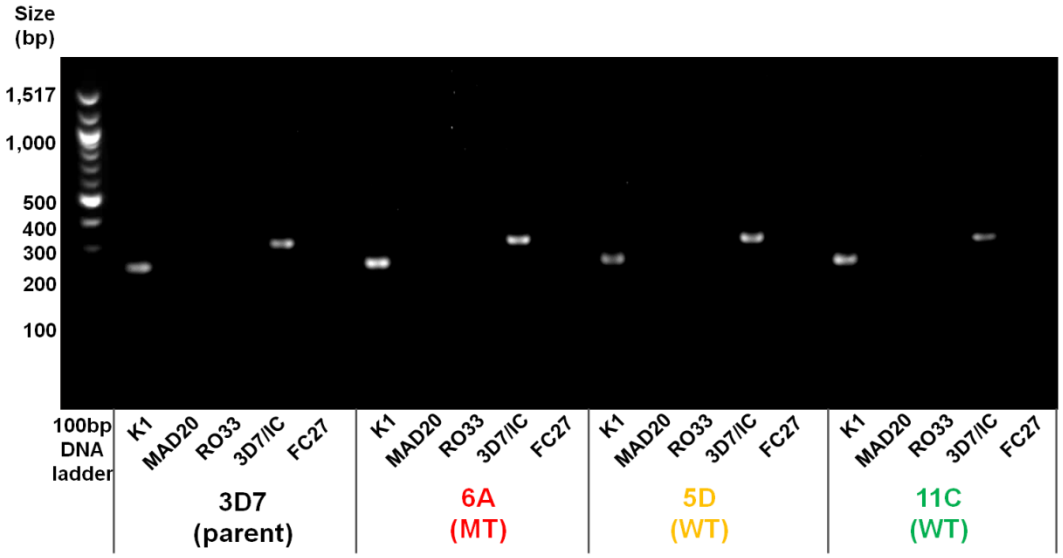

Figure 3-2. Genotyping result of the five 3D7 clones. 5µl of PCR product from genotyping reactions for parent 3D7 and clones 6A, 11C and 5D ran on a 2% agarose gel.

3.2.2 Investigation of global transcriptional differences between 3D7 clones and during culture adaptation

In the background of periodic gene expression of *Plasmodium*, differential gene expression may involve parasites expressing increased level of a gene at any particular stage(s) of the IDC or constitutively throughout the IDC, resulting in higher basal level of transcripts. Parasites may also change their timing of gene expression, represented by a shift in the peak timing of expression by a fraction of the cycle which we demonstrate in Chapter 5. In this section, we identified genes that showed a difference in either level of expression stage-wise or in terms of overall level of expression among the single clones of a culture-adapted strain 3D7 (i) or during the course of culture adaptation of a fresh isolate from a patient (ii) (Figure 3-3). For all analyses, genes coding for rRNAs were removed and genes belonging to variant surface antigen family (*var*, *rif*, *stevor*) were analyzed separately (Section 3.2.8).

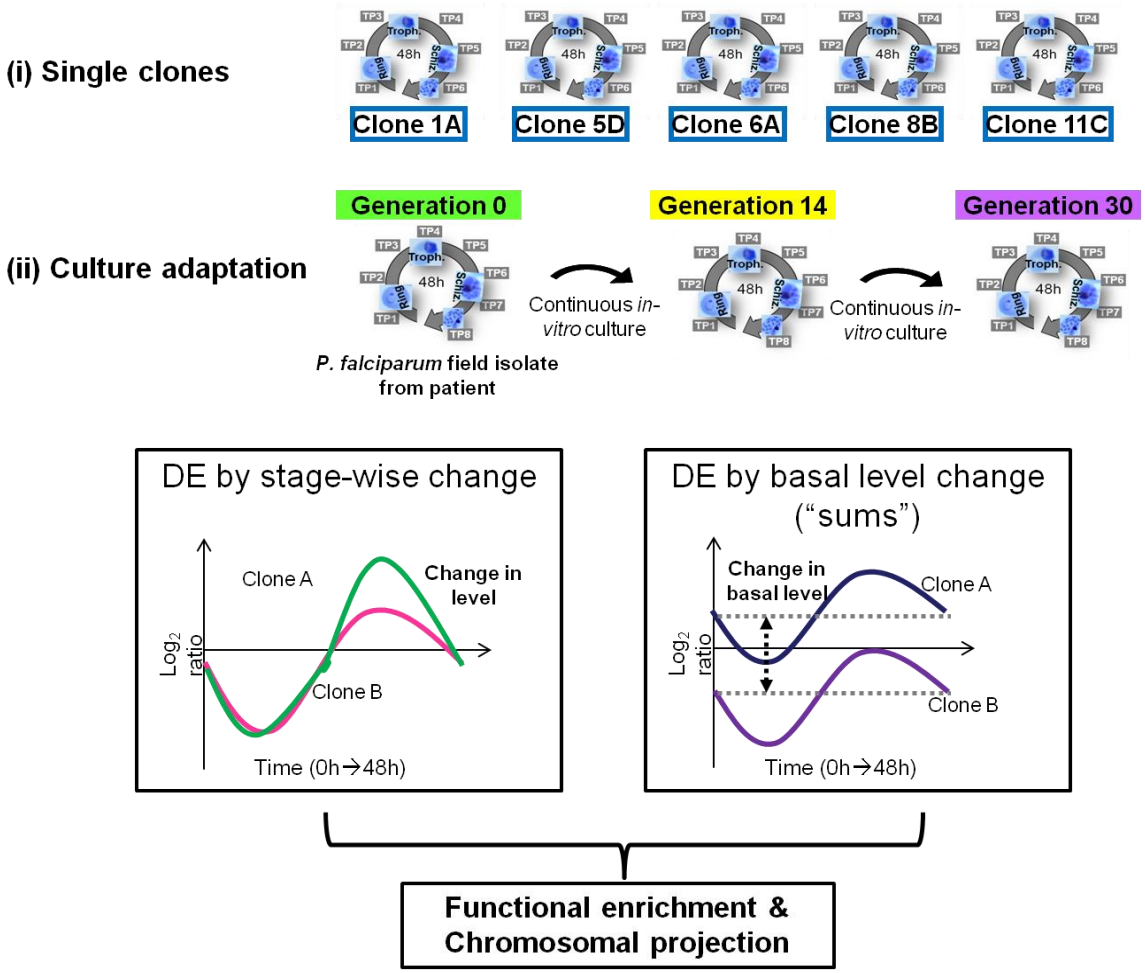

Figure 3-3. Analysis approaches for detecting transcriptional changes. Outline of analysis approach used to identify transcriptional changes between single 3D7 clones and between isolates during culture adaptation from host to *in vitro* conditions. Differentially expressed genes were defined as those showing a change at a specific stage of the IDC or genes that change in terms of levels throughout the IDC.

3.2.3 Establishing the transcriptomes and mapping parasite's age to *in vitro* transcriptome

The transcriptome for each clone was assembled by including only microarray features that were highly confident (see Materials and Methods Chapter 2). Following background subtraction, the cy5/cy3 ratios for each MOE (molecular element) was averaged to obtain the ratios for each gene. After carrying out fast fourier transformation, we observed that all five 3D7 clones' transcriptomes were highly similar to the parent 3D7 transcriptome, reflecting a high degree of stage-specific transcription and periodic gene expression of almost all genes as well as normal

developmental progress over 48 hr (Figure 3-4A). Likewise, the transcriptomes generated from the *ex vivo* (G0) and *in vitro* (G11/14 and G30) time course experiments of the culture adaptation experiment were good quality and showed a high degree of stage specificity in global gene expression (Figure 3-4B). There was no marked difference in overall transcriptomes from G0 to G30 for both isolates (Figure 3-4B). As we note that there may be certain variability in the starting time of harvest for each clone time course experiment, thus we mapped the individual sampling time points for each clone to a reference *in vitro* transcriptome to estimate the time of harvest. Previously, we generated a 2 hour resolution of the IDC transcriptome from a tightly synchronized culture of Dd2 lab strain in our lab which was used here as the reference transcriptome (for data processing; see Chapter 2 section 2.9.). The maximum spearman rank correlation coefficient of each sample time point to a reference time point (2-48 hpi) was considered as the best estimate of the parasite's stage/age and all sampling time points were plotted onto a graph (Figure 3-4C). All sample time points for the clones gave high maximum spearman rank correlation value (>0.6) to the reference transcriptome (Figure 3-4B) while the maximum SRCC values for all culture adapted samples were mostly above 0.5 (with the exception of MS6 G0 TP1, 2 and MS6 G30 TP1). There was no difference in the maximum SRCC values between the clones' TPs nor between sample TPs from the *ex vivo* G0 culture and G11/G14 or G30 cultures. The parasites progressed from rings to schizonts over 48 hours of sampling. These indicate that cultures were similar in synchronicity between generations and between clones. However, we observed that each clone/isolate progressed at different rates from ring to schizont across 48 hours despite growing under same culture conditions and regular sampling of the synchronized culture every 8 hours (Figure 3-4C and D). This reflected a natural

variation in the developmental rate of the parasite from clone to clone through the IDC. Furthermore, it reemphasized the importance of mapping samples to a high-resolution reference transcriptome which avoids comparing samples with different stage proportions to each other resulting in spurious results. The highest frequency of samples mapped within 4 windows of 4-hour time intervals corresponding to mid ring (10-14 hpi), mid trophozoite (22-26 hpi), mid schizont (32-36 hpi) and late schizont (38-42 hpi) stages for the study of 3D7 clones (Figure 3-4C). Similarly, the four windows of mid ring: 8-12 hpi, late ring: 14-16 hpi, trophozoite: 22-26 hpi and early schizont: 28-32 hpi were selected for the study of transcriptional variation in culture adaptation (Figure 3-4D). Hence, transcriptional differences were analyzed at these four stages.

3.2.4 (i) Genes with a change in level of expression between 3D7 clones

To identify genes that display variation in level of expression among single clones, the standard deviation of gene expression ratios for each gene was calculated for sampling time points that fell within each time interval window. Taking only genes with standard deviation (SD) values larger than mean of the SD plus 2 Standard Deviations of SD (ie. outside the 95% confidence interval) for each time interval, we obtained between 122 to 184 genes that were the most differentially expressed among the clones. To find genes which are differentially expressed based on the overall level of transcript abundance over the IDC, we used a "sums" approach to find the area under the curve for each clone and calculated the pair-wise fold change difference in "sums" between every 2 clones. Taking a 6-fold change in difference in "sums" as the cut-off (since this represents a 3-fold change in at least 2 time points), we observed a total of 245 genes that were differentially expressed in more than 50% of all pair-wise comparisons.

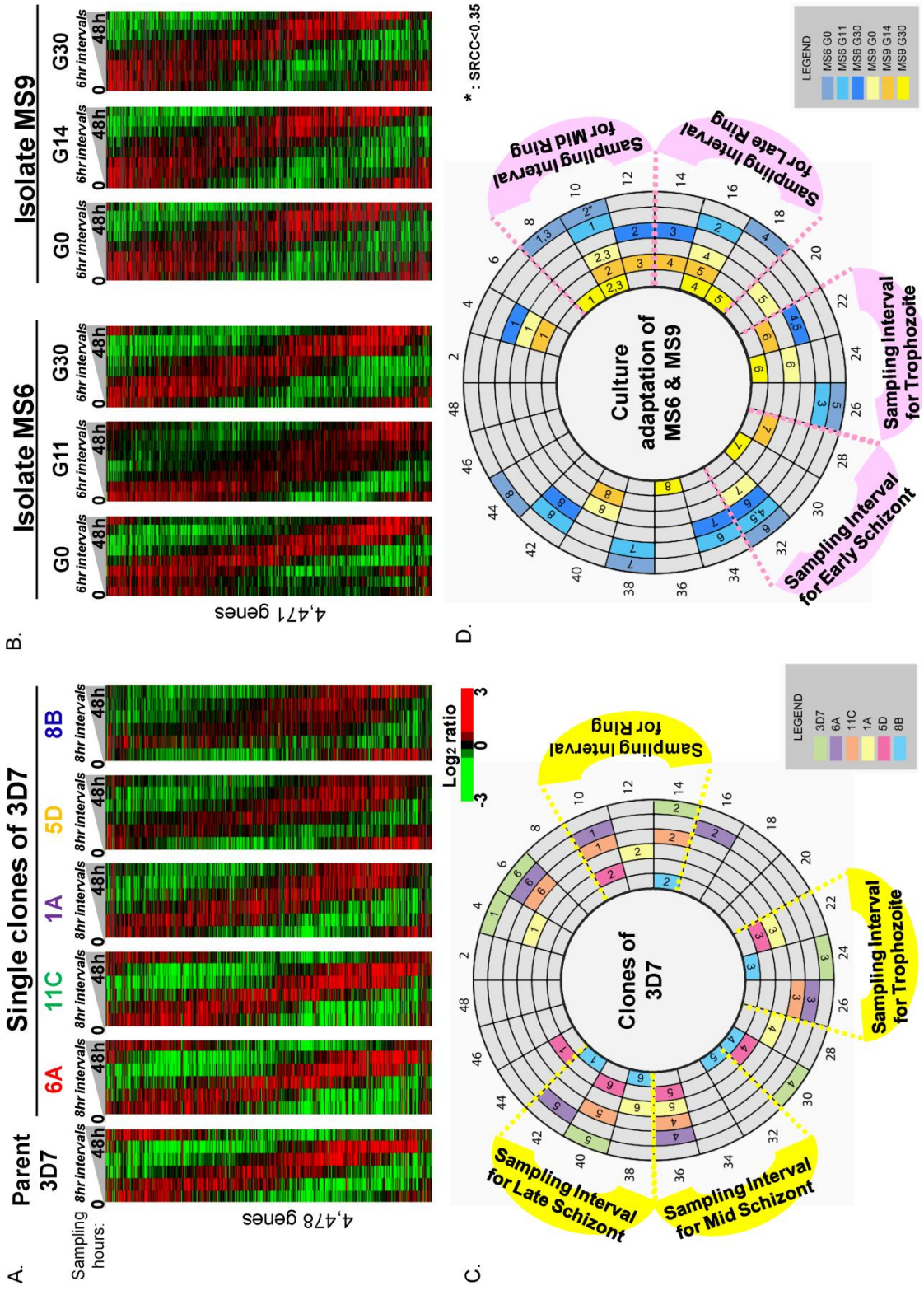

Figure 3-4 . Transcriptomes generated for each time course and age estimation.
A. Heat maps of mean-centered $\log_2$ expression ratios for each of the single 3D7 clones sampled over 48 hr and ordered by the timing of peak expression (FFT). 4,478 genes were found to be commonly present in at least 5 out of the 6 sampled time

points in all 5 clones and missing data was imputed by KNN. B. Transcriptomes established from *ex vivo* and *in vitro* lifecycles of MS6 at generations 0 (G0), 11 (G11) and 30 (G30) and MS9 at generations 0 (G0), 14 (G14) and 30 (G30) using FFT of the log_2 ratios. 4,471 genes were found to be commonly present in at least 5 out of the 8 sampled time points for each generation and missing data was imputed by KNN. C. Mapping of the sample time point (TP 1 – 8) relative to *in vitro* reference IDC (measured in Hours Post Invasion (hpi); shown by numbers 2 to 48 outside the circle). To determine parasite's age, age estimation was calculated as a best fit Spearman rank correlation. In yellow boxes are the selected time intervals (Ring: 10-14 hpi, Trophozoite: 22-26 hpi, Mid Schizont: 32-36 hpi and Late schizont: 38-42 hpi) for analysis of differentially expressed genes among the 5 clones. Pink boxes show the selected stages (mid ring: 8-12 hpi, late ring: 14-16 hpi, trophozoite: 22-26 hpi, and early schizont: 28-32 hpi) for analysis of differential expression during the culture adaptation process of 2 field isolates. TPs with * indicates that the maximum SRCC value was below the cut-off of 0.35 which was excluded from further analysis.

We combined the results from both analysis and obtained a total of 480 (8.8%) genes with differential expression among the clones (Figure 3-5A and B). 69 genes (16.7%) were predicted to possess a PEXEL motif which was significantly over represented considering that only 410 genes (7.4%) in the *P. falciparum* genome is predicted to have a PEXEL motif (hypergeometric distribution ; p-value = 3.5×10^{-8}). 120 genes (33.3%) had at least 1 paralog and belonged to multi-gene families (hypergeometric distribution; p-value = 1.8×10^{-8}).

3.2.4.1 Functional enrichment analysis of differentially expressed genes between clones

Functional enrichment analyses using hypergeometric test was carried out for the 480 genes to investigate their biological functionalities. It was observed that pathways for merozoite invasion (*eba-175, 140, 181, Rh1, surf, mtrap, msp*), molecular motor machinery, Maurer's cleft proteins and parasite's exported proteins (*hyp, phistb, phistc*) which are associated with host cell remodeling and surface antigen presentation including early transcribed membrane protein (*etramp*), mature-parasite-infected erythrocyte surface antigen (*mesa*), knob-associated histidine-rich protein

(*kahrp*), ring-infected erythrocyte surface antigen (*resa*), ring-exported protein 1, 3, 4 (*rex*), skeleton-binding protein 1, cytoadherence linked asexual protein 3.2 (*clag*), fatty acyl-coA synthesis (*pfacs* 1, 3, 7, Acyl-coA binding proteins) and family of protein kinases were significantly enriched (p-value < 0.05) (Figure 3-5C). The cluster was also enriched for genes belonging to the chromatin assembly pathway in particular encoding 4 histone proteins (histone 2A, 2B, 3 and 4) and those coding for 5 zinc finger – CCCH proteins (PFI1335w, PF13_0314, MAL8P1.70, PFE1245w, PFI0325c). Interestingly, we observed that 7 out of 27 group of transcription factors containing the ApiAP2 domain (PFF1100c, PF14_0271, PF13_0267, PFF0670w, PF10_0075, PF11_0442, PFF0200c::PfSIP2) varied in their level of expression frequently between clones (Figure 3-5E). Since these genes are highly involved in cell cycle regulation as well as transcriptional regulation, their varying expression levels could result in cell cycle shifts and activation or repression of certain sets of genes. Hemoglobin digestion and ferriprotoporphyrin IX polymerization pathway was also significantly DE among the clones (p-value = 0.04) and comprise of genes coding for histidine-rich protein III, plasmepsin I and 2 falcipains 2A and 2B which are physically located next to each other on the chromosome. Several enzymes which localize to Maurer's cleft (MC) were also in the group of DE genes such as PF13_0141:: L-lactate dehydrogenase and PF14_0598:: glyceraldehyde-3-phosphate dehydrogenase, hence implicating a role in the variation of nutrient acquisition between parasites. Of the total 21 FIKK protein kinases encoded in the *P. falciparum* genome, 8 (38%) were DE. The FIKK serine/threonine protein kinases are kinases unique to Apicomplexan that have expanded to include 21 members [161]. 2 genes - *fikk7.1* (MAL7P1.144) and *fikk12* (PFL0040c) were shown to phosphorylate the RBC membrane skeletal proteins and gene knock outs led to the altered mechanical

properties, specifically loss in rigidity of the infected RBC [162], albeit without any growth defects under *in vitro* culture conditions. The differential expression of both these genes in our data supports the hypothesis that DE genes are not necessary for the growth of the parasites in culture but may play crucial roles in other stages or *in vivo*. Moreover in *P. berghei*, 23 of 73 (31%) of the protein kinases are redundant in the asexual blood stages and have roles in either sporogony or gametocyte stages [163]. Molecular motor machinery involving myosin, actin and dynein are especially important for biological process of gliding motility in sporozoite stage and merozoite invasion in the asexual blood stage and the DE associated with this pathway is parallel to invasion-specific ligands being DE.

Other individual genes that were differentially expressed but not enriched for any particular pathways include several sexual stage proteins such as *P. falciparum* gamete antigen 27/25 and gametocyte-implicated protein fragment, genes involved in REDOX activities such as superoxide dismutase, cytochrome C oxidase copper chaperone, 1-cys peroxiredoxin and glutamate dehydrogenase, and molecular chaperones involved in stress response (*hsp70*, *hsp86*, hsp70/90 organizing protein, *dnaj*) among 175 hypothetical proteins (Figure 3-5E). In addition, we noted the differential expression of the *pfmc-2tm* Maurer's cleft 2 transmembrane protein (MAL7P1.5) known to be clonally variant and undergoes expression switching [164]. No drug resistance markers or transporters, except for only 1 gene, PFL1410c, coding for an ABC transporter, was significantly differentially expressed and further characterized (Chapter 6).

Chromosomal distribution of the 480 DE genes

The chromosomal distribution of the 480 genes were plotted and it was observed that the genes were significantly enriched at telomere and sub-telomeric ends of the chromosomes (hypergeometric distribution; p-value = 5 x 10^{-13}). Next, we investigated if the genes occurred in significantly enriched clusters by using hypergeometric testing of enrichment of genes in a 100 kb window with 1 kb frame

A.

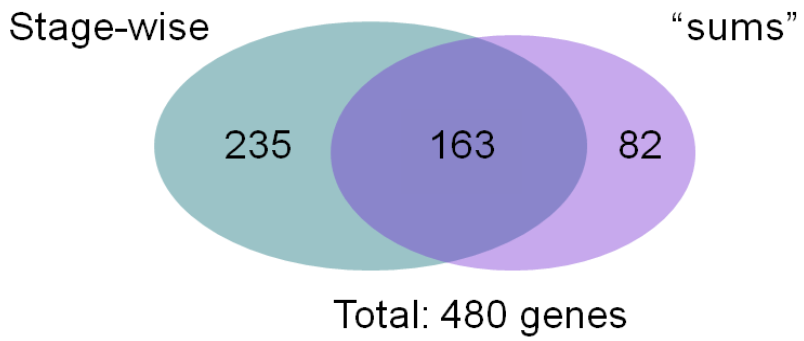

B

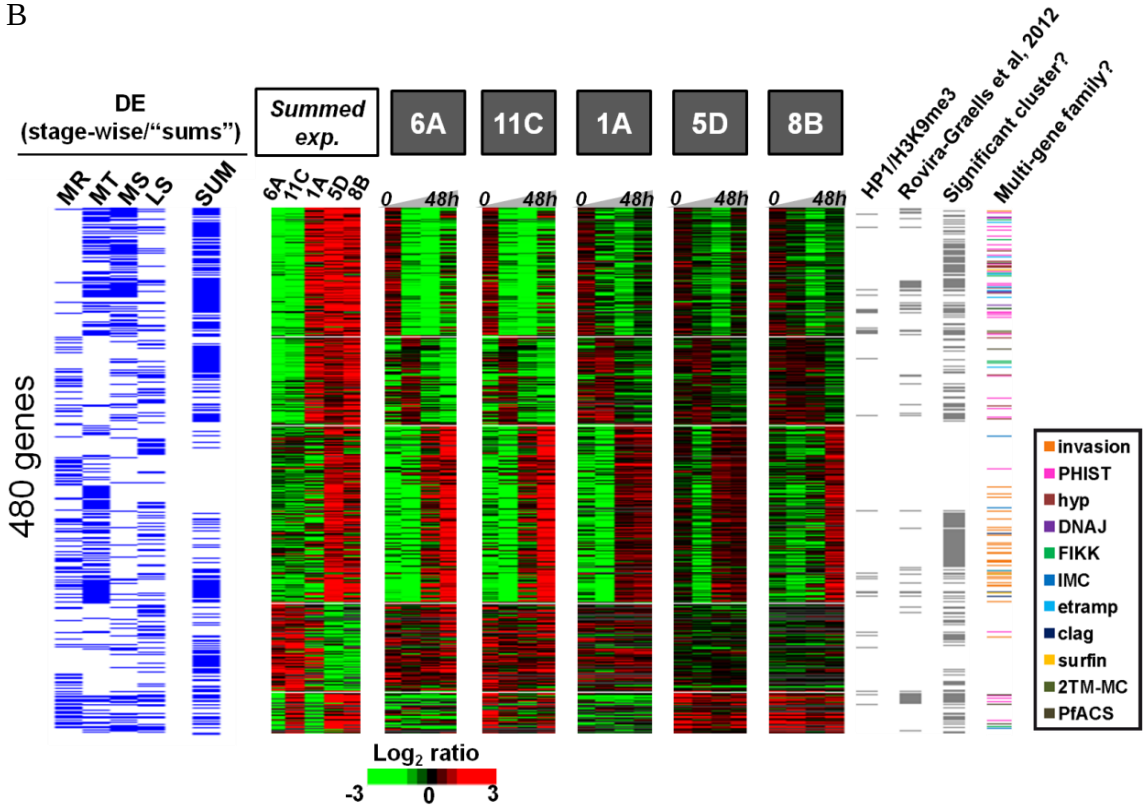

C.

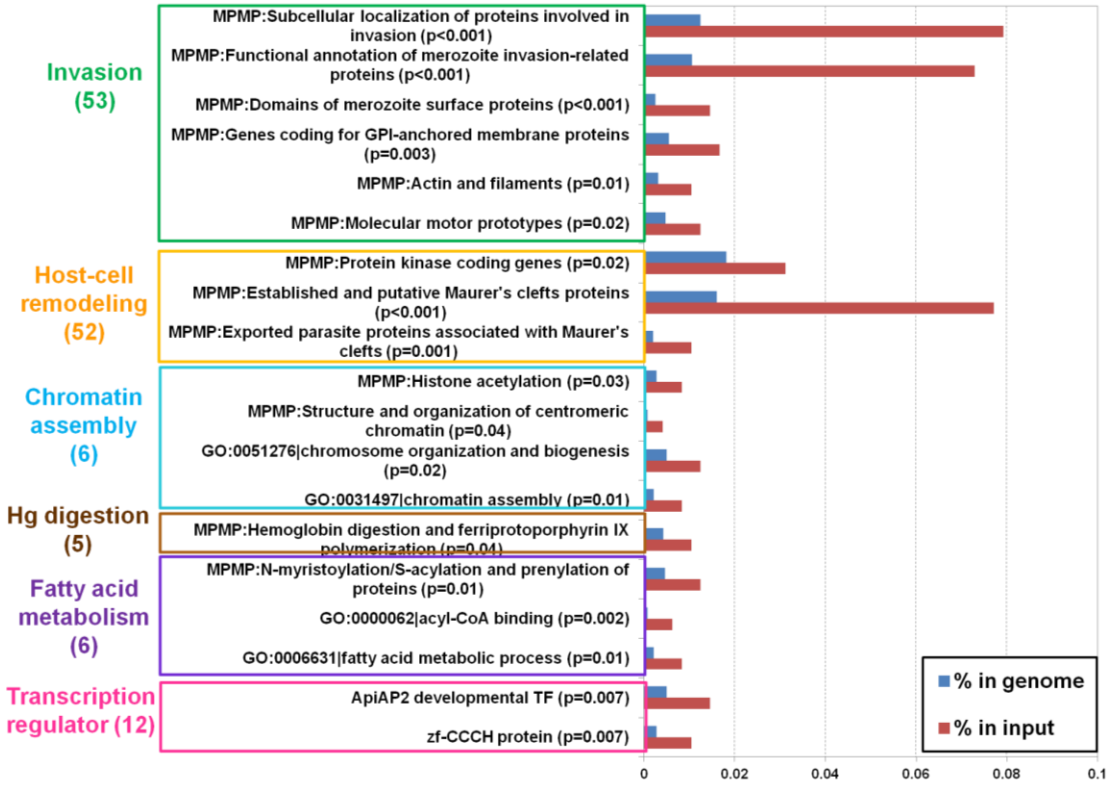
Invasion (53)
MPMP:Subcellular localization of proteins involved in invasion (p<0.001)
MPMP:Functional annotation of merozoite invasion-related proteins (p<0.001)
MPMP:Domains of merozoite surface proteins (p<0.001)
MPMP:Genes coding for GPI-anchored membrane proteins (p=0.003)
MPMP:Actin and filaments (p=0.01)
MPMP:Molecular motor prototypes (p=0.02)
Host-cell remodeling (52)
MPMP:Protein kinase coding genes (p=0.02)
MPMP:Established and putative Maurer's clefts proteins (p<0.001)
MPMP:Exported parasite proteins associated with Maurer's clefts (p=0.001)
Chromatin assembly (6)
MPMP:Histone acetylation (p=0.03)
MPMP:Structure and organization of centromeric chromatin (p=0.04)
GO:0051276|chromosome organization and biogenesis (p=0.02)
GO:0031497|chromatin assembly (p=0.01)
Hg digestion (5)
MPMP:Hemoglobin digestion and ferriprotoporphyrin IX polymerization (p=0.04)
Fatty acid metabolism (6)
MPMP:N-myristoylation/S-acylation and prenylation of proteins (p=0.01)
GO:0000062|acyl-CoA binding (p=0.002)
GO:0006631|fatty acid metabolic process (p=0.01)
Transcription regulator (12)
ApiAP2 developmental TF (p=0.007)
zf-CCCH protein (p=0.007)
% in genome
% in input
0
0.02
0.04
0.06
0.08
0.1

D.

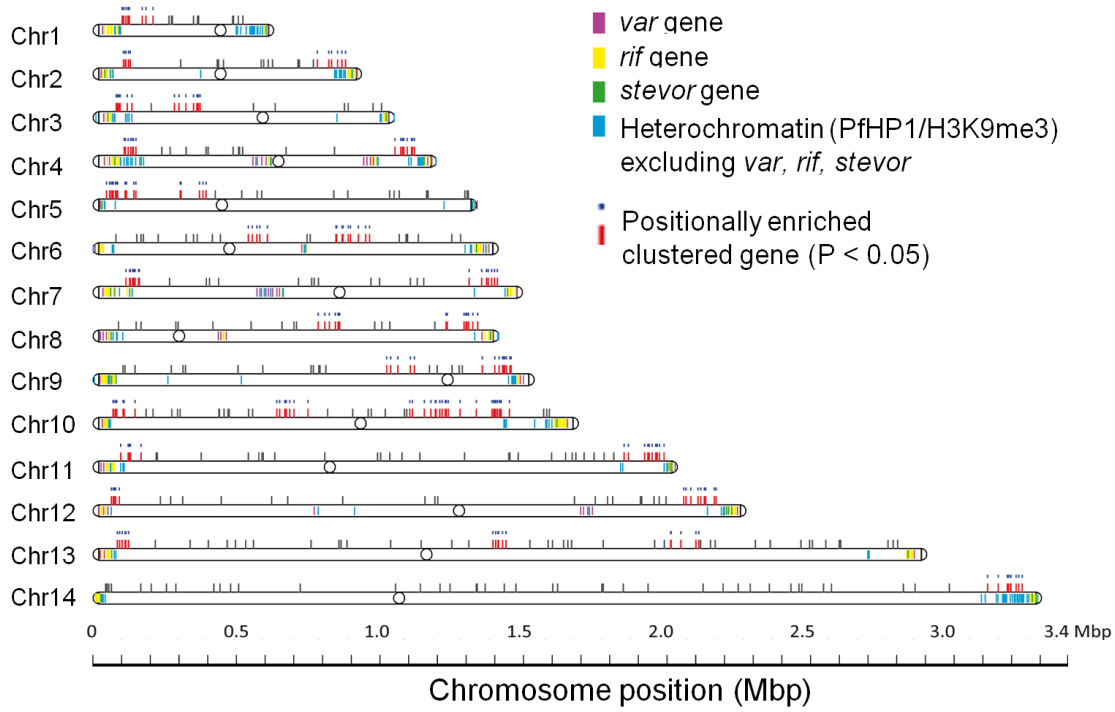
Chr1
Chr2
Chr3
Chr4
Chr5
Chr6
Chr7
Chr8
Chr9
Chr10
Chr11
Chr12
Chr13
Chr14
var gene
rif gene
stevor gene
Heterochromatin (PfHP1/H3K9me3) excluding var, rif, stevor
Positionally enriched clustered gene (P < 0.05)
0
0.5
1.0
1.5
2.0
2.5
3.0
3.4 Mbp
Chromosome position (Mbp)

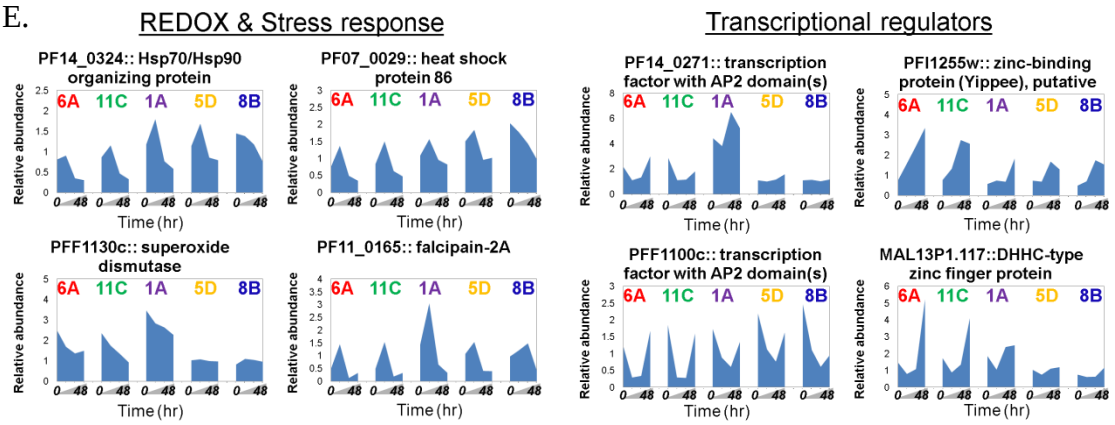

Figure 3-5. Analysis of differentially expressed genes between 3D7 clones. A. Venn diagram showing the overlap between DE genes identified from the analysis methods of stage-specific change in expression ("stage-wise") or change in overall level of expression in the 4 selected TPs ("sums"). B. Heat maps depicting the microarray ratios of the differentially expressed genes between the single 3D7 clones detected by either the stage-wise approach or the "sums" method (blue bars) along with the mean-centered summed gene expression ratios for each clone over the 4 selected TPs. In grey are our DE genes which are found to be associated with HP1 protein or known to be DE from Rovira-Graells et al, 2012 study or genes found in positionally enriched clusters. Genes belonging to multigene family of *Plasmodium* are shown in the most right column (colored bars). C. List of functional pathways (MPMP: Malaria Parasite Metabolic Pathways; GO: Gene Ontology Database) significantly enriched in the group of 480 differentially expressed genes with the p-values. The graphs depict the % of pathway-related genes in the genome (blue) and % of pathway-related genes in the group of 480 genes (red). The number of genes from the group belonging to each functional category is listed in brackets. Hg: hemoglobin; met.: metabolism; T.F.: transcription factor. D. Plot of the chromosomal distribution of the 254 differentially expressed genes showing significantly positional enriched clusters (red bars with blue dots) calculated by hypergeometric testing with cut-off of p-value < 0.05. Shown are the position of the *var* (purple), *rif* (yellow), *stevor* (green) genes of 3D7 and genes found to be associated with the PfHP1 protein on the chromosomes in cyan (after excluding *var*, *rif* and *stevor* genes). E. Relative transcript abundance of several differentially expressed genes across each clone's IDC.

shift. We observed the presence of 29 significantly positional enriched clusters (p-value < 0.05) comprising of 43.7% of all DE genes (210 genes) which were biased towards the sub-telomeric ends of all 14 chromosomes (Figure 3-5D). Of the 29 detected clusters, 18 of these were located near genes coding for variant surface antigens (*var, rif, stevor*) which are known to be clonally variant (Figure 3-5D). The *P. falciparum* heterochromatin protein 1 (PfHP1) has been shown to be physically associated with H3K9me3 histone marks at the sub-telomeric ends of chromosomes

and associates with clonally variant genes such as *var*, *rif* and *stevor* multi-gene families along with 177 other genes [146]. Hence, we investigated the overlap between the DE genes and those associated with PfHP1 protein. A total of 28 out of the 177 non-VSA genes (15.8%) associated with PfHP1 were differentially expressed in our data (Figure 3-5D cyan bars) signifying an enrichment of PfHP1 genes (hypergeometric distribution; p-value = 9×10^{-4}) and possible association between HP1 marks and transcriptional variation.

3.2.4.2 Clonal expression differences is largely independent of copy number polymorphisms

Since it is known that there is much variation in copy number at chromosomal ends of *in vitro* cultured *Plasmodium* [164], hence to ascertain if the differences in gene expression between clones were due to differences in genetic composition (ie. SNPs or copy number polymorphisms present), we carried out comparative genomic hybridization (CGH) of the 5 clones relative to parental 3D7 using our microarray chip (Table 3-1). Analysis of the CGH data of these 5 clones found that for almost all the 480 genes, there was no difference in copy number or SNPs present that resulted in the differential expression. However, for the handful of genes (~15 genes excluding VSA) found with CNVs located on chromosome 2 and 12 sub-telomeric ends, there was a strong positive association between gene copy number and basal level of expression. Further analysis showed that there were telomeric and sub-telomeric deletions at the ends of these 2 chromosomes in clones 1A and 6A which resulted in loss of expression of these genes.

Table 3-1. List of genes found to have CNVs in the 5 clones of 3D7.
The CNV state of gain (+1) or loss (-1) or no change (0) for each clone relative to the parent 3D7 strain is shown.

chr	Gene associated with CNV segment	1A	6A	5D	8B	11C
2	PFB0075c:: *Plasmodium* exported protein (hyp9), unknown function	-1	-1	0	0	0
2	PFB0080c:: *Plasmodium* exported protein (PHISTb), unknown function	-1	-1	0	0	0
2	PFB0085c:: DNAJ protein, putative	-1	-1	0	0	0
2	PFB0090c:: RESA-like protein with PHIST and DnaJ domains	-1	-1	0	0	0
2	PFB0095c:: erythrocyte membrane protein 3, PfEMP3	-1	-1	0	0	0
2	PFB0100c:: knob-associated histidine-rich protein, KAHRP	-1	-1	0	0	0
2	PFB0105c:: *Plasmodium* exported protein (PHISTc), unknown function	-1	-1	0	0	0
2	PFB0106c:: *Plasmodium* exported protein, unknown function	-1	-1	0	0	0
12	PFL0005w:: erythrocyte membrane protein 1, PfEMP1	-1	-1	0	0	0
12	PFL0010c:: rifin	-1	-1	0	0	0
12	PFL0020w:: erythrocyte membrane protein 1, PfEMP1	-1	-1	0	0	0
12	PFL0025c:: rifin	-1	-1	0	0	0
12	PFL0030c:: erythrocyte membrane protein 1, PfEMP1	-1	-1	0	0	0
12	PFL0035c:: acyl-CoA synthetase, PfACS7	-1	-1	0	0	0
12	PFL0040c:: Serine/Threonine protein kinase, FIKK family	-1	-1	0	0	0
12	PFL0045c:: *Plasmodium* exported protein (PHISTc), unknown function	-1	-1	0	0	0
12	PFL0050c:: *Plasmodium* exported protein (PHISTb), unknown function	-1	-1	0	0	0
12	PFL0055c:: RESA-like protein with PHIST and DnaJ domains	-1	-1	0	0	0
12	PFL0060w:: *Plasmodium* exported protein, unknown function	-1	-1	0	0	0
12	PFL0065w:: conserved *Plasmodium* protein, unknown function	-1	-1	0	0	0
12	PFL2655w:: rifin	0	0	-1	0	0
12	PFL2665c:: erythrocyte membrane protein 1, PfEMP1	0	0	-1	0	0
11	PF11_0479:: conserved *Plasmodium* protein, unknown function	+1	0	0	0	0
11	PF11_0480:: sporozoite asparagine-rich protein	+1	+1	-1	-1	-1
10	PF10_0399:: rifin	0	+1	0	0	0
10	PF10_0400:: rifin	0	+1	0	0	0

3.2.5 (ii) Genes varying in level of expression during culture adaptation

We investigated whether the transcriptomes of two field isolates, MS6 and MS9, were preserved during culture adaptation and if any genes were differentially expressed as a result of the adaptation process from *in vivo* to *in vitro* conditions. Similar to the analysis for 3D7 clones, genes that display variation in level of expression between the 3 generations of each field isolate were identified using the same analysis approach of stage-wise DE and overall "sums" in total expression throughout the asexual lifecycle between any 2 generations in multiple pair-wise comparisons

(Chapter 3.2.5) for each isolate. 494 and 430 genes were differentially expressed across the 3 generations (0, 11/14 and 30) in MS6 and MS9 respectively (Figure 3-6A). Of which, 182 genes were commonly differentially expressed during the culture adaptation process of either of the two isolates. Hence, we identified a total of 742 genes that were differentially expressed between parasite generations over the course of culture adaptation (Figure 3-6A). These genes were stage-specific and peaked at either ring or schizont stages (Figure 3-6A). There was a significant overlap of 284 genes (38.3%) which are found in this list and among the 480 genes shown to be differentially expressed between clones of 3D7 (binomial distribution; p-value = 1.4×10^{-118}). However, only 10.1% of these DE genes were found to be DE between any 2 parasite lines in a study by Rovira-Graells et al, 2012. After excluding *var*, *rif* and *stevor* genes, surprisingly only ~5.9% of genes differentially expressed in culture adaptation were known to be associated with PfHP1 protein and marks of heterochromatin region, suggesting that the other 94% of DE genes had other mechanisms underlying variant expression.

3.2.5.1 Functional enrichment of genes differentially expressed during culture adaptation

Functional enrichment analysis of these 742 DE genes reveals that pathways over represented were highly similar to those observed in the list of DE genes between single 3D7 clones. They comprise of invasion, host-cell remodeling such as Maurer's cleft proteins, protein kinases, fatty acid metabolism (*pfacs*), histones 2a, 2b, 3 and 4 in chromatin assembly. Additional pathways consisting of cytoskeleton organization, centriole proteins and mitotic centrosome structure also came up, which were not observed in the DE genes between clones. Although certain pathways such as hemoglobin digestion and transcriptional regulators (ApiAP2 domain and zinc finger

domain proteins) were enriched in the DE genes between single clones and not for DE genes in culture adaptation, we observed that several genes belonging to these pathways were also differentially expressed in culture adaptation but not giving rise to significant p-value cut-off of 0.05. They include falcipain 2a and 8 ApiAP2-related genes of PF14_0271, PF11_0091, PFF0670w, PF11_0442, PF11_0404, MAL8P1.153, PFF0200 (PfSIP2) and PFL1085w. 4 zinc finger proteins of MAL8P1.70 PF11_0357, PFC0610c, PFD0765w were also observed as DE.

Of the 742 genes, more than a third was found in positionally enriched clusters on the chromosomes (hypergeometric distribution, p-value < 0.05). Similar to the DE genes in 3D7 clones, we observed a significant enrichment of genes towards the sub-telomeric ends of the chromosomes (hypergeometric distribution; p-value = 7.7×10^{-6}). On comparison of enriched clusters in the DE genes from both studies, we found that 4 sub-telomeric clusters on chromosomes 4, 7, 9 and 11 representing 49 genes were commonly observed.

A

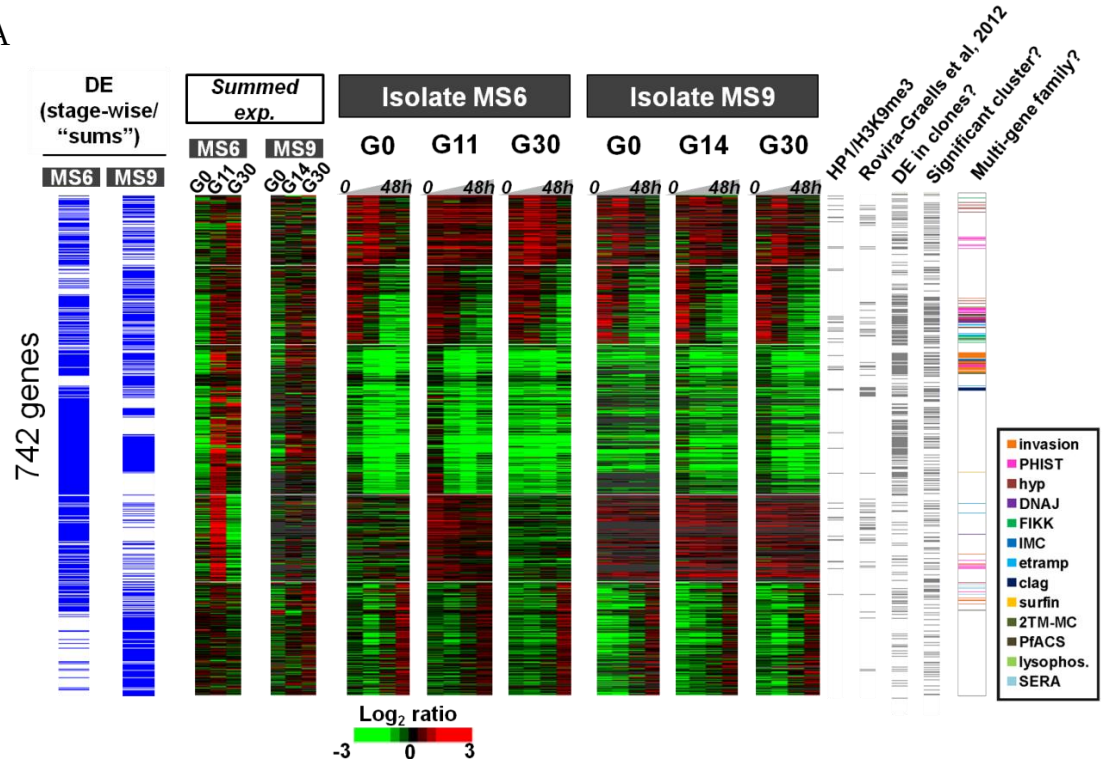

B.

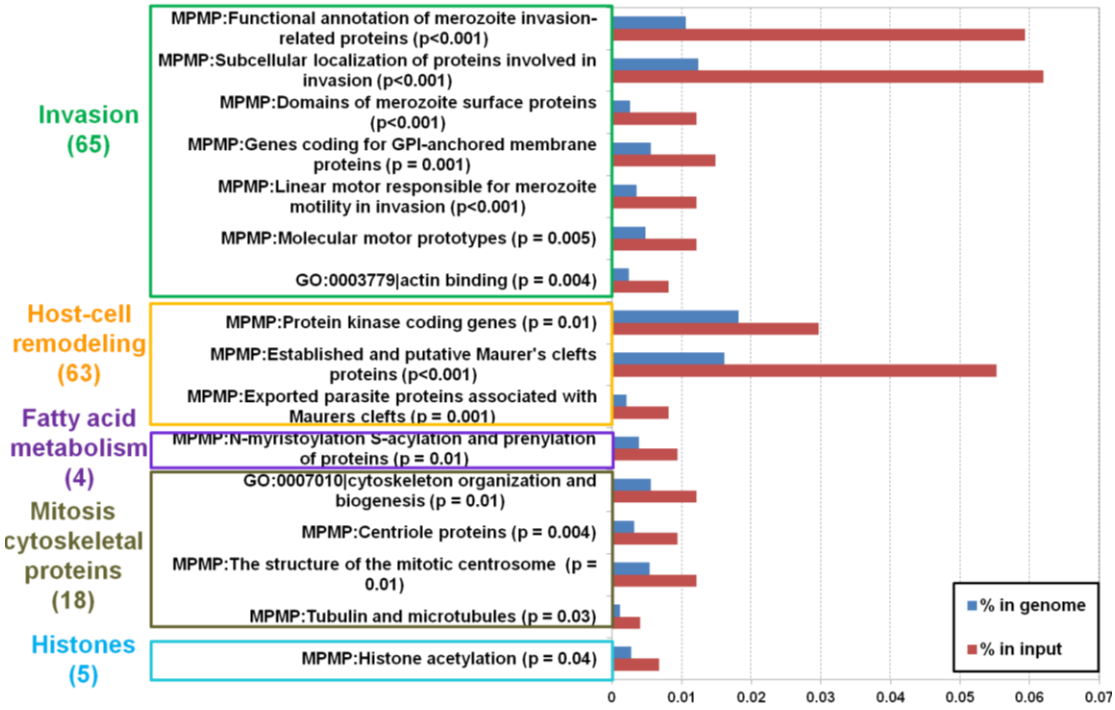

C.

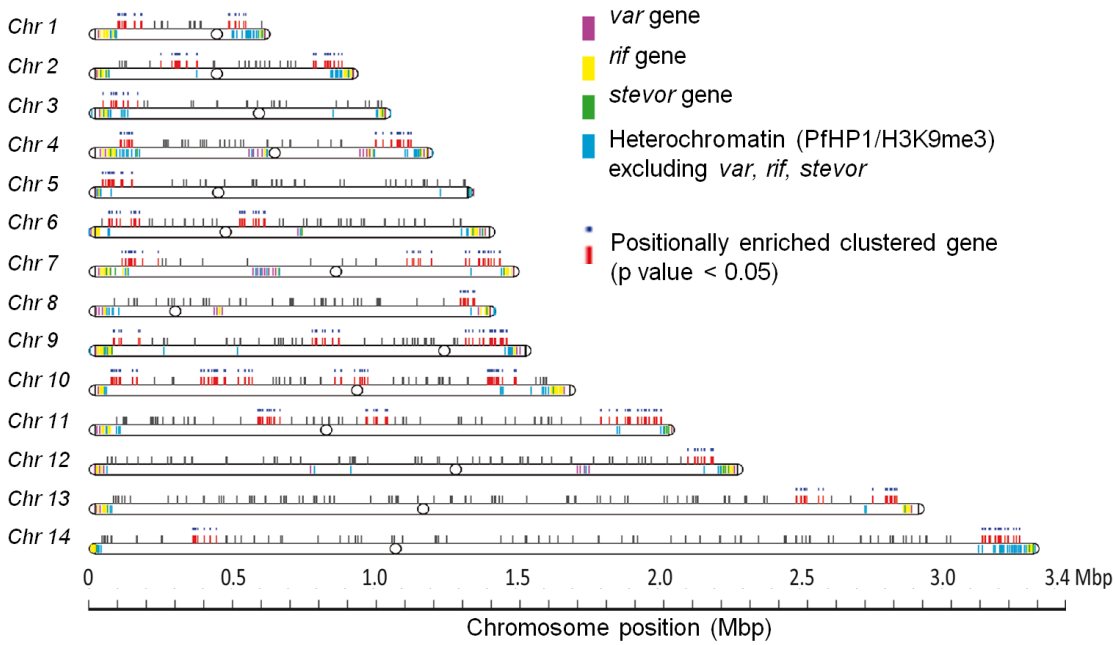

Figure 3-6. Analysis of differentially expressed genes during culture adaptation. A. Heat maps depicting the microarray ratios of the differentially expressed genes between generations in culture detected by either the stage-wise approach or the "sums" method in MS6 or MS9 isolate (blue bars) along with the mean-centered

summed gene expression ratios for each isolate at each generation over the 4 selected TPs. In grey are our DE genes which are found to be associated with HP1 protein or known to be DE from Rovira-Graells et al, 2012 study or DE in our study of single 3D7 clones or genes found in positionally enriched clusters. Genes belonging to multigene family of *Plasmodium* are shown in the most right column (colored bars). B. List of functional pathways (MPMP: Malaria Parasite Metabolic Pathways; GO: Gene Ontology Database) significantly enriched in the group of 742 differentially expressed genes with the p-values. The graphs depict the % of pathway-related genes in the genome (blue) and % of pathway-related genes in the group of 742 genes (red). The number of genes from the group belonging to each functional category is listed in brackets. C. Plot of the chromosomal distribution of the 742 differentially expressed genes showing significantly positional enriched clusters (red bars with blue dots) calculated by hypergeometric testing with cut-off of p-value < 0.05. Shown are the position of the *var* (pruple), *rif* (yellow), *stevor* (green) genes of 3D7 and genes found to be associated with the PfHP1 protein on the chromosomes in cyan (after excluding *var, rif* and *stevor* genes).

3.2.6 Maurer's Cleft Export and Merozoite invasion genes are most variable in expression during culture-adaptation of isolates

We sought to identify genes that changed in the overall level of expression from one generation to another using the "sums" approach to identify any trends in expression of DE genes over culture adaptation. More than 95% of the genes did not show any transcriptional difference between G30 and G0 or between G11 and G0 (Figure 3-7). 40 (1%) to 170 (4%) genes varied in expression between any 2 generations for both isolates MS9 and MS6 (Figure 3-7). Interestingly, we observed that a larger number of genes were highly expressed in G30 and G11 compared to G0 while fewer genes had lower expression levels in G30 and G11 than G0 for both isolates (Figure 3-7). While 224 genes were up-regulated in expression in G11 and/or G30, only 36 were down-regulated over time in MS6 isolate. Likewise for MS9, 84 genes had higher expression in G14 and/or G30 but only 22 had lowered expression in these generations. In total, 312 (7%) and 130 (3%) genes were differentially expressed between any 2 generations for isolate MS6 and MS9. K-means clustering was carried out on these genes separately for both isolates and the variation in expression levels

was summarized by 4 major patterns: (i) increased expression from G0 to G11 and maintenance of higher expression from G11/G14 to G30, (ii) maintenance of similar expression levels between G0 and G11/G14 and increased expression from G11/G14 to G30, (iii) increased expression from G0 to G11/G14 followed by decreased levels in G30 and (iv) decreasing level from G0 to G30 over time.

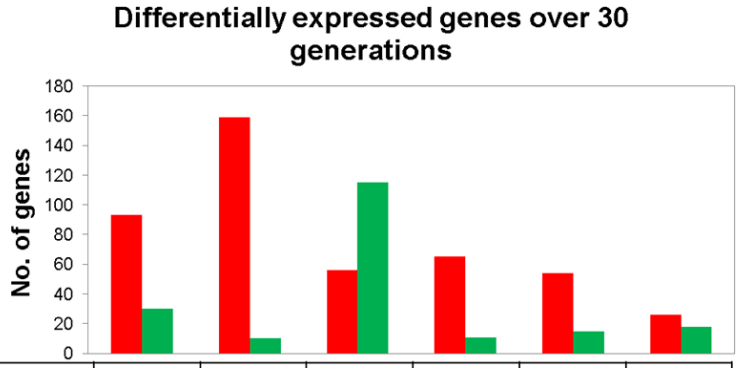

	G30/G0	G11/G0	G30/G11	G30/G0	G14/G0	G30/G14
Isolate	MS6			MS9		
Positive change	93 (2.27%)	159 (3.88%)	56 (1.37%)	65 (1.59%)	54 (1.32%)	26 (0.63%)
Negative change	30 (0.73%)	10 (0.24%)	115 (2.81%)	11 (0.27%)	15 (0.37%)	18 (0.44%)
Total	123 (3.00%)	169 (4.12%)	171 (4.17%)	76 (1.86%)	69 (1.68%)	44 (1.07%)

Figure 3-7. Bar plots of the DE genes between every 2 generations. Plotted are the number of genes differentially expressed between G0 and G11/G14, G0 and G30 and G11 and G30 defined by having more than 6-fold difference in the summed $\log_2$ ratios across the 4 selected hpi windows for isolates MS6 and MS9 in multiple pair-wise comparisons. Red bars indicate the genes with a positive change and green bars indicate negative change with respect to the fold-difference in each pair-wise comparison as shown. The total number and % of differentially expressed genes for each comparison are listed.

3.2.6.1 Functional enrichment analysis of the k-means clusters

Functional enrichment analysis of the genes for each pattern of varying transcriptional levels was performed to identify over-represented functionalities in these clusters. We observed that for both isolates, multiple pathways relating to merozoite invasion and exported proteins associated with Maurer's clefts were enriched in clusters (i) and (ii)

(p-value<0.05) for genes showing increased transcript abundance with adaptation to laboratory conditions (Figure 3-8). For cluster (iii) where genes decreased in expression levels from generation 11 to 30 after an increase from G0 to G11, there was an also an enrichment of genes (p-value<0.05) relating to these same pathways of host cell remodeling (Maurer's cleft proteins) and merozoite invasion as well as lactate dehydrogenase activity in MS6 (Figure 3-8). In MS9, host cell remodeling (Maurer's cleft proteins), endopeptidase activity and fatty acid metabolic processes in MS9 were enriched (Figure 3-8). Importantly, we observed that these MC genes that were differentially expressed over the generations were mostly different members for the 2 clones. For example, while MC genes: PF14_0761 and PFD1170c were found in MS9 cluster (iii), MC genes: PF10_0164, PFD1120c, PF11_0039, PF13_0197, PFB0120w, PFD0310w and PF10_0019 were found MS6 cluster (iii). This suggests that although the main functionally enriched pathways are similar between the 2 clones, yet the individual genes found within these pathways differ. In addition, it suggests a general transcriptional plasticity associated with genes relating to invasion and Maurer's cleft such as *phists* and *etramps*. Genes coding for sexual stage development was also DE in both isolates. While the expression level of sexual stage protein precursor (PFD0310w) increased in MS6 at G11 and then decreased in G30, the gene were more highly expressed in both G30 and G14 compared to G0 in MS9 (Figure 3-8B (iii) and C (ii)), signifying that transcriptional variation of transmission stage related genes is stochastic over time.

A smaller proportion of genes exhibited lowered expression over 30 generations, mainly hypothetical genes among several interesting ones which were enriched for endopeptidase and superoxide dismutase activities for MS6 and invasion and prenyltransferase and selenocysteine biosynthesis activities for MS9.

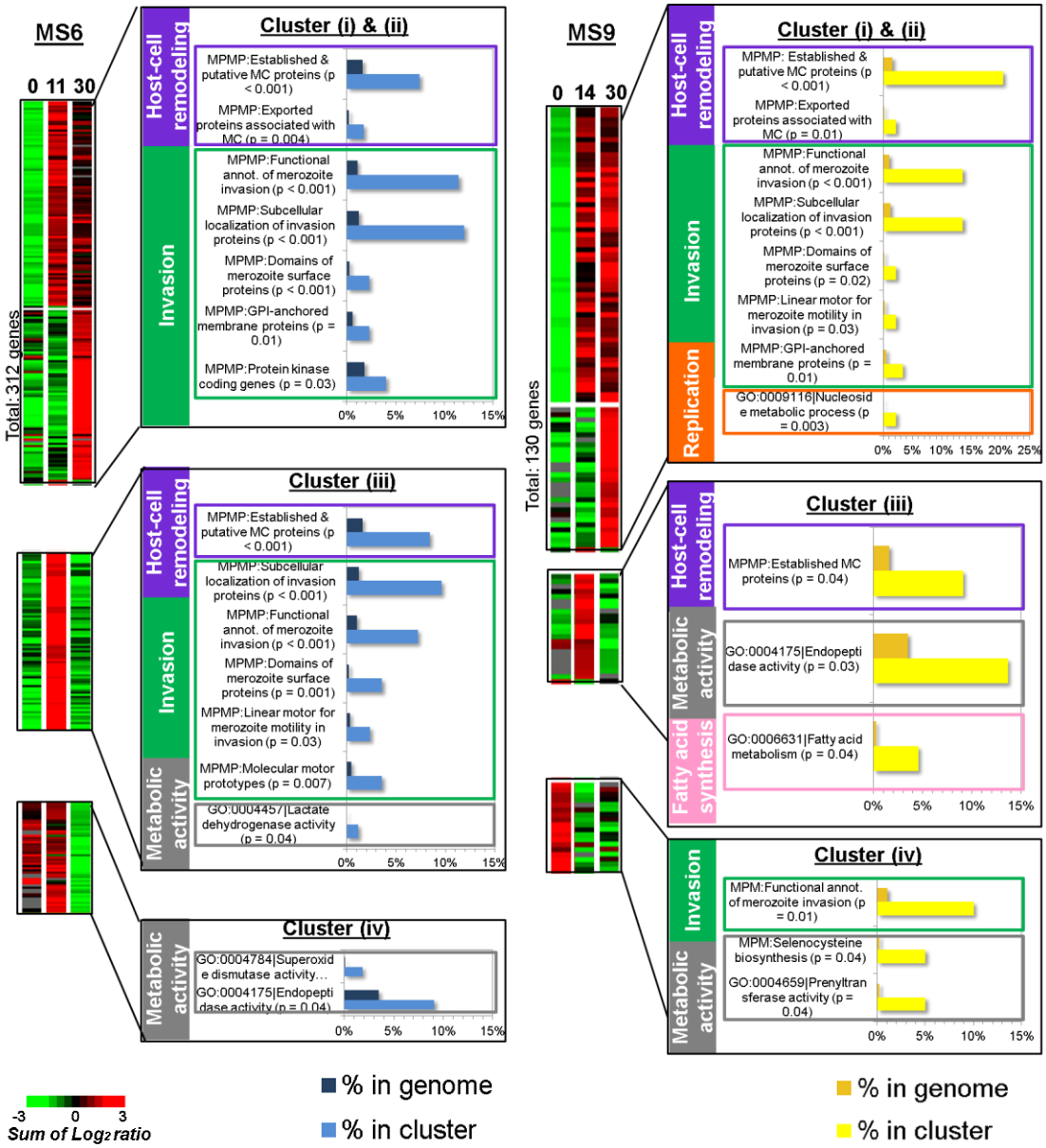

Figure 3-8. Functional enrichment analysis of genes found to be differentially expressed between generations of isolates MS6 and MS9. Heat maps represent the log_2 transformed and mean-centered "sums" (summed transcript abundance) of the 312 (MS6) or 130 (MS9) DE genes which are grouped by the pattern of expression trend during culture adaptation as determined from K-means clustering. Genes found within the clusters were tested for functional over representation by hypergeometric testing using MPMP and GO databases and depict significantly enriched pathways (p-value < 0.05). MC: Maurer's cleft. Yellow (MS9) and blue (MS6) Bars indicate the % enriched in cluster while orange (MS9) and dark blue (MS6) bars indicate the % enriched in genome for each pathway.

3.2.7 Is differential expression between the isolates maintained *in vitro*?

Comparison of the distribution of differentially expressed genes revealed that there was a significantly larger number of genes that were differentially expressed between the 2 field isolates at all 3 generations than between any 2 generations of an isolate (Figure 3-9A) (Student's t-test; p-value = 7.1×10^{-4}). This suggests that differential expression brought about by culture adaptation were significantly lesser than the differential expression between any 2 field isolates. Next, we determined if the same genes are consistently differentially expressed between the 2 field isolates, MS6 and MS9, after culture adaptation to 11 and 30 generations as compared to *ex vivo* culture. The overall distribution of difference in summed expression ratios between MS6 and MS9 was similar and highly correlated between G0, G11/14 and G30 (Pearson correlation coefficient (PCC) = 0.87 for G11 and G0 and PCC = 0.82 for G30 and G0) (Figure 3-9B). Taking only genes with difference in summed expression greater than mean ± 2SD of the distribution of fold changes, we found that 129, 151 and 127 genes were differentially expressed between MS6 and MS9 in the *ex vivo* culture (G0) and culture adapted cultures (G11/14 and G30) respectively. There was significant overlap in the number of genes differentially expressed between the 2 isolates at G0, G11 and G30 (binomial distribution; p-value <0.001) (Figure 3-9C). Moreover, the direction of change for the overlapping differentially expressed genes was the same in all 3 generation (Figure 3-9B). In addition, for the DE genes that was only considered as DE in G0 but not in G11 and G30 based on the cut-offs, no difference in direction of change for almost all these DE genes was observed in both G11 and G30, except for a few hypothetical proteins. Functional enrichment of the DE genes in G0 showed that the genes were enriched for invasion, Maurer's cleft, fatty acid synthesis, folate biosynthetic pathway and DNA replication (hypergeometric distribution; p-value <

0.05). Likewise, we see pathways for MC, invasion, folate biosynthesis and fatty acid metabolism also over-represented in G11 and G30 (hypergeometric distribution; p-value < 0.05). Hence, although we observed differences in the total number of genes DE in the *ex vivo* generation compared to the *in vitro* generations, the functions related to these DE genes do not differ. The most conserved DE genes between MS6 and MS9 belonging to the same enriched pathways in every generation were GTP cyclohydrolase I and dihydrofolate synthase (*dhfs*) in the folate biosynthesis process. While MS6 had higher expression of *dhfs*, GTP cyclohydrolase I was down-regulated (Figure 3-9D). Interestingly, DNA replication related genes such as DNA replication licensing factor *mcm5* and *mcm4* were up-regulated in MS6 (Figure 3-9D), although the levels of these genes slowly tapered with *in vitro* culture, resulting in this pathway enriched *ex vivo* (G0) but not *in vitro* (G11 and G30).

A.

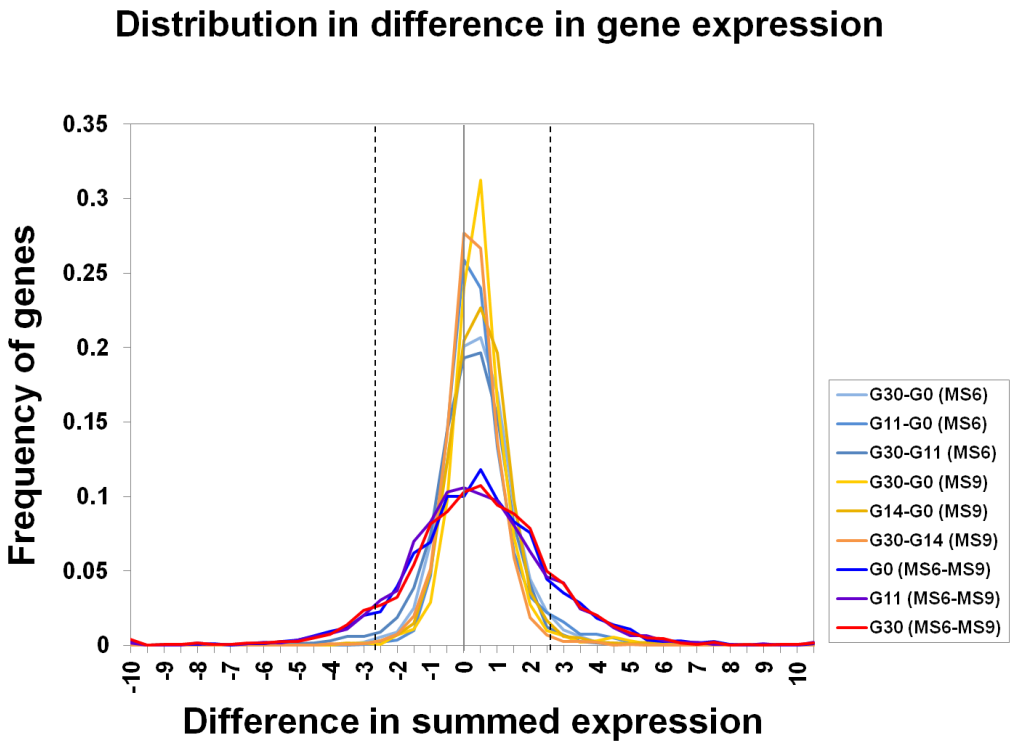

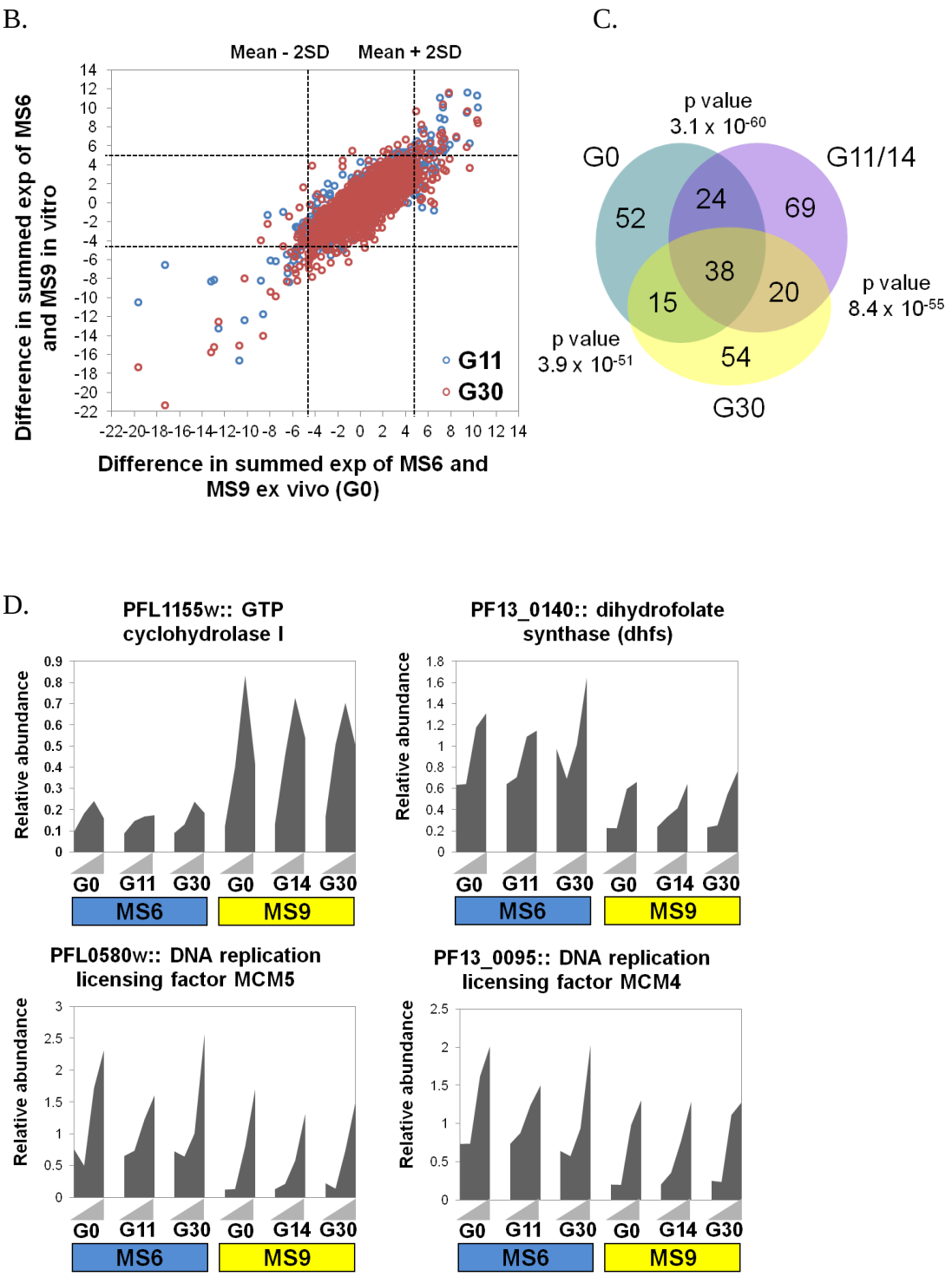

Figure 3-9. Analysis of transcriptional differences between MS6 and MS9. A. Histogram showing the distribution of the difference in summed gene expression levels over the IDC between every paired lifecycle transcriptomes i.e. between generations of MS6 or MS9 isolate or between the 2 isolates at each generation. B. Scatter plot of the difference in summed gene expression levels of MS6 and MS9 in *ex vivo* culture, G0, compared to *in vitro* cultures, G11 (blue) and G30 (red). C. Venn diagram of the overlap of DE genes between MS6 and MS9 in the *ex vivo* culture (G0) and *in vitro* cultures (G11 and G30). D. Relative transcript abundance level across the IDC of the genes involved in folate biosynthesis (top panels) and DNA replication (bottom panels) for G0, G11/14 and G30 of MS6 and MS9 isolates.

3.2.8 VSA expression in 3D7 clones

3.2.8.1 Timing of expression of Variant Surface Antigens

The expression of variant surface antigens (*var*, *rif*, *stevor*) was analyzed in these selected clones of 3D7 origin in order to verify their identities as single clones. It was observed that unlike *var* gene expression where almost all full length transcripts of the 60 member family (93%-100%) were present, only less than half of the 152-member *rif* family (28% to 49%) and 30-member *stevor* family (21% to 38%) were detected on our microarray chip (Figure 3-10). More than half of the members of the *rif* and *stevor* gene families are possibly expressed at other stages of the lifecycle such as in sexual stage gametocytes or sporozoites [165]. Alternatively, their expression may be repressed during the asexual stage under *in vitro* culture conditions and are expressed only in the environment of the human host [166].

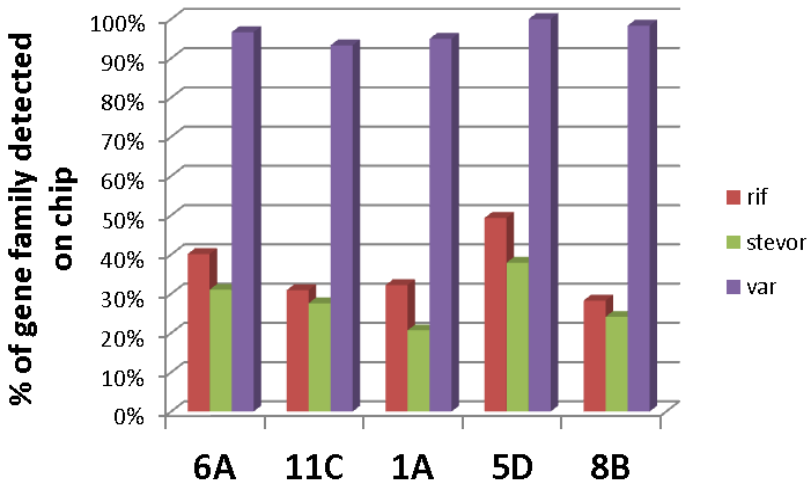

Figure 3-10. Proportion of *var*, *rif* and *stevors* detected in the 3D7 clones. Shown are the percentages of members in the VSA family expressed by the 5 clones of 3D7 during the intraerythrocytic stage of *P. falciparum*. A total of 246 probes mapping specifically to 60 member *var* gene family, 175 probes mapping to 152 member *rif* gene family and 30 probes mapping to 30 member *stevor* gene family were designed for our microarray chip.

The expression of all *var* genes was highly synchronous and peaked throughout the ring stage from early ring (4 hpi) to late rings (18 hpi) with the highest levels in mid rings (10-12 hpi) and dramatically decreased in trophozoites (Figure 3-11A) in all clones. Whereas the expression of majority of *rif* genes peaked from mid/late ring to early trophozoite (12-22 hpi) (Figure 3-11B), which follows closely behind the stage of peak *var* expression as previously reported [167]. In contrast, there was larger variability in the peak of *stevor* gene expression with several genes overlapping with *rif* expression (late ring/early trophozoite) while others were expressed in mature schizont stages (36-40 hpi) (Figure 3-11C). The observed diversity in timing of peak expression of *rif* and *stevor* family members suggests their involvement in other biological functions other than antigenic variation and cytoadherence in asexual parasites. Recently, stevor proteins have been implicated to be involved in merozoite invasion and biogenesis of the merozoite surface coat[168]. On the other hand, the tight regulation and uniformity in timing of *var* gene expression is a reflection of the importance of this antigenic gene family in the survival of the iRBC through antigenic switching and immune evasion in the host.

A.

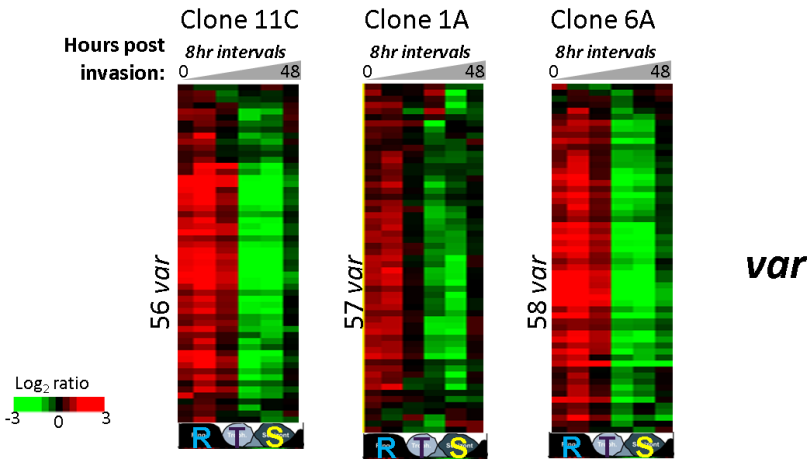

B.

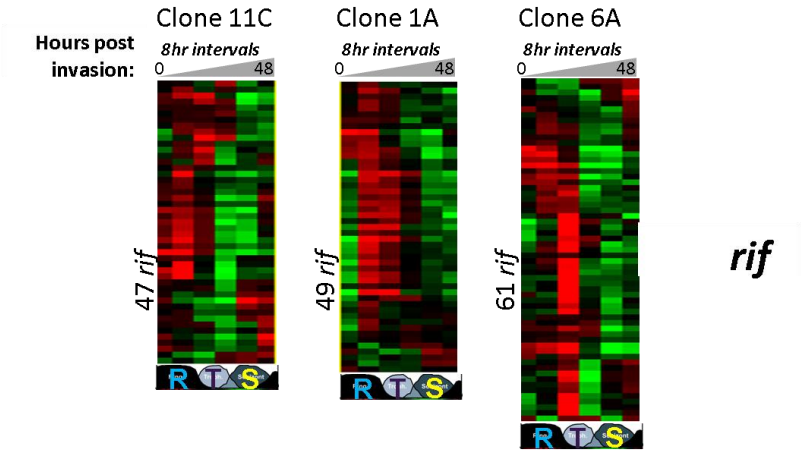

C.

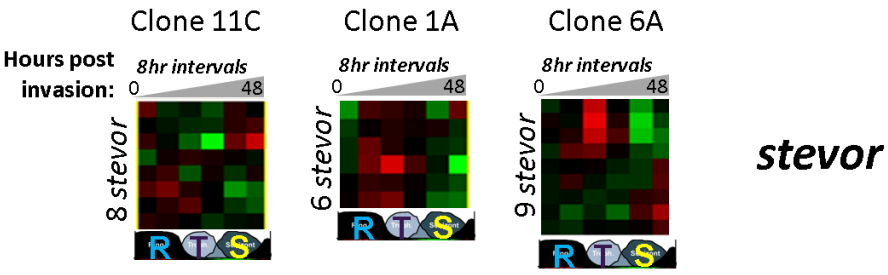

Figure 3-11. Timing of expression of *var*, *rif* and *stevor* genes during the IDC. Heat maps of the mean-centered microarray $\log_2$ ratios showing the timing of peak expression of *var*, *rif* and *stevor* genes across the 48hour IDC from ring (R) to trophozoite (T) and to schizont (S) stage.

3.2.8.2 3D7 Clones are derived from a single parasite

Since studies have shown that a single *P. falciparum* parasite only expresses a single *var* gene member at any one time and the other 59 members are silenced, thus we verified whether the clones were derived from a single parasite by determining the expression level of the *var* gene family. Only full length *var* genes were considered and pseudogenes, *var*-like and truncated *var* genes were excluded. It was observed that between one (clone 6A) to three full length transcripts (clones 11C, 5D and 8B) were dominantly present in each of the clones. Surprisingly, there was no dominant *var* transcript expressed in clone 1A and all transcripts were detected at levels lower

than the parent 3D7 (Figure 3-12A). All 60 members of *var* family were expressed in the parent 3D7 without any single dominant *var* gene which is as expected of a long term culture comprising of a population of parasite clones with heterogeneous expression of *var* genes where all *vars* are randomly expressed [160]. Of the 5 clones, 6A shows the most marked difference in dominant *var* gene transcript level, with the gene PFL1970w expressed at 468-fold above the reference pool and 144 times higher than the mean background transcript abundance. Both clones 11C and 5D expressed the same 2 dominant *var* genes, PFL0030c (*var2CSA*), a type E sub-subtelomeric *var* and MAL7P1.56, a type C2 central *var*, albeit at 3-4 times lower for 5D (Figure 3-12 A). There were 2 dominant *var* transcripts present for clone 8B - PFL1960w, a type C1 central *var* and PFD0020c, a type A1ST subtelomeric *var*. Overall, we observed that the clones expressed dominant *vars* (except for 1A) and hence, each clone was likely to be derived from a single parasite.

3.2.8.3 *rif* gene expression is clonally variant in the presence of a dominant *var*

Besides the *var* family, we observed expression differences in *rif* and *stevors* among the clones. There were 1-3 dominant *rif* transcripts present in the 4 clones (11C, 5D, 6A and 8B) which expressed 1-2 dominant *vars* (Figure 3-12B). Interestingly, clone 6A with a single dominant *var* also expressed a single *rif* (PF11_0021) at 77-fold higher than the reference pool (Figure 3-12B). Although clones 11C and 5D expressed the same 2 dominant *var* transcripts, yet they differed with respect to dominant *rif* genes. While clone 11C expressed 2 dominant *rif* genes - PFD0055w and PFL0025c (Figure 3-12B), clone 5D expressed a single *rif*, PFL2625w, along with intermediate expression of PFL0010c and PFL0025c (Figure 3-12B). In both of these clones, we observed that the presence of the dominant *var2csa* gene, PFL0030c, was associated with high levels of the downstream neighboring *rif* gene, PFL0025c. This

relationship could work both ways and the *rif* gene PFL0025c when highly expressed could result in the active transcription of the neighboring *var* gene, PFL0030c.In clone 8B, 2 *rif* genes (PFF1575w and PFD0025w) were strongly expressed at 13-fold higher than the reference pool (Figure 3-12B). Surprisingly, the dominant *rif* (PFD0025w) is neighboring to the dominant *var* (PFD0020c) although transcription occurs on different DNA strands. Either there exists a shared promoter motif in the intergenic region which is recognized bi-directionally, or their expression is controlled by presence of epigenetic marks (e.g. H3K4me3) at this locus. This will result in the genes found within that locus to be located at permissible sites of active gene expression on the nuclear periphery [131]. The most surprising finding is that clone 1A having all the *var* genes silenced (expressed lower than 3D7), expresses several *rif* genes at similar or higher levels than for the other clones as well as parent 3D7. Similar to the absence of a dominant *var*, there is no dominant *rif* observed in clone 1A (Figure 3-12B). Taken together, the absence of a dominant *var* and *rif* in clone 1A and presence of 1-3 dominant *var* and *rif* in the other 4 clones supports the theory that there is mutually exclusive expression of *rif* family on condition there is dominant expression of a *var* member or vice versa. Hence, it is likely that their allelic exclusive expressions are regulated by the same mechanism of perinuclear positioning and chromatin modification states.

3.2.8.4 *stevor* gene expression is not mutually exclusive

All 5 clones did not show any mutually exclusive expression of the *stevor* family (Figure 3-12C) which is contrary to earlier reports that *stevor* transcription is clonally variant with only 1-3 *stevors* expressed in each clone [164, 169]. Nevertheless, we observed that certain clones such as 1A and 8B expressed the same or almost identical

A.

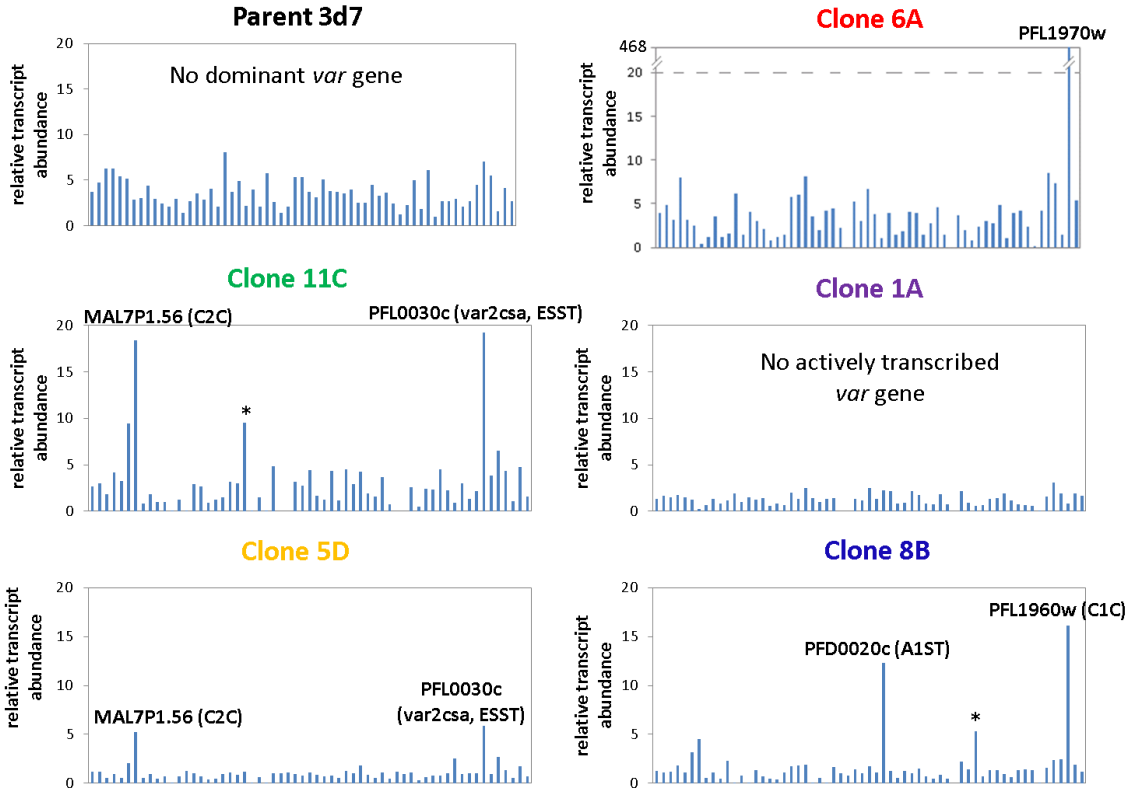
Parent 3d7
No dominant *var* gene
relative transcript abundance
Clone 6A
PFL1970w
468
Clone 11C
MAL7P1.56 (C2C)
PFL0030c (var2csa, ESST)
*
Clone 1A
No actively transcribed *var* gene
Clone 5D
MAL7P1.56 (C2C)
PFL0030c (var2csa, ESST)
Clone 8B
PFL1960w (C1C)
PFD0020c (A1ST)
*

B.

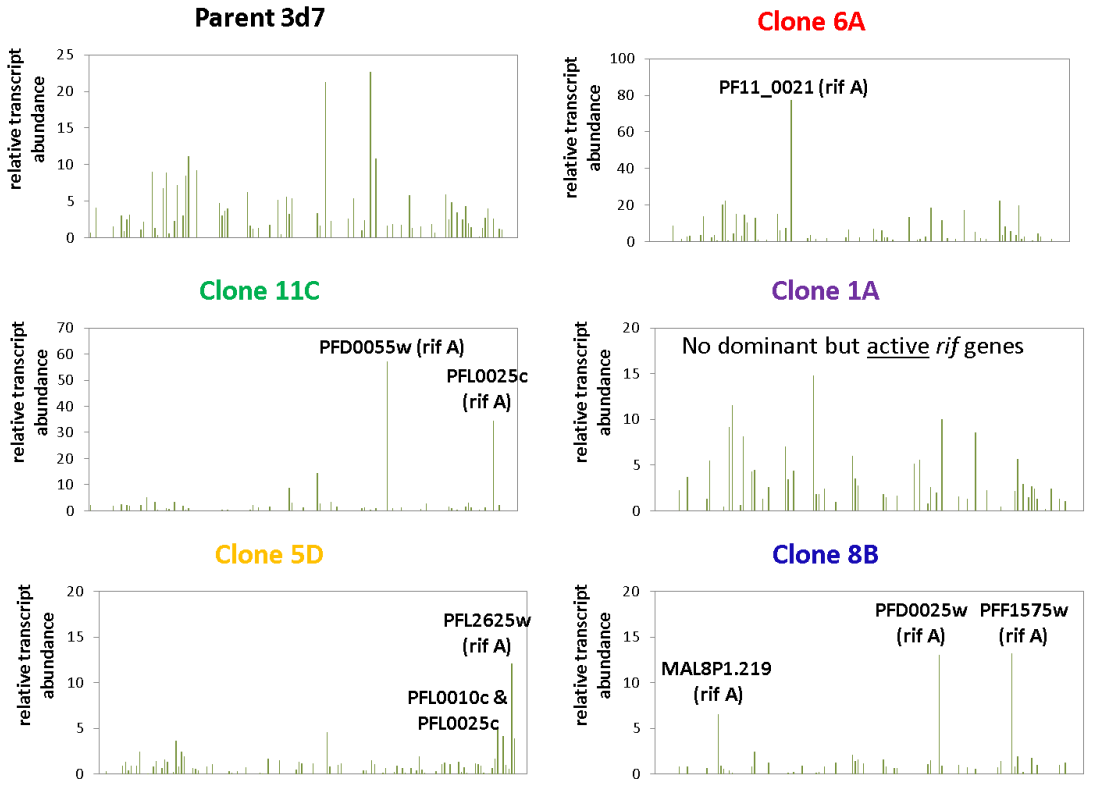
Parent 3d7
relative transcript abundance
Clone 6A
PF11_0021 (rif A)
Clone 11C
PFD0055w (rif A)
PFL0025c (rif A)
Clone 1A
No dominant but active *rif* genes
Clone 5D
PFL2625w (rif A)
PFL0010c & PFL0025c
Clone 8B
PFD0025w (rif A)
PFF1575w (rif A)
MAL8P1.219 (rif A)

C.

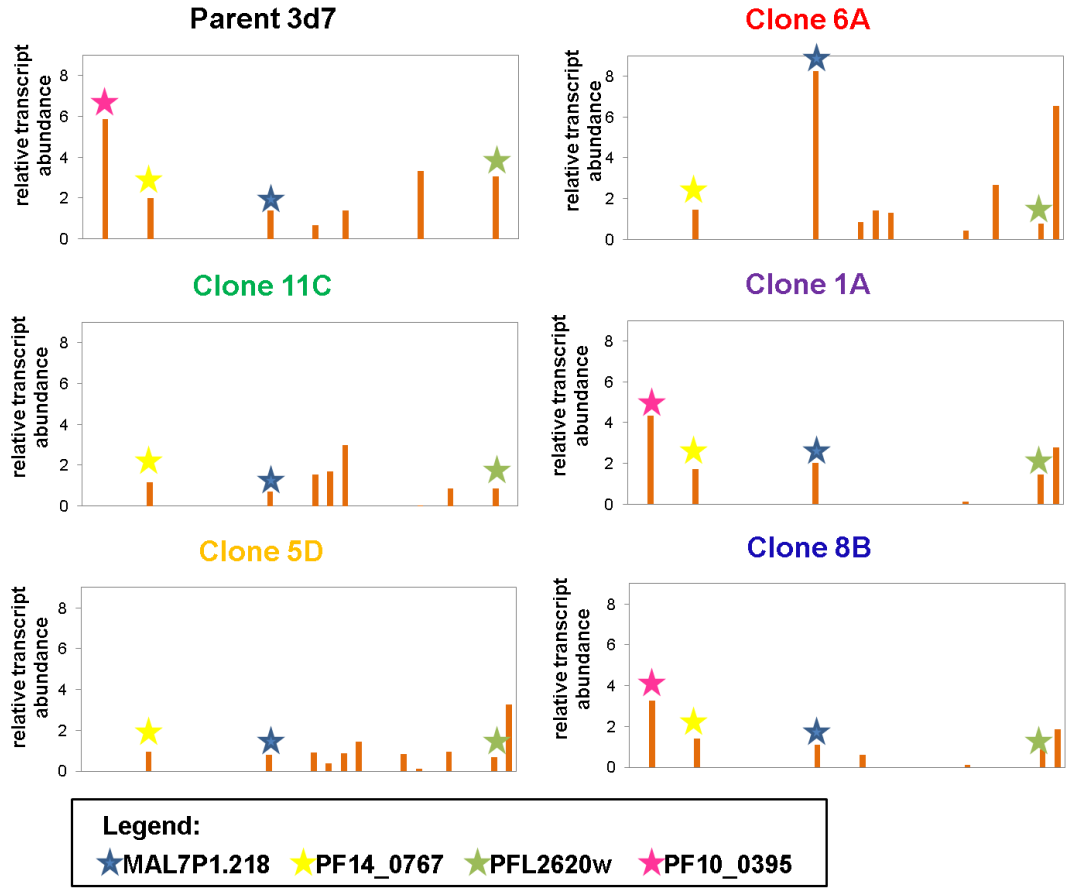

Figure 3-12. *var*, *rif* and *stevor* gene expression levels in the 3D7 clones. Shown above are the relative abundance (non-mean centered, non-log transformed averaged microarray ratio) of A. *var* gene transcripts B. *rif* gene transcripts and C. *stevor* gene transcripts for each clone and parent 3D7 relative to the reference pool. * indicates that <50% probes have signal for that particular *var* gene, hence transcript may be truncated. Only genes with signal above the background + 2SD for at least 50% of probes designed for a gene at the stage of peak expression were plotted. Data shown is the sampling time point for each clone where the maximum total *var/rif/stevor* transcript abundance is observed.

set of *stevor* genes (Figure 3-12C). Despite clone 1A and 8B sharing the same expression pattern of *stevor* genes, yet clone 1A did not display expression of any dominant *var* unlike 8B which had 2 dominant *var* transcripts (Figure 3-12A and C). This observation supports that mutual exclusion of *var* genes does not correlate with the expression of selected *stevor* genes. PF10_0395 is the most highly expressed

stevor in the parent 3D7 at 5.85 fold above the reference pool (Figure 3-12C pink star), which support the data from two previous reports [164, 170] that PF10_0395 is a commonly occurring 3D7 *stevor* gene. Our data suggests that there is either a greater predisposition for this particular *stevor* gene to be transcribed in each individual parasite at every generation or there is a small sub-population of parasites that highly expresses this *stevor* gene already pre-existing in the initial 3D7 culture. The observation that this member is the most highly expressed *stevor* in only 2 out of 5 clones (40%) supports the latter. Of the 30-membered *stevor* family, the most commonly expressed *stevor* genes were PFL2620w, MAL7P1.218 and PF14_0767 whose transcripts were detected in all 5 clones as well as the parent 3D7 (Figure 3-12 C blue, yellow, green stars). Both PF10_0395 and PF14_0767 code for *stevor* proteins that are exported to Maurer's clefts and subsequently expressed on the surface of the iRBC in late trophozoite and schizont stages [166, 169]. Expression of *stevor* genes has been found to be significantly correlated to erythrocyte rigidity and thus plays a role in the sequestration of the infected red blood cells into deep tissues of the host [171]. The overlapping expression of these particular *stevor* genes in the clones may indicate that these are *stevors* essential for cytoadherence in mature stages of the parasite in the host environment and necessary for parasite survival.

3.2.8.5 Clonally variant multi-gene family of *var, rif* and *stevor* in clones

Given that there were 5 clones selected, it is surprising that the repertoire of dominant *var* gene is limited, with only 1 upsA *var* gene, 2 upsC genes, and 1 type B/C gene dominantly expressed among the 5 clones together with var2csa. Moreover, 2 clones, 11C and 5D share the same 2 dominant strain-transcendant *var* genes. Clones 6A and 8B express completely different *vars*, while clone 1A does not express any Figure 3-12A). Overall, we observed that dominant *var* and *rif* members are independent of a

clone's genotype and two clones that have same copy numbers can express different or the same dominant *var* members, thus confirming the role of epigenetic regulation on *var* gene expression. The absence of a single dominant *var* gene being expressed in clone 1A is surprising. One possibility is the occurrence of sequence polymorphisms in the dominant *var* gene simultaneously at various sites. Alternatively, the switching rates might be higher for that dominant *var* gene since *var* genes have different switching rates [160, 172], and thus the expression was reduced to background levels within 20 generations and without having switched to other *var* members. Despite clones 11C and 5D having the same 2 dominant *var* genes, they express different dominant *rif* genes. These points to the 5 clones being non-identical and clonally distinct from each other, with the likelihood that clones 11C and 5D *var* switching patterns are highly similar. 3 out of 5 clones (60%) expressed a upsC *var* due to upsA and upsB *var* genes having higher switching rates than upsC [172]. 2 clones that express a upsC *var* also express var2csa gene dominantly supporting studies that showed that some parasites, especially those expressing upsC *var* genes, may favorably switch to transcribing *var2csa* , between the 15^{th} and 33^{rd} generation of *in vitro* culturing [173]. Var2csa protein, expressed on the iRBC surface , is crucial for the binding of iRBC to host placenta endothelial cells expressing Chrodroitin Sulphate A receptors in pregnancy malaria [174], thereby allowing the parasite to evade immune clearance. It is a well conserved protein found across different strains of *P. falciparum*, such as HB3 and IT4 that cytoadhere to host cells [126]. Recently, a study reported a surprisingly high prevalance of var2csa protein expression in field samples of young Tanzanian children which suggests that var2csa has a role as binding ligand in childhood malaria [175]. The importance of var2csa expression is

shown in 2 out of the 5 clones, and may be a safety net set out by the parasite to ensure binding to host cells and survival long enough to stay in the genetic pool.

3.2.9 *var* gene expression levels changes over 30 generations in culture

A.

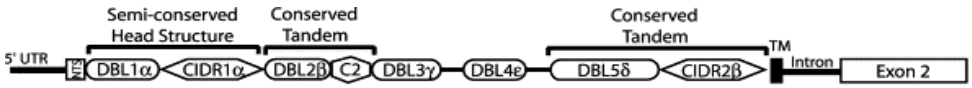

B. C.

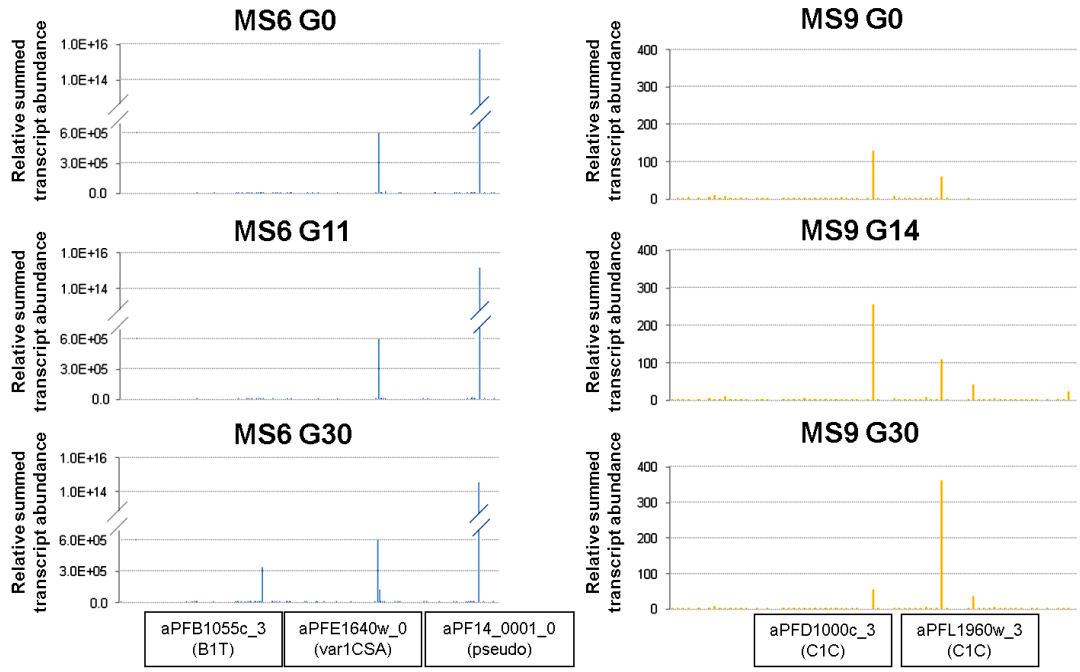

Figure 3-13. Changes in *var*, *rif* and *stevor* gene expression during culture adaptation. A. Canonical structure of a *var* gene comprising of DBL domains and CIDR1 regions (Source: [176]). *Var* probes on our chip are designed for the conserved sequence of the DBL and CIDR domains. B. Relative summed transcript abundance of all 324 *var* gene probes on the chip and filtered for presence in >60% of TPs in each of the 3 generations for MS6 (B.) and MS9 (C.). In boxes are the probes for the *vars* that dominate in total expression levels in the culture. Only probes that had signal above the background + 2SD in at least 60% of the time course (i.e. 5 out of 8 TPs) for each of the 3 generations were considered and KNN imputation of missing data was carried out.

Besides identifying overall transcriptional changes occurring during culture adaptation, we investigated how variant surface antigen family of *var* genes coding for PfEMP1 protein changed in expression levels over 30 generations. Especially since a single *var* member is known to be expressed in a parasite, the expression of *vars* in these isolates would reflect the number of sub clonal types present. Since the probes designed on the microarray chip was specific for only 3D7 *var* genes, and there is a huge repertoire of *var* genes in isolates, hence we compared the expression levels of all 324 probes on our chip that mapped to *vars* including the known 60 member full length *vars* as well as truncated and pseudo *vars*. On comparing the summed transcript abundance for each probe at G0, G11/14 and G30, we observed 2 *var* gene probes were dominant for both isolates at G0, freshly obtained from the patient. Probes for PFL1960w and PFD1000c, both upsC type *vars*, gave high expression ratios for MS9 and probes for PF14_0001, a pseudo truncated *var*, and PFE1640w which codes for var1CSA, showed very high expression ratios for MS6 (Figure 3-13A and B). This indicates that at most 2 sub clones formed the majority of the parasites for each isolate culture. However, for MS9, while the expression of var1CSA gene (PFE1640w_0) remained constant at G11 and G30, the pseudo *var* PF14_0001_0 probe decreased in expression at G11 and G30 (Figure 3-13A). Moreover, a third additional *var* probe, PFB1055c_3 increased in expression dramatically in G30 (Figure 3-13A). Likewise for MS9, we observed unstable levels of *var* probe expression levels during the course of culture adaptation. There was an increase followed by a decrease in expression of PFD1000c_3 probe in G14 and G30 and an overall increase in expression of PFL1960w_3 probe in G11 and G30. In the case of MS6, either the dominant *var* gene (PF14_0001) is switching its expression to another *var* member (PFB1055c), indicating that the culture is undergoing clonal

diversification over time, or there is a minority sub-clonal type expressing this particular *var* gene, PFB1055c in G0 and a clonal expansion of this sub-clone with a clonal reduction in that expressing PF14_0001. Similarly for MS9, we observed that one dominant *var* is being replaced by another *var*, albeit both were the same *var* type upsC. Studies of adapting field isolates to culture have shown that ups A, B, D and E *var* genes tend to lose their expression in culture even within the first 5-30 generations, whereas upsC centromeric *var* expression is relatively more stable [158, 159].

3.3 Discussion

In our study we sought to identify all genes differentially expressed between single 3D7 clones as previous studies may not detect to full extent genes which show variable expression [129]. Overall, we observed that transcriptionally variable genes in single clones are associated with exportome machinery, host-cell interactions (PfEMP1), antigenic presentation and merozoite invasion. Genes encoding for fatty acid synthesis, stress response of molecular chaperones, REDOX, transcriptional regulators, sexual-stage along with hemoglobin digestion form the next level of transcriptionally variant genes. Our study identified similar sets of genes transcribed differently between single parasite lines as reported from a recent study [129]. However, we also identified differential expression in additional gene sets coding for REDOX proteins (superoxide dismutase, cytochrome C oxidase) as well as hemoglobin degradation and heme polymerization (histidine-rich protein III, plasmepsin I, falcipain-2A). As an extension to the study of single clones, we investigated transcriptional changes during culture adaptation and compared differentially expressed genes between clones and those which change during the course of culture adaptation. Overall, we observed a significant overlap of 284 differentially expressed genes in culture adaptation and between single clones of 3D7

(binomial distribution; p-value < 0.001) (Figure 3-14). These genes mainly code for proteins involved in exportome machinery, host-cell remodeling, host-parasite interactions and invasion process.

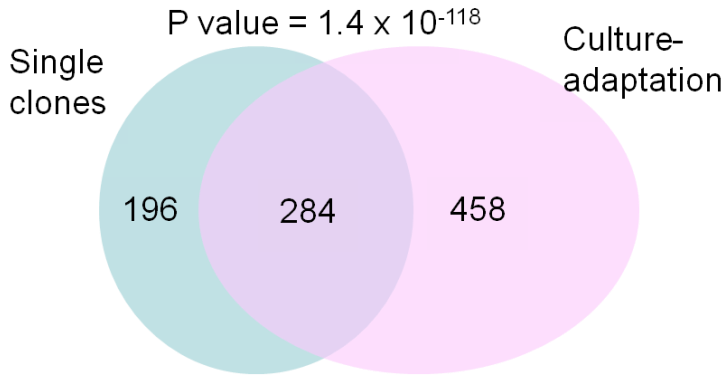

Figure 3-14. Venn diagram showing the number of DE genes identified from the study of transcriptional variation in single clones and during culture adaptation process and the number of DE genes overlapping.

3.3.1 Expression differences in Maurer's clefts and invasion-related genes are not directed transcriptional responses to changing growth conditions

We can conclude that genes representing these functionalities of merozoite invasion and host-cell remodeling (Maurer's cleft proteins) define the list of transcriptionally variable genes between any 2 parasites (5% variable genes). This suggests that there are parasite to parasite differences in the remodeling of the parasite's host cell, diversity in expressed ligands involved in invasion mechanisms and host-parasite interactions. Moreover, we did not find any housekeeping gene or one that is linked to metabolic growth, replication rates or stress response being commonly positively selected for during the culture adaptation of both isolates. This could be due to the nutrient rich culture conditions without external selection pressures which allows for parasites to grow without restriction that undermines the identification of genes that act as rate-limiting factors of parasite growth. Hence, our results demonstrate that

these differences in expression detected over the course of culture adaptation is not specifically related to *in vitro* culture adaptation conditions or a directed growth response to changing environmental (nutrient, stress) condition from host to culture but a general diversification in expression of these genes. This again reiterates that the parasite has a core of stable transcriptional profiles with only 2-5% genes which is consistently variable between any 2 parasite lines [129]. Our findings support the bet-hedging strategy model where diversification in expression of such genes may give the parasite population a higher chance for long-term survival [129].

On another note, our results indicate that the culture conditions are highly suitable for long-term *in vitro* culture of *P. falciparum*, as the transcriptional changes associated with each isolate's culture adaptation are not directly associated with any selection or stimulus. Furthermore, none of the metabolic pathways such as glycolysis, TCA cycle, translation and nitrogen metabolism that are distinctive to the alternate physiological states seen in *in vivo* parasites were differentially expressed during culture adaptation. Hence, it may seem to support that physiologically states seen *in vivo* would remain *in vitro* if these were culture adapted. However, the parasites we studied exhibited typical ring-like transcriptomes when freshly obtained from patients. Thus, to ascertain whether culture adaptation does erase transcriptional profiles associated with the distinct metabolic states, we need to carry out the same culture adaptation experiment using isolates that display such phenotypes. Nevertheless, our results show that since Maurer's clefts and invasion-related genes are always changing in culture, it forms the stochastic background noise which needs to be taken into account when carrying out any comparative transcriptomic studies involving cell lines.

In contrast, genes coding for aminoacyl tRNA biosynthesis, DNA mismatch base repair and ATPase coupled proton transport functions are the least variable in

expression levels between clones, signifying that 1) expression of these genes has to be tightly regulated in order for the parasite to survive or 2) these genes are not under the influence of any immune or environmental pressure. Studies have found that tight regulation of hydrogen transporting ATPase activity is necessary for the survival of plants. In *Plasmodium*, the precise regulation of intracellular pH by these proton pumps may be required for optimal cell growth as the pH would affect the level of enzymatic activities. Moreover, studies have found that the ATP hydrolysis changes the oscillations of nuclear chromatin compaction states which is suggested to play a role in regulation of transcription [177]. Hence, the tight regulation of transcription timing in *Plasmodium*, specifically at non-sub-telomeric regions may stem from the conservation of ATPase coupled proton transport pathways.

3.3.2 Role of differential gene expression and implications for cell survival

Essentiality of differentially expressed genes in *in vitro* cultures?

Several genes which show differential expression may not be essential for survival of the parasite under *in vitro* culture conditions as evidenced by the ability of two clones (6A and 1A) to survival even with the absence of genes involved in *var* gene presentation (KAHRP) as well as a acyl-coA synthetase. Since these genes are commonly found as members of gene families, there are redundancies in gene function. Hence, decreased expression of one member may not be limiting to a parasite's growth as other members may compensate for the lack. Immune evasion and changing host cell environments drives the expansion of these families [178]. Since the parasite survives within the host RBC for almost the entire duration of the IDC, it needs to ensure that the microenvironment within the host RBC is suitable and that the parasite is able to evade host cell immune responses while obtaining its

unique nutrient requirements from the external environment of host serum. In the context of a host, a certain level of expression of genes pertaining to host-cell binding, oxidant defense or nutrient acquisition is required for escaping and overcoming any immune assaults and obtaining the necessary metabolites for optimal survival. In contrast, in the nutrient-rich environment without any selection pressure such as the *in vitro* culture, the expression of these non-housekeeping genes is diversified without compromising the parasite's survival.

3.3.3 Is REDOX a stochastic expression or directed transcriptional responses?

The phenomenon of differential expression in *Plasmodium* clones has its advantages and may be essential for the overall propagation of the species. Diversity in expression levels of these genes in individual parasites increases the chances of a sub-population to survive in a multitude of different host environments and through harsh, stressful conditions on the pretext of a bet-hedging strategy as proposed recently [129]. However, this does not exclude a possibility that the parasite may also exhibit directed transcriptional responses to a local stimulus which allows for better adaptation to that condition. Transcription of chaperones and redox enzymes may be regulated by the parasite's local redox state. A study in mice showed that the modulation in mitochondria redox state which was driven by an increase in ROS in mice resulted in higher transcription and elevated mRNA levels of nuclear genes, thioredoxin and *sod2*, which are targeted to the mitochondria [179]. Increased expression of *sod* was also associated with lengthening of the cell cycle [180]. Interestingly, we observed that the clone 1A with heightened levels of *sod* throughout the IDC also required a longer time (~8 hr longer than other clones) to complete a lifecycle as it progressed to mid schizonts after 48 hour of sampling. ROS has also been shown to promote expression of glutamate dehydrogenase in plants [181]. Hence, variable expression of redox

genes (*sod*), glutamate dehydrogenase and chaperones (heat-shock proteins 70 and 86) in clones may be the parasite's direct transcriptional responses and adaptive states under environmental and oxidative stress by increasing its antioxidant defense. However, studies in *Plasmodium* have shown that parasites subjected to heat shock treatment do not result in changes as robust as in yeast or humans [182] even though febrile temperatures did induce significant up-regulation of *hsp70* and *hsp86* by 5.3 and 2.4 fold respectively along with other biological functions [151].

3.3.4 Transcriptionally variable genes are enriched at the Sub-telomeres of Chromosomes in positionally enriched clusters

It is interesting to note that there is a propensity for genes which were found to be differentially expressed in both clones and culture adaptation to be located towards chromosomal ends, indicative of a certain level of transcriptional "looseness" at the regions. These usually comprise of invasion-related genes or those involved in exportome machinery. Hence, the physical location of genes may be another factor which contributes to the level of transcriptional variation between parasites. Transcriptional responses of *var* genes to biological stress (oxidative stress and glucose deprivation) is dependent on the sequence of promoters and physical position of the *var* genes as sub-telomeric *vars* were found to be repressed while the centrally located *vars* were induced in expression [183]. However, it is not known of the association of transcriptional variation of non-VSA genes and location on the chromosomes. The mechanism controlling such variation in transcriptional levels is worth further exploring. A study has shown that there is an overlap between PfHP1 (heterochromatin protein 1) binding sites and sub-telomeric multi-gene exported protein families as well as invasion proteins [146], several of which were observed to be differentially expressed in our study. Yet only 5.8% of DE genes in single clones

and 5.9% of DE genes in culture adaptation were associated with PfHP1 protein. Hence, for the other ~95% DE genes, there are likely other mechanisms controlling their differential expression from clone to clone. In addition, the presence of positionally-enriched clusters of the differentially expressed genes indicates there is co-regulation in gene expression based on position in the chromosome and could indicate that their variant expression is related to bistable chromatin microdomains present at these clusters. As suggested, these regions of bistable domains may switch from transcriptionally-repressive heterochromatin to transcriptionally-permissive euchromatin states spontaneously from one clone to another and through different generations as shown to be the case for the invasion-related gene *eba-140* [133]. It would be interesting to investigate the driving molecular factors that underlie the variegated expression of these other genes, such as *rex*1,3, 4, zinc binding proteins and AP2 transcriptional regulators and falcipains by sequencing the promoters upstream of these genes and carrying out chromatin immunoprecipitation sequencing (ChiP-Seq) for various histone marks in these clones in order to determine whether the transcriptional variation in gene expression is correlated to levels of histone marks at these gene clusters. In addition, one should look at the heritability of gene expression levels of these clonally variant genes over consecutive generations and couple this with chromatin immunoprecipitation-chip experiments using antibodies targeting proteins like modified histone tail marks or the HP1 which occupies mainly sub-telomeric gene families [146]. The levels of these enrichment marks may have a role in the change in expression level of these genes by modifying the chromatin states at these chromosomal ends. Sequencing these single parasite lines as well as performing ChIP on chip experiments on single clones would give us a more accurate

picture of the contribution of epigenetic plasticity on transcription levels between clones.

3.3.5 Is change in expression levels during culture adaptation largely A) stochastic differences in expression levels between clones or B) selection driven changes in proportions of sub-clones in population over time?

We propose two models to explain the transcriptional variation observed and process of culture adaption. As mentioned, clones can diversify their transcription levels of certain genes when grown in culture over time. In the first model, we hypothesize that the parasites although clonal in the beginning produces progenies which vary in gene expression levels with regards to invasion and Maurer's cleft genes, a result of stochastic transcriptional variation [129] (Figure 3-15A). In the second model of selection driven transcriptional change, different sub-clones pre-existed in the initial field isolate culture and during the process of long–term culture adaptation of the field isolate, the proportion of abundance of one to the other may change over the course of culturing, with the initially dominant one now being overtaken by the other sub-clone (Figure 3-15A). Differences in cycle time, number of merozoites and general fitness of the clone leads to differences in growth rates and can cause a fitter clone to outcompete the other [184]. This means that overall gene expression differences we observed in relation to culture adaptation process is the result of comparing populations of parasites with differences in proportions of sub-clones.

One way to verify which of the two models explains the variation leading to transcriptional differences between clones/isolates is to carry out limiting dilutions of a field isolate (with multiplicity of infection of 1) to obtain single clones, subsequently culture them over several generations and perform transcriptional

profiling of the synchronized cultures across the IDC at each successive generation (eg. generations 5, 6 and 7). Since *var* gene expression is the best indicator of a culture's clonality because a parasite only expresses a single *var* member in any generation, we can determine if the global expression profiles are preserved and whether the group of genes, which were identified as transcriptionally variant, does change in expression over successive generations. If the same *var* dominant member is expressed in 2 successive generations of a single clonal population, yet the parasites display differences in expression of the exportome and invasion-related genes, then model 1 supporting the idea of stochastic gene expression of these multi-gene families is correct. However, we cannot exclude that the scenario depicted by model 2 arises in the adaptation of a field isolate to *in vitro* culture conditions. To verify if model 2 is true, the single clones derived from the field isolate by limiting dilution can be cultured for 30 generations and monitored for growth rates in terms of invasion rates and length of IDC and importantly, how many clones survive the course of adaptation to culture for 30 generations. To extend a step further, we can mix the two clones having the highest and lowest growth rates and monitor the expression of each clone's dominant *var* gene in the population along with the expression of the known transcriptionally variant genes across generations. Overtime, if we observe the *var* gene expression of the fitter clone increases proportionately to the *var* gene expression of the other clone, then we can conclude that the clone with higher growth rates has outcompeted the clone with lower growth rates and that the fitness of individual parasites in the field isolate population does change the proportions of sub-clones during culture adaptation. Moreover, if the ratio between the two clones' dominant *var* expression is similar to the ratio between the clones' expression of the other transcriptionally variant genes, then we can conclude that fitness and growth

rates of the clones did contribute largely to the transcriptional variation observed during the culture adaptation process in our study and the second model is true.

In light that there was no metabolic, growth-related or cell-cycle associated pathway and no specific genes that were selected for during the culture adaptation process of both isolates to strongly suggest that a particular pre-existing sub-clone was selected for, our results support the first model. Moreover, the broad transcriptional difference between isolates are maintained throughout from *ex vivo* culture to *in vitro* culture at 30 generations and the changes in the transcriptional levels were significantly smaller in magnitude between generations of an isolate than between isolates. Furthermore, looking at *var* gene expression of all probes for MS6 and MS9, we observed that despite *var* gene expression signature being highly conserved at generations 0 and 11 (Figure 3-13B), yet we observed transcriptional variation in genes associated with host-cell remodeling and invasion. Regardless of these scenarios, a clone that is subjected to long-term culturing over years will very likely undergo genetic mutations usually in the unstable chromosomal ends which will produce sub-clones in the population and may result in greater transcriptional differences (Figure 3-15B).

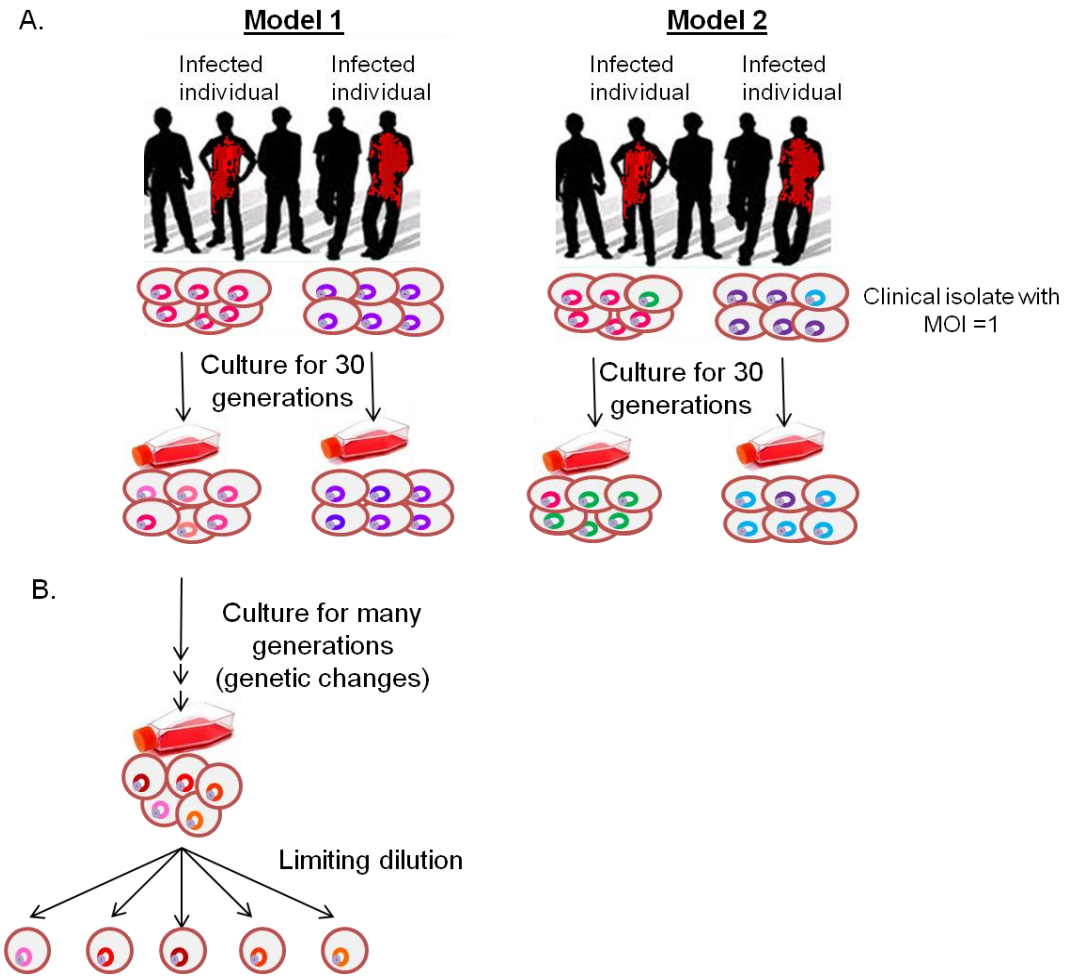

Figure 3-15. Model describing transcriptional variation over culture adaptation.
A. Proposed model illustrating the changes that occur in a parasite population (with multiplicity of infection = 1) over culture adaptation. Model 1: stochastic gene expression difference of certain gene sets such as Maurer's cleft and invasion-related genes occurs between *ex vivo* and *in vitro* cultures as a form of transcriptional diversification from the original clonal population. Model 2: Heterogeneity of clones may be present in a field isolate. A clone of small minority can outcompete to become the predominant clone within the parasite culture if it has better growth and invasion rates under *in vitro* culture conditions. B. Although limiting dilution of the starting field sample gives rise to a single isogenic clone, spontaneous duplications and deletions in the genome often occurs during long term *in vitro* culture and produces clones with genetic diversity adding to the another layer of transcriptional differences.

Chapter 4 : Transcriptional profile associated with Artemisinin resistant field isolates

4.1 Introduction

Artemisinin combination therapy (ACT) is recommended by the World Health Organization as the first-line treatment for falciparum malaria in all endemic regions [185, 186]. The excellent effectiveness and tolerability of ACTs brought new enthusiasm into world-wide efforts to eliminate human malaria which until today accounts for 243 million cases of infection and 863,000 deaths per annum [187]. The core components of ACTs - artemisinin and its derivatives, provide an important alternative to quinoline and antifolate-based compounds. Resistance to these older compounds that emerged on the Thai-Cambodian border and subsequently spread across the world has severely compromised their use and contributed to a dramatic rise in malaria morbidity prior to introduction of the ACTs in the late 1990's [188-191]. Learning from past mistakes, much effort is being invested in proper management of ACTs in order to sustain their efficacy and prevent the spread of resistance [20]. In spite of these efforts, there have been sporadic reports of artemisinin resistance *in vivo* and *in vitro* for many years (from Yunnan Province, Southwest China [152], Vietnam [71] and French Guiana [76]). Although the biological and clinical significance of these reports were uncertain [192], these early warning signs suggested a possibility of emergence of malaria parasites resistant to artemisinin [193-195]. Recently, unequivocal evidence of reduced artemisinin susceptibility from Western Cambodia has been reported [66]. Curiously, this was also the epicenter of chloroquine and sulfadoxine-pyrimethamine resistance. Dondorp et al. (2009) documented markedly prolonged parasite clearance times (median pct 84

hours (interquartile range 60 to 96 hours) in Pailin, Western Cambodia. This compares with a median pct of 48 hours (36 to 66 hours) on the Western border of Thailand [46, 66]. Since this study, reports of delayed parasite clearance and early treatment failure have emerged and been confirmed in other parts of the region, including the Thai-Myanmar border [66] (Figure 4-1). Although it has yet to be established whether artemisinin resistance has spread westward [185], the possibility of the spread of resistant parasites through Asia to Africa would be disastrous.

A.

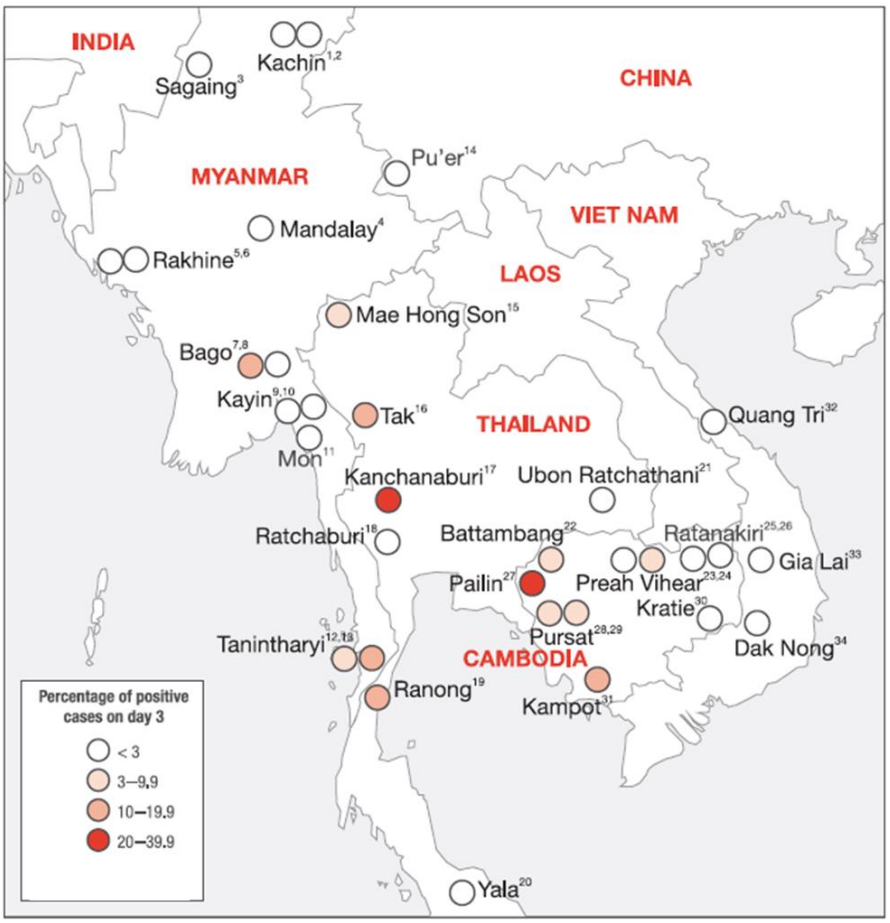

B.

Figure 4-1. Percentage of artemisinin resistant cases across South East Asia between 2006 and 2010. A. Percentage of total malaria cases in each site of early treatment failure represented by persisting malaria parasites in the patient on day 3 post treatment with ACT (e.g. Artesunate and mefloquine). B. Percentage of total malaria cases of late treatment failure indicated by recrudescence of parasites at day 28 post treatment with ACT. (Source:[46])

The mechanism of artemisinin resistance is unknown. The resistant phenotype detected in Western Cambodia does not associate with any polymorphisms in the established drug resistance markers [66]. *In vitro* susceptibility testing of parasites which are cleared abnormally slowly *in vivo,* showed essentially no shift in IC_{50} (50% inhibition concentration) values *in vitro* [66]. This apparent discrepancy between the experimental and the clinical data may be explained by the reduced susceptibility of

Plasmodium parasites at only the ring stage (first third) of its 48 hours intraerythrocytic developmental cycle (IDC) [66, 196]. Another phenomenon that has been suggested to explain artemisinin resistance is an increased propensity for these parasites to form "dormant" (or quiescent) rings under artemisinin exposure [197, 198]. However, this process, suggested by *in vitro* studies, is unlikely to explain the slow first order decline in parasitemia with time that was observed in Western Cambodian patients treated with artemisinin-based drugs [199]. The reduced artemisinin susceptibility phenotype of the resistant malaria parasites exhibits a heritable pattern with 56-58% of the variation in clearance rates explained by a parasite genetic basis [200]. Identifying the genetic determinants will be crucial for understanding the molecular basis of artemisinin resistance and will also provide an important molecular tool for epidemiological surveys. Here we carry out genome-wide gene expression analyses in order to identify key elements of a transcriptional profile underlining artemisinin resistance. We show that the *P. falciparum* parasites with slow clearance after artemisinin treatment exhibit reduced expression levels of generic metabolic (e.g. glycolysis, nucleotide metabolism) or cellular (e.g. DNA replication) pathways in the ring and trophozoite stages but strong increased expression of essentially all functionalities associated with protein synthesis, folding and trafficking in the schizont stages. This specific "tune-up" of the transcriptional pattern in these resistant *P. falciparum* isolates is associated with altered expression of a number of genes involved in cell cycle regulation, transcription regulation, chromatin remodeling as well as intracellular signaling. Altogether these results provide the first set of testable genetic markers associated with artemisinin resistance.

4.2 Results

4.2.1 Gene expression associated with artemisinin resistance

The main purpose of these studies was to characterize the transcriptional profile associated with artemisinin resistance in field isolates of *P. falciparum* [66]. For this, we conducted DNA microarray analyses of parasites collected from patients in Pailin, Western Cambodia which had slow parasite clearance (detectable parasitemia 78-96 hrs following administration of ACTs; isolates CP025, CP037 and CP040; Figure 4-2).

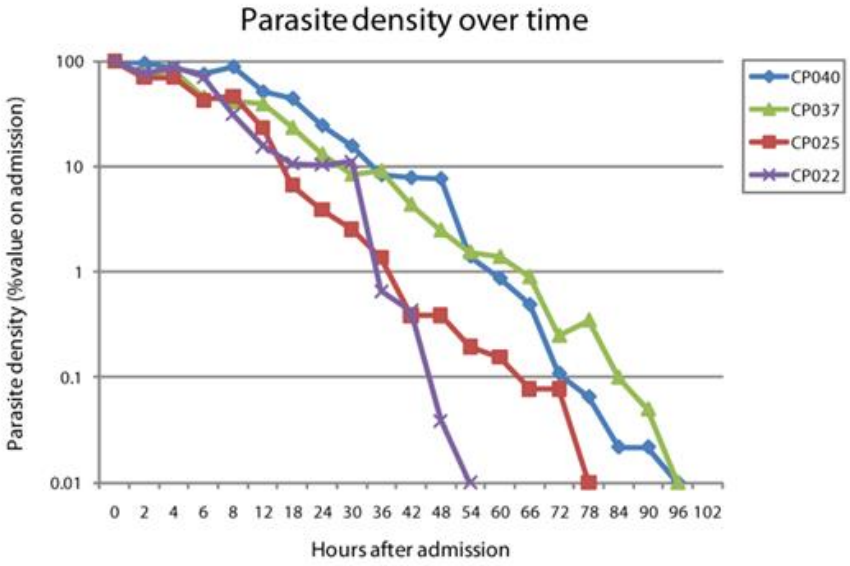

Sample	Arm	treatcode	para0	prr24	prr48	modelpc50	modelpc90	pct
CP 022	AS7(Split)	2	103,996	9.63	2,599.92	7.17	18.46	54.00
CP 025	AS7(Split)	2	20,598	25.75	257.48	5.41	17.98	**78.00**
CP 037	AS7	1	80,384	7.62	40.19	8.55	29.24	**96.00**
CP 040	MAS3	3	73,852	4.08	13.07	13.86	30.82	**96.00**

Treatment arms:

1. AS7 - artesunate 6mg/kg once daily for 7 days;
2. AS7(Split) - artesunate 3mg/kg twice daily for 7 days;
3. MAS3 - artesunate 8mg/kg once daily for 3 days followed by mefloquine;

Figure 4-2. Parasite density over course of treatment and treatment outcomes. Plot of the parasite densities (relative to starting parasite numbers on admission) from the time of patient's first admission date up to 100 hours after admission. Of the 4 isolates from Pailin, Cambodia, only 3 (CP025 (red), CP037 (green), CP040 (blue)) display significant delayed parasite clearance time (pct) of 78 and 96 hours from the patients after treatment while CP022 (purple) parasites was cleared earlier at 54 hours after treatment. The initial parasite numbers upon admission (para0) and parasite reduction ratio at 24 hours (prr24) and 48 hours (prr48) are included in the table. The prr24 and prr48 is the ratio between the parasite count on admission and at 24 hours or 48 hours respectively as determined from microscopy. The modelpc50 and modelpc90 are the time to 50% or 90% reduction in parasite density (hours) following treatment. Artesunate and mefloquine treatment regimens administered are listed.

For comparison we analyzed transcriptomes of additional Southeast Asian isolates collected from Xepon, Savannakhet Province, Laos (isolates BMT061, BMT076, BMT077, XPN003), from Mae Sot, Thailand (isolates NHP2094, NHP4459, NHP4460), and one additional isolate from Pailin (CP022) with normal clearance (~54 hour). At the time of collection, all isolates exhibited high synchronicity; ~100% parasites were at the ring stage. Parasites were then cultured for up to 48 hours *in vitro* and total RNA was isolated from samples harvested at regular intervals of 2-8 hr.

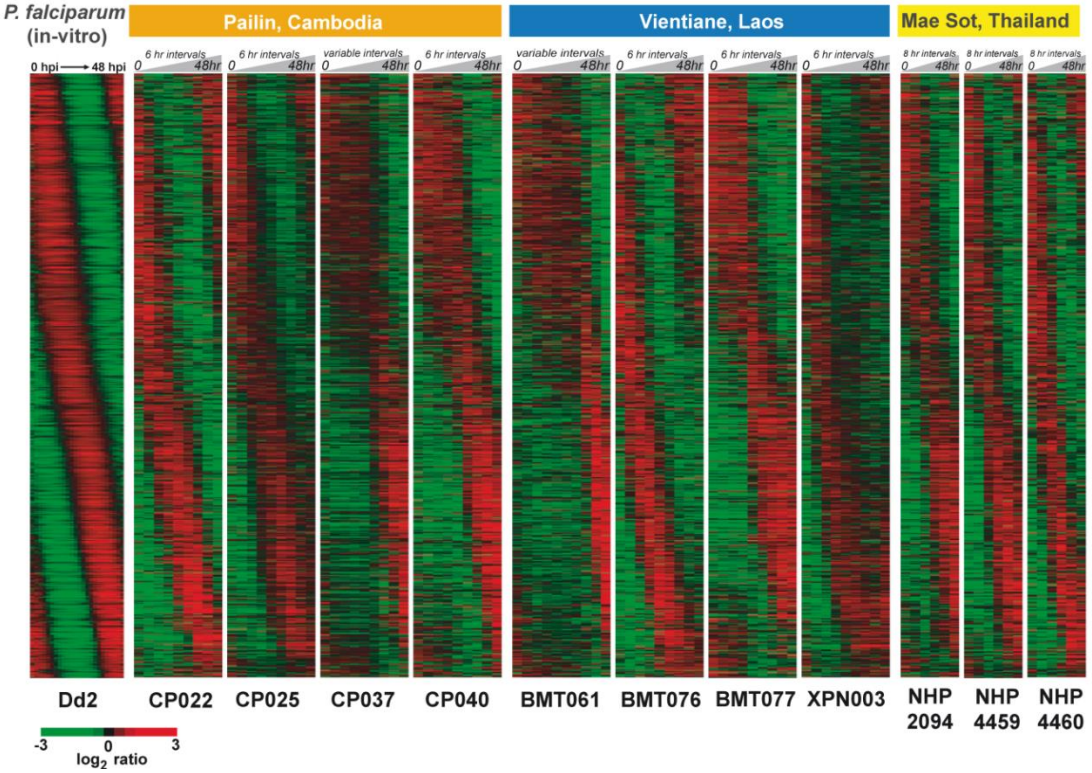

Figure 4-3. *Ex vivo* transcriptomes generated of the field isolates from S.E. Asia. Transcriptomes of the *ex vivo* IDC of all 11 field isolates from the 3 geographical locations measured over 48 hour sampling time. Only genes with at least 80% of time points with a positive signal were included for each of these transcriptomes. The phaseograms were constructed by ordering the mean-centered $\log_2$ microarray expression ratios to the genes ordered by phase calculated from the Fast Fourier Transformation of the Dd2 reference *in vitro* lifecycle.

Similar to previous experiments on *in vitro* adapted isolates [96], these *ex vivo* samples displayed extensive stage specificity in transcriptional regulation during their 48-hour IDC (Figure 4-3). However, in contrast to the *in vitro* conditions, the assembled *ex vivo* transcriptional profiles indicate considerable differences in the rates of stage progression (Figure 4-4A; Figure 4-3). Using a Spearman-rank/Pearson correlation method, we identified a best fit of the "age" of each *ex vivo* experimental point based on peak correlation values using the previously generated *P. falciparum* IDC transcriptome *in vitro* [86]. Here we observed that while at the time of blood collection, all parasite populations correspond to the ring stages (10-16 hours post invasion, hpi), the subsequent IDC development was subjected to significant fluctuations (Figure 4-4B). 5 out of the 11 isolates (BMT061 and BMT077 from Laos, NHP2094 from Thailand and CP040 and CP037 from Cambodia) exhibited an initial developmental arrest in the ring stage for 16-24 hours post collection (Figure 4-4B). In spite of this initial arrest, these isolates reactivated their IDC progression and developed unidirectionally through trophozoite and schizont stages. The progress of the *ex vivo* cultured *P. falciparum* isolates through these later stages was also uneven. The most extreme example is the Lao isolate BMT077 that showed additional arrests in the trophozoite and early schizont stages at 30 to 48 hours post collection (Figure 4-4A and B). Overall, the developmental shifts in the IDC progression do not correlate with the site of collection, thus excluding the possibility of experimental bias due to culturing techniques in each field laboratory. These data support the previous observation of Lemieux et al (2008) who showed that the ages of 25 *P. falciparum* isolates cultured *ex vivo* for 48 hours fell into a large interval of 20-44 hpi [101].

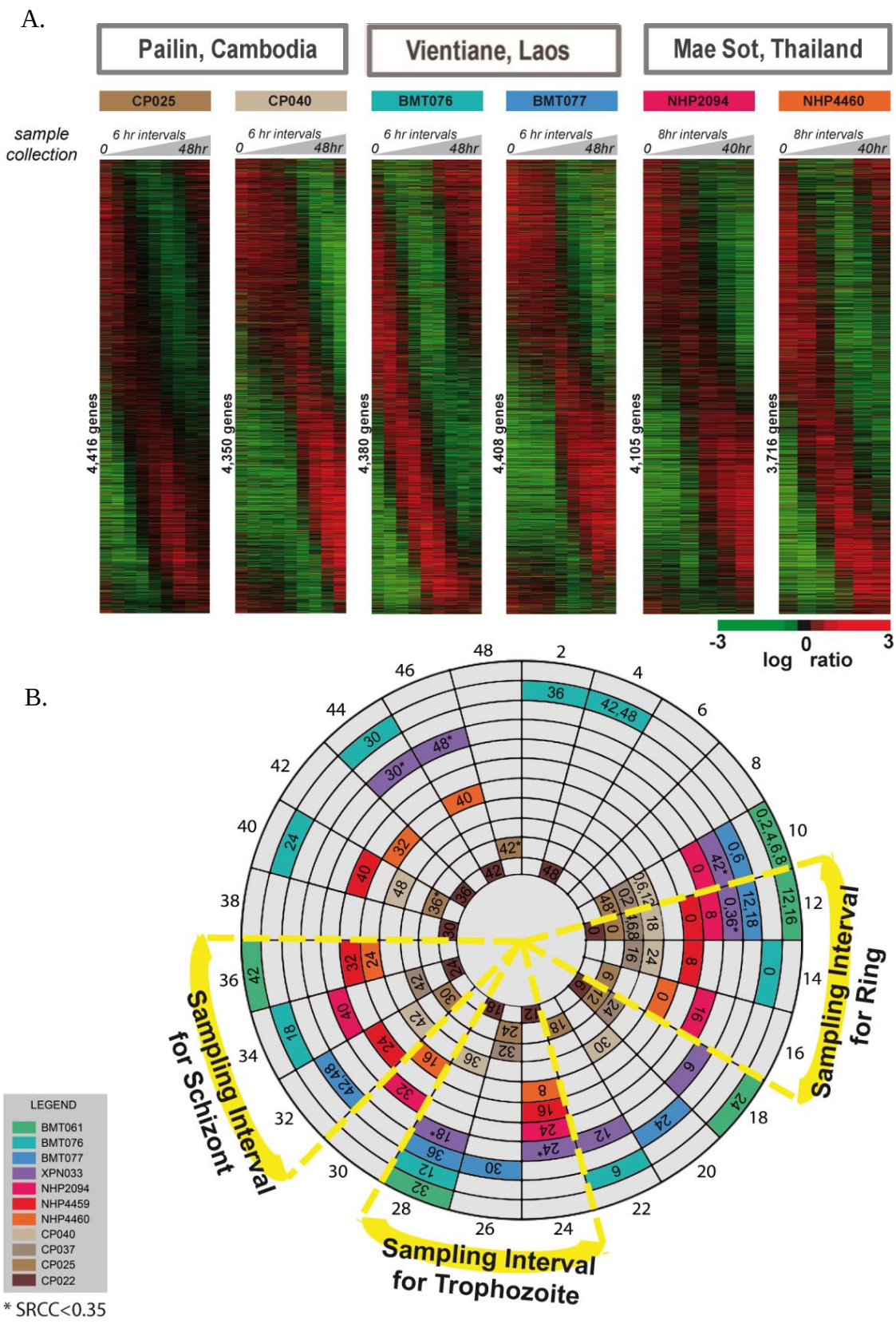

Figure 4-4. Transcriptome analyses of the *ex vivo* cultured *P. falciparum* parasites. A. Transcriptomes of the *ex vivo* IDC of 6 field isolates (representative set of total 11 transcriptomes generated in this study) from the 3 geographical locations over 48 hour

sampling time. The heat maps represent the mean-centered $\log_2$ microarray expression ratios for the *P. falciparum* genes that were ordered according to the phase calculated by the Fast Fourier Transformation for the reference *in vitro* IDC transcriptome. B. Age estimate of the *ex vivo* culture time points for all 11 field isolates. Each colored box represents age estimate (hpi; shown by numbers outside the circle) of the isolate sample relative to the *in vitro* reference IDC transcriptome calculated as a best fit Correlation (Spearman rank, see materials and methods). Indicated within each box is the sampling collection time with respect to the first sampling time denoted by 0h that correspond to the initial sample collection from the infected patients prior to culturing. Sampling times with * represent Spearman Rank correlation value less than 0.35 which indicates a deteriorating synchronicity in the later IDC time points and were excluded from the analysis. Time points included in 3 windows (yellow frame) corresponding to rings at 12-16 hpi, trophozoites at 24-28 hpi and schizonts at 32-36 hpi were selected for further analysis.

In addition, the correlation coefficients between the mRNA profiles of field isolate time points and the *in vitro* control transcriptome are above 0.55 which demonstrates a good synchronicity of the *ex vivo* cultures (Figure 4-5). Taken together, these data show that careful assessment of the parasite stage of development (age) at any experimental time point using a reference dataset is essential in *ex vivo* analyses of *Plasmodium* parasites. Overall, the developmental shifts in the IDC progression do not correlate with the site of collection, thus excluding the possibility of experimental bias due to culturing techniques in each field laboratory.

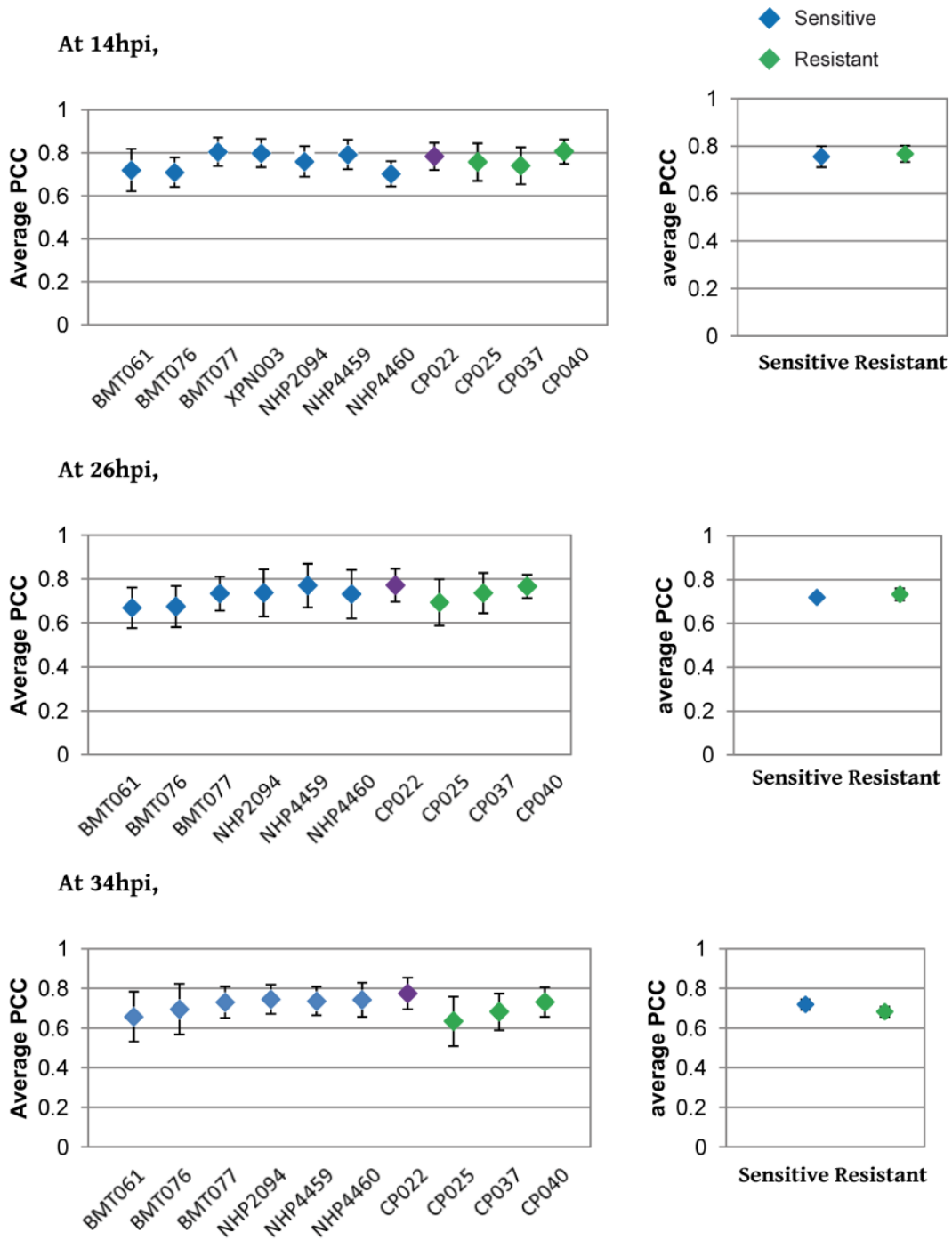

Figure 4-5. Distribution of Pearson correlations between all isolates for the three stages. Including isolate time points that correspond to the 3 stages – 14 hpi, 26 hpi and 34 hpi, graphs shown are average pearson correlation calculated from multiple pairwise comparisons between all isolates (graphs on left panel) and the average of the PCC for the resistant and sensitive parasites (graphs on right panel) at 14 hpi (a), at 26 hpi (b) and at 34 hpi (c). Error bars represent the standard deviation of all the pair-wise comparisons.

To identify genes whose expression is associated with artemisinin resistance, we compared global transcription levels between the three artemisinin resistant isolates and the remaining sensitive isolates by analyzing steady state mRNA levels in 3 developmental stages; ring (12-16 hpi: hours post invasion), trophozoite (24-28 hpi) and schizont (32-36 hpi) (Figure 4-4B). For that, we included the experimental time points that show highest correlation value to the *in vitro* reference transcriptome [86] within these sampling intervals (Figure 4-4B). Overall, we identified 160 (3.9%), 198 (4.9%) and 373 (9.2%) genes that are up-regulated and 278 (6.9%), 344 (8.5%) and 232 (5.7%) genes that are down-regulated in the resistant parasites (p-value < 0.01) at the ring, trophozoite and schizont stages, respectively (Figure 4-6).

Interestingly, the majority of the genes over-expressed in the ring stage of the resistant parasites correspond to trophozoite- specific genes (peak mRNA abundance in the normal IDC) and the genes over-expressed in the schizont stages represent mainly ring and trophozoite specific transcripts (Figure 4-6). The genes up-regulated in the trophozoite stage are evenly distributed between ring and schizont specific transcripts. This indicates that the transcriptional up-regulations associated with artemisinin resistance constitute either accelerated timing of transcription of trophozoite and schizont genes at the ring stage, or prolonged expression of ring and trophozoite transcripts in the schizont stage. Intriguingly, this pattern was not observed for down-regulated genes whose expression in artemisinin resistant parasites coincides with their expected stage specificity, albeit at lower levels than expected in the artemisinin sensitive isolates (Figure 4-6). Taken together, these results suggest that artemisinin resistance is associated with specific modifications of the IDC transcriptional cascade that involve a large number of genes and presumably alter the levels and temporal distributions of biological and cellular functions.

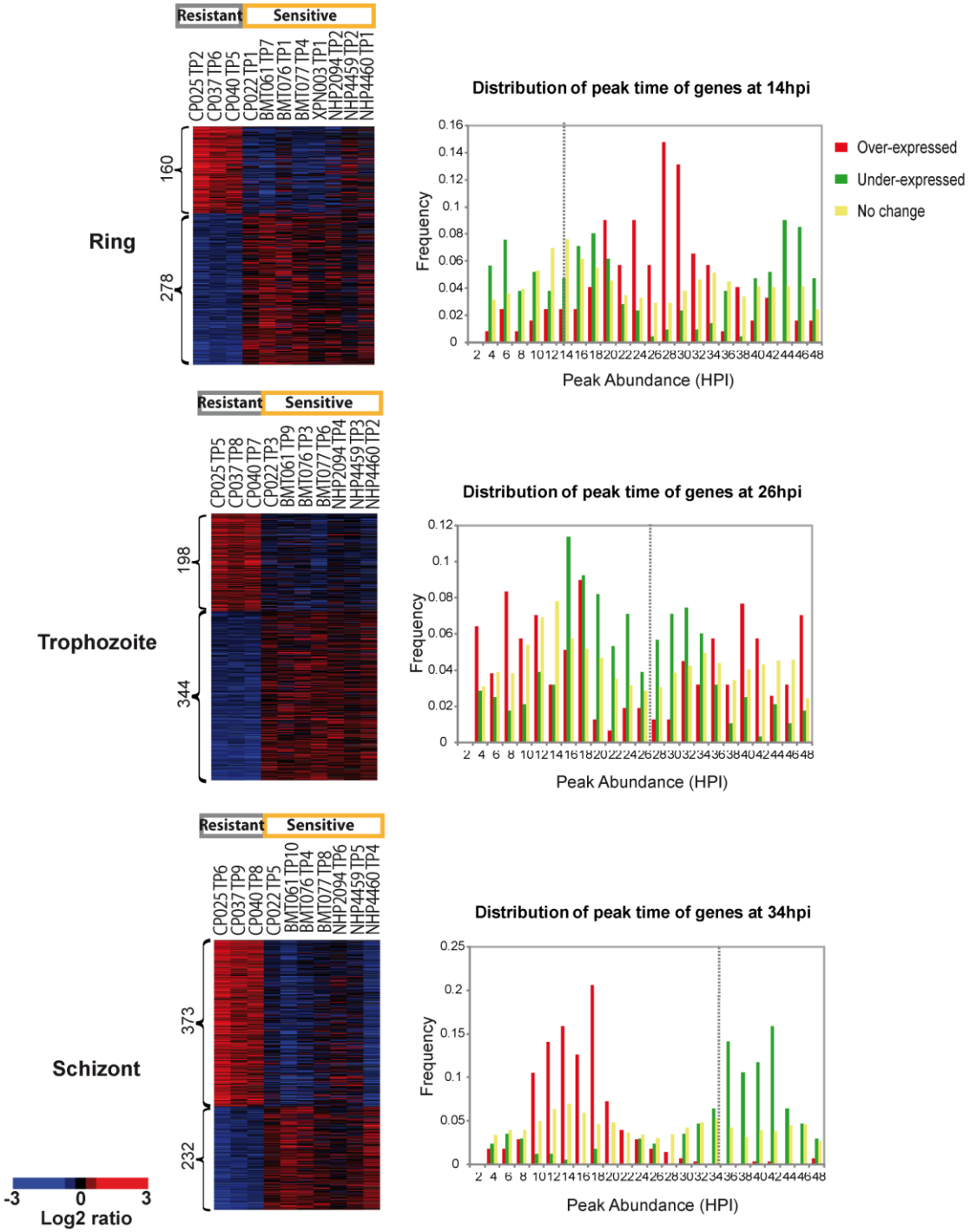

Figure 4-6. DE genes between the artemisinin resistant and sensitive parasites. Clusters of genes with significant differential expression (p-value < 0.01) between the resistant (grey) and susceptible (orange) parasites at ring (14 hpi), trophozoite (26 hpi) and schizont (34 hpi) stages. Shown are the mean-centered expression $\log_2$ ratios for these genes ranked by the z-score based on the differential expression between the resistant and susceptible isolates. Graphs represent the frequency distribution of the peak abundance time in the IDC transcriptome for each group of genes: over-expressed (red bars), under-expressed (green bars) or no significant change in expression (yellow bars). The grey lines represent the middle of the time IDC interval used for the analysis (e.g. ring, (14 hpi), trophozoite (26 hpi) and schizonts (34 hpi).

4.2.2 Functional analysis of artemisinin resistance associated genes

To evaluate the physiological relevance of the identified differential gene expression, we utilized Gene Set Enrichment Analysis (GSEA) [110] to explore functional assignments of genes associated with artemisinin resistance (Figure 4-7; Supplementary Figure 1). We found that genes down-regulated at ring and trophozoite stages represent well established biochemical and cellular pathways such as glycolysis, pentose phosphate shunt, REDOX, nucleotide and glutathione synthesis, and the TCA cycle (Figure 4-7 and Figure 4-8). Under normal growth, these pathways reach transcriptional peaks during the early stages of the IDC, so down-regulation indicates reduced expression in young parasites. In addition, we observed a significant down-regulation of genes associated with DNA replication and protein degradation in the trophozoite and schizont stages (Figure 4-7A and B; Supplementary Figure 1, Supplementary Figure 2). This down-regulation may represent a delayed onset of expression that normally starts during at the ring/trophozoite transition. At the schizont stage, the artemisinin resistant parasites were characterized by marked over-expression of genes that belong to many pathways associated with protein synthesis, folding and trafficking (Figure 4-7A and B). These include genes involved in ribosome assembly and maturation, chaperone-assisted protein folding, translational initiation and elongation (Supplementary Figure 1 and Supplementary Figure 2). In addition, we observed up-regulation of several additional pathways such as RNA metabolism and hemoglobin degradation, both of which could contribute to increased capacity of protein synthesis in these parasites by boosting global levels of RNA transcripts and concentration of amino acids produced by the food vacuole (Supplementary Figure 1 and Supplementary Figure 2).

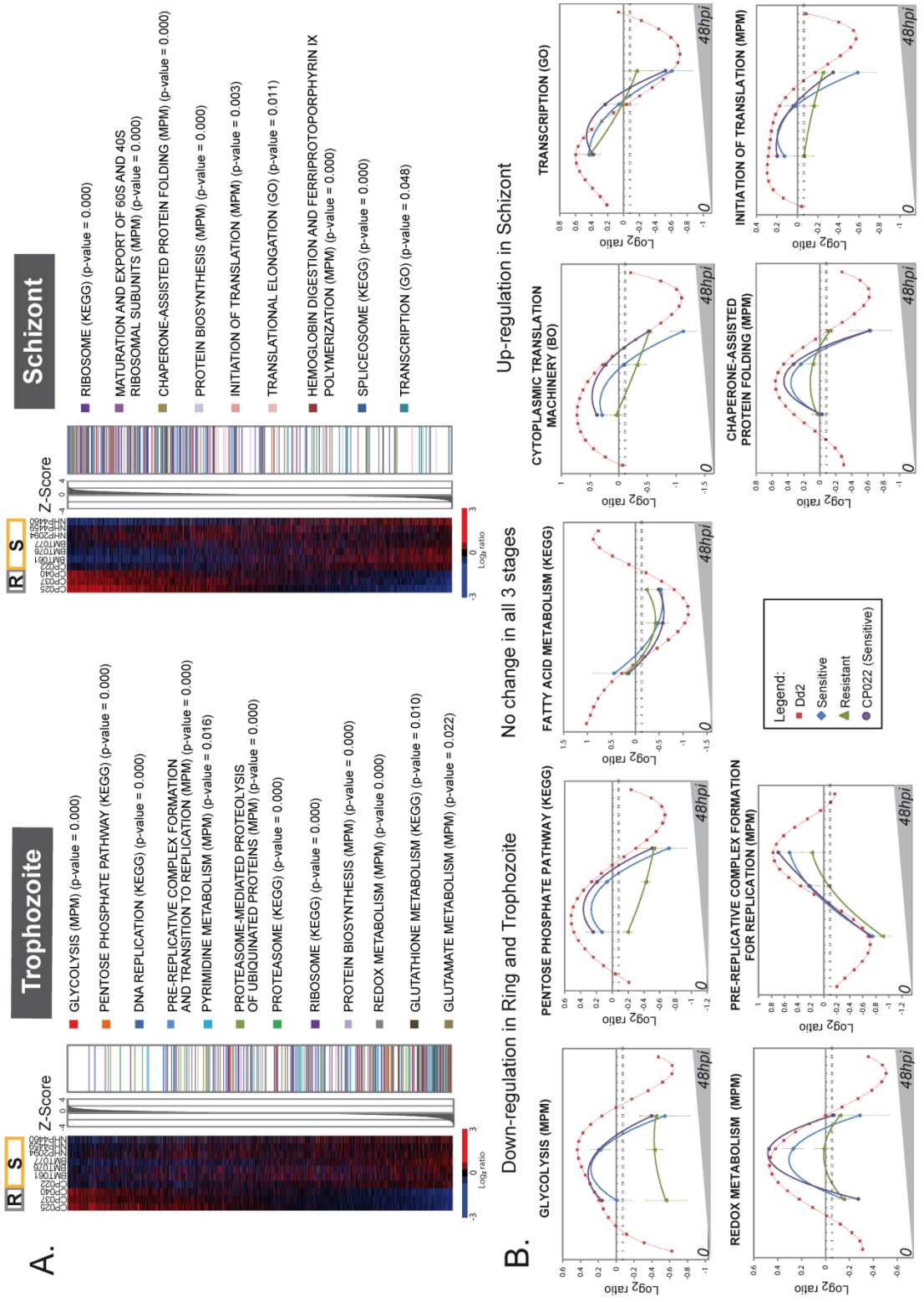

Figure 4-7. Functional analyses of DE genes in the artemisinin resistant parasites. A. The heat maps depict differential gene expression in the trophozoite and schizont stages and the mean-centered $\log_2$ ratios of mRNA levels between the resistant and susceptible isolates (for the complete set of all stages, see Supplementary Figure 1). Here the genes were ranked according to descending z-score (SNR) by correlating the expression profiles to the phenotypic class. Gene Set Enrichment Analysis (GSEA) revealed functional pathways down-regulated in trophozoites and up-regulated in

schizonts of the resistant parasites shown in the side bar diagrams and ordered by the nominal p-value. Positions of the genes belonging to each identified pathway are indicated by the colored bars in the corresponding z-score ordered gene distribution. (b) Graphs illustrate several functional pathways with significant differential expression between the resistant and susceptible parasites in the three stages. Data points represent the average $\log_2$ expression ratio for the isolates in each of the groups and across all genes belonging to the pathway for ring (14 hpi), trophozoite (26 hpi) and schizont (34 hpi) stages of the resistant (green triangle) and susceptible (blue diamond) isolates. Plotted are best fit polynomial curves and error bars that indicate the standard deviation amongst the isolates. Included are the average expression ratios for the artemisinin sensitive Cambodian isolate, CP022 (purple circle). For reference, the data are projected onto the centered mRNA abundance profiles of the *in vitro* IDC transcriptome (red square).

Investigating individual genes in the affected pathways, we observed that while in some cases the differential expression affects most genes (such as glycolysis or REDOX), in other pathways (such as translational initiation or proteasome degradation), only a fraction of genes exhibit differential expression (Supplementary Figure 3). These latter genes may represent crucial regulatory or rate limiting steps in these biological processes.

In summary, our data suggest that the specific modulation of the IDC transcriptional cascade observed in artemisinin resistant parasites has at least two major physiological implications that include: down-regulation of metabolic and cellular pathways in the first half of the IDC (up to 28 hpi) and prolonged transcription up-regulation of functionalities associated with protein synthesis and their supporting activities in the late stages (~36 hpi). Interestingly, this transcriptional program was observed in all three Western Cambodian isolates with the delayed clearance but not in the isolate collected in the same region (CP022) that had a normal clearance time (Figure 4-7B; Supplementary Figure 2). This suggests that the altered transcriptional pattern is not a simple reflection of geographical or other generic differences between *P. falciparum* isolates but is indeed associated with artemisinin resistance.

4.2.3 Differential expression of regulatory proteins contribute to artemisinin resistance

Artemisinin resistance in Western Cambodia was shown to exhibit a genetically inheritable pattern [200]. Thus it is feasible to speculate that the broad transcriptional changes associated with this phenotype may have resulted from a small number of genetic mutations in key regulatory proteins such as global transcription factors, chromatin remodeling-associated proteins or cell cycle regulators. We sought to explore the transcriptional data to find further clues for such underlying genetic determinants. For that, we inspected the genes whose expression was changed consistently in the three individual stages as these may be linked with a putative genetic variation (possibly in their regulatory elements). To identify such genes, we determined the rank product score for differentially expressed genes and classified them based on their differential expression in all 3 stages (Figure 4-8A). Interestingly, the rank distribution was skewed towards lower values where larger numbers of genes show lower than expected rank scores (Figure 4-8A). This indicates that there are more genes consistently down-regulated in the artemisinin resistant parasites in all three stages compared to the up-regulated genes that tend to be over-expressed in only one or two of the IDC developmental stages. Functional enrichment analyses of the top 5% of genes from both extremes of the distribution (Figure 4-8A grey boxes) did not uncover any additional functional groups compared to the stage-wise GSEA (Figure 4-7), however, visual inspection of these gene groups identified 41 putative transcription regulators, of which 22 are under-expressed and 19 are over-expressed. These include transcription factors, RNA binding proteins, cell cycle regulators, chromatin remodeling associated proteins, histone modification enzymes as well as histones (Figure 4-8B and C).

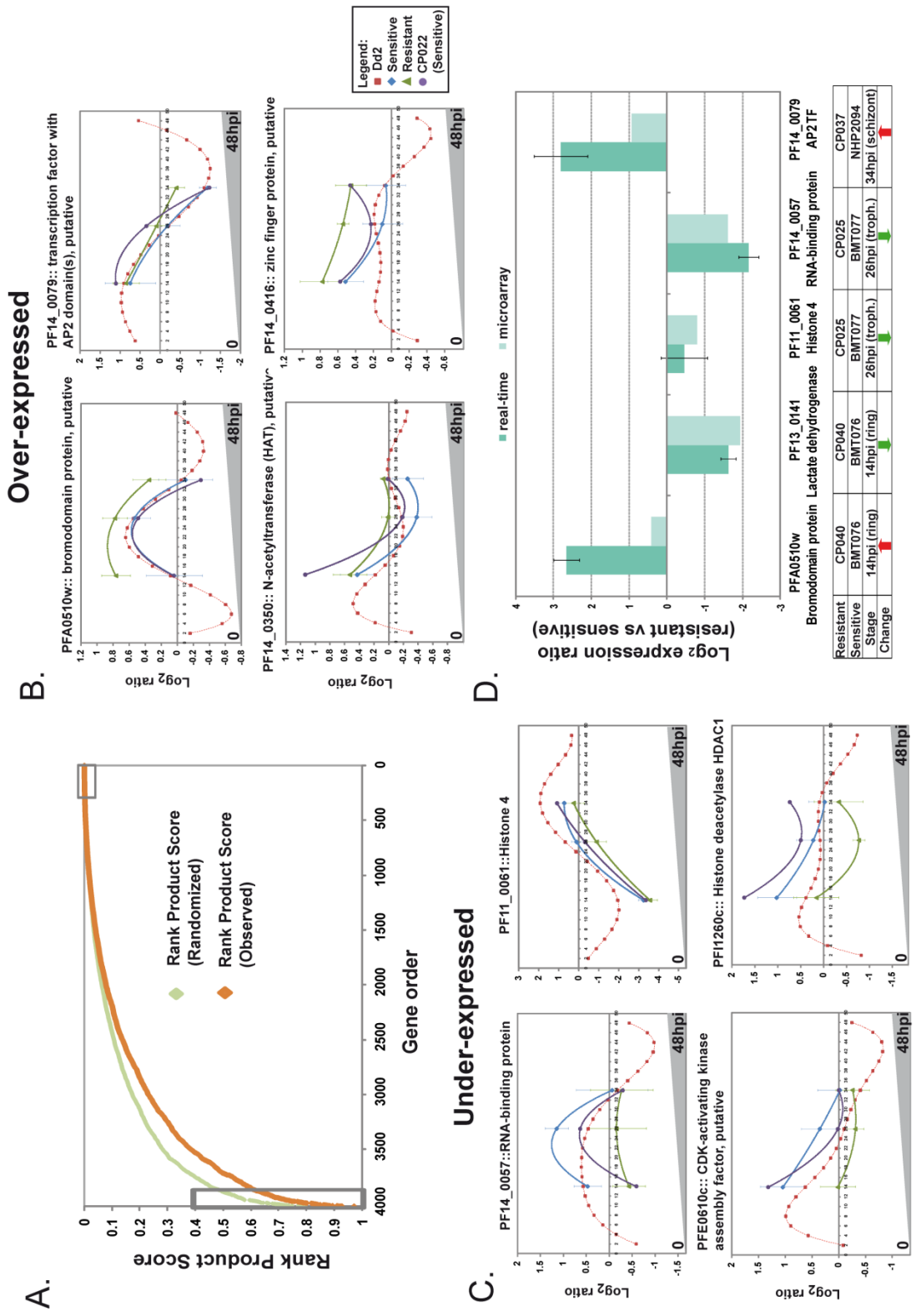

Figure 4-8. Classification of differentially expressed genes across the whole IDC and validation of differential expression of 5 genes by qPCR. A. Plot of the Ranked Product Score for all 4,015 genes calculated from the geometric mean of the ranked z-scores of the genes in the 3 stages in the generated transcriptome (orange) and in the randomized dataset (green) (for details see material and methods). The graphs represent 4 over (B.) and 4 under-expressed (C.) genes in the resistant parasites with

potential regulatory functions present in the top 5% of each extreme of the rank product distribution, respectively (A. grey boxes). Data points represent the mean $\log_2$ expression ratios of the genes in the resistant (green triangle), susceptible Lao and Thai (blue diamond), and susceptible Cambodian isolates (CP022, purple circle) across the three selected stage intervals. The data are projected onto the gene expression profiles analyzed by the *in vitro* IDC transcriptome (red square). Error bars reflect the standard deviation of the $\log_2$ ratios for each data point. D. Bars represent the $\log_2$-transformed fold change measured from relative quantification of a resistant versus a sensitive isolate using *PFC0965w* as a reference control gene in real-time PCR experiments (teal) and plotted alongside the microarray expression ratios (light blue). Error bars reflect the standard deviation of the $\log_2$ ratios over triplicates.

The most remarkable examples are strong down-regulation of genes coding for histone deacetylase 1 protein (*pfhdac1*) (PFI1260c), recently proposed to play a major role in the transcriptional regulation [201], and CDK-activating kinase assembly factor (PFE0610c) whose paralogue was shown be associated with HDAC1 in *P. falciparum* [202]. Also, the artemisinin resistant parasites show a considerable up-regulation of the AP2 containing transcription factor (PF14_0079), bromo-domain containing protein (PFA0510w), putative histone acetyltransferase (*hat*; PF14_0350), zinc finger protein (PF14_0416), and the *P. falciparum* homologue of yeast histone chaperone Rttp106-like transcriptional regulator (PFE0870w). In addition to these DNA interacting regulatory proteins, we identified 10 genes encoding the RNA-recognition motif (RRM) that are involved in regulating mRNA stability or translational repression. Quantitative real-time PCR carried out with 4 of these genes (PFA0510w, PF14_0079, PF11_0061 and PF14_0057) further confirmed that these genes are significantly differentially expressed between the resistant and sensitive isolates (Figure 4-8D). Differential expression of these genes encoding regulatory factors may contribute to the global changes in the transcriptome observed in the artemisinin resistant parasites.

4.2.4 Copy number variations (CNV) and genotypes of artemisinin resistant isolates

Several recent studies have demonstrated a frequent occurrence of gene copy number variants (CNV) in *P. falciparum* and linked these to differential gene expression in field isolates and laboratory strains [115]. This can contribute to the variability in drug sensitivities observed among isolates [55, 115, 178, 203-207]. We carried out comparative genomic hybridizations with genomic DNA of the four Cambodian and two Lao isolates and demonstrated that CNV profiles exhibit a clear segregation between these two groups (Figure 4-9A). Among the 138 genes occurring within the 93 CNV detected segments are Histone 4, GTP cyclohydrolase I (*pfgch1*), *hyp4/5* exported proteins, *phist* genes and Maurer's cleft two transmembrane proteins (*pfmc-2tm*) [115, 178, 203-205, 207]. Increased copy number of *pfgch1* has been previously linked with resistance to antifolate antimalarial drugs and its amplification in the Cambodian isolates (p-value = 0.002) may reflect the prolonged use of these drugs in this region [208]. Other newly identified CNVs include several hypothetical genes; an autophagocytosis associated protein and Zn^{2+}/Fe^{2+} permease (data not shown). Overall we observed strong similarities amongst the Cambodian isolates, however none of the identified CNV could be associated with artemisinin resistance. This genetic coherence among the four Cambodian isolates contrasts with their transcriptional heterogeneity and indicates that copy number differences are strongly associated with differentiation in geographical origins. More genetic studies with large number of isolates will be required to assess the role of CNVs in artemisinin resistance (see Chapter 6).

A.

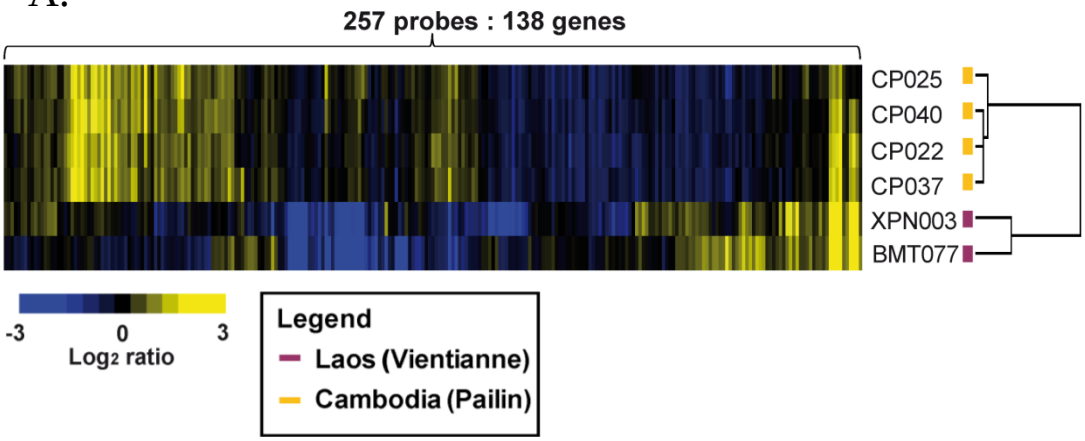

B.

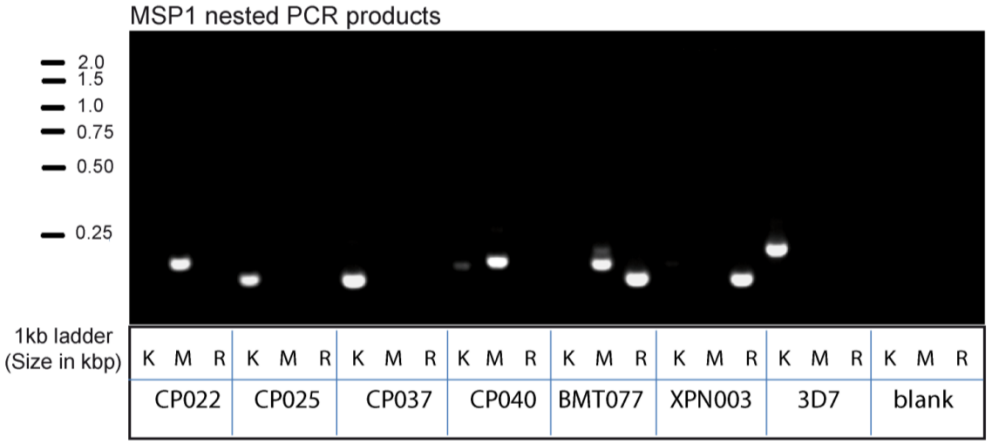

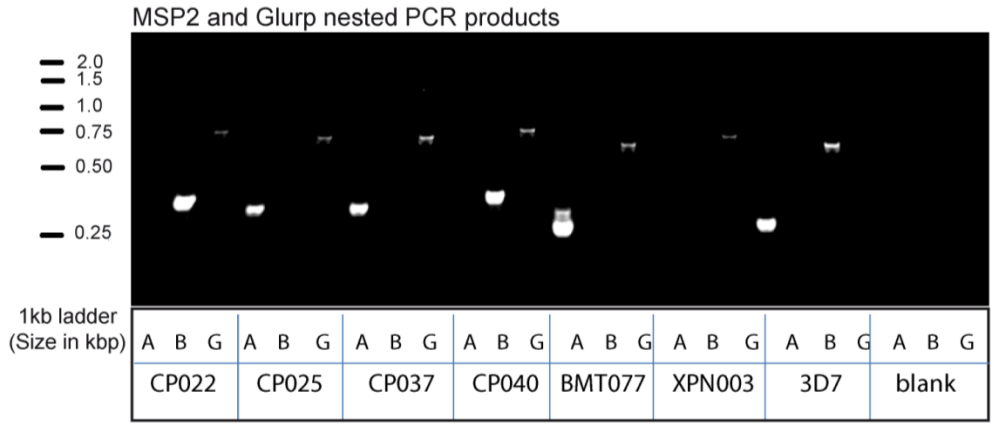

Legend:

K: K1	M: MAD20	R: R033
A: IC/3d7	B:FC27	G: Glurp

C. SNPs detected in codons of drug-resistant genes

Common SNPs

Pfmdr1	86	130	184	1034	1042	1109	1246
CP022	AAT(N)	GAA(E)	TTT(F)	AGT(S)	AAT(N)	GTA(V)	GAT(D)
CP025	AAT(N)	GAA(E)	TAT(Y)	AGT(S)	AAT(N)	GTA(V)	GAT(D)
CP037	AAT(N)	GAA(E)	TAT(Y)	AGT(S)	AAT(N)	GTA(V)	GAT(D)
CP040	AAT(N)	GAA(E)	TTT(F)	AGT(S)	AAT(N)	GTA(V)	GAT(D)
BMT077	AAT(N)	GAA(E)	TAT(Y)	AGT(S)	AAT(N)	GTA(V)	GAT(D)
XPN003	AAT(N)	GAA(E)	TAT(Y)	AGT(S)	AAT(N)	GTA(V)	GAT(D)
3d7	AAT(N)	GAA(E)	TAT(Y)	AGT(S)	AAT(N)	GTA(V)	GAT(D)

Novel SNPs

Pfmdr1	79	171	208	214	1181
CP022	GGT(G)	ATC(I)	TGC(C)	AAG(K)	AAA(K)
CP025	GTT(V)	ATC(I)	TGC(C)	CAG(Q)	AAA(K)
CP037	GTT(V)	ATA(I)	TGC(C)	AAG(K)	ACA(T)
CP040	GGT(G)	ATC(I)	TGC(C)	AAG(K)	ACA(T)
BMT077	GGT(G)	ATC(I)	TGC(C)	AAG(K)	AAA(K)
XPN003	GGT(G)	ATC(I)	TGC(C)	AAG(K)	ACA(T)
3d7	GGT(G)	ATA(I)	TGT(C)	AAG(K)	AAA(K)

Common SNPs

Pfdhps	431	436	437	540	581	613
CP022	ATA(I)	GCT(A)	GGT(G)	GAA(E)	GCG(A)	GCC(A)
CP025	ATA(I)	GCT(A)	GGT(G)	GAA(E)	GCG(A)	GCC(A)
CP037	ATA(I)	GCT(A)	GGT(G)	GAA(E)	GCG(A)	GCC(A)
CP040	ATA(I)	GCT(A)	GGT(G)	GAA(E)	GCG(A)	GCC(A)
BMT077	ATA(I)	TCT(S)	GCT(A)	AAA(K)	GCG(A)	GCC(A)
XPN003	ATA(I)	GCT(A)	GGT(G)	GAA(E)	GCG(A)	GCC(A)
3d7	ATA(I)	TCT(S)	GGT(G)	AAA(K)	GCG(A)	GCC(A)

Figure 4-9. CGH analysis and genotyping of artemisinin resistant isolates. Sequencing of drug-resistant genes to determine haplotypes. A. The heat map represents hierarchical clustering of CGH signal (against 3D7 genome) for 257 microarray oligonucleotide elements representing 138 genes in 93 CNV regions identified by GADA analysis (see material and methods). B. Visualization of *msp1*, *msp2* and *glurp* nested PCR products of the 6 isolates on a 2.5% agarose gel shows distinctive patterns of product sizes for each clone, except for CP025 and CP037. C. Tables depict the commonly and rarely found single nucleotide polymorphisms (SNPs) found based on the codon position (top row) and the sequenced bases of the various isolates and corresponding amino acid in brackets. Highlighted in yellow are the codons with mutations compared to wild type 3D7.

In addition to the CGH analysis, we carried out "standard" genotyping of genes coding for merozoite surface proteins: *msp1*, *msp2* and glutamate-rich protein: *glurp* together with sequencing of drug-resistant markers: multidrug resistant protein 1 (*pfmdr1*) and dihydropteroate synthase (*pfdhps*). This analysis revealed that the four Cambodian and two Lao isolates are genetically distinct from each other carrying different alleles of the tested genes (Figure 4-9B). Of these, CP025 and CP037 appeared highly related, exhibiting identical *msp1* and *msp2* nested PCR products of KO33 and IC/3d7 alleles (Figure 4-9B). However, these two isolates differ in 2 non-synonymous SNPs of codons K214Q and K1181T and a synonymous SNP in codon 171 in the *pfmdr1* gene (Figure 4-9C). In addition, CP025 and CP037 exhibit subtle differences in their CNV pattern as measured by CGH (Figure 4-9A). Interestingly, we found that none of the 6 isolates carry the N86Y *pfmdr1* mutation (Figure 4-9C) whose presence is frequent in many Southeast Asian regions [78] and which is commonly associated with chloroquine resistance and mefloquine hypersensitivity [209]. Furthermore, we observed significant haplotype sharing amongst analyzed isolates such as CP040 and CP022 that share the "NEFSNVD" haplotype of *pfmdr1*, containing the non-synonymous Y184F mutation. Moreover, CP025, CP037, CP040, CP022 and XPN003 share the IAGEAA haplotype of *pfdhps* with non-synonymous triple mutants S436A, G437A and K540E, which were previously linked to resistance to sulfadoxine-pyrimethamine [210, 211]. The mutations in *dhps* may reflect the selection pressure as a result of an extensive antifolate drug use in this region over several decades.

4.3 Discussion

4.3.1 Mechanism of artemisinin resistance

Artemisinin resistance of *P. falciparum* is a major threat to malaria control. Understanding its molecular basis is thus essential for determining treatment strategies, mapping the spread of resistance and guiding elimination [81, 197, 200, 212-214]. Mutations or amplification of genes encoding transporters or target enzymes have been identified as resistance mechanisms to other antimalarial drugs. It is possible that resistance to artemisinin is unlike these classical mechanisms *in vitro* but instead results from a complex series of genetic and epigenetic events affecting multiple pathways. Here we showed that artemisinin resistant parasites are characterized by a specific modulation of the IDC transcriptome that affects a broad spectrum of genes and biological functions. First, we detected a specific down-regulation of many ring stage-specific metabolic pathways such as energy metabolism, nucleotide synthesis etc. Second, the progress to mature schizont stages was marked by significant increase in transcription of genes associated with essentially all functionalities involved in protein metabolism (Figure 4-7 and 4-11). Based on these two observations, we propose a plausible model for molecular basis of the artemisinin resistance observed in these Cambodian isolates that is founded on two (possibly independent) events: (i) Limited metabolic activity of the ring stages could lead to lower levels of hemoglobin digestion, less ferrous ions produced and thus reduced activation and conversion of artemisinin drugs to reactive intermediates [215]. This effect may be linked to the high prevalence of hemoglobinopathies, especially Hemoglobin E and α-thalassemia in this area conferring increased oxidant stress [216, 217]. This is possibly compounded by decades of unregulated artemisinin use in Western Cambodia which may select for parasites with greater resistance to oxidant

stress during the ring form development. Alternatively, the lower metabolic activities of the ring stages may be a prerequisite of the ability of the resistant parasite to become dormant under the artemisinin pressure as demonstrated by several *in vitro* analyses [197, 198]. Although this phenomenon is unlikely to be the major factor in artemisinin resistance, it is worth noting that the results obtained in our study are in agreement with the transcriptional analyses of the *in vitro* derived artemisinin tolerant parasites that include mRNA levels of the hypoxanthine phosphoribosyl transferase (PF10_0121), a cell cycle regulator (PFE1415w) and a Heat Shock Protein 70 kDa (PF08_0054) (Figure 4-10) [197].

(ii) The increased activity of protein metabolism may contribute to the resistance by withstanding the damaging effects of artemisinin on parasite's proteins by increasing rates of protein turnover and synthesis and thus compensate for loss of active proteins. This is consistent with the presumed artemisinin mode of action in which the drug inflicts substantial damage to the parasite cell either by an oxidative stress (via reactive free radicals) or by direct alkylation of a wide spectrum of cellular components such as proteins, heme, and lipids [35-38, 218, 219].

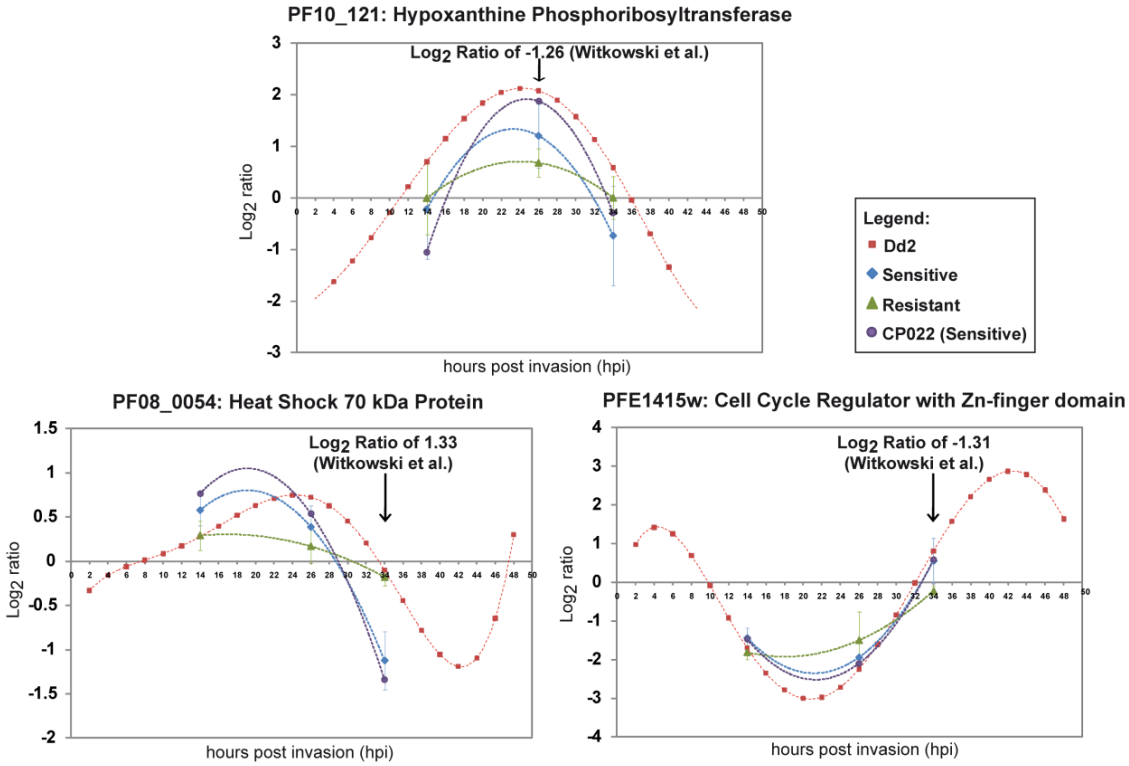

Figure 4-10. Transcriptional profiles of the 3 genes in the artemisinin resistant parasites compared with previous data published [197]. The mean expression $\log_2$ ratio (data point) and SD (error bars) among the resistant (green triangle) and sensitive (blue diamond) isolates for each stage are plotted for the genes: PF10_0121 - hypoxanthine phosphoribosyltransferase (rank 3207/4029; p-value = 0.1), PF08_0054 - Heat Shock Protein 70 kDa (rank 14/4041; p-value = 4×10^{-4}) and PFE1415w- cell cycle regulator (rank 3837/4041; p-value = 0.01) and the polynomial represents the best fit curve through the data points. The arrow indicates the approximate stage in which significant increased or lowered expression was observed in artesunate-tolerant parasites and the fold change [197].

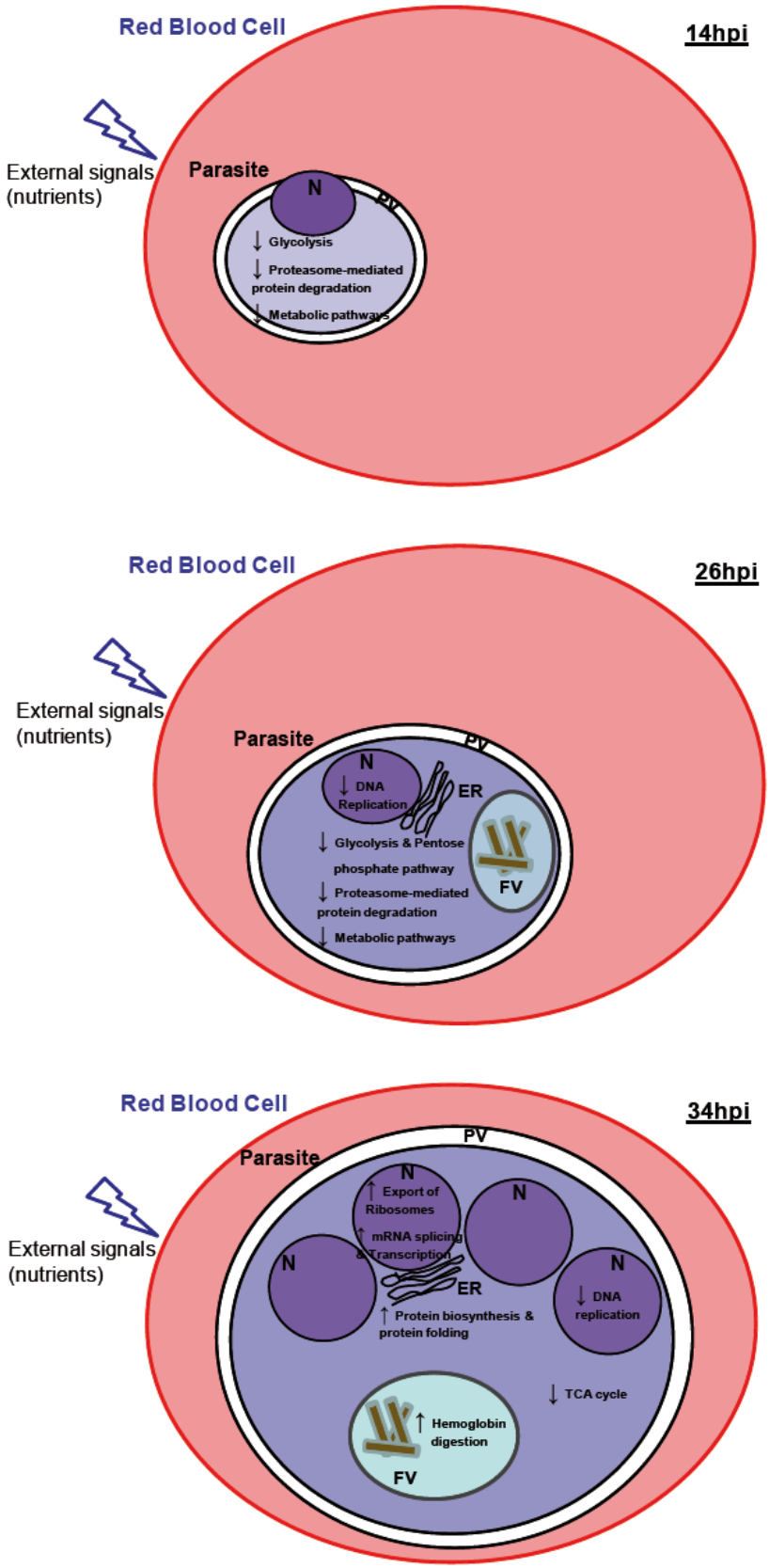

Figure 4-11. Model depicting the changes in the expression of various cellular and metabolic pathways observed from the transcriptional profiling of artemisinin resistant parasites at ring, trophozoite and schizont stages of the IDC.

4.3.2 Transcriptional regulation and artemisinin resistance

It is important to note that the differences in mRNA levels linked to artemisinin resistance were not the most dramatic transcriptional differences detected among the field isolates. Functional enrichment analysis of genes that vary the most in their expression among the 11 field isolates irrespective of their artemisinin sensitivities, revealed a distinct set of functionalities that varied in gene expression amongst field isolates in general. These include mainly genes encoding proteins of host-parasite interactions, Maurer's cleft proteins, invasion-related proteins, as well as factors of fatty acid metabolism, glycolysis and hemoglobin digestion (Figure 4-12). This indicates that the observed transcriptional differences between artemisinin resistant and sensitive strains may represent a new event in transcriptional differentiation of field isolates that does not occur in other parasite populations. Although very little is known about molecular factors of transcriptional regulation in *P. falciparum*, a number of previous studies [98, 99, 152, 201, 220] have indicated the existence of broad range regulatory mechanisms that affect large groups of genes controlling the progression of the *Plasmodium* life cycle. Although more studies that involve large epidemiological surveys followed by extensive molecular analyses will have to be carried out to support such putative mechanisms, here we explored genes whose expression was affected in all three developmental stages in the resistant Western Cambodian parasites. One of the most remarkable examples of consistently down-regulated genes is *pfhdac1* and its putative interacting proteins partner CDK-activating kinase, both of which show dramatic down-regulation in all three developmental stages (Figure 4-8). In our recent study, we showed that HDAC activities play a highly dynamic role in regulating the transcriptome of the *Plasmodium* life cycle and that their inhibition leads to widespread transcriptional

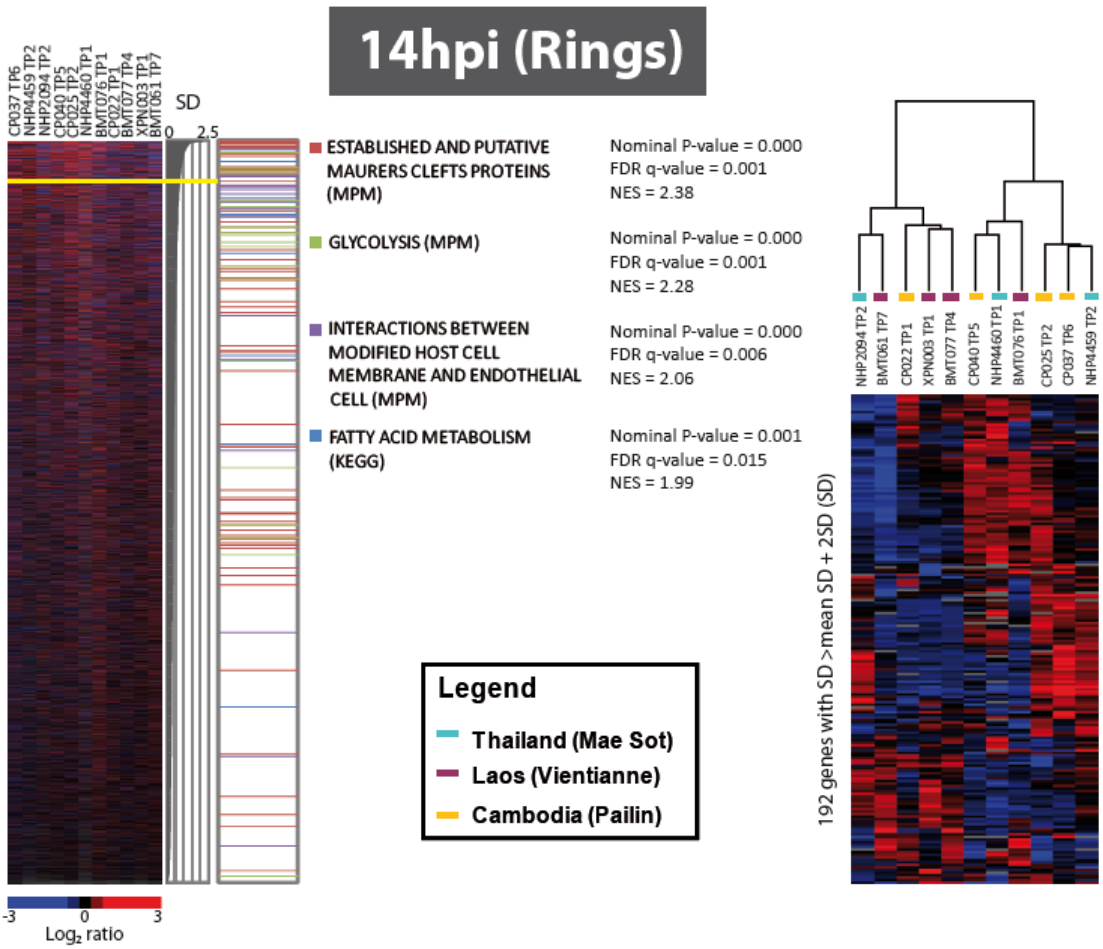
14hpi (Rings)
CP037 TP6
NHP4459 TP2
NHP2094 TP2
CP040 TP5
CP025 TP2
NHP4460 TP1
BMT076 TP1
CP022 TP1
BMT077 TP4
XPN003 TP1
BMT061 TP7
SD
0
2.5
ESTABLISHED AND PUTATIVE MAURERS CLEFTS PROTEINS (MPM)
Nominal P-value = 0.000
FDR q-value = 0.001
NES = 2.38
GLYCOLYSIS (MPM)
Nominal P-value = 0.000
FDR q-value = 0.001
NES = 2.28
INTERACTIONS BETWEEN MODIFIED HOST CELL MEMBRANE AND ENDOTHELIAL CELL (MPM)
Nominal P-value = 0.000
FDR q-value = 0.006
NES = 2.06
FATTY ACID METABOLISM (KEGG)
Nominal P-value = 0.001
FDR q-value = 0.015
NES = 1.99
Legend
Thailand (Mae Sot)
Laos (Vientianne)
Cambodia (Pailin)
NHP2094 TP2
BMT061 TP7
CP022 TP1
XPN003 TP1
BMT077 TP4
CP040 TP5
NHP4460 TP1
BMT076 TP1
CP025 TP2
CP037 TP6
NHP4459 TP2
192 genes with SD >mean SD + 2SD (SD)
-3
0
3
Log2 ratio

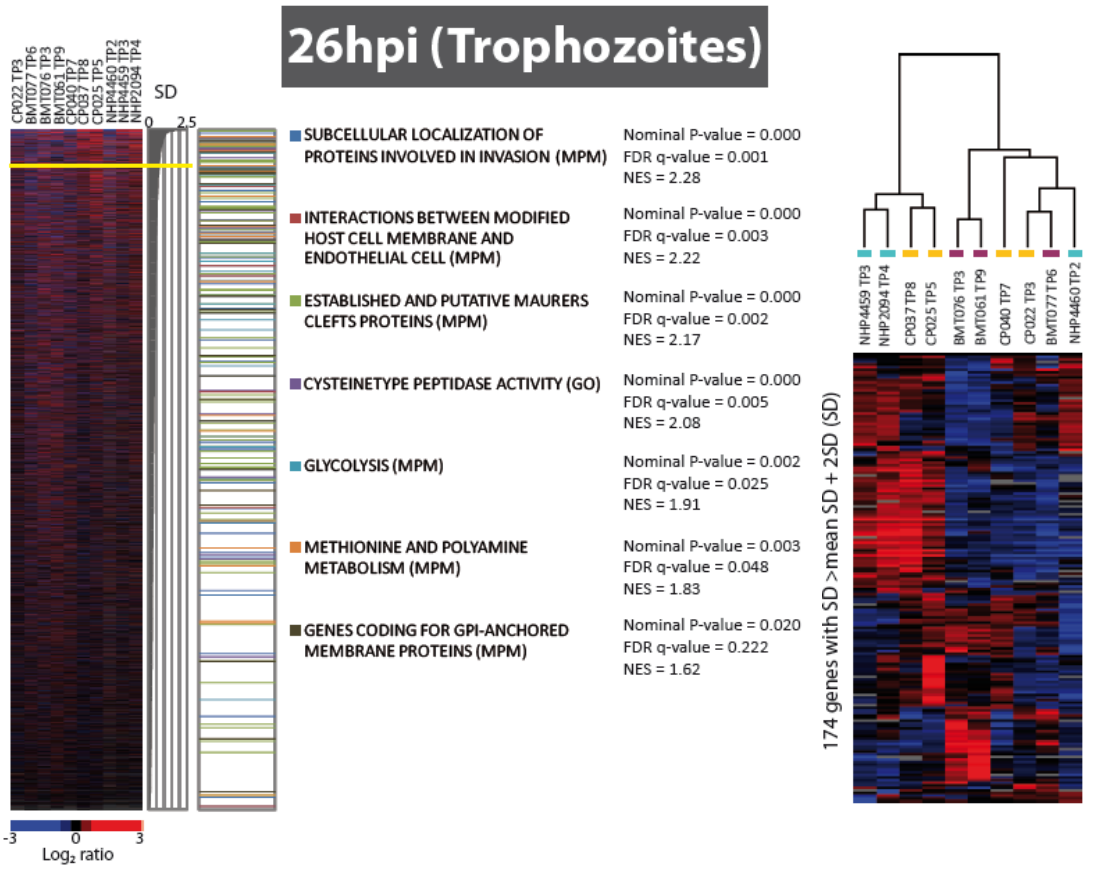
26hpi (Trophozoites)
CP022 TP3
BMT077 TP6
BMT076 TP3
BMT061 TP9
CP040 TP7
CP037 TP8
CP025 TP5
NHP4459 TP2
NHP4460 TP2
NHP2094 TP4
SD
0
2.5
SUBCELLULAR LOCALIZATION OF PROTEINS INVOLVED IN INVASION (MPM)
Nominal P-value = 0.000
FDR q-value = 0.001
NES = 2.28
INTERACTIONS BETWEEN MODIFIED HOST CELL MEMBRANE AND ENDOTHELIAL CELL (MPM)
Nominal P-value = 0.000
FDR q-value = 0.003
NES = 2.22
ESTABLISHED AND PUTATIVE MAURERS CLEFTS PROTEINS (MPM)
Nominal P-value = 0.000
FDR q-value = 0.002
NES = 2.17
CYSTEINETYPE PEPTIDASE ACTIVITY (GO)
Nominal P-value = 0.000
FDR q-value = 0.005
NES = 2.08
GLYCOLYSIS (MPM)
Nominal P-value = 0.002
FDR q-value = 0.025
NES = 1.91
METHIONINE AND POLYAMINE METABOLISM (MPM)
Nominal P-value = 0.003
FDR q-value = 0.048
NES = 1.83
GENES CODING FOR GPI-ANCHORED MEMBRANE PROTEINS (MPM)
Nominal P-value = 0.020
FDR q-value = 0.222
NES = 1.62
NHP4459 TP3
NHP2094 TP4
CP037 TP8
CP025 TP5
BMT076 TP3
BMT061 TP9
CP040 TP7
CP022 TP3
BMT077 TP6
NHP4460 TP2
174 genes with SD >mean SD + 2SD (SD)
-3
0
3
Log2 ratio

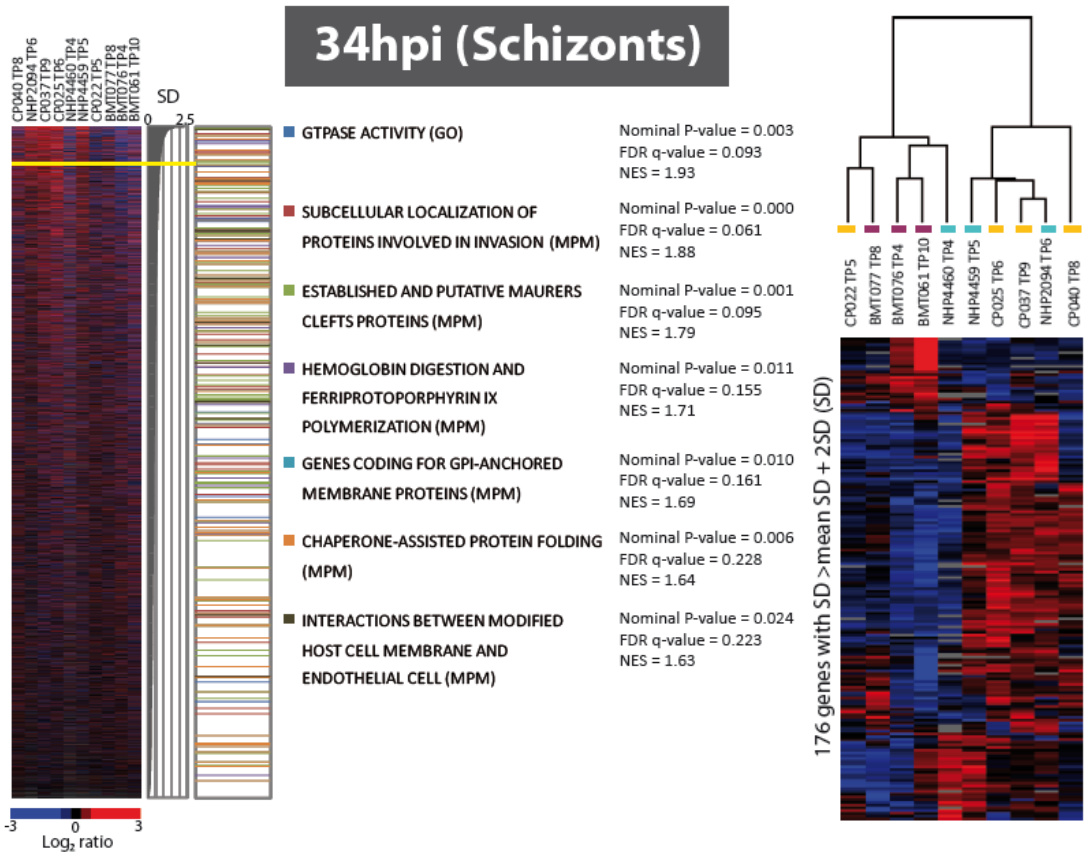

Figure 4-12. Functional analysis and clustering based on general differences in gene expression among field isolates without phenotypic classification. Left panel: Clusters are represented by the $\log_2$ expression ratios for all genes ordered according to the standard deviation (SD) for each gene in a descending manner. GSEA [110] performed on this pre-ranked list of genes identified these functional gene sets as differentially expressed among field isolates without any phenotypic classification for the 3 stages. Right panel: Hierarchically clustered isolates for the genes showing greatest variation in expression ratios (taking genes with SD value at the 95th percentile cut off).

changes. Intriguingly, the transcription profile of the resistant parasites is reminiscent of the effect of HDAC inhibitors on the *P. falciparum* gene expression in which most gene induction represent accelerated transcription in the ring and trophozoite stages and prolonged mRNA expression during the schizont stage [201]. Another gene whose differential expression is significant is histone 4 (PF11_0061). Histone 4 is the only nucleosomal subunit present as a single copy gene and thus its down-regulation could have severe implication on the nucleosomal assembly during the *P. falciparum*

schizont stage. Depletion of histone 4 in both yeast and human cells causes an arrest or dramatic delay in the progression of the S-phase, which is caused by insufficient nucleosomal assembly and subsequently inhibition of DNA synthesis [221, 222]. We observed a modest but statistically significant decrease of histone 4 in the artemisinin resistant *P. falciparum* parasites (Figure 4-8D) that could analogously lead to a delayed onset of schizogony and thus prolonged expression of genes associated with the typical trophozoite functions such as protein synthesis and hemoglobin digestion (Figure 4-7). In summary, these genetic studies suggest that while the Western Cambodian isolates are not identical isogenic clones, they share a recent common ancestor that is evident from their CNV profiles. Hence, the highly unique and also uniform CNV pattern identified in these parasites may represent a genetic background that contributes to development of artemisinin resistance and possibly other drug resistant phenotypes in this region. Since the CNV profiles were similar among the four Cambodian isolates regardless of their tolerance level to artemisinin, more studies will be needed to understand their role in regulating transcriptional levels in artemisinin resistant parasites. More importantly, the coherence of CNV profiles among the Cambodian isolates indicates that the parasites in this region share a recent common ancestor. Similar conclusion was made by an admixture study carried out in Southeast Asia that demonstrated a sub-group of recently expanded parasite populations in Western Cambodia [223]. This could be a result of intense administration of a successive number of antimalarials from chloroquine to mefloquine to sulfadoxine-pyrimethamine to treat malaria cases in the Western Cambodian region over the last 80 years. It is plausible that a population with a restricted genotype has emerged with a genetic background that has higher propensity to give rise to resistance of the *P. falciparum* parasites to artemisinin.

Chapter 5 : PfMRP2 Multi-Drug Resistance Protein Pump

5.1 Introduction

Genes with temporal differences in expression between clones include PFL1410c

In addition to the microarray analysis of transcription variation among single clones (Chapter 3.2.4) by level of expression, we also analyzed the microarray data for differentially expressed genes based on differential timing of expression. Genes which have the highest PCC values of 0.9 include housekeeping genes, such as glutathione synthetase involved in REDOX pathway and chromatin assembly protein. In contrast, only 10 genes (0.2% of genome) had PCC < -0.4 and had expression profiles anti-correlated between clones (Figure 5-1A). Half of them code for hypothetical proteins. Of particular interest is PFL1410c (*pfmrp2),* which is the gene with the most pronounced negative correlation (r = -0.97 between clone 8B and 6A). The mRNA expression profile of clones 1A and 6A was found to be anti-correlated with the profile of clones 11C, 5D, 8B and parent 3D7. While its peak of expression occurs in early/mid rings in clone 11C, 5D, 8B and parent 3D7, the expression is highest at the early/mid schizont stage in clones 6A and 1A (Figure 5-1B). PFL1410c was also observed to be significantly differentially expressed among the 5 clones, and fell within the top 10% of the list of 480 differentially expressed genes between 3D7 clones. For each clone, we found a high correlation between the probe microarray ratios for all the four probes designed for PFL1410c gene. This confirmed that the negative correlation in timing of expression between the clones was due to change in timing of expression of the full length mRNA transcript.

A.

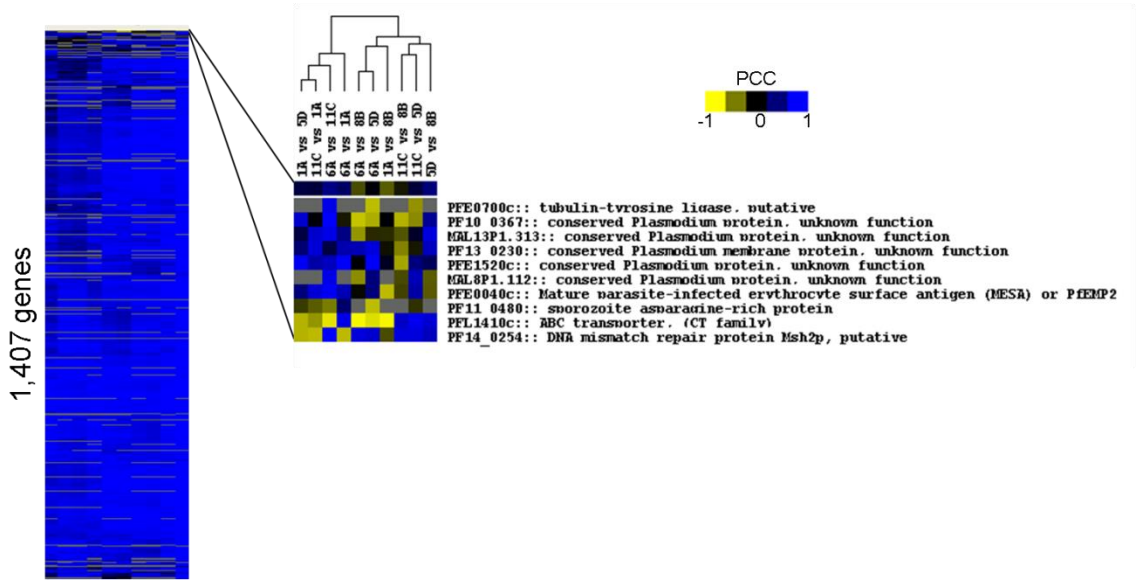

B.

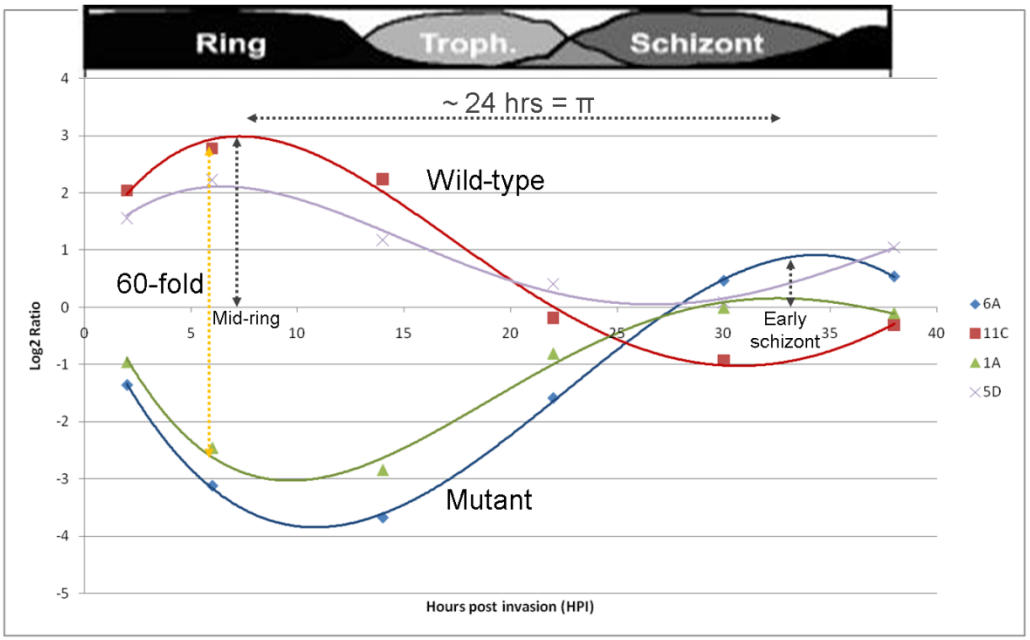

Figure 5-1. DE genes between 3D7 clones with anti-correlated expression profiles across the IDC. A. Heat map of the pair-wise PCCs for 1,407 genes with at least 2-fold change in all clones and the 10 genes which are found to be anti-correlated in gene expression (PCC<-0.4 in any pairwise comparison and >2-fold change across the lifecycle) using several matched hpi to represent the ring, trophozoite and schizont stages. B. Gene expression profile of PFL1410c across the 48 hour IDC for clones 6A/mut (mutant), 1A/mut (mutant), 11C/wt (wild-type) and 5D/wt (wild-type). Shown are the microarray $\log_2$ ratios for each sampling time point.

Interestingly, PFL1410c codes for PfMRP2 (multidrug resistance-associated protein). In *P. falciparum*, MRPs have been suggested to function in redox metabolism pathway, allowing parasite and infected red blood cell to release glutathione conjugates (GSSG/GSH) synthesized by the glutathione synthase enzyme, into the extra-cellular medium [224]. The other known multi-drug resistant pump protein homologue in *P. falciparum* is PfMRP1 (*PFA0590w*), which is similarly expressed between the clones. PfMRP1 has been shown to have an important role in mediating CQ resistance with knock out cell lines having increased accumulation of glutathione, increased sensitivity to CQ and other antimalarials and are unable to survive beyond 5% parasitemia in culture, suggesting that this protein is crucial for normal physiological growth [89]. The mutant *Pfmrp1* gene carrying the 1466K allele was found to be associated with recrudescent infections following sulfadoxine-pyrimethamine treatment [225] while treatment with artemether-lumefantrine drug resulted in a selection of the I876V polymorphism of *Pfmrp1* gene in African parasites showing late treatment failure [226]. Recently, the F1390I SNP found among Thai-Myanmar field isolates was shown to be associated significantly with *in vitro* IC_{50}s of various antimalarials such as artemisinin, mefloquine and lumefantrine [227]. These findings support the functional role of PfMRP1 protein in mediating drug resistance to antimalarial therapy.

However, the function of MRP2 in *P. falciparum* is still under debate since the timing of its peak gene expression does not coincide with the expression of glutathione synthase even though expression of MRP1 coincides with expression of glutathione synthase, suggesting different functional roles (Figure 5-2). In *P. falciparum*, MRP1 and MRP2 have been shown to be located on the parasite plasma membrane in the blood stage of the parasite [89, 228, 229]. Syntenic orthologues of MRPs are found in

the other 4 *Plasmodium* species sequenced to date; PV124085 in *P. vivax*, PKH_144590 in *P. knowlesi*, PY05035 in *P. yoelii yoelii* and PBANKA_144380 in *P. berghei* (PlasmoDB v8.1). This signifies that this protein may be important for the proper functioning of any *Plasmodium* parasite. PfMRP2 is most closely related to human MRP of the ABC transporter subtype C, and is shown to be localized to the plasma membrane [230] or to membrane-bound lysosomal vesicles [231]. Human MRP has been shown to be able to transport a variety of substrates including HIV protease inhibitors, such as saquinavir, ritonavir and lopinavir [232]. Additionally, over-expression of this protein mediates multiple chemotherapeutic resistance in cancer cells caused by increased efflux of anticancer drugs [233, 234]. However, PfMRP2 has not yet been shown to be associated with antimalarial drug resistance.

Despite reports showing that SNPs are detected in *pfmrp*2 gene in field isolates, there has yet to be any clear evidence that these mutations are associated with *in vitro* drug sensitivities [235, 236]. The 2 well known transporters in *P. falciparum* that confers drug resistance in the parasite are PfCRT (chloroquine resistance transporter) and PfMDR1 (multi-drug resistance protein; P-glycoprotein) [51, 55, 237-239]. However, mutations and copy number differences in the known drug-resistance genes alone have not been sufficient to completely explain discrepancies in drug resistance between isolates [236, 240, 241]. The genetic background of various strains is suggested to play a role in mediating the level of CQ resistance as different parasite strains transfected with the same mutant *pfcrt* gene did not give identical CQ inhibitory concentrations [241, 242]. Genome-wide association studies performed in hundreds of field isolates across geographical regions have also been unable to identify and validate determinants contributing to drug resistance other than the known drug resistance markers *pfcrt* and *pfmdr1* [223, 240, 243].

Hence, we hypothesize that MRP2 plays a role in mediating drug efflux and drug resistance in *Plasmodium*. Since the clones naturally differ in expression of this gene, it presents a good model to study the role of MRP2 by first determining the drug sensitivity of the clones to antimalarials. We aimed to characterize the localization and level of MRP2 protein and correlate it to mRNA abundance, in particular to explain the differential expression between clones. On the other hand, we investigated the promoter activity of *pfmrp2* gene in the 5 clones in order to uncover the driving factor behind the differential *pfmrp2* gene expression levels.

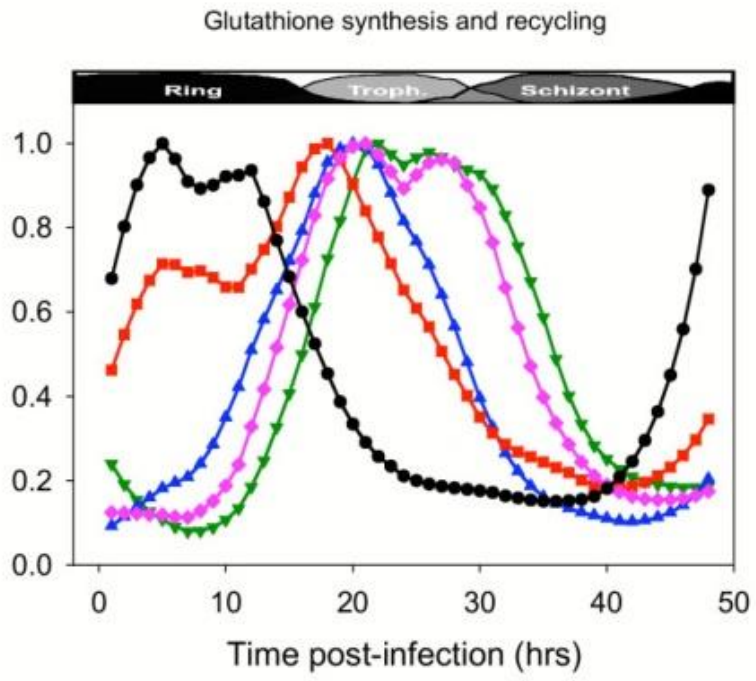

Figure 5-2. Expression profiles of various genes involved in the glutathione synthesis and recycling pathway of the *Plasmodium* IDC. Glutathione synthetase: green line, *pfmrp2*: black line and *pfmrp1*: pink line. (Source: [244])

5.2 Results

5.2.1 Characterization of Clones phenotype - Drug Sensitivity (Fitness)

After deriving the single clones from limiting dilution, the clones were characterized for their sensitivity to antimalarial drugs, CQ and MEF. Drug assays were performed on highly synchronized cultures of clone 11C showing the wild type mRNA expression profile (labeled as "11C/wt") and clone 6A showing the mutant mRNA profile (labeled as "6A/mut") at 3 stages of the IDC: mid ring, mid trophozoite and mid schizont. The parasites were exposed to different concentrations of the drugs till the next generation of new rings, where the % parasitemia of healthy rings were counted. The drug assays were carried out in duplicates and at 3 different generations (triplicates). Surprisingly, the IC values of mefloquine varied significantly in both trophozoite and schizont stages between clones 6A/mut and 11C/wt and of chloroquine in trophozoite stage between clones (Figure 5-3). From the IC_{50} values, we observed that clone 6A/mut was significantly less sensitive than clone 11C/wt to CQ in trophozoite stage (1.9 fold, Student's t-test; p-value = 0.02) while this clone was 2.4 and 1.8 fold less sensitive than 11C/wt to MEF in trophozoite (p-value = 0.06) and schizont (p-value = 0.007) stages (Figure 5-3). Decreased sensitivity of clone 6A/mut to the 2 drugs was reflected in higher IC_{90} values (Figure 5-3). There was no significant difference in IC values between clones in ring stages to either drug (Figure 5-3). Regardless of clone type, the parasites were generally more sensitive to both drugs in ring stage (IC_{50} of MEF: 11-14 nM; IC_{50} of CQ: 23-25 nM) compared to later stages (IC_{50} of MEF: 15-66 nM; IC_{50} of CQ: 31-82 nM).

A.

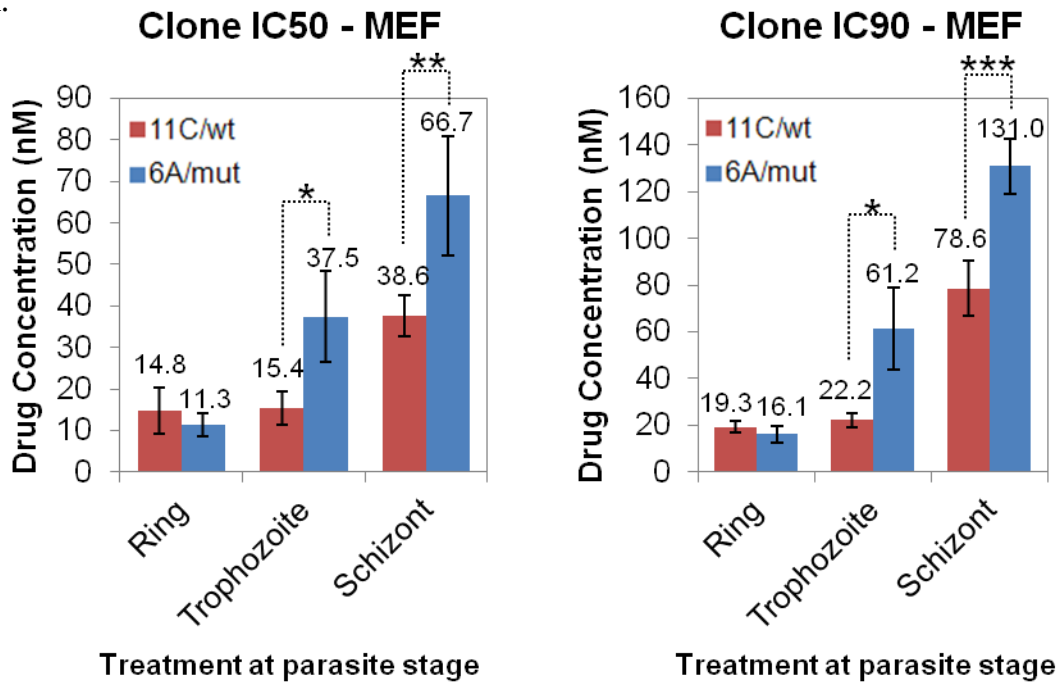

B.

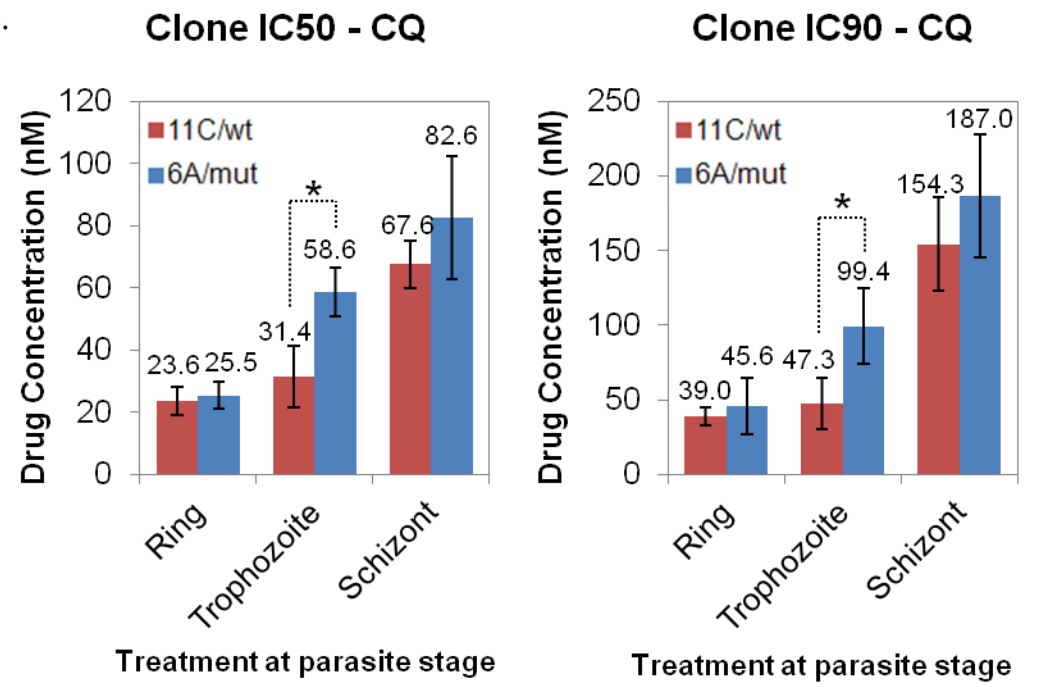

Figure 5-3. Inhibitory concentrations of clones 11C/wt and 6A/mut to mefloquine and chloroquine treated at various stages in the IDC. IC_{50} and IC_{90} values (nM) of clones 11C/wt and 6A/mut treated at mid ring (10 hpi), mid trophozoite (24 hpi) and mid schizont (34 hpi) stages with mefloquine (A) or chloroquine (B) drugs were determined from drug assays done in triplicate. Error bars represent the standard deviations of the IC_{50}/IC_{90} measurements. *: p-value <0.05; **: p-value<0.01; ***: p-value<0.001 calculated using Student's t-test.

5.2.2 Characterization of PfMRP2 protein expression levels

Protein data shows that the MRP2 protein is made up of 2108 amino acids and is 248.3 kDa in size. It is predicted to have 11 transmembrane alpha-helices making up 2 transmembrane domains along with 2 nucleotide-binding domains (ATP-binding cassettes). A schematic diagram of the PfMRP2 protein is shown in Figure 5-4.

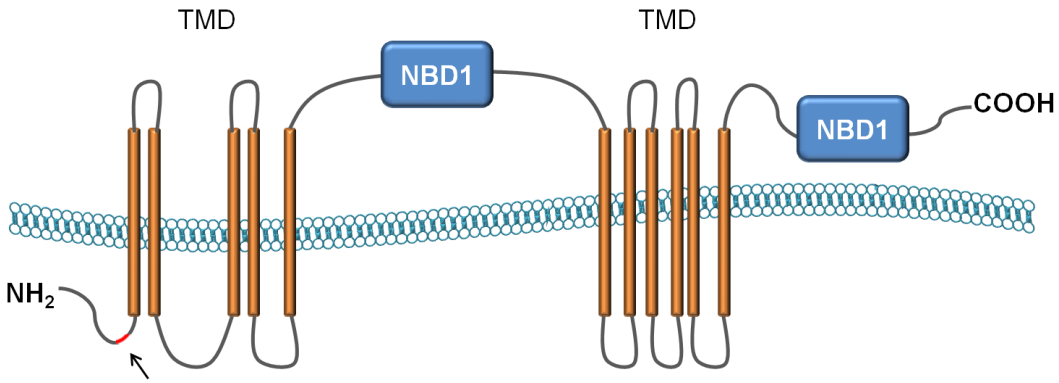

Figure 5-4. Diagrammatic prediction of PfMRP2. Shown is the PfMRP2 protein in the parasite lipid bilayer with respect to the prediction from bioinformatics software TMHMM v2, showing the 2 nucleotide binding domains (NBD) and 2 transmembrane domains (TMD) comprised of 11 transmembrane helices. In red is the span of the 13 amino acid hydrophilic sequence at the N-terminus of the protein where the generated anti-PfMRP2 peptide antibody recognizes.

The question of whether differential mRNA expression profiles in the clones led to differential protein levels expressed was investigated. Antibodies specifically targeting to the PfMRP2 were first raised by synthesizing a 13 amino acid peptide hapten based on selecting a suitable epitope from the predicted protein structure sequence. The amino acid sequence, KNHTNKFHKRKKE, spanning the 101st to 113th position of the protein from the N-terminal (Figure 5-4 black arrow) was chosen based on a good score for hydrophilicity, antigenicity and accessibility using the Bcell Parker Hydrophilicity Prediction and Bcell Emini Surface Accessibility Prediction algorithms. This epitope was predicted to be away from the transmembrane domains and accessible to antibody. The hapten was then conjugated to a mcKLH large carrier

protein that would make the antigen immunogenic. 4 BALB/c mice were then immunized with this immunogen (see Materials and methods section 2.10.) and serum from the final bleed was used to test PfMRP2 protein binding specificity.

Equal amounts of parasites were harvested from highly synchronized cultures of the clone 6A/mut and 11C/wt every 6 hours over the 48 hr IDC. The same volumes of parasite lysates (ie. total protein from equal number of parasites) were ran on the 6% SDS-PAGE gel for all samples and the membrane probed with the anti-PfMRP2 antibody and anti-actin antibody used as a loading control and normalization reference. SDS-PAGE and immuno-blotting analysis revealed a doublet band of 250 kDa, corresponding to the expected size (248.3 kDa) of PfMRP2 protein (Figure 5-5A). In addition, we observed ~130 kDa and <50 kDa bands that may represent processed forms of PfMRP2 (the full length and processed form of PfMRP2 were detected by four antibodies that were generated in separate immunizations) (Figure 5-5B) whereas the negative control of pre-immune sera did not give any bands. To quantify the levels of protein expression, we calculated the sum of the PfMRP2 band intensities for each lane measured by densitometry (Biorad Densitometer, USA) and normalized this optical density (OD) value by the ratio of the actin between the 2 clones for each TP (Figure 5-5A and C). We observed that there was greatest amount of the PfMRP2 protein at trophozoite stage for the clone 11C/wt. However, for clone 6A/mut, highest intensity of the protein bands was detected at later stages in schizonts (Figure 5-5A and C). Overall, there was more PfMRP2 protein expressed in the mutant clone in the second half of the IDC, from early trophozoites to late schizonts, compared to the wild-type clone (Figure 5-5A and C). Interestingly, the 2-fold decreased sensitivity to CQ and MEF for clone 6A/mut in trophozoite and schizont stages but not in ring stage coincides with the increased level of MRP2 protein at

these same stages, suggesting a positive correlation between protein levels and parasite resistance to these drugs. As a whole, the results confirm that the differential timing and abundance of mRNA levels resulted in differential levels of translated MRP2 protein.

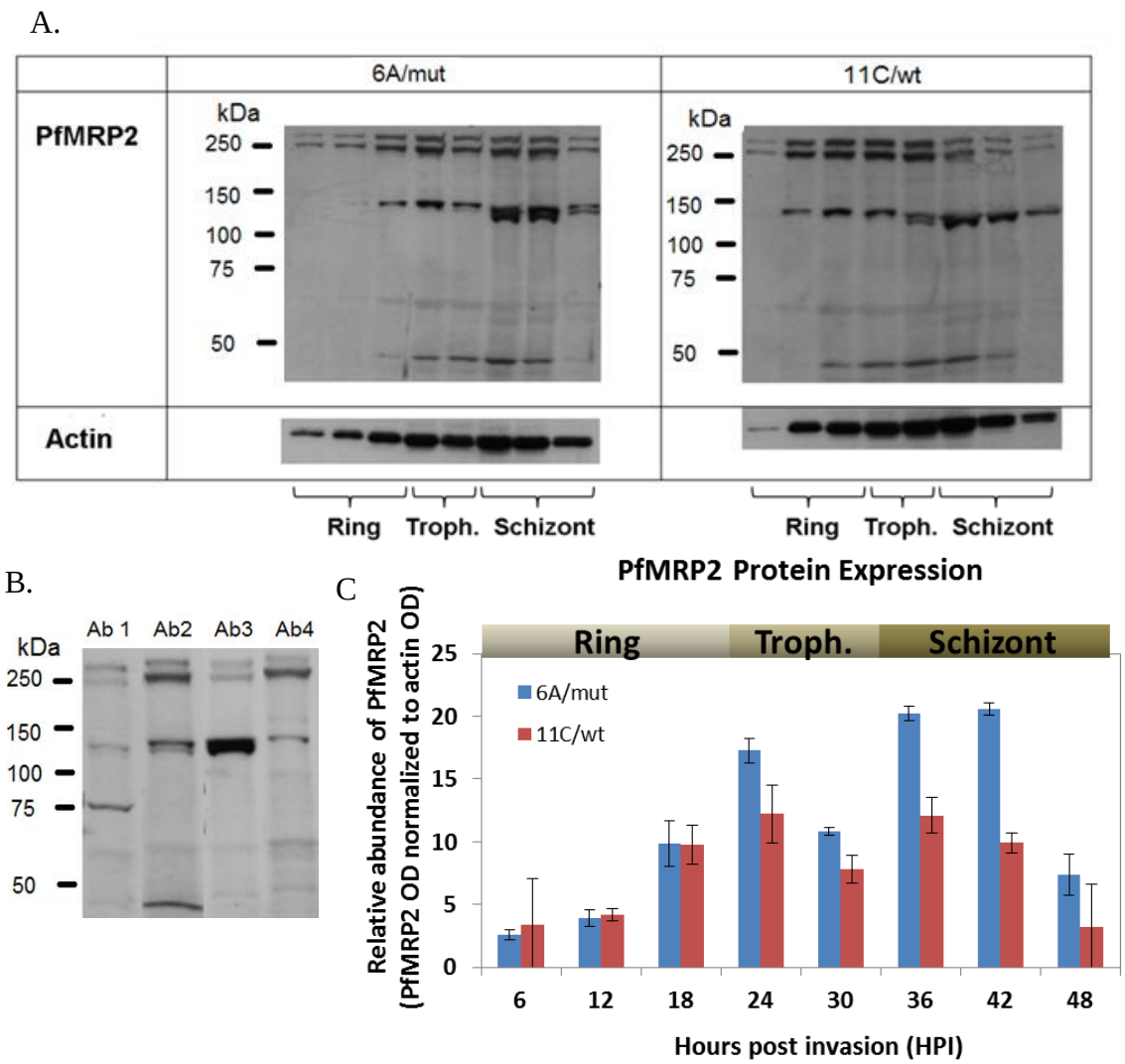

Figure 5-5. PfMRP2 protein expression level of clones 11C/wt and 6A/mut. A. Immunoblot image of the PfMRP2 protein bands detected for each clone sampled at 6 hr intervals over the 48 hr asexual lifecycle. Total protein amounts corresponding to equal number of parasites per time point sample was probed using the anti-PfMRP2 polyclonal peptide antibody. The same samples were probed with actin as a loading control. B. Immunoblot image of the protein bands detected by probing 3D7 total parasite proteins with the 4 anti-PfMRP2 peptide mouse antibodies (Ab1, Ab2, Ab3, Ab4) which were generated in parallel. C. Relative protein expression levels of PfMRP2 measured by densitometer (Biorad, USA). The protein profiles represent the summed abundance of all bands determined by their optical density (OD) over the lifecycle for clone 6A/mut (blue) and 11C/wt (red) and normalized to the ratio of actin between clones. Error bars represent the standard deviation of OD values over three technical replicates.

PfMRP2 protein Cleavage analysis by PEST

We sought to find why a 130 kDa protein band was observed on the blot. Thus, we ran a protease cleavage analysis using PEST algorithm. The results gave a single potential PEST motif of 60 amino acids (RSNDNTPNNNNTDNNNTSDNNNTSNNNNTSDNNNTSDNNNTSDNNNTSNNNNTDNNNTSN) between 940th and 1001st amino acid in the protein with a high probability score of +10.63. Using this value, the predicted size of the cleaved 940 amino acid product was estimated to be 940/2108 x 248.3 kDa = 111 kDa in size, which is similar to the observed protein band size of ~130 kDa.

5.2.3 Localization of PfMRP2 in *P. falciparum* by IFA

PfMRP2 protein localization in the parasites was characterized by immunofluorescence assays using polyclonal anti-PfMRP2 antibodies. Parasites sampled from a highly synchronized culture were visualized every 6 hours over the IDC. Although PfMRP2 signal was observed in all blood stages, the signal intensity and pattern differed during the development of the parasite (Figure 5-6A). In the ring stage (Figure 5-6A), PfMRP2 staining was concentrated to the periphery of the parasite, developed into a punctuated signal enveloping the parasite in trophozoite stage (Figure 5-6A) and later appeared discrete and punctuated around individual merozoites in the mature schizont stage just prior to rupture and invasion (Figure 5-6A). Throughout the asexual blood stage, the MRP2 signal did not overlap with the DAPI signal, indicating that this protein was not found in the nucleus (Figure 5-6A overlay). Schizonts dual-labeled with the anti-PfCRT and anti-PfMRP2 antibodies showed no overlapping signals indicating that PfMRP2 did not associate with the parasite digestive vacuole (Figure 5-6D). The punctuated staining pattern was reproduced by all four polyclonal anti-PfMRP2 antibodies generated independently in

A.

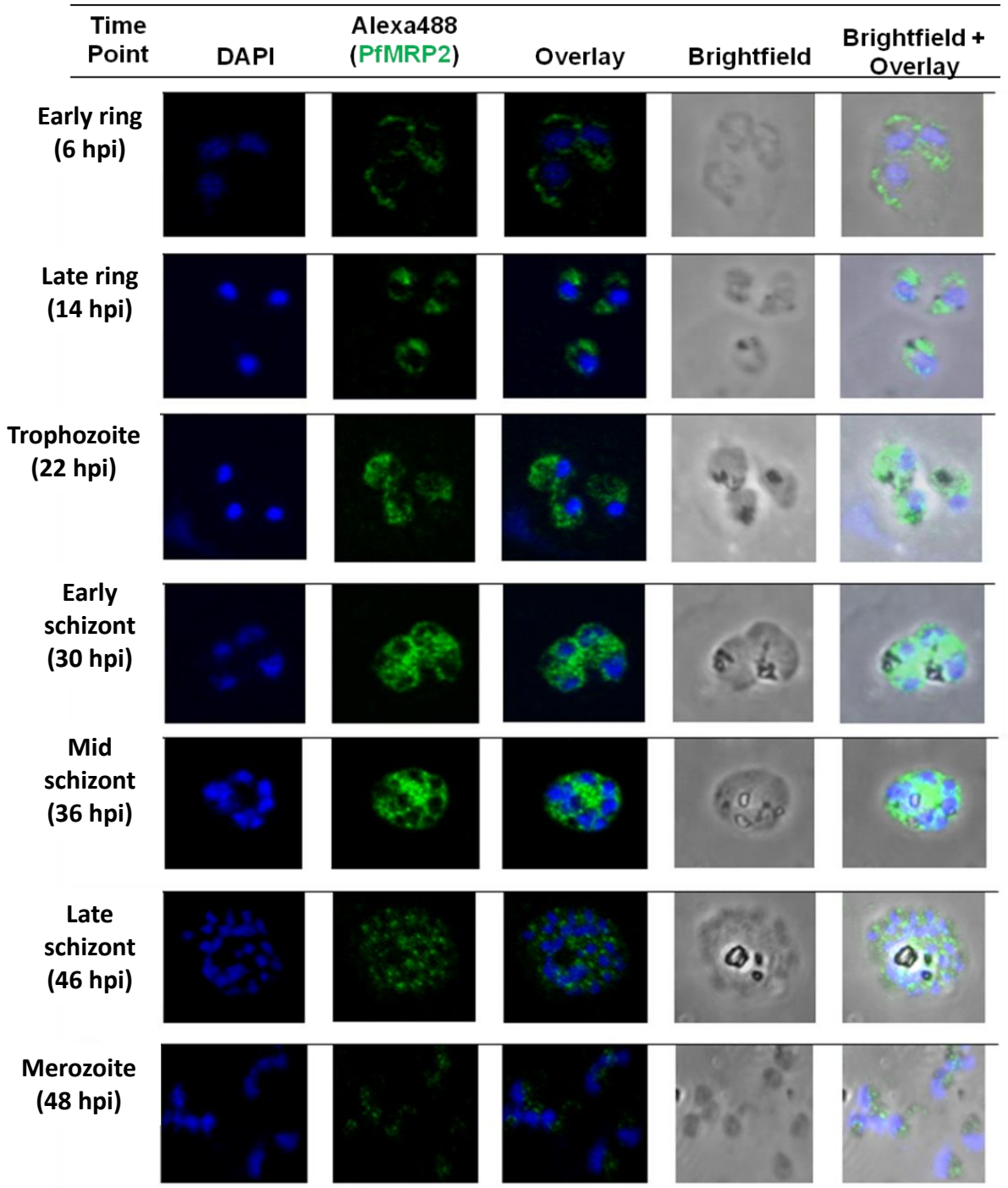

Figure 5-6. Localization of PfMRP2 protein in 3D7 by immunofluorescence assays. Immunofluorescence assay images of 3D7 parasites using polyclonal anti-PfMRP2 mouse antibody followed by Alexa Fluor 488-conjugated anti-mouse Ig (green). Nuclei were stained with DAPI (4′,6′-diamidino-2-phenylindole; blue). A. Parasites were visualized every 6 hours across the IDC from ring to trophozoite to schizont and merozoites. B. Immunofluorescence assay images of 3D7 parasites using each of the 4 polyclonal anti-PfMRP2 mouse antibodies. C. Pre-immune serum was used as a negative control. D. Immunofluorescence assay of dual-labeled early/mid schizonts with anti-PfMRP2 (Alexa488; green) antibody and digestive vacuole specific PfCRT antibody (Alexa594; red) and nuclei stained with DAPI (blue).

B.

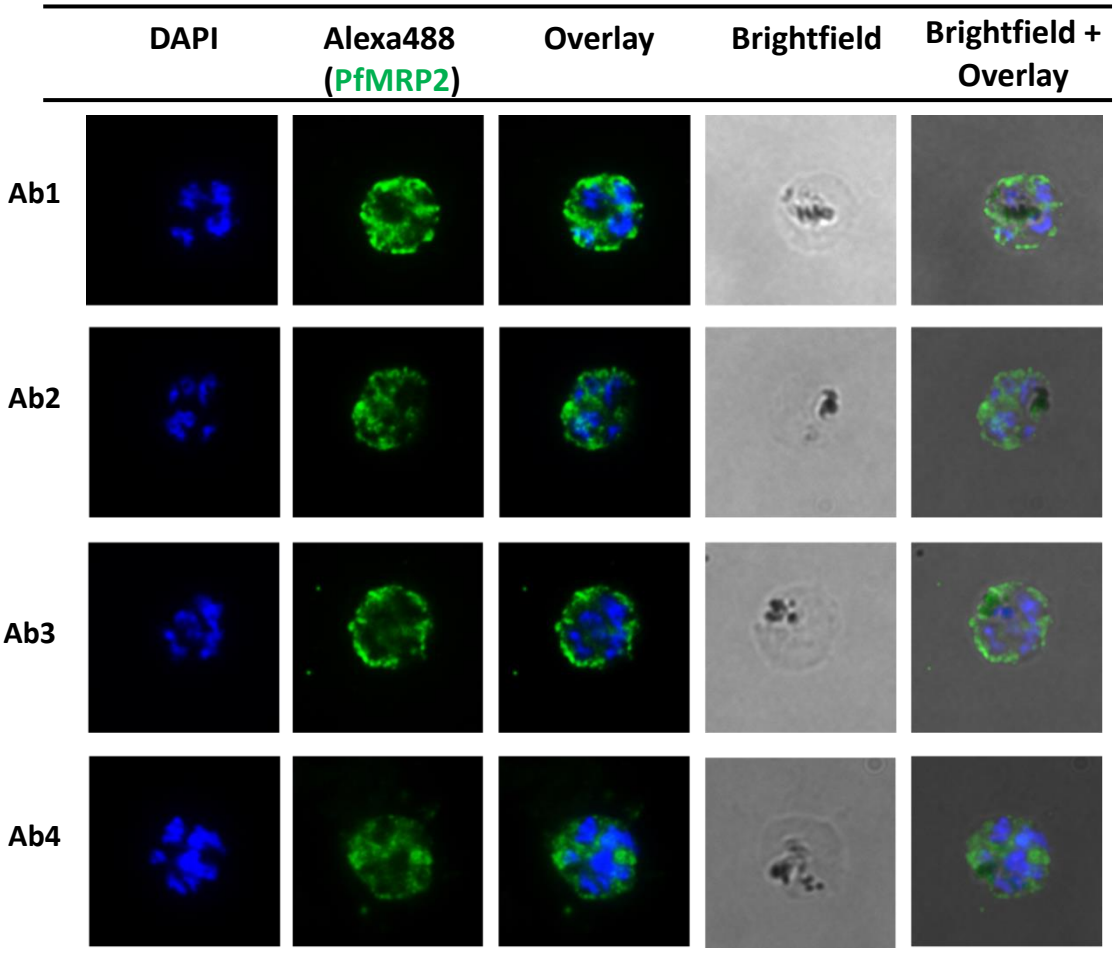
DAPI
Alexa488 (PfMRP2)
Overlay
Brightfield
Brightfield + Overlay
Ab1
Ab2
Ab3
Ab4

C.

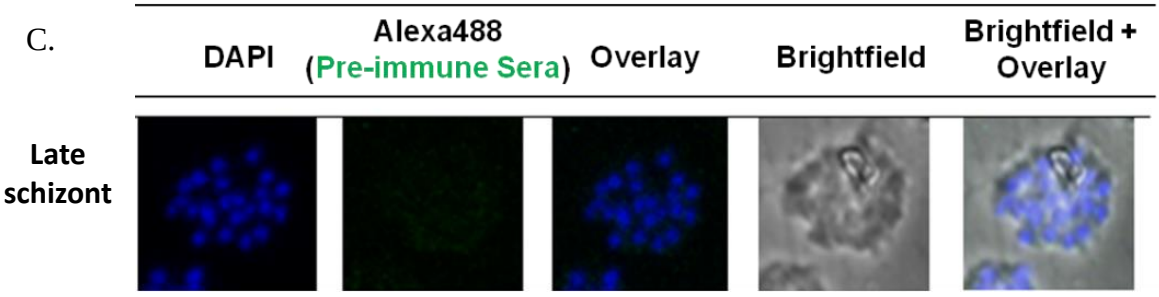
DAPI
Alexa488 (Pre-immune Sera)
Overlay
Brightfield
Brightfield + Overlay
Late schizont

D.

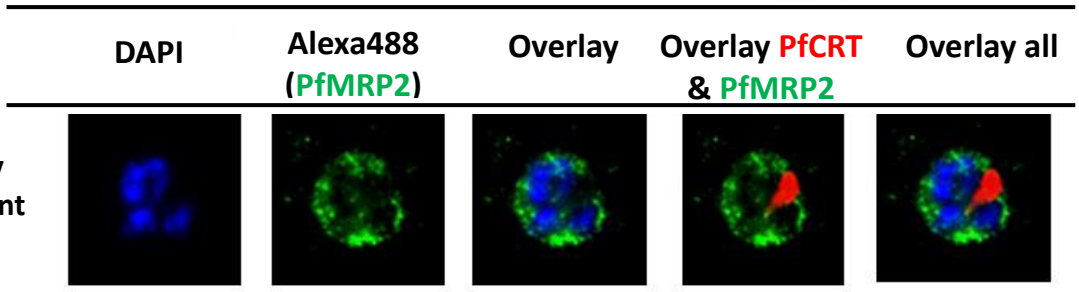
DAPI
Alexa488 (PfMRP2)
Overlay
Overlay PfCRT & PfMRP2
Overlay all
Early schizont

separate immunizations (Figure 5-6B) and no signal was present in the negative control of pre-immune serum (Figure 5-6C). This further confirms the specificity of the derived antibody and by that the localization of the PfMRP2 protein to putative membranous structures. Taken together, the results suggest the protein localizes to discrete sub-cellular, membrane-bound compartments and parasite's plasma membrane which is as expected for a MRP transporter and consistent with the expected intracellular pattern observed for PfMRP1and PfMRP2 [89, 228]. Similarly, mammalian MRPs have been shown to localize to both the plasma membrane [230] and internal vesicular structures [231].

5.2.4 Deletion polymorphisms within the 5' UTR of *pfmrp2* gene

To understand the molecular basis of the differential expression, it was imperative to study how the *pfmrp2* gene was regulated and expressed differently with a shift in timing of maximum expression between the 2 clone groups. While 3 clones (11C/wt, 5D/wt and 8B/wt) showed expression timing of *pfmrp2* similar to 3D7 (PlasmoDB v8.1), 2 clones (6A/mut and 1A/mut) expressed this gene at a different stage of the IDC. We hypothesized that the difference in transcript levels was due to polymorphisms occurring in the promoter region (presumably 1-2 kb) upstream of the gene for clones 6A/mut and 1A/mut. Hence, we designed primers specific for the first 2 kb region of the 5'UTR of *pfmrp2* (Figure 5-7A; orange bars). Surprisingly, while PCR using these primer pairs 2.2, 3.3 and 4.4 gave the expected product sizes for clones 5D/wt, 8B/wt and 11C/wt as indicated in Figure 5-7A, no PCR product was obtained for clones 1A/mut and 6A/mut (Figure 5-7C). However, PCR with 2 primer pairs designed for the ORF of *pfmrp2* (13.13: 0^{th} to 504^{th} position and 14.14: 447^{th} to 878^{th} position) gave positive products of the correct corresponding sizes for all 5 clones (Figure 5-7C), confirming that the deletion is specific to the 5' UTR of the 2

clones and the lack of product is not a reflection of the quality of the genomic DNA template. The closest upstream gene to *pfmrp2* on the same strand is PFL1430c, which is 14,829 bp away, while the closest neighboring gene, PFL1415w, found on the opposite strand is 5,777 bp away. To define the size of the deletion in the 5'UTR, primers spanning across the 14.8 kb 5' region upstream of the gene was designed and PCR was carried out on these additional 12 primer pairs (Figure 5-7A; purple bars). All 12 reactions gave PCR products of expected sizes for clone 11C/wt, but no product was obtained for primer pairs 4.9, 4.10, 4.12, 3.9, 3.10, 3.12, 2.9, 2.10, 2.12 and 1.10 with clone 6A/mut genomic DNA template (Figure 5-7A and B). However, PCR with primers 1.9 and 1.12 gave products of approximately 2.2 kb and 6.2 kb for clone 6A/mut which is about 4 kb smaller than the expected size of 6.2 kb and 10.2 kb as obtained for clone 11C/wt (Figure 5-7B). PCR was also carried out with the primer pair 5.10 (forward primer in the ORF) to check if the deletion was found in only clones 1A/mut and 6A/mut and the results confirm likewise (Figure 5-7D). These results indicate that the deletion segment for clones 1A/mut and 6A/mut occurs approximately between the -20th and - 6,212th position upstream of the *pfmrp2* start codon.

The PCR products for the 5 clones were sequenced using the BigDye sequencing method to identify the precise breakpoint of where the deletion segment starts in the 5' UTR of the clones 1A/mut and 6A/mut. Multiple sequence alignment revealed that the sequences of the 5 clones from the coding region until 248th base upstream of the start codon are highly identical to the 3D7 reference sequence taken from PlasmoDB v8.1 (Figure 5-8A). Sequence of the mutant (drug resistant) clones did not follow the 3D7 reference sequence from approximately 250 bp upstream, just before a long 45

poly(dA:dT) tract known as an A-tract, whereas the wild type clones followed the 3D7 sequence (Figure 5-8A).

A.

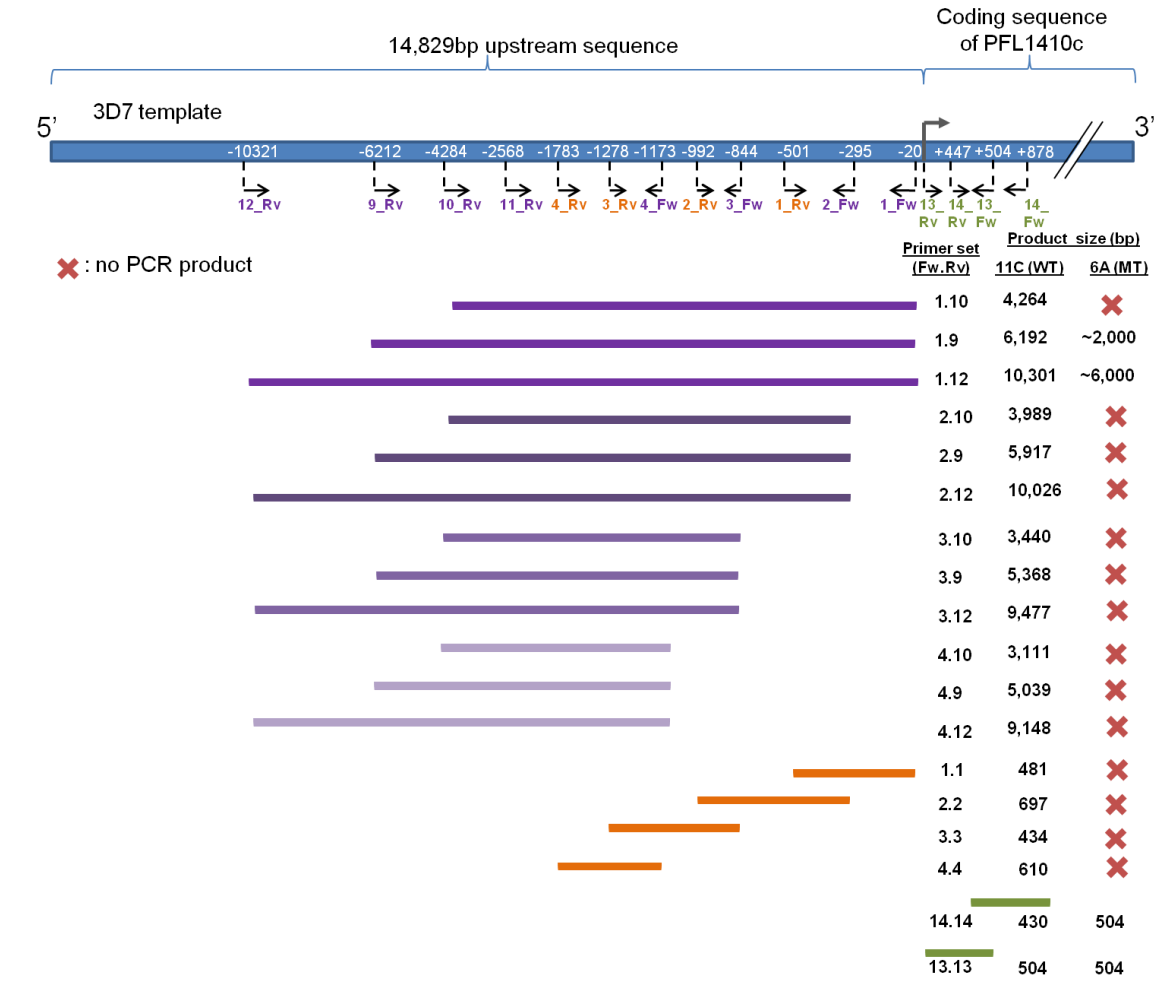

B.

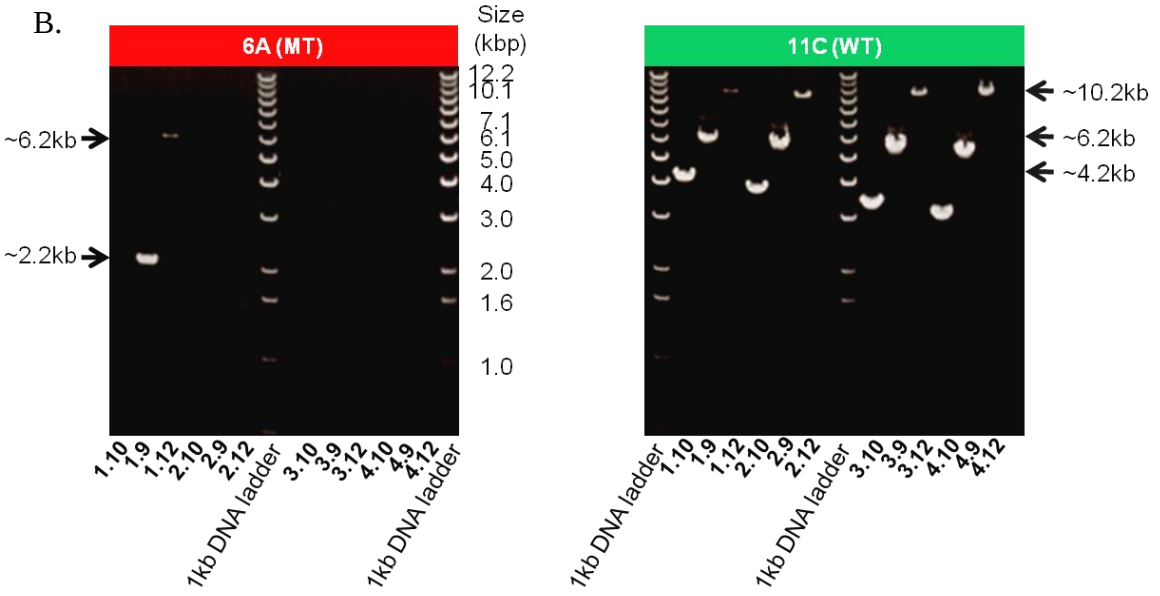

C. D.

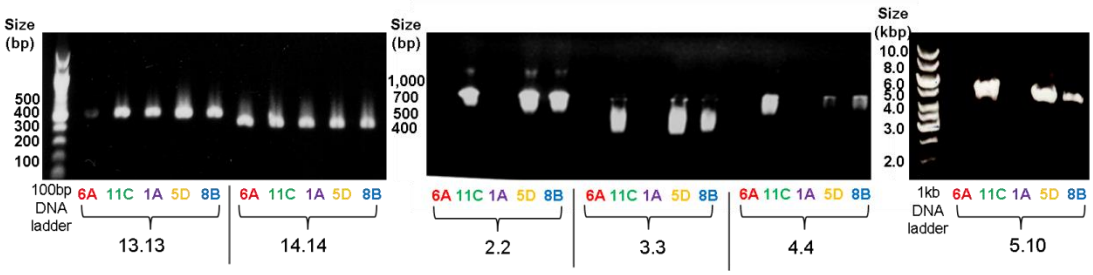

Figure 5-7. Mapping of *pfmrp2* promoter polymorphisms by PCR. A. Map of upstream regions of the 3D7 *pfmrp2* gene showing the panel of primer pairs (purple and orange) used and their positions on the upstream 5' UTR of the gene on the reverse strand. Listed are the sizes of the PCR products obtained for clones 11C/wt and 6A/mut for the various primer pairs. All clone 11C/wt PCR products are of the expected sizes. Included are 2 primer pairs spanning the ORF of the gene (green) as positive control for presence of the gene. B. Agarose gel picture of PCR products for the various primer pairs showing the truncated products of 1.9 and 1.12 and deleted product of 1.10 for clone 6A/mut and full length products for clone 11C/wt for all primer pairs (sizes are stated for 1.10, 1.9 and 1.12 primer pairs). C. Agarose gel picture of PCR products showing the full length products obtained for all 5 clones for the primer pairs covering the ORF (13.13 and 14.14), and (D.) full length products obtained for only clones 11C/wt, 5D/wt and 8B/wt for primer pairs 2.2, 3.3, 4.4 and 5.10 but no PCR products for clones 6A/mut and 1A/mut.

In order to find the other break point site in the mutant clone, we sequenced the 2 kb cloned promoter construct of 6A/mut. Pair-wise alignment of the partial promoter sequence mapped to -4,345th position from *pfmrp2* gene (Figure 5-8A). In addition, microarray data showed that the upstream gene PFL1415w is present for all 5 clones. CGH data also gave a detectable signal for the intergenic probe at -4850th from the start codon of PFL1410c. Based on the PCR and sequencing results, we conclude that clones 1A/mut and 6A/mut have a deletion of 4.1 kb in the 5'UTR promoter region of *pfmrp2* gene with a break point at the -248th position and the sequence resuming from the -4,345th position upstream based on multiple sequence alignments (Figure 5-8A and B). Interestingly, we observed that both the break point occurs at a DNA site comprised of a stretch of 14 direct repeats of (TA) followed by a long homopolymer T stretch (>24 nt) (Figure 5-8A), suggesting that these highly homologous sequences in these 2 segments of the DNA may play a role in the deletion of the large DNA

fragment. However, unlike PFL1410c gene which shows 2 distinct, anti-correlated mRNA expression profiles for the 2 groups of clones, the upstream gene PFL1415w which shares a common intergenic region as PFL1410c, does not differ in its mRNA expression among the 5 clones (Figure 5-8B). This proves that the 4.1 kb deletion in this intergenic region did not have any effect on the expression of PFL1415w gene and the promoter for this gene lies within ~1.4 kb upstream of its start codon.

A.

B.

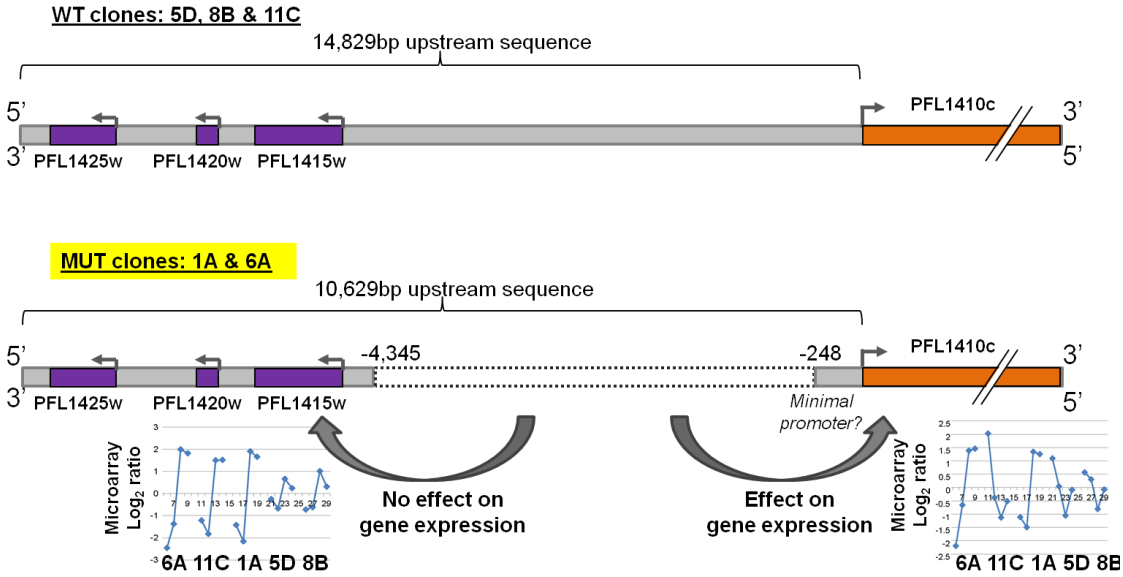

Figure 5-8. Sequence alignment showing deletion in upstream sequence of *pfmrp2*. A. Sequence alignment of WT: wild type clones and MUT: mutant clones compared to 3D7 sequence (PlasmoDB v8.1) showing the 200 bp segment of gene and the upstream, non-coding region of *pfmrp2* gene where the double break points occur (grey dotted lines). Numbers indicate the base position relative to the start codon. 2 constructs of 6A of size 300 and 500 bp were sequenced to verify the deletion break point is at -4,345th bp from start codon. B. Schematic diagram of the upstream regions of WT and MUT clones showing the breakpoint sites and deletion segment in the MUT clones (grey dotted box), along with the upstream genes on the opposite strand (purple). The numbers are relative to the PFL1410c (*pfmrp2*) gene start codon. Graphs depict the expression pattern of the gene PFL1415w and PFL1410c for each clone over the 48 hour IDC.

5.2.5 Activity of Mutant vs Wildtype Promoter (Firefly Luciferase reporter assay)

In order to determine if this deletion in the 5' UTR of the gene had a direct effect on the discrepency in transcript expression profiles between the mutant and wild type expressing clones, we carried out transfections involving a dual-luciferase reporter gene assay with the 2 kb upstream promoter sequence of the gene for clone 11C/wt and 6A/mut as constructs controlling the firefly luciferase activity.

The 2 kb sequence in the 5' UTR of *pfmrp2* for clones 6A/mut and 11C/wt were cloned upstream of the firefly luciferase gene into the Pf86 vector by replacement of the 5' *pfhsp86* sequence with the sequence of interest to generate the vectors: PF86-5'UTR-WTmrp2-FL and PF86-5'UTR-MUTmrp2-FL (Figure 5-9).

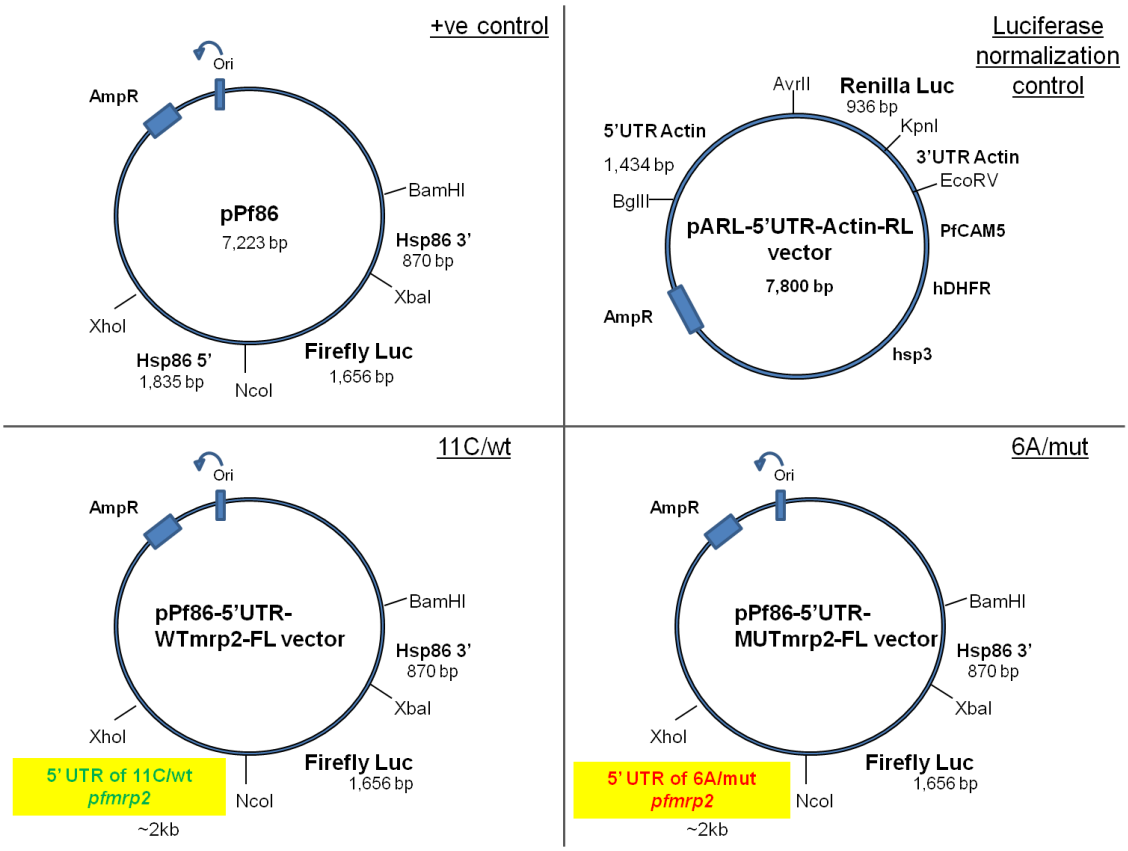

Figure 5-9. Schematic of plasmid constructs created with *pfmrp2* promoter sequence. Plasmids created include 2 vectors with firefly luciferase activity driven by the constructs of *pfmrp2* 5' 2 kb promoter regions – 6A/mut and 11C/wt, the Pf86 plasmid (positive control for firefly luciferase activity) and the pARL-5'UTR-Actin-RL plasmid containing renilla luciferase (loading control and normalization reference).

From the transfection experiments and after normalizing to renilla luciferase activity, we observed a significant difference in the level of the firefly luciferase activity between the 2 transfected cell lines in all 3 stages (one-sample Student's t-test at 95% confidence interval; Shapiro-Wilk normality test proves normality of data). The cell line containing the plasmid with the 2 kb promoter construct of clone 6A/mut

consistently gave significantly higher firefly luciferase activity compared to the cell line containing the plasmid with clone 11C/wt 2 kb promoter, in ring (mean 1.88 fold; p-value = 0.02), trophozoite (mean 2.00 fold; p-value = 0.001) and schizont (mean 2.35 fold; p-value = <0.001) stages (Figure 5-10B). This reflects a generally more active promoter and higher transcriptional activity of the mutant 2 kb 5' UTR sequence than the wild type 2 kb sequence. More importantly, the results indicate that within the 2 kb 5'UTR sequence of the *pfmrp2* gene, there are promoter elements (silencer/enhancer) that regulate the level of gene transcript over the course of the IDC. These results also confirm that the 4.1 kb deletion in the 5'UTR of the mutant clones has a direct effect on the transcriptional activity and result in different transcript levels of *pfmrp2*.

A.

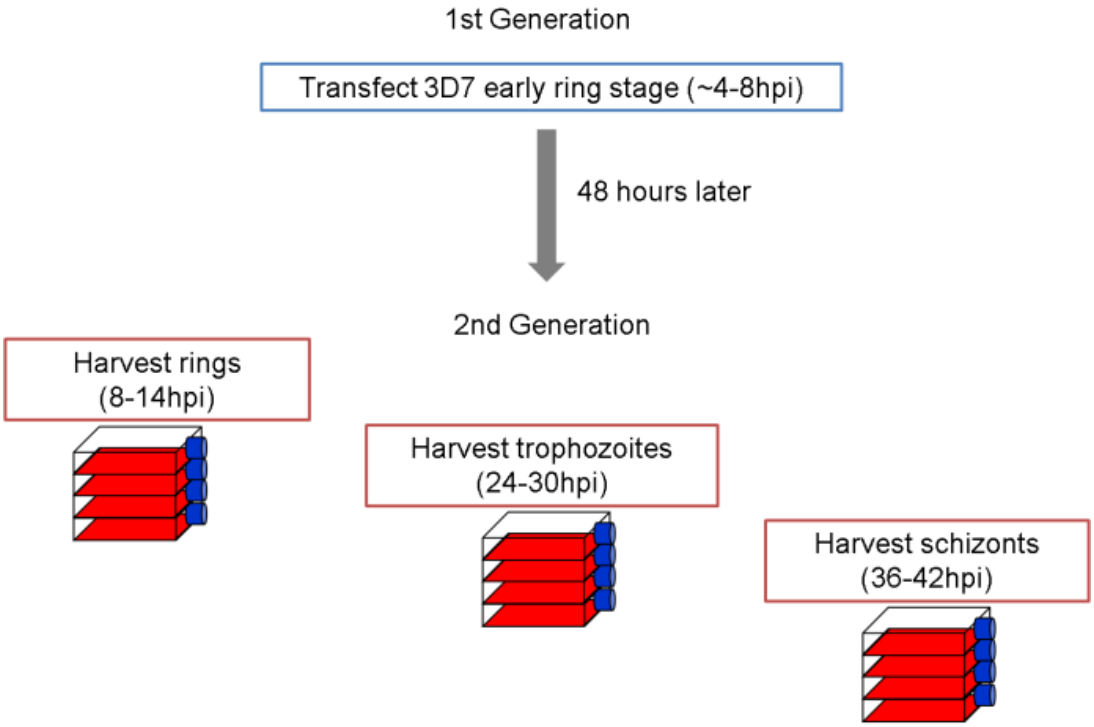

B.

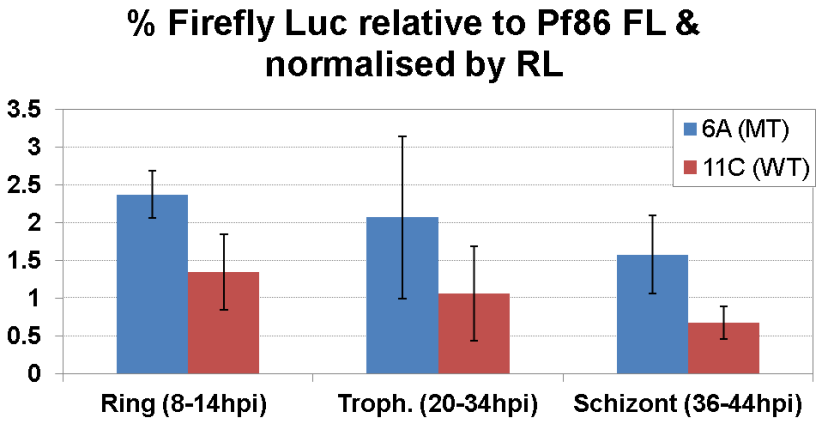

Figure 5-10. Firefly luciferase activity of *pfmrp2* mutant and wild type promoters. A. Overview of Pf episomal transient transfection experiment. Equal ratio of the plasmid of interest and RL plasmid was transfected into a highly synchronized culture of 3D7 at the early ring stage at 6 hpi. The cells were grown for one generation and then measured for bioluminescence levels i.e., firefly/renilla luciferase activity in the subsequent generation at ring, trophozoite and schizont stages to determine the promoter activity of the *pfmrp2* 2 kb sequence in this reporter gene assay. The experiment was done in triplicates independently. B. For each stage of the IDC, bars indicate the averaged firefly luciferase (FL) activity of clone 6A/mut (blue bars) versus clone 11C/wt (red bars) constructs relative to positive control of Pf86 FL and normalized to the same level of RL activity in each transfected cell line. Error bars indicate the standard deviation of the FL activity over 3 independent transfection experiments.

5.3 Discussion

5.3.1 Deletion in promoter region drives differential expression of *pfmrp2* gene

The phenomenon of a large deletion of 4.1 kb in the upstream promoter region of a gene resulting in the differential expression of the gene is so far unprecedented in *P. falciparum* biology. This is the first observation showing the association between promoter deletion and change in timing of gene expression in the IDC. Furthermore, the break point sites giving rise to this deletion were found to be associated with the presence of stretches of TA repeats (n>13) followed by a long poly T tract (>25 nt).

Poly(A/T) tracts are known to encourage polymerase slippage during DNA replication and may have led to the deletion breakpoint at the 248th nucleotide. This 4.1 kb deletion could be casued by chromosome breakage and healing type deletions such as Microhomology-mediated end joining (MMEJ), Single strand annealing (SSA) or Non-homologous end joining (NHEJ) repair mechanisms (Figure 5-11). In MMEJ and SSA, after the double strand break (DSB) occurs, 5'to 3' resection takes place and either the 5-25 (MMEJ) or >30 (SSA) base pair repeat homologous sequences flanking the DSB allows for the alignment of the broken strands prior to joining and repair by DNA ligases (Figure 5-11). This process, especially SSA, involves flap trimming and often leads to deletion of large genomic sequences in between the repeat sequences [245, 246]. Alternatively, non-allelic homologous recombination where intrachromosomal crossing-over occurs between lengths of homologous sequences may randomly occur during replication and give rise to the deletion region [245, 247] (Figure 5-11). Our results also showed that the conservation of the first 248 nucleotides of the 5'UTR across all clones suggest that it could funtion as a minimal core promoter site for binding of the transcription initiation complex.

How does this 4.1 kb deletion in the UTR vary the timing of *pfmrp2* gene expression? Interestingly, the mRNA expression profile of the neighbouring gene, PFL1415w is similar to the mutant expression profile of PFL1410c regardless of whether the deletion is present in the intergenic region between both genes. This suggests that there may be a bidirectional promoter element which dictates the expression profile to peak in trophozoite/early schizont stage. In addition, the data also suggests that within the 4.1 kb deletion harbours a unidirectional transcription regulatory element that shifts the gene expression timing to a profile that peak in early ring stage, resulting in

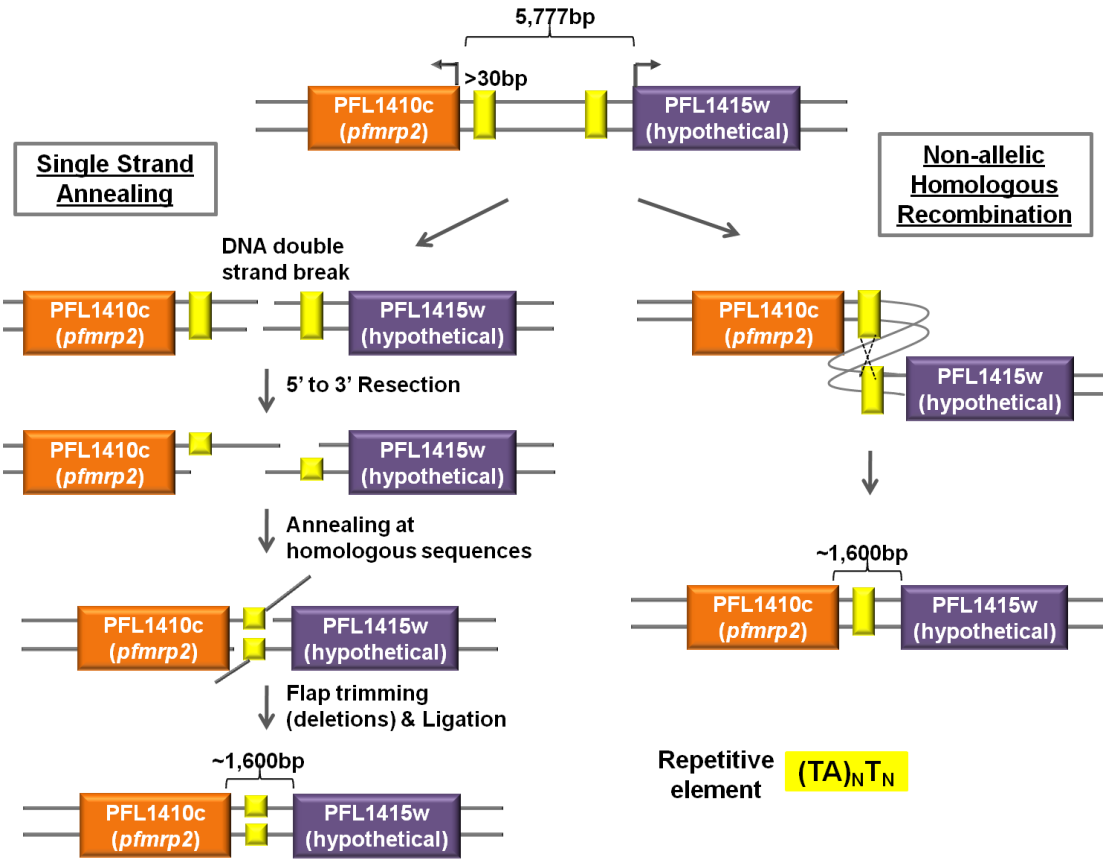

Figure 5-11. Proposed mechanism of the 4.1 kb deletion in the intergenic genomic sequence upstream of PFL1410c. This occurs either through single strand annealing double strand break repair mechanism or through intra-chromatid non-allelic homologous recombination during DNA replication to result in a truncated intergenic region of ~1.6 kb. In yellow are the homologous sequences of >30 nucleotides found upstream of both PFL1410c and PFL1415w genes that are required for the repair or crossing over.

the wild type PFL1410c expression pattern. A scan of predicted regulatory motifs identified by the FIRE program of the *P. falciparum* HB3 transcriptome [248] showed that a probable motif is present between the 700 to 800th position upstream of the gene's start codon which is related to timing of expression. ChIP-chip data shows that the stage-specific enrichment of H3K9ac and H3K14ac modifications at the 500th bp position upstream of start codon is highly positively correlated (PCC = 0.7) with the wild type mRNA transcript expression (Gupta et al, manuscript submitted). The absence of this 4.1 kb segment and hence lack of these histone modification marks in

the mutant clones point to the potential of particular histone modification marks in eliciting an effect on the timing of *pfmrp2* gene expression. Further studies include carrying out ChIP-Chip on these clones to determine the potential role of the histone marks on gene regulation. More constructs are needed in order to define the relationship between promoter activity and the mRNA transcript level in these 2 clones and to identify the promoter element which regulates the stage-specific timed transcription.

5.3.2 Role of PfMRP2 in CQ/MEF resistance

A study showed that selection of chloroquine-resistant *P. berghei* parasites did not result in any *pfmrp2* gene amplification or increased mRNA expression, although the discontinued administration of CQ drug when carrying out the experiments may have resulted in the lack of any observable increased gene expression [249]. An additional confounder was that the study compared the mRNA levels extracted from a mixture of different intraerythrocytic stages instead of looking at parasites at a particular stage.

Our data suggest that MRP2 protein is important for mediating resistance to antimalarials of CQ and MEF in the parasite. A study had found that efflux of glutathione conjugates is 2-fold higher for drug-resistant compared to drug-sensitive strains (Dd2 and 3D7) in the presence of inhibitors of glutathione synthesis, thus showing that Dd2 strain is able to preserve intracellular glutathione and intracellular thiol redox environment more efficiently than 3D7 under stressed conditions. This suggests that glutathione transport as well as glutathione metabolism could be involved in mediating drug resistance since reduced glutathione (GSH) assists in heme detoxification and protects parasites from cytotoxicity [88]. Since MRPs are involved in this pathway, MRP2 may play a role in mediating drug efflux and drug

resistance in this manner. It has been confirmed that PfMRP1 functions to efflux GSSG and GSH-drug adducts out of the parasite as knock out of PfMRP1 leads to increased accumulation of GSSG, CQ and QN within the parasite and results in a small but significant 1.6-fold increased sensitivity of the parasite to chloroquine and various antimalarials [89]. There was however no association of mefloquine sensitivity to knock out of PfMRP1. Unlike the export function of PfMRP1, PfMRP2 is believed to be an importer of GSH from the host cell into the parasite, seeing that GSH synthesis by glutathione synthase only peak in trophozoite stages and the parasite requires a source of GSH during the early asexual stages [244]. GSH is an important molecule needed for removal of H_2O_2 as well as for degradation of the toxic metabolite, free heme (ferriprotoporphyrin IX), into ferrous ions, Fe^{2+}, during hemoglobin digestion in the parasite's digestive vacuole [250]. Both CQ and MEF are quinolines that bind to free heme and thereby inhibit the polymerization to hemozoin. The accumulation of the toxic free heme leads to oxidative stress and membrane damage within the parasite which finally causes cell lethality [251]. It was suggested that parasites resistant to CQ had higher levels of intracellular GSH enabling lessened accumulation of the toxic ferriprotoporphyrin IX and greater cell survival [252, 253]. Another study showed that addition of exogenous GSH also enables CQ-sensitive parasites to withstand 2-fold more CQ, although this was associated with reduced drug accumulation within the parasite as a consequence of increased efflux of GSH-drug adduct from the parasite [89]. Taken together, a larger pool of reduced glutathione (GSH) enables the cells to resist quinolines. Elevated levels of the PfMRP2 protein in the trophozoite and schizont stage of the clone 6A/mut can either cause increased GSH concentrations in these mature asexual stages or lead to a

reduction in the GSSG and drug levels within the parasite, allowing the cell to withstand the toxic effects of the drug.

From the IFA results, PfMRP2 is found in the cytoplasmic membrane-bound vesicles and the plasma membrane of the parasite during the trophozoite and schizont stage which is similar to the localization of MRPs in human cells. In multi-drug resistant cancer cells, MRPs on membrane-bound vesicles have been shown to sequester substrates away from the nucleus of the cell, thereby preventing the compounds from eliciting their mode of action [231]. Hence, the presence of PfMRP2 on the membranes of vesicles may allow sequestration of antimalarial CQ and MEF drugs away from their target sites of the parasite's digestive food vacuole. PfMRP2 on the parasite's plasma membrane may function to import reduced glutathione from the external environment or export GSSG and GSH-drug adducts out of the parasite. Future work include experiments to measure the levels of GSH and GSSG/drug accumulated levels in the drug-sensitive and drug-resistant parasite clones at baseline levels and in the presence of antimalarial drugs known to elicit oxidative damage. Attempting genetic knock out of *pfmrp2* gene would be feasible if this protein is not essential for the survival of the parasite. If this is an essential protein, episomal overexpression of this protein can be carried out instead. The knock-out or over-expressing cell line can be characterized for drug sensitivities towards mefloquine and chloroquine in drug assays to determine the role of this protein in mediating drug responses. To ascertain if PfMRP2 functions to transport GSH or GSSG, the levels of these glutathione molecules can be measured in the knock-out or over-expressed transfectants.

5.3.3 From Gene expression to Protein expression to Phenotype

Based on the results, we propose a model where a deletion polymorphism of 4.1 kb in the 5'UTR promoter region of the *pfmrp2* gene alters and leads to a shift in the time of maximum expression of the gene (Figure 5-12 (1)). The result is a higher level of the MRP2 protein produced in trophozoite and schizont stages (Figure 5-12 (2)) which is accompanied by decreased drug sensitivities towards CQ and MEF. The effect on drug sensitivity is mediated either through increased drug efflux or increased GSH import across the parasite plasma membrane or increased drug sequestration into membrane-bound vesicles (Figure 5-12 (3)). Since CQ and MEF drugs induce oxidative stress within the parasite due to their inhibition of polymerization of heme to hemozoin during hemoglobin digestion, increased GSH levels would enable degradation of the accumulated toxic heme in the digestive vacuole and thus lessen the oxidative stress inflicted upon the parasite (Figure 5-12 (4)). Hence, increased transport of PfMRP2 makes the parasite more resistant to drugs by either increasing GSH import and/or decreasing drug accumulation within the parasite. Based on our results, we propose that PfMRP2 may be an important modulator of CQ and MEF resistance in field isolates. Since this mutant expression profile arose independently of any drug selection in our single clones, this mutant expression of PfMRP2 protein could be frequent in field isolates. The importance of PfMRP2 as a molecular marker of drug resistance in field isolates can be further strengthened by determining the presence of the deletion in the promoter of the *pfmrp2* gene in MEF or CQ resistant field isolates and correlating the deletion to measured *ex vivo* IC_{50}s. The implication of finding such a relationship is far reaching. Besides, being beneficial to the field of Malaria drug resistance where drug resistant markers have so far been limited to a handful of gene candidates. This also provides a framework to dissect the gene

expression differences between clones and isolates to uncover genes crucial for regulating phenotypic growth rates and drug sensitivities.

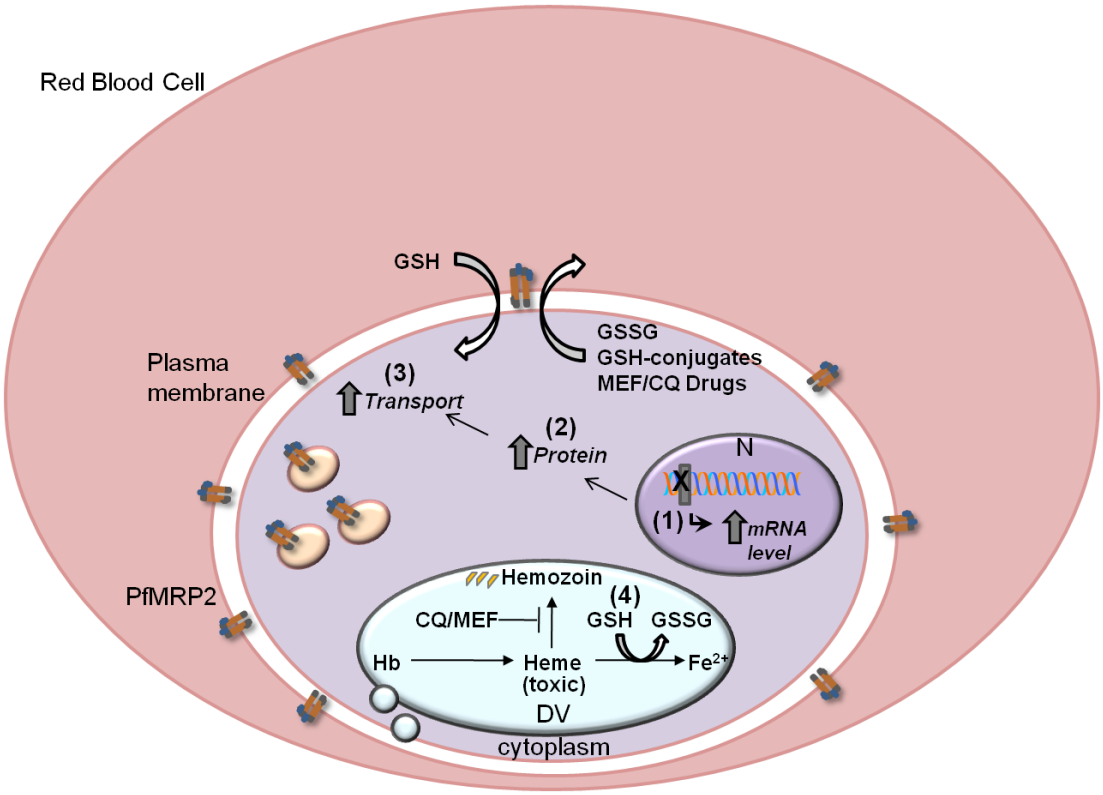

Figure 5-12. Proposed model showing the underlying association of drug resistance in mutant clones and deletion polymorphism in *pfmrp2* promoter.
The deletion in the 5'UTR promoter of *pfmrp2* gene leads to differential mRNA profiles (1) and higher levels of PfMRP2 protein translated in the 2nd half of the IDC (2), resulting in increased transport of glutathione molecules (either import of GSH or efflux of GSH-drug conjugates) (3). Increased GSH levels allow the parasite to degrade free heme to non-toxic products (4) while increased efflux of the drug/GSH – conjugates prevents drug accumulation within the parasite, hence enabling the parasite to withstand higher concentrations of CQ and MEF antimalarial drugs. N: nucleus; DV: digestive vacuole; Hb: hemoglobin

Chapter 6 : Conclusion and Future Directions

The study of single clones from a parent clonal line of 3D7 has given rise to the question of what defines a clone. And how long is a clone stable for? 3D7 was originally cloned by limiting dilution from NF54 when it was first isolated from a patient in the Netherlands airport. However, our studies and others have observed the impact of long term *in vitro* culture on the genotype of the parasite i.e. the presence of clonal lines that are non-isogenic within the parent population through a sampling of 5 clones. With the exclusion of copy number variants, we further identified genes which were clonally variant and non-mutually exclusive in expression between the single clones of 3D7 using microarray-based transcriptional profiling. Some of these were identified in other studies as clonally variant such as exported proteins (*phist*, *hyp*) invasion-related, transmission-related, Maurer's cleft associated, *fikk* protein kinases and a number of zinc finger or ApiAP2-domain containing transcriptional regulators [129]. Besides these, we identified additional genes, namely hemoglobin digestion-related falcipain and histidine-rich protein, REDOX related genes such as superoxide dismutase and molecular chaperones of heat shock proteins which exhibited a diversification in the level of gene expression between clones. While previous studies found that invasion phenotypes and cytoadherent characteristics were epigenetically regulated in the parasite, these findings indicate that epigenetic mechanisms may be involved in the regulation of metabolic phenotypes. In a broad perspective, our findings hint that parasites may have the capacity to either modulate their redox "lifestyle" in order to proliferate in a variety of unique host cell environments (eg. redox disequilibrium arising from G6PD deficiency or hemoglobinopathies) or parasites expressing suitable levels of redox-related enzymes/transporters to survive in particular stressful host conditions may have a selective advantage *in vivo*. It would

be interesting to follow up with functional genetic studies to understand the physiological roles of these genes in enabling parasite's survival under various environmental pressures and in the presence of drugs.

From the study involving the adaptation of an isolate to *in vitro* culture conditions, we observed that parasites consistently display transcriptional variation of pathways relating to host-remodeling (Maurer's cleft genes), invasion process and family of fatty acyl-coA synthetases and protein kinases from one generation to another generation. Despite that these same pathways were likewise differentially expressed between both field isolates, yet we found that other genes such as the anti-folate drug resistance related genes, DHFS and GTP cyclohydrolase I, and DNA replication-related genes were expressed at significantly higher levels in one isolate compared to the other throughout the entire adaptation process spanning over 60 days. This suggests that the expression levels of these pathways related to the drug response or replication and cell cycle regulation are highly conserved and distinguish an isolate from another. Sequencing of these two isolates would reveal the contribution of underlying genetic difference to the observed transcriptional differences. Overall, we did not detect increased/decreased expression of any specific metabolic pathways or growth-related genes common to both isolates, suggesting that neither selection of pre-existing parasites occurred nor did the adaptation of the field isolates to culture drive direct transcriptional responses in the parasite's growth. Taken together, we can conclude that these genes showing transcriptional variation are not subjected to tight regulation of expression levels in order for the parasite to survive under *in vitro* culture conditions. Moreover, these genes form the background of constant transcriptional variation which acts as a confounder in the analysis of genome-wide association and perturbation studies using comparative transcriptomic approaches.

Overall, these studies emphasize the importance of finding the right markers to use in identifying clones in a parasite population. Our findings have demonstrated that the "standard" genotyping techniques using *msp* alleles have failed to distinguish non-isogenic clones arising from long term culture adaptation. We need better genetic markers that can differentiate clones more accurately. Alternatively, the use of expression or epigenetic markers is worth exploring in future since certain inheritable and clinically relevant traits may not arise solely from genetic factors.

Notably, we present *ex vivo* transcriptional profiles associated with artemisinin resistance of field isolates where down-regulation of major metabolic and cellular activities in ring and trophozoite stage reflect a lowered active growth and metabolism of the parasite compared to sensitive isolates, allowing them to escape the cytotoxic effects of the drug by decreased drug activation. These resistant parasites express higher levels of protein synthesis related function in the schizont stage, which may suggest that these parasites catch up with these early processes in the second half of the blood stage. Future work to culture adapt these resistant parasites that are associated with this distinct transcriptional profile *ex vivo* would be crucial and to characterize transcriptional changes over the course of culture adaptation. This would allow us to determine if physiological distinct states are preserved in culture. Furthermore, functional genetic experiments can be performed on these stable lines to understand the mechanism of drug resistance. Transcriptional profiling of a larger number of isolates which display delayed clearance phenotype may enable us to narrow down and identify a few candidate genes whose gene expression is highly correlated to artemisinin resistance. This would be particularly useful as *in vitro* correlates of drug resistance seeing that there are none available.

Lastly, we have shown that structural polymorphisms including indels in promoter regions of genes (*Pfmrp2*) which naturally occur in nature have broad implications on the gene expression timing and expression level of the downstream gene. More importantly, these changes at the genomic level relate to phenotypic variation in terms of characteristics such as parasites fitness and drug sensitivities. These findings give weight to the role of SNPs in non-coding regulatory regions which should be studied further and related to data from transcriptional profiling. Our results also highlight the role of PfMRP2 protein in resistance to drugs which induce oxidative stress and as a potential resistance marker for use in the field.

Role of redox in parasite's physiology and regulation of drug responses

Taken together, we propose that the observation of cell to cell transcriptional variation in redox enzymes, heat shock proteins and hemoglobin digestion associated enzymes which all have a common goal of parasite's detoxification process and maintaining redox equilibrium may reflect the parasite's flexibility in surviving in changing host environments or increased the chance of survival in the presence of oxidative damaging antimalarial drugs. In the case of PfMRP2, we have shown how a genetic copy number polymorphism in the promoter of the gene can play a role in modifying the expression level of the protein which correlates with the increasing tolerance to CQ and MEF compounds that are known to induce oxidative stress either through inhibition of heme polymerization or directly generating ROS. This in turn suggests that the protein's function may be linked to the transport of GSH into the parasite. However, for *in vivo* artemisinin-resistant field isolates, we did not observe elevated expression of resistance thioredoxin or glutathione pathways, despite that artemisinin is reported to produce oxidative damage in the parasite. Resistance to antimalarial such as artemisinin may be mediated through other means such as slowing down the

ring stage development or metabolism. The effect of this is decreased hemoglobin digestion which has a two-fold advantage to the parasite in withstanding the cytotoxic effects of the drug. Firstly, less amount of toxic heme would be generated and secondly, a reduced pool of activated artemisinin would be present since ferrous iron generated from hemoglobin digestion is required to activate the drug.

Chapter 7 : Appendix

Supplementary Figures

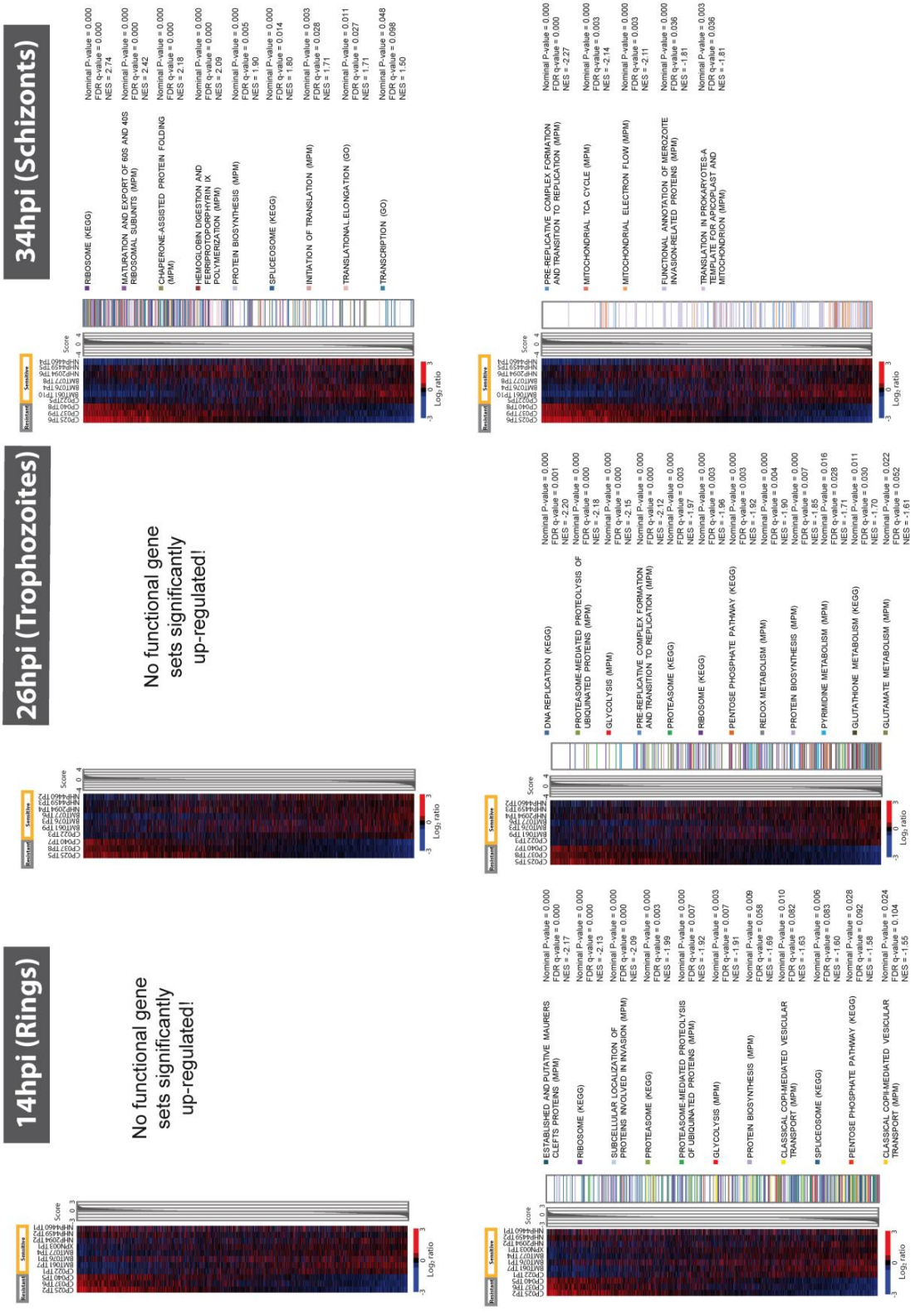

Supplementary Figure 1 – Functional analyses of differential expression in all stages of the artemisinin resistant parasites. For each of the 3 stages, genes were ranked according to the z-score by correlating the expression profiles to the phenotypic class. The mean-centered $\log_2$ ratios for each gene of the resistant (CP025, CP037, and CP040) and sensitive (CP022, BMT061, BMT076, BMT077, XPN003, NHP2094, NHP4459, NHP4460) isolates are represented in these clusters. Gene Set Enrichment Analysis [110] of the ranked clusters gave rise to gene sets down-regulated in rings and trophozoites and up-regulated in schizonts in the resistant parasites as shown ordered by the nominal p-value, false discovery rate (FDR) q-value and Normalized Enrichment Score (NES). Significant gene sets were based on cut-off p-value of 0.05 and FDR q-value of 0.25.

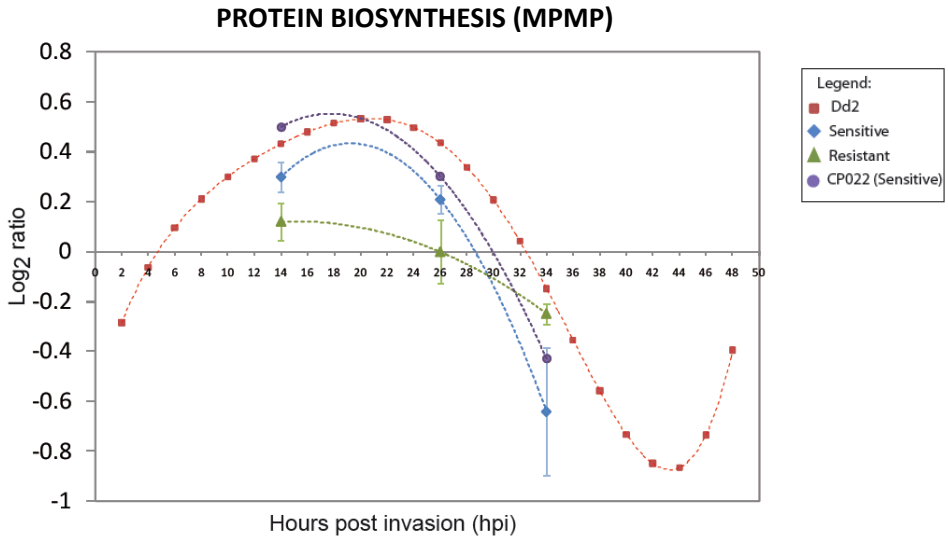

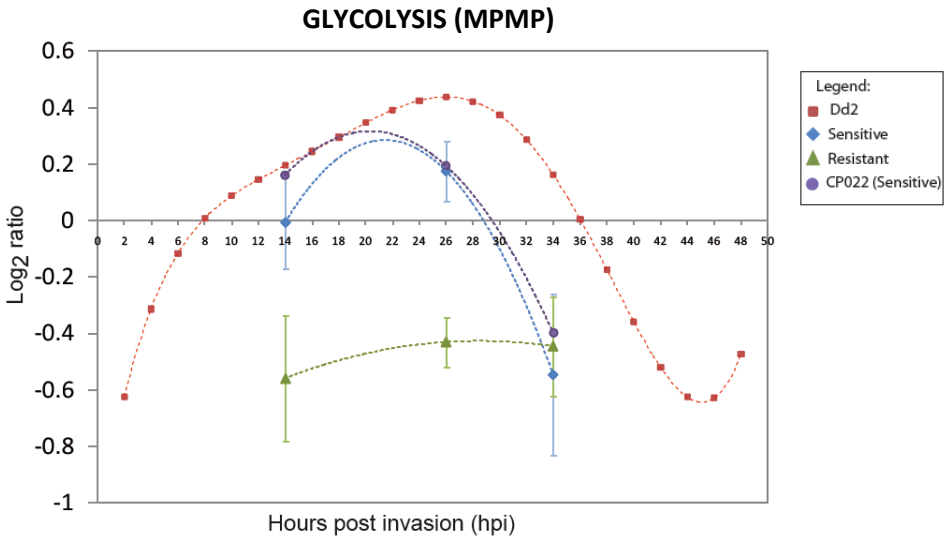

PENTOSE PHOSPHATE PATHWAY (KEGG)

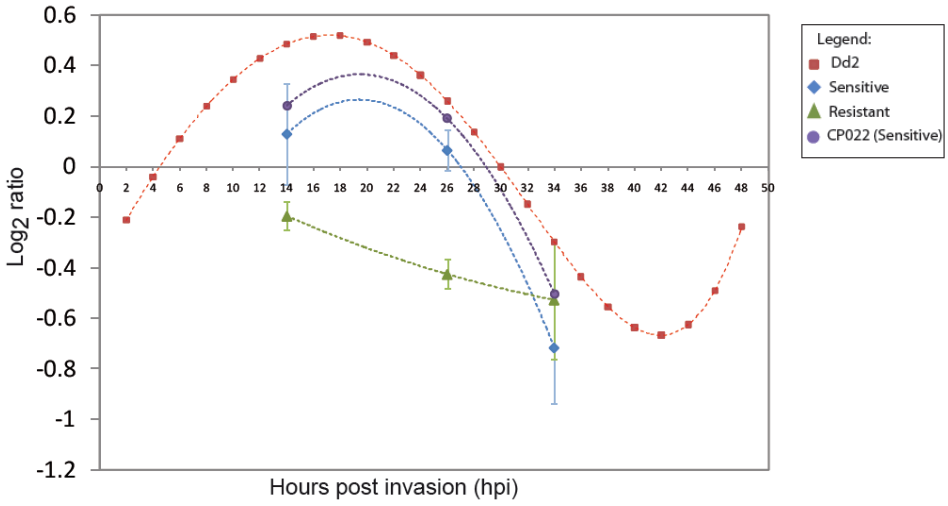

GLUTAMATE METABOLISM (MPM)

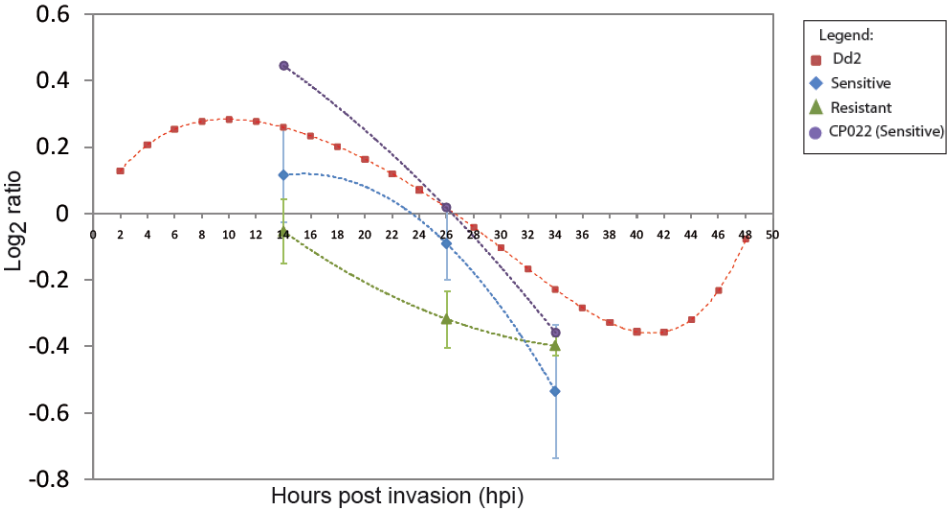

PURINE METABOLISM (MPMP)

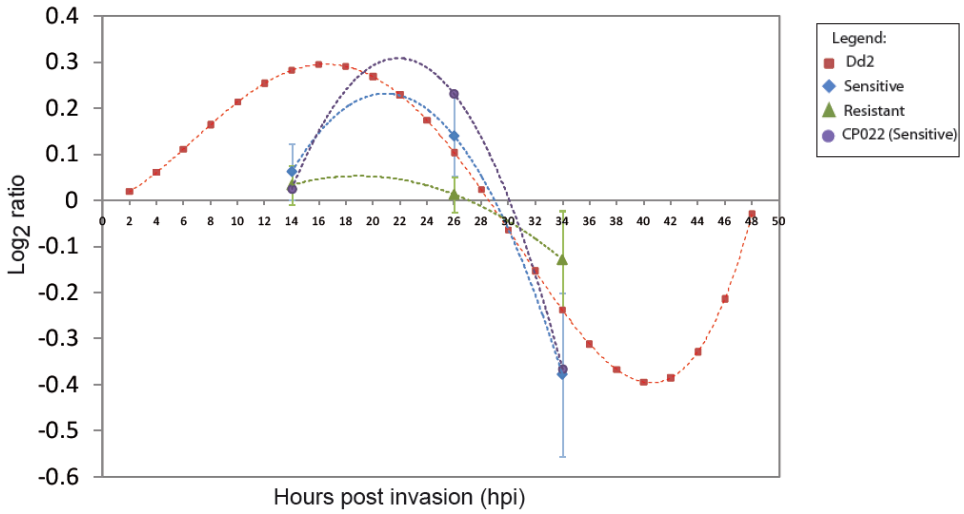

PROTEASOME-MEDIATED PROTEOLYSIS OF UBIQUINATED PROTEINS (MPMP)

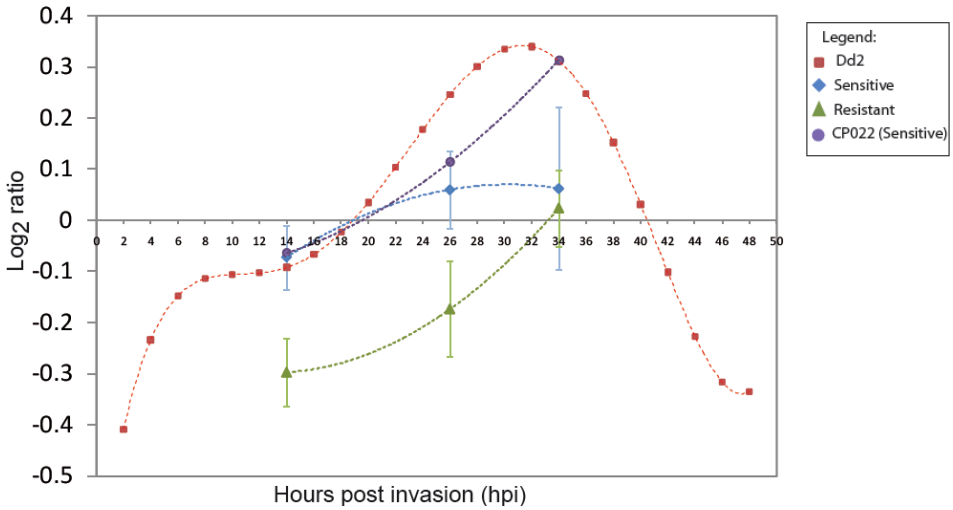

REDOX METABOLISM (MPMP)

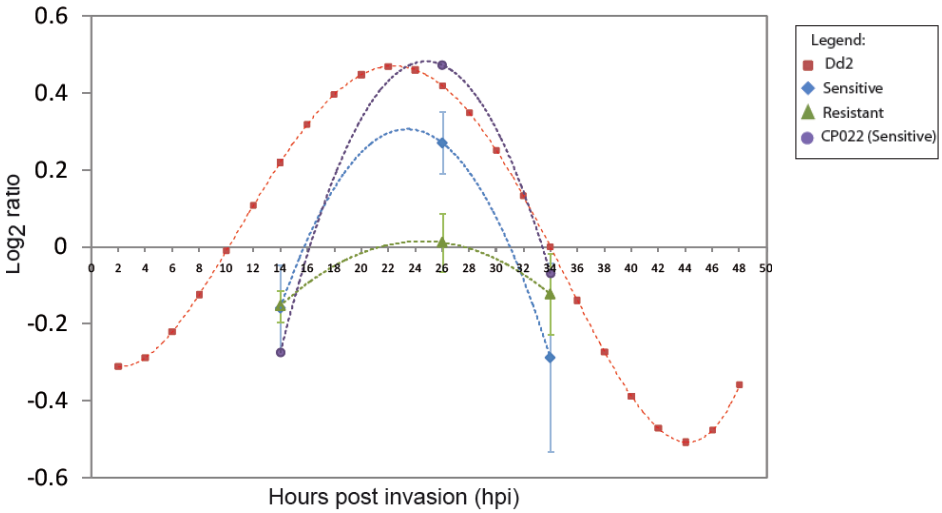

GLUTATHIONE METABOLISM (MPMP)

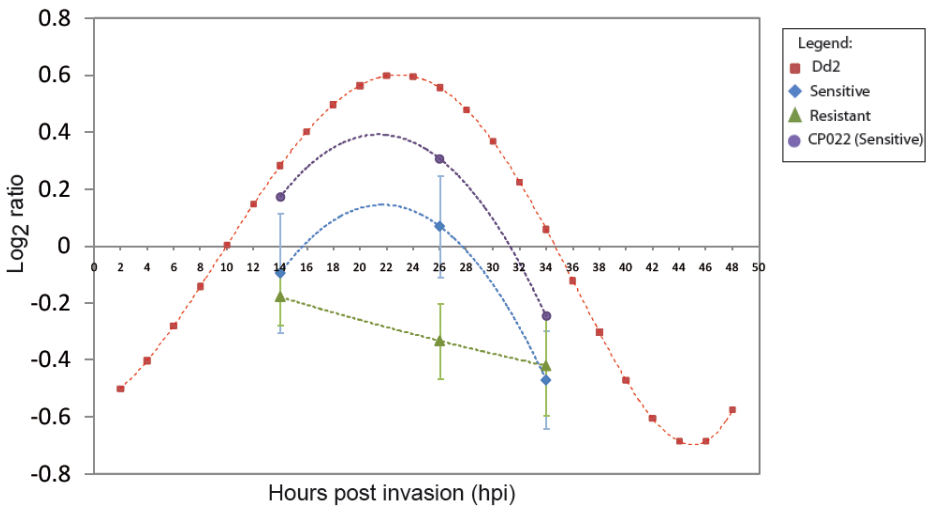

PYRIMIDINE METABOLISM (MPMP)

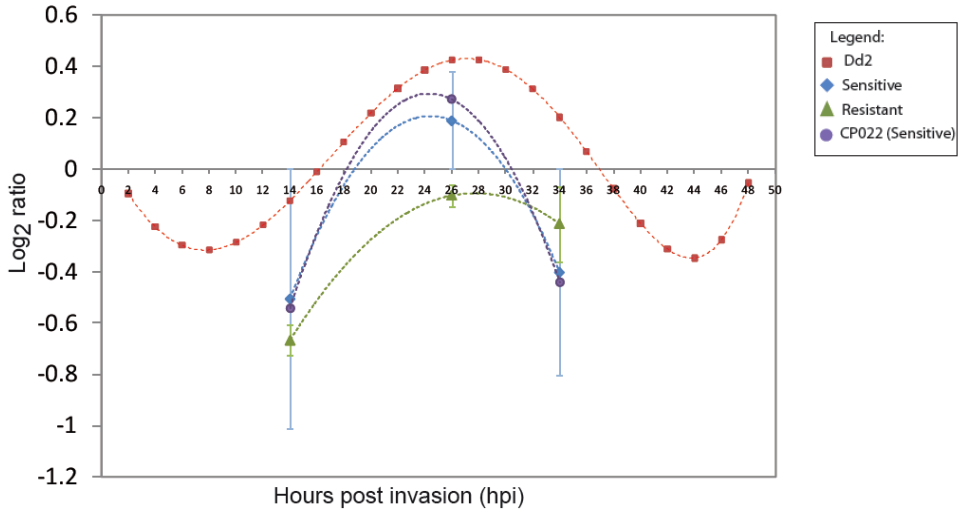

DNA REPLICATION (KEGG)

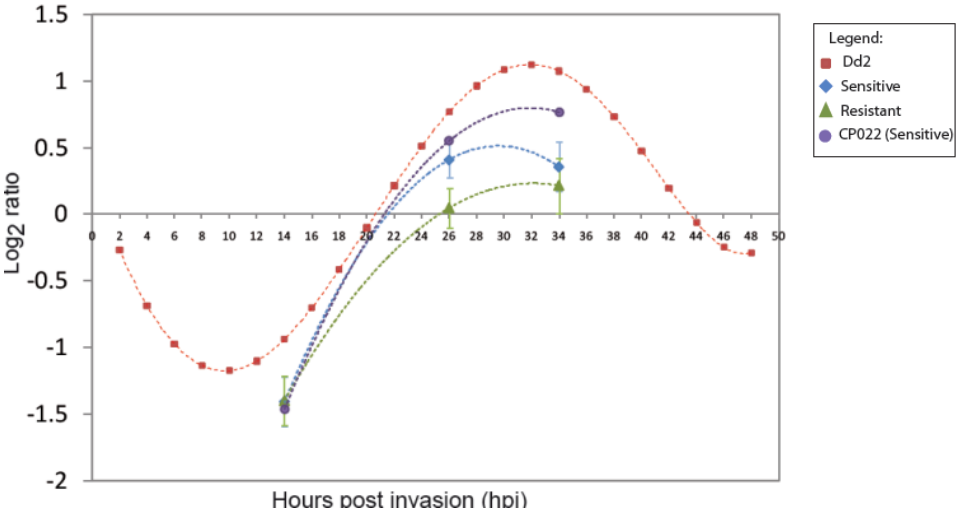

PRE-REPLICATIVE COMPLEX FORMATION AND TRANSITION TO REPLICATION (MPMP)

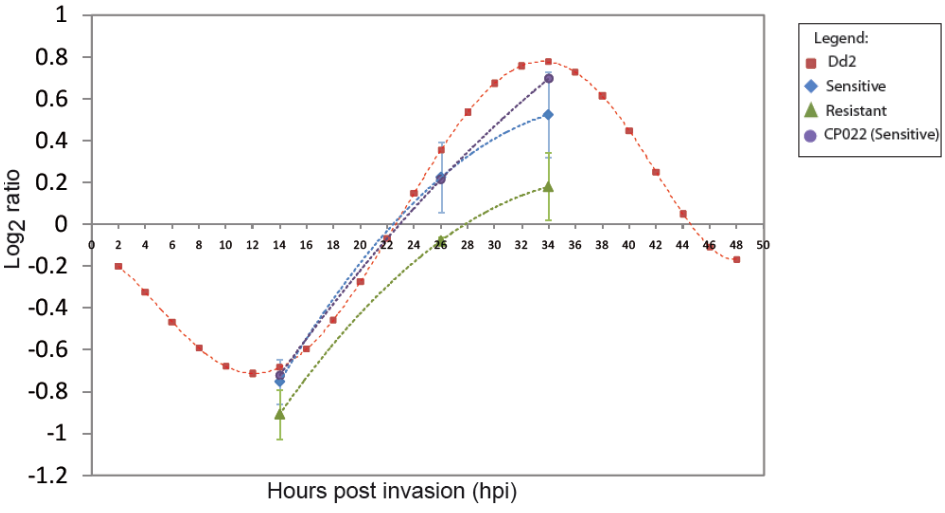

MITOCHONDRIAL TCA CYCLE (MPMP)

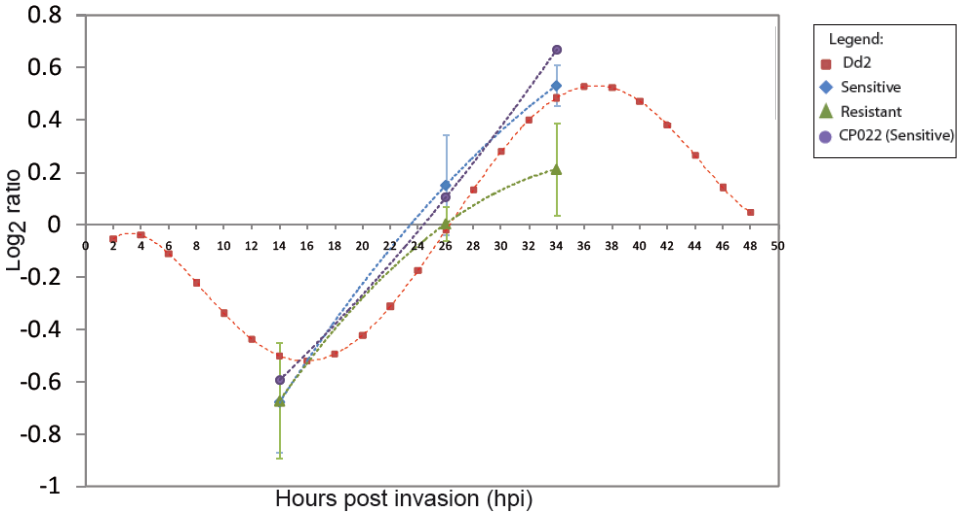

TRANSLATIONAL ELONGATION (GO)

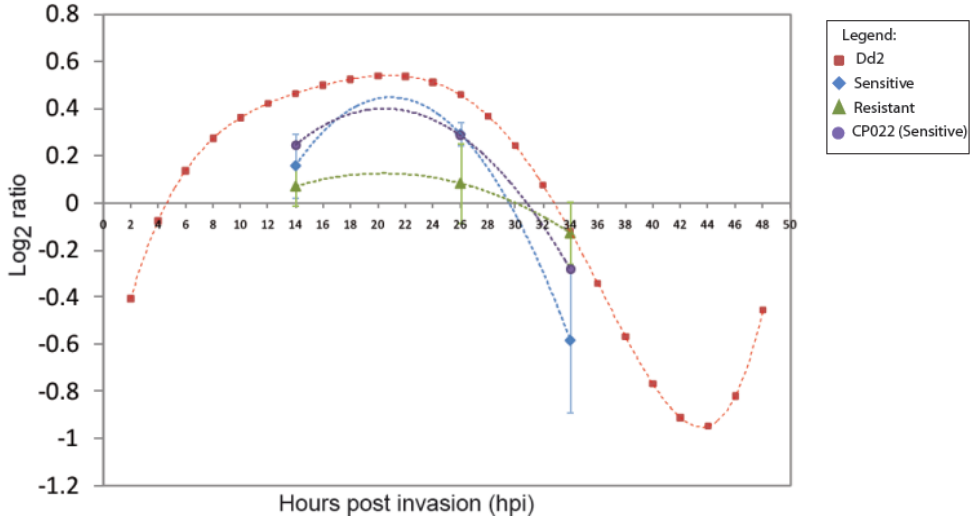

CLASSICAL COPI-MEDIATED VESICULAR TRANSPORT (MPMP)

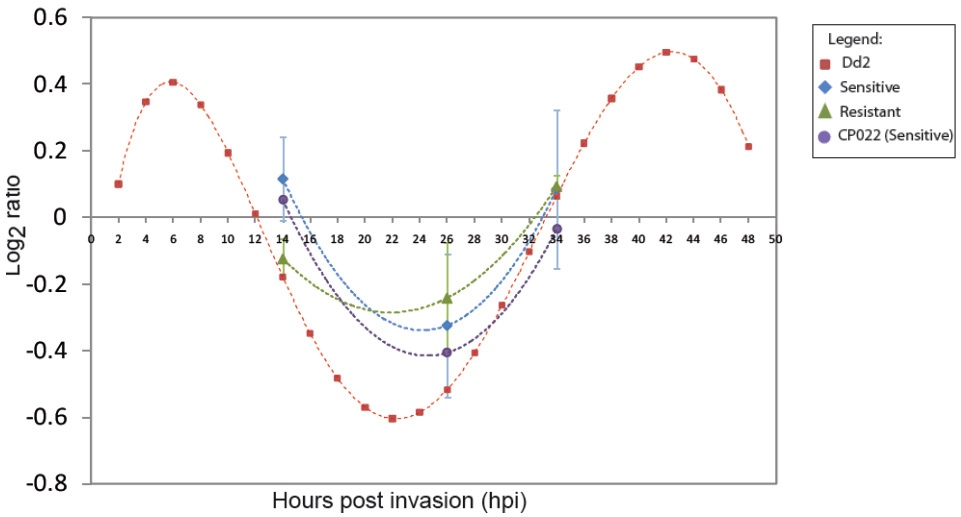

EARLY RING TRANSCRIPTS (BO)

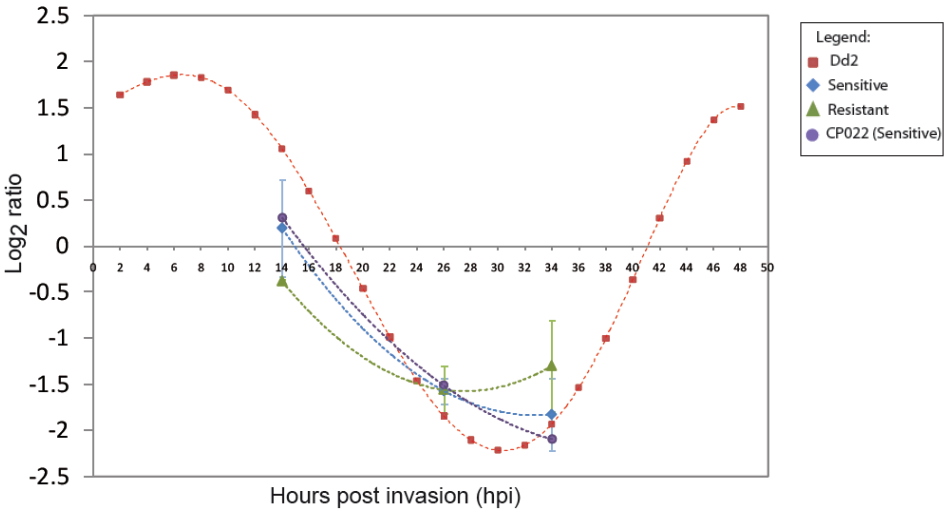

MATURATION & EXPORT OF 60S AND 40S RIBOSOMAL SUBUNITS (MPMP)

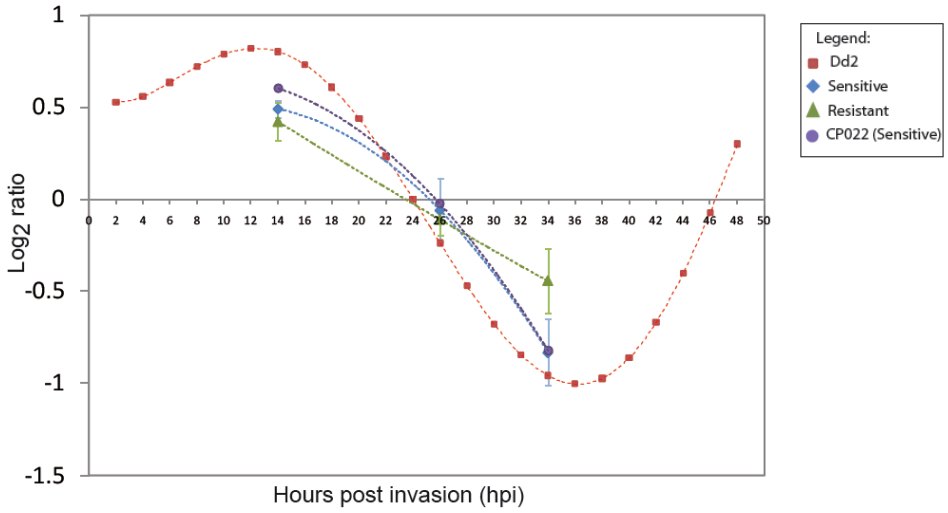

CYTOPLASMIC TRANSLATION MACHINERY (BO)

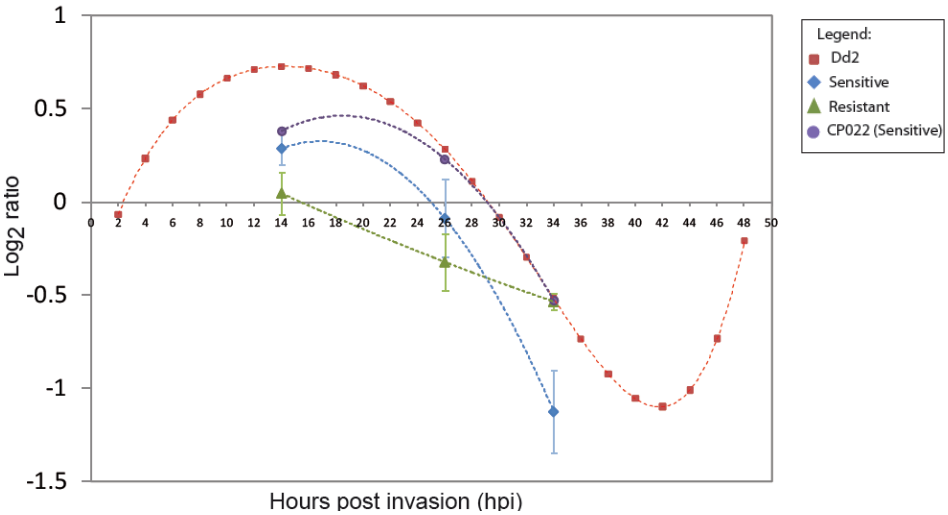

HEMOGLOBIN DIGESTION & FERRIPROTOPOPHYRIN IX POLYMERIZATION (MPMP)

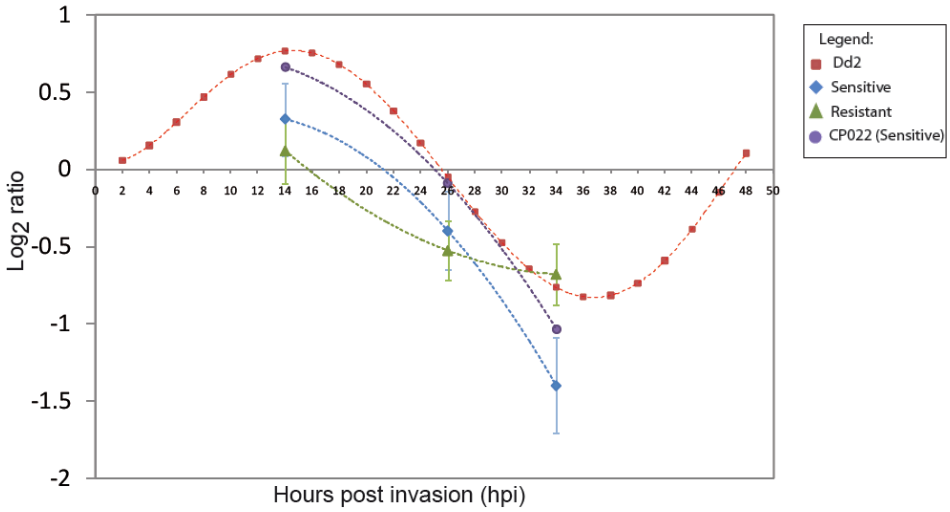

PROTEASOME (KEGG)

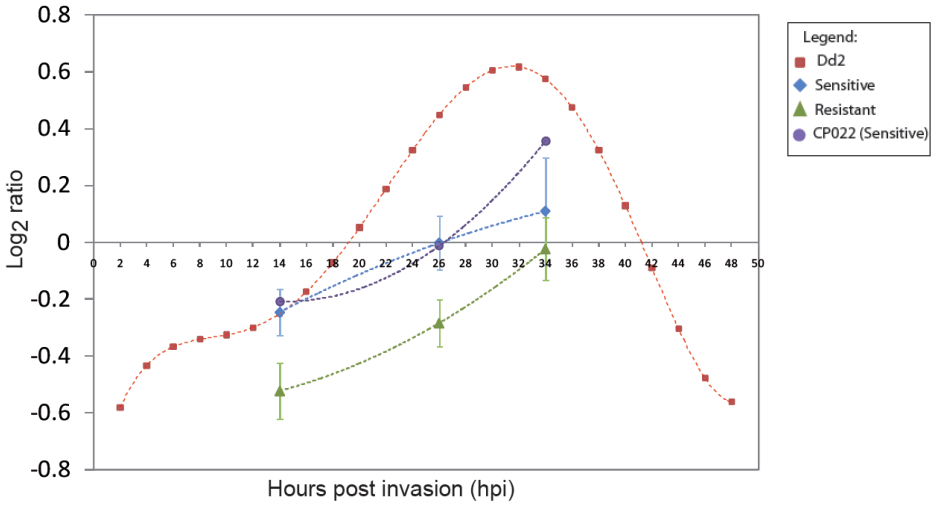

INITIATION OF TRANSLATION (MPMP)

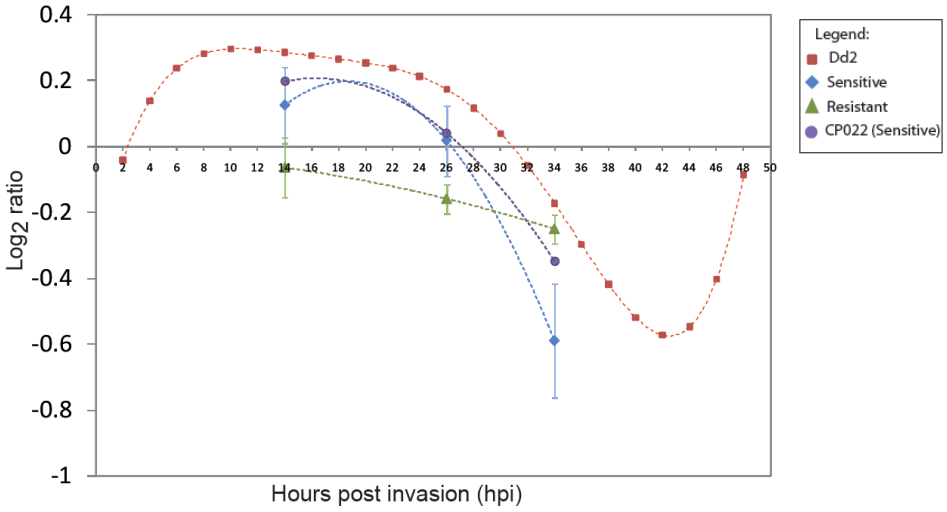

SPLICEOSOME (KEGG)

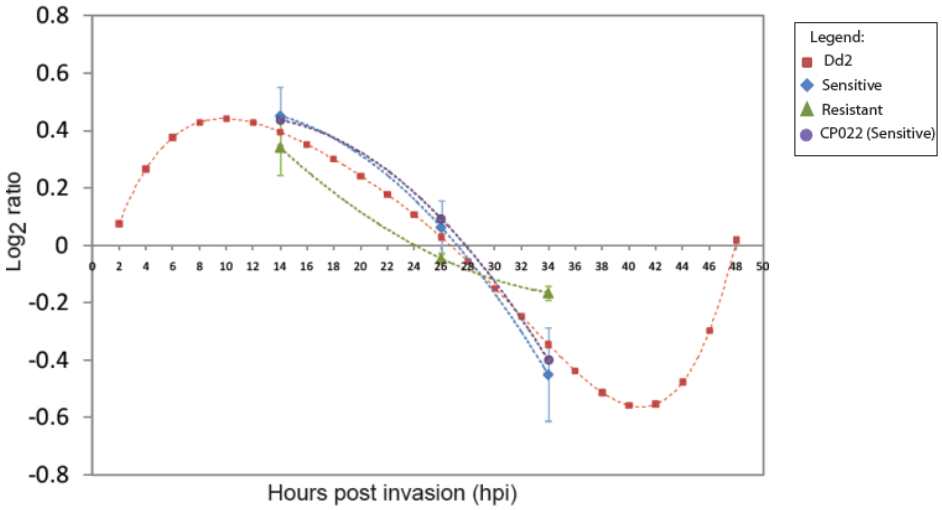

CHAPERONE-ASSISTED PROTEIN FOLDING (MPMP)

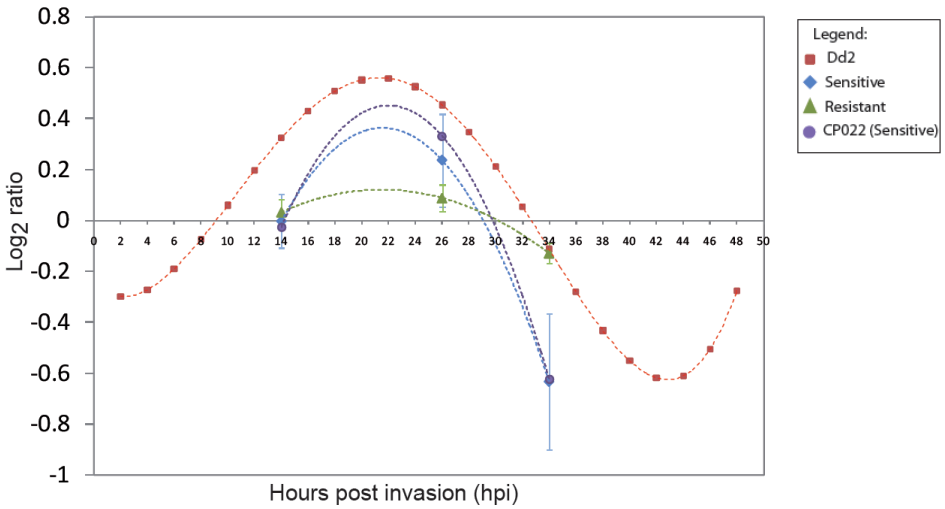

INTERACTIONS BETWEEN MODIFIED HOST CELL MEMBRANE AND ENDOTHELIAL CELL (MPMP)

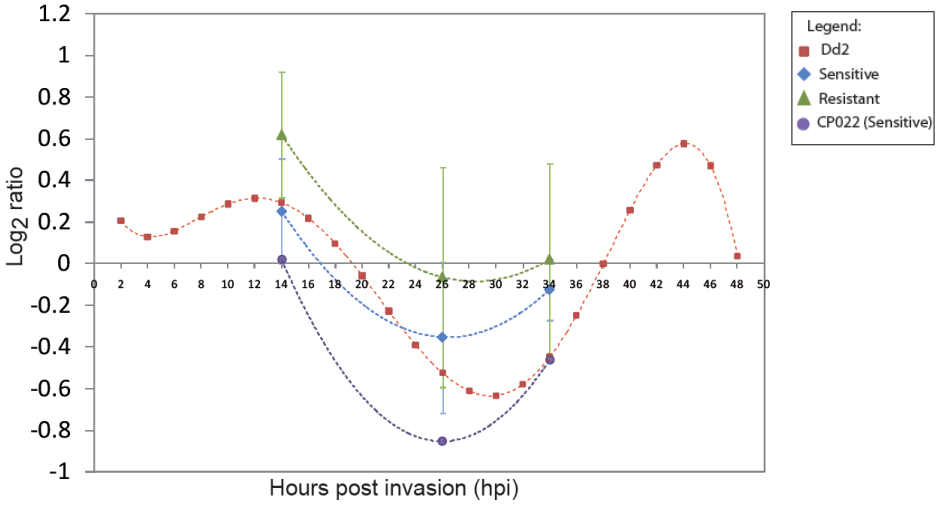

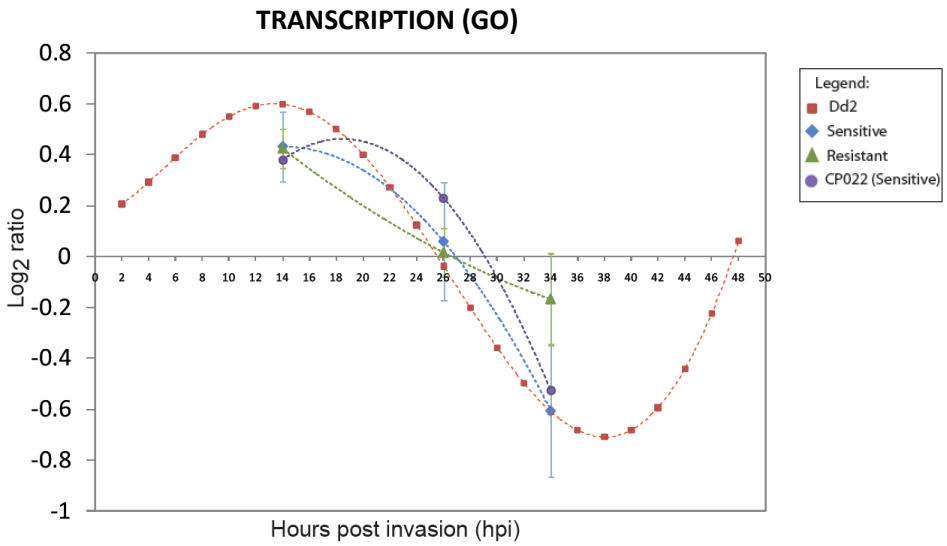

Supplementary Figure 2 – Functional pathways with significant differential expression in in rings, trophozoites and schizonts of artemisinin resistant parasites. Gene sets (functional groups) which are denoted in the graphs are obtained from various data sets of previous studies [111, 114, 254] and plotted are all pathways that are significantly differentially expressed in artemisinin resistant parasites in at least one IDC stage. For each pathway, each data point at ring (14 hpi), trophozoite (26 hpi) and schizont (34 hpi) of the resistant (green triangle) and sensitive (blue diamond) series was calculated from the average of the expression $\log_2$ ratio of a gene across all isolates in that phenotypic group (resistant or sensitive) and then averaged for all the genes associated with that pathway. Best fit polynomial curves were plotted (lines). Error bars indicate the standard deviation among the isolates. Included separately are the average expression ratios of all genes belonging to that pathway for CP022 isolate (purple circle) from Pailin, Cambodia and reference strain (red square).

Glycolysis (MPM)
Log2 ratio
Hours post invasion (hpi)
Legend:
Dd2
Sensitive
Resistant
CP022 (Sensitive)
GLYCOLYSIS 14hpi
GLYCOLYSIS 26hpi
GLYCOLYSIS 34hpi
Log2 ratio
glycerol kinase, putative
glycerol-3-phosphate dehydrogenase, putative
6-phosphofructokinase, putative
phosphoglycerate mutase, putative
enolase
triose-phosphate isomerase
hexokinase
Phosphoglycerate kinase
pyruvate kinase, putative
glyceraldehyde-3-phosphate dehydrogenase
L-lactate dehydrogenase
FAD-dependent glycerol-3-phosphate dehydrogenase...
phosphoglycerate mutase, putative
oxidoreductase, putative
ATP-dependent phosphofructokinase, putative
glucose-6-phosphate isomerase
fructose-bisphosphate aldolase
Aquaglyceroporin

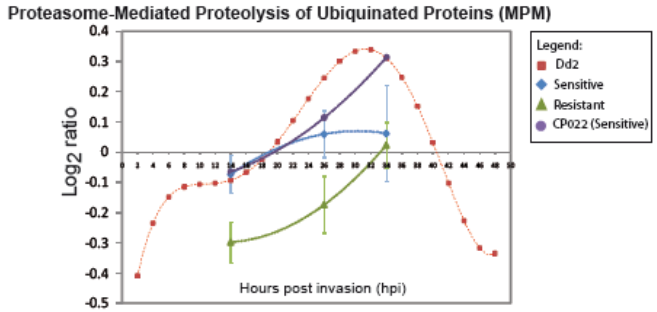
Proteasome-Mediated Proteolysis of Ubiquinated Proteins (MPM)
Log2 ratio
Hours post invasion (hpi)
Legend:
Dd2
Sensitive
Resistant
CP022 (Sensitive)

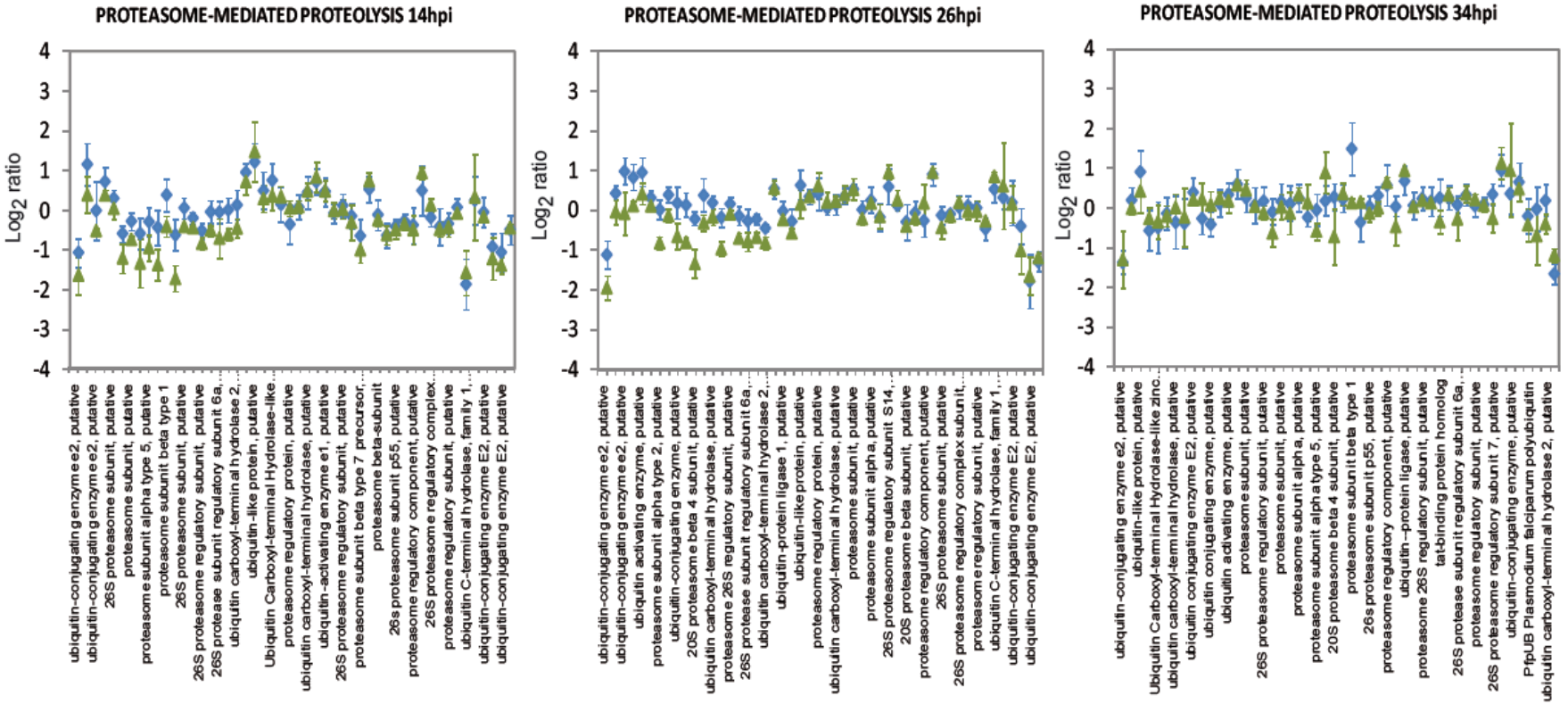
PROTEASOME-MEDIATED PROTEOLYSIS 14hpi
PROTEASOME-MEDIATED PROTEOLYSIS 26hpi
PROTEASOME-MEDIATED PROTEOLYSIS 34hpi
Log2 ratio

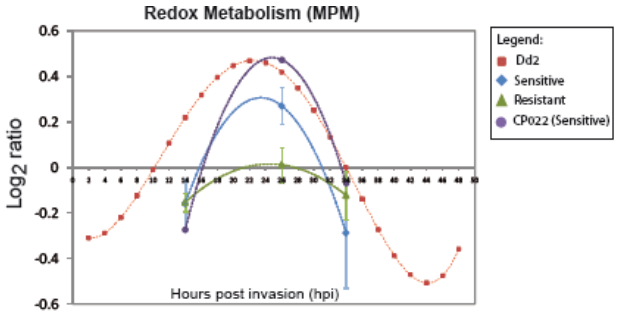
Redox Metabolism (MPM)
Log2 ratio
Hours post invasion (hpi)
Legend:
Dd2
Sensitive
Resistant
CP022 (Sensitive)

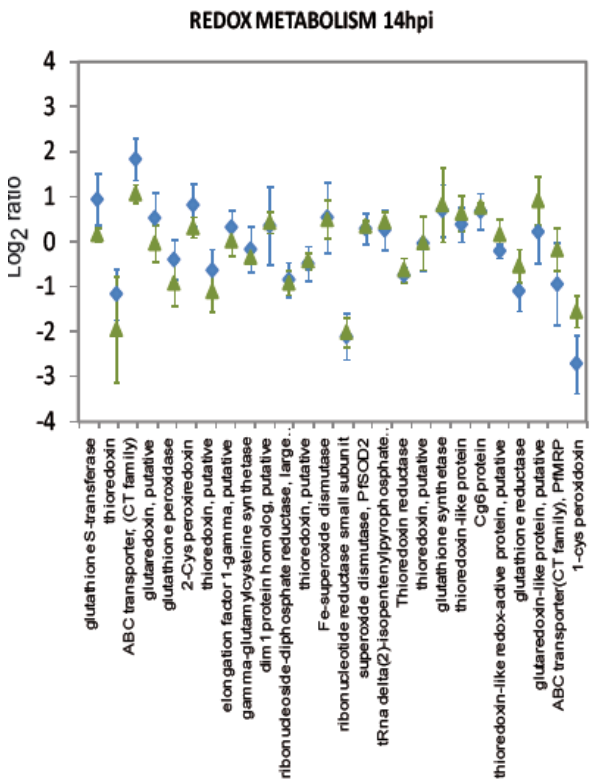
REDOX METABOLISM 14hpi
Log2 ratio
glutathione S-transferase
thioredoxin
ABC transporter, (CT family)
glutaredoxin, putative
glutathione peroxidase
2-Cys peroxiredoxin
thioredoxin, putative
elongation factor 1-gamma, putative
gamma-glutamylcysteine synthetase
dim 1 protein homolog, putative
ribonucleoside-diphosphate reductase, large...
thioredoxin, putative
Fe-superoxide dismutase
ribonucleotide reductase small subunit
superoxide dismutase, PfSOD2
tRna delta(2)-isopentenylpyrophosphate...
Thioredoxin reductase
thioredoxin, putative
glutathione synthetase
thioredoxin-like protein
Cg6 protein
thioredoxin-like redox-active protein, putative
glutathione reductase
glutaredoxin-like protein, putative
ABC transporter(CT family), PfMRP
1-cys peroxiredoxin

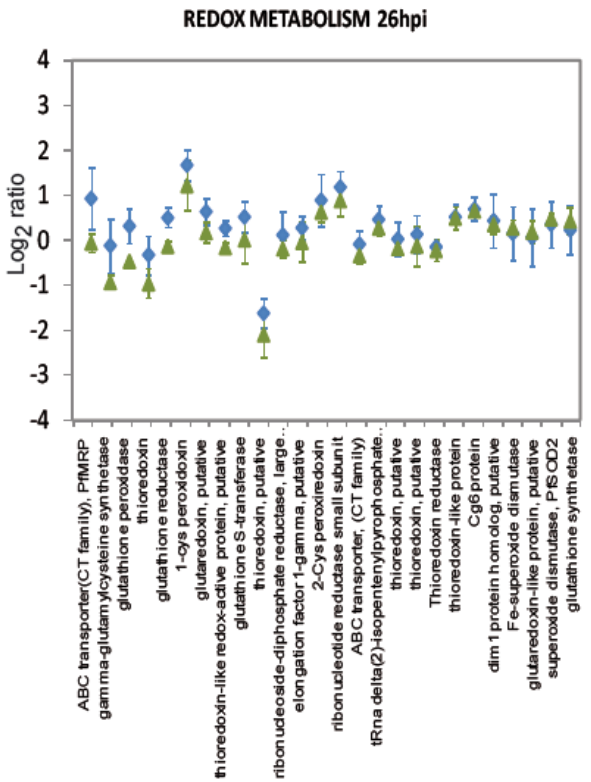
REDOX METABOLISM 26hpi
Log2 ratio
ABC transporter(CT family), PfMRP
gamma-glutamylcysteine synthetase
glutathione peroxidase
thioredoxin
glutathione reductase
1-cys peroxiredoxin
glutaredoxin, putative
thioredoxin-like redox-active protein, putative
glutathione S-transferase
thioredoxin, putative
ribonucleoside-diphosphate reductase, large...
elongation factor 1-gamma, putative
2-Cys peroxiredoxin
ribonucleotide reductase small subunit
ABC transporter, (CT family)
tRna delta(2)-isopentenylpyrophosphate...
thioredoxin, putative
thioredoxin, putative
Thioredoxin reductase
thioredoxin-like protein
Cg6 protein
dim 1 protein homolog, putative
Fe-superoxide dismutase
glutaredoxin-like protein, putative
superoxide dismutase, PfSOD2
glutathione synthetase

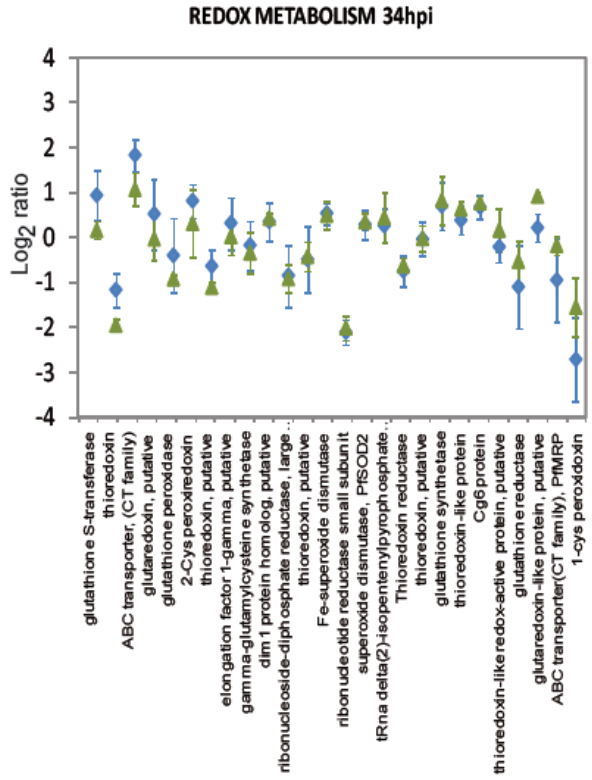
REDOX METABOLISM 34hpi
Log2 ratio
glutathione S-transferase
thioredoxin
ABC transporter, (CT family)
glutaredoxin, putative
glutathione peroxidase
2-Cys peroxiredoxin
thioredoxin, putative
elongation factor 1-gamma, putative
gamma-glutamylcysteine synthetase
dim 1 protein homolog, putative
ribonucleoside-diphosphate reductase, large...
thioredoxin, putative
Fe-superoxide dismutase
ribonucleotide reductase small subunit
superoxide dismutase, PfSOD2
tRna delta(2)-isopentenylpyrophosphate...
Thioredoxin reductase
thioredoxin, putative
glutathione synthetase
thioredoxin-like protein
Cg6 protein
thioredoxin-like redox-active protein, putative
glutathione reductase
glutaredoxin-like protein, putative
ABC transporter(CT family), PfMRP
1-cys peroxiredoxin

INITIATION OF TRANSLATION 14hpi
Log2 ratio
4
3
2
1
0
-1
-2
-3
-4
eukaryotic initiation factor, putative
eukaryotic translation initiation factor 2, beta, putative
initiation factor 2 subunit family, putative
eukaryotic translation initiation factor 3, subunit 6, putative
eukaryotic translation initiation factor, putative
eukaryotic translation initiation factor 3 subunit, putative
RNA-binding protein, putative
eukaryotic translation initiation factor 3 subunit 7, putative
translation initiation factor E4, putative
eukaryotic translation initiation factor 2b, subunit 2, putative
eukaryotic translation initiation factor 2 gamma subunit, putative
eukaryotic translation initiation factor 3 subunit 10, putative
eukaryotic translation initiation factor 2 alpha subunit, putative
homologue of human HSPC025
eukaryotic translation initiation factor 3 subunit 8, putative
translation initiation factor-like protein
polyadenylate binding protein, putative
translation initiation factor eIF-1A, putative
Plasmodium falciparum asparagine-rich protein
polyadenylate-binding protein, putative
Ser/Thr protein kinase, putative
cell cycle regulator protein, putative
translation initiation factor E2-2b alpha subunit, putative
eukaryotic translation initiation factor 3 37.28 KDa subunit, putative
eukaryotic translation initiation factor 5, putative
translation initiation factor IF-2, putative
translation initiation factor EF-1, putative
INITIATION OF TRANSLATION 26hpi
Log2 ratio
4
3
2
1
0
-1
-2
-3
-4
eukaryotic initiation factor, putative
eukaryotic translation initiation factor 3, subunit 6, putative
eukaryotic translation initiation factor 3 subunit, putative
eukaryotic translation initiation factor, putative
RNA-binding protein, putative
cell cycle regulator protein, putative
polyadenylate-binding protein, putative
eukaryotic translation initiation factor 2 alpha subunit, putative
eukaryotic translation initiation factor 2 gamma subunit, putative
polyadenylate binding protein, putative
eukaryotic translation initiation factor 3 subunit 7, putative
translation initiation factor 2, beta, putative
Plasmodium falciparum asparagine-rich protein
translation initiation factor eIF-1A, putative
translation initiation factor-like protein
eukaryotic translation initiation factor 3 37.28 KDa subunit, putative
translation initiation factor E4, putative
eukaryotic translation initiation factor 5, putative
eukaryotic translation initiation factor 3 subunit 8, putative
eukaryotic translation initiation factor 3 subunit 10, putative
homologue of human HSPC025
translation initiation factor EF-1, putative
translation initiation factor 2b, subunit 2, putative
translation initiation factor IF-2, putative
Ser/Thr protein kinase, putative
initiation factor 2 subunit family, putative
translation initiation factor E2-2b alpha subunit, putative
INITIATION OF TRANSLATION 34hpi
Log2 ratio
4
3
2
1
0
-1
-2
-3
-4
translation initiation factor EF-1, putative
RNA-binding protein, putative
Plasmodium falciparum asparagine-rich protein
translation initiation factor-like protein
polyadenylate binding protein, putative
translation initiation factor eIF-1A, putative
eukaryotic translation initiation factor 3, subunit 6, putative
translation initiation factor IF-2, putative
polyadenylate-binding protein, putative
eukaryotic translation initiation factor 2 alpha subunit, putative
eukaryotic translation initiation factor 2 gamma subunit, putative
cell cycle regulator protein, putative
initiation factor 2 subunit family, putative
eukaryotic translation initiation factor 3 subunit, putative
translation initiation factor E2-2b alpha subunit, putative
eukaryotic translation initiation factor 3 37.28 KDa subunit, putative
eukaryotic translation initiation factor 5, putative
eukaryotic translation initiation factor 3 subunit 7, putative
eukaryotic translation initiation factor 2, beta, putative
Ser/Thr protein kinase, putative
eukaryotic initiation factor, putative
eukaryotic translation initiation factor 3 subunit 8, putative
homologue of human HSPC025
eukaryotic translation initiation factor 2b, subunit 2, putative
eukaryotic translation initiation factor, putative
translation initiation factor E4, putative
Initiation of Translation (MPM)
Log2 ratio
0.4
0.2
0
-0.2
-0.4
-0.6
-0.8
-1
Hours post invasion (hpi)
Legend:
Dd2
Sensitive
Resistant
CP022 (Sensitive)

Supplementary Figure 3. Relative expression of individual genes related to four DE functional pathways in artemisinin resistant parasite. Top: Example of four functional gene sets with significant differential expression between resistant and sensitive parasites and the relative gene expression of all members of the gene sets at the three stages. Each set of data points are the average $\log_2$ expression ratios of the isolates in a group and averaged for all the genes in that pathway at 14, 26 and 34 hpi. The curves are the best fit polynomial curves to the data points. Bottom: Each of the 3 graphs plotted are the average $\log_2$ gene expression ratios of the isolates in the resistant (green triangle) or sensitive (blue diamond) group with the standard deviation represented by error bars in each particular pathway at 14, 26 or 34 hpi.

Supplementary Tables

Supplementary Table 1. List of Primer sequences used in all experiments.

Gene	Description	Forward Primer	Reverse Primer	Anneal Temp.
Study: Genotyping of Parasites (Section 3.)				
msp1	Conserved sequence	M1-OF: CTAGAAGCTTTAGAAGATGCAGTATTG	M1-OR: CTTAAATAGTATTCTAATTCAAGTGGATCA	61C
msp1	K1 allele	M1-KF: AAATGAAGAAGAAATTACTACAAAAGGTGC	M1-KR: GCTTGCATCAGCTGGAGGGCTTGCACCAGA	61C
msp1	MAD20 allele	M1-MF: AAATGAAGGAACAAGTGGAACAGCTGTTAC	M1-MR: ATCTGAAGGATTTGTACGTCTTGAATTACC	61C
msp1	RO33 allele	M1-RF: TAAAGGATGGAGCAAATACTCAAGTTGTTG	M1-RR: CATCTGAAGGATTTGCAGCACCTGGAGATC	63C
msp2	Conserved sequence	M2-OF: ATGAAGGTAATTAAAACATTGTCTATTATA	M2-OR: CTTTGTTACCATCGGTACATTCTT	55C
msp2	FC27 allele	M2-FCF: AATACTAAGAGTGTAGGTGCARATGCTCCA	M2-FCR: TTTTATTTGGTGCATTGCCAGAACTTGAAC	55C
msp2	3D7/IC allele	M2-ICF: AGAAGTATGGCAGAAAGTAAKCCTYCTACT	M2-ICR: GATTGTAATTCGGGGGATTCAGTTTGTTCG	55C
glurp	Conserved sequence	: G-OF: TGAATTTGAAGATGTTCACACTGAAC	G-OR: GTGGAATTGCTTTTTCTTCAACACTAA	58C
glurp	RII repeat region	G-NF: TGTTCACACTGAACAATTAGATTTAGATCA	G-OR: GTGGAATTGCTTTTTCTTCAACACTAA	58C

Gene	Description (Fw.Rv)	Forward Primer	Reverse Primer	Anneal Temp.
Study: Polymorphisms within the 5'UTR promoter of *pfmrp2* gene (PFL1410c) (Section 3.)				
pfmrp2	ORF (13.13)	13_Fw: +504 ACAACATTTGAACCGCCT	13_Rv: +1 ATGATGAGACGGAGAAGCG	55C
pfmrp2	ORF (14.14)	14_Fw: +447 ATTTGTTGCTGTGTGTATTGAG	14_Rv: +878 CTGTTGGTTGAATCTTTGCTTTC	55C
pfmrp2	ORF (15.15)	15_Fw: +2370 ACTTGGGAATGTGGGTTCAG	15_Rv: +2856 ATCTGTGTTATTATTATTTGGCGTG	55C
pfmrp2	5'UTR (1.1)	1_Fw: -20 ACTTTACTATATGGTGATAAGTT	1_Rv: -501 TTAACATAGCAGTTTTGAAATAT	55C
pfmrp2	5'UTR (2.2)	2_Fw: -295 CTGGGAACTGGAGGTGCT	2_Rv: -992 CCTTAAATATCTTCTTACATTTGTTTATCG	55C
pfmrp2	5'UTR (3.3)	3_Fw: -844 GTATAAACAGATGCTCAATATA	3_Rv: -1278 ATGACAAGAATAATAACGACAAAA	55C
pfmrp2	5'UTR (4.4)	4_Fw: -1173 TAAATAAACACAGCTCATACAAATAA	4_Rv: -1783 TGAAGAGTGAATGTGCCTTATA	55C
pfmrp2	5'UTR (1.9)	1_Fw: -20 ACTTTACTATATGGTGATAAGTT	9_Rv: -6212 TATTACACCTTTCTTTACATTTCGG	53.5C
pfmrp2	5'UTR (1.10)	1_Fw: -20 ACTTTACTATATGGTGATAAGTT	10_Rv: -4284 TTATCAAACCGTATCTCTACTCG	53.5C
pfmrp2	5'UTR (1.12)	1_Fw: -20 ACTTTACTATATGGTGATAAGTT	12_Rv: -10321 1AAAGAGAACCACTGAAGGC	53.5C
pfmrp2	5'UTR (2.9)	2_Fw: -295 CTGGGAACTGGAGGTGCT	9_Rv: -6212 TATTACACCTTTCTTTACATTTCGG	53.5C
pfmrp2	5'UTR (2.10)	2_Fw: -295 CTGGGAACTGGAGGTGCT	10_Rv: -4284 TTATCAAACCGTATCTCTACTCG	53.5C
pfmrp2	5'UTR (2.12)	2_Fw: -295 CTGGGAACTGGAGGTGCT	12_Rv: -10321 1AAAGAGAACCACTGAAGGC	53.5C

Gene	Description (Fw.Rv)	Forward Primer	Reverse Primer	Anneal Temp.
pfmrp2	5'UTR (3.9)	3_Fw: -844 GTATAAACAGATGCTCAATATA	9_Rv: -6212 TATTACACCTTTCTTTACATTTCGG	53.5C
pfmrp2	5'UTR (3.10)	3_Fw: -844 GTATAAACAGATGCTCAATATA	10_Rv: -4284 TTATCAAACCGTATCTCTACTCG	53.5C
pfmrp2	5'UTR (3.12)	3_Fw: -844 GTATAAACAGATGCTCAATATA	12_Rv: -10321 1AAAGAGAACCACTGAAGGC	53.5C
pfmrp2	5'UTR (4.9)	4_Fw: -1173 TAAATAAACACAGCTCATACAAATAA	9_Rv: -6212 TATTACACCTTTCTTTACATTTCGG	53.5C
pfmrp2	5'UTR (4.10)	4_Fw: -1173 TAAATAAACACAGCTCATACAAATAA	10_Rv: -4284 TTATCAAACCGTATCTCTACTCG	53.5C
pfmrp2	5'UTR (4.12)	4_Fw: -1173 TAAATAAACACAGCTCATACAAATAA	12_Rv: -10321 1AAAGAGAACCACTGAAGGC	53.5C
pfmrp2	5'UTR (11.11)	11_Fw: +610 ATCATAATAGCAAAGGAGGGC	11_Rv: -2568 AAGGGAGGATAAAGGGTCC	53.5C
pfmrp2	5'UTR (5.5)	5_Fw: +739 GCCCTTTCCCTCTTCACTA	5_Rv: -13740 ATTTCTTCACATCTATTTACGATTG	53.5C
pfmrp2	5'UTR (5.6)	5_Fw: +739 GCCCTTTCCCTCTTCACTA	6_Rv: -13712 CACCACTTATTCTTTCTAATCTATTC	53.5C
pfmrp2	5'UTR (5.7)	5_Fw: +739 GCCCTTTCCCTCTTCACTA	7_Rv: -12863 ACATTGCCATAGGACCCAAG	53.5C
pfmrp2	5'UTR (5.8)	5_Fw: +739 GCCCTTTCCCTCTTCACTA	8_Rv: -7341 CAACATTTGTATCATCACCCA	53.5C
Study: Real-time PCR & sequencing of selected genes for artemisinin resistance (Section 3.)				
Pfmdr1	*mdr1*, 1st fragment	P1_Fw: TGTATGTGCTGTATTATCAGGA	P1_Rv: CTCTTCTATAATGGACATGGTA	52°C
Pfmdr1	*mdr1*, 2nd fragment	P3_Fw: GAATTATTGTAAATGCAGCTTTA	P3_Rv: GCAGCAAACTTACTAACACG	52°C

Gene	Description	Forward Primer	Reverse Primer	Anneal Temp.
Pfdhps	*dhps*	P8_Fw: TTGAAATGATAAATGAAGGTGCTAGT	P8_Rv: CCAATTGTGTGATTTGTCCA	52°C
Pfcrt	*crt*, 1st fragment	**P10_Fw:** CTTGTCTTGGTAAATGTGCTC	**P10_Rv:** GAACATAATCATACAAATAAAGT	52°C
Pfcrt	*crt*, *2nd* fragment	P18_Fw: TCCTTATTTGGAAATAAAAAGGGAAATT	P18_Rv: TAAGTGATATCTAAAAAGGAGTAAAT	52°C
Pfcrt	*crt*, 3rd fragment	P11_Fw: ACAATTATCTCGGAGCAGTTA	P11_Rv: CATGTTTGAAAAGCATACAGGC	52°C
Pfcrt	*crt*, 4th fragment	P16_Fw: CTTTTTCCAATTGTTCACTTCTTG	P16_Rv: TCTTACATAGCTGGTTATTAAAT	52°C
Pfcrt	*crt*, 5th fragment	P12_Fw: ACCATGACATATACTATTGTTAG	P12_Rv: TTATAGAACCAAATAGGTAGCC	52°C
PFA0510w	Bromodomain protein	PFA0510w_Fw : GAAGAAACCAAACCTATTTACGAT	PFA0510w_Rv: TCGTCTTGATAAACTTCCGAAA	53°C
PF13_0141	L-lactate dehydrogenase	PF13_0141_Fw: ACATTACTGTAGGTGGTATCCC	PF13_0141_Rv: TGCCTTCATTCTCTTAGTTTCAG	53°C
PF11_0061	Histone 4	PF11_0061_Fw: AAGAGGTAAGGGAGGTAAAGGTT	PF11_0061_Rv: ACAATATCCATAGCAGTGACGG	53°C
PF14_0057	RNA-binding protein:	PF14_0057_Fw: GATGAAGTCCCAGCAAAATCT	PF14_0057_Rv: CACAAAAGCCCAGTCTACAT	53°C
PF14_0079	apiAP2 TF	PF14_0079_Fw: AGAAAGCGAAACATCCTCCT	PF14_0079_Rv: TCATCTTCATCTTTAGTGCTTGA	53°C
PFC0965w	Hypothetical protein	PFC0965w_Fw: ATTCGGTTGGTGGTATGAACG	PFC0965w_Rv: GTAAGTCTATGTCCGCTACGA	53°C
Study: Miscellaneous PCR (Section 6.)				
PFB0095c	PfEMP3	PFB0095c_Fw: TGTCTGGTGATTGTATGG	PFB0095c_Rv: TAAATGGATGACCTGCTG	50C
PFB0100c	KAHRP	PFB0100c_Fw: AAGGAAATGACGGTGAAG	PFB0100c_Rv: TTTATTTGTTGCGGCATT	50C

Chapter 8 : References

1. Chaturvedi LN: *The teachings of Bhagavad Gita.* New Delhi: Sterling Publishers; 1991.
2. Cox FE: **History of human parasitology.** *Clin Microbiol Rev* 2002, **15:**595-612.
3. **World malaria report 2010.** Geneva: World Health Organization; 2010.
4. **World malaria report 2008.** Geneva World Health Organization; 2008.
5. Miller LH, Baruch DI, Marsh K, Doumbo OK: **The pathogenic basis of malaria.** *Nature* 2002, **415:**673-679.
6. Su X, Hayton K, Wellems TE: **Genetic linkage and association analyses for trait mapping in Plasmodium falciparum.** *Nat Rev Genet* 2007, **8:**497-506.
7. Nabarro DN, Tayler EM: **The "roll back malaria" campaign.** *Science* 1998, **280:**2067-2068.
8. RollBackMalariaPartnership: **THE GLOBAL MALARIA ACTION PLAN.** Roll Back Malaria Partnership; 2008.
9. Rehwagen C: **WHO recommends DDT to control malaria.** *Bmj* 2006, **333:**622.
10. Lengeler C: **Insecticide-treated bednets and curtains for preventing malaria.** *Cochrane Database Syst Rev* 2000**:**CD000363.
11. Parise ME, Ayisi JG, Nahlen BL, Schultz LJ, Roberts JM, Misore A, Muga R, Oloo AJ, Steketee RW: **Efficacy of sulfadoxine-pyrimethamine for prevention of placental malaria in an area of Kenya with a high prevalence of malaria and human immunodeficiency virus infection.** *Am J Trop Med Hyg* 1998, **59:**813-822.
12. Curtis CF: **Should the use of DDT be revived for malaria vector control?** *Biomedica* 2002, **22:**455-461.
13. **First Results of Phase 3 Trial of RTS,S/AS01 Malaria Vaccine in African Children.** *N Engl J Med* 2011.
14. Targett GA: **Malaria vaccines 1985-2005: a full circle?** *Trends Parasitol* 2005, **21:**499-503.
15. Alonso PL, Sacarlal J, Aponte JJ, Leach A, Macete E, Milman J, Mandomando I, Spiessens B, Guinovart C, Espasa M, et al: **Efficacy of the RTS,S/AS02A vaccine against Plasmodium falciparum infection and disease in young African children: randomised controlled trial.** *Lancet* 2004, **364:**1411-1420.
16. Alonso PL, Sacarlal J, Aponte JJ, Leach A, Macete E, Aide P, Sigauque B, Milman J, Mandomando I, Bassat Q, et al: **Duration of protection with RTS,S/AS02A malaria vaccine in prevention of Plasmodium falciparum disease in Mozambican children: single-blind extended follow-up of a randomised controlled trial.** *Lancet* 2005, **366:**2012-2018.
17. Plebanski M, Locke E, Kazura JW, Coppel RL: **Malaria vaccines: into a mirror, darkly?** *Trends Parasitol* 2008, **24:**532-536.
18. Greenwood D: **Conflicts of interest: the genesis of synthetic antimalarial agents in peace and war.** *J Antimicrob Chemother* 1995, **36:**857-872.
19. Rehwagen C: **WHO ultimatum on artemisinin monotherapy is showing results.** *Bmj* 2006, **332:**1176.
20. Nosten F, White NJ: **Artemisinin-based combination treatment of falciparum malaria.** *Am J Trop Med Hyg* 2007, **77:**181-192.
21. Warhurst DC: **Antimalarial interaction with ferriprotoporphyrin IX monomer and its relationship to activity of the blood schizontocides.** *Ann Trop Med Parasitol* 1987, **81:**65-67.
22. Egan TJ, Ncokazi KK: **Quinoline antimalarials decrease the rate of beta-hematin formation.** *J Inorg Biochem* 2005, **99:**1532-1539.
23. Ginsburg H, Ward SA, Bray PG: **An integrated model of chloroquine action.** *Parasitol Today* 1999, **15:**357-360.

24. Radfar A, Diez A, Bautista JM: **Chloroquine mediates specific proteome oxidative damage across the erythrocytic cycle of resistant Plasmodium falciparum.** *Free Radic Biol Med* 2008, **44:**2034-2042.
25. Chong CR, Sullivan DJ, Jr.: **Inhibition of heme crystal growth by antimalarials and other compounds: implications for drug discovery.** *Biochem Pharmacol* 2003, **66:**2201-2212.
26. Foley M, Tilley L: **Quinoline antimalarials: mechanisms of action and resistance and prospects for new agents.** *Pharmacol Ther* 1998, **79:**55-87.
27. Robert V, Molez JF, Trape JF: **Short report: gametocytes, chloroquine pressure, and the relative parasite survival advantage of resistant strains of falciparum malaria in west Africa.** *Am J Trop Med Hyg* 1996, **55:**350-351.
28. Ramkaran AE, Peters W: **Infectivity of chloroquine resistant Plasmodium berghei to Anopheles stephensi enhanced by chloroquine.** *Nature* 1969, **223:**635-636.
29. Buckling A, Ranford-Cartwright LC, Miles A, Read AF: **Chloroquine increases Plasmodium falciparum gametocytogenesis in vitro.** *Parasitology* 1999, **118 (Pt 4):**339-346.
30. Kumar N, Zheng H: **Stage-specific gametocytocidal effect in vitro of the antimalaria drug qinghaosu on Plasmodium falciparum.** *Parasitol Res* 1990, **76:**214-218.
31. Jefford CW: **Why artemisinin and certain synthetic peroxides are potent antimalarials. Implications for the mode of action.** *Curr Med Chem* 2001, **8:**1803-1826.
32. Scholl PF, Tripathi AK, Sullivan DJ: **Bioavailable iron and heme metabolism in Plasmodium falciparum.** *Curr Top Microbiol Immunol* 2005, **295:**293-324.
33. Posner GH, Oh CH, Wang D, Gerena L, Milhous WK, Meshnick SR, Asawamahasadka W: **Mechanism-based design, synthesis, and in vitro antimalarial testing of new 4-methylated trioxanes structurally related to artemisinin: the importance of a carbon-centered radical for antimalarial activity.** *J Med Chem* 1994, **37:**1256-1258.
34. Anne Robert CBSALLBM: **Heme alkylation by artemisinin and trioxaquines.** *J Phys Org Chem* 2006, **19:**562-569.
35. Asawamahasakda W, Ittarat I, Pu YM, Ziffer H, Meshnick SR: **Reaction of antimalarial endoperoxides with specific parasite proteins.** *Antimicrob Agents Chemother* 1994, **38:**1854-1858.
36. Yang YZ, Little B, Meshnick SR: **Alkylation of proteins by artemisinin. Effects of heme, pH, and drug structure.** *Biochem Pharmacol* 1994, **48:**569-573.
37. Bhisutthibhan J, Pan XQ, Hossler PA, Walker DJ, Yowell CA, Carlton J, Dame JB, Meshnick SR: **The Plasmodium falciparum translationally controlled tumor protein homolog and its reaction with the antimalarial drug artemisinin.** *J Biol Chem* 1998, **273:**16192-16198.
38. Bhisutthibhan J, Meshnick SR: **Immunoprecipitation of [(3)H]dihydroartemisinin translationally controlled tumor protein (TCTP) adducts from Plasmodium falciparum-infected erythrocytes by using anti-TCTP antibodies.** *Antimicrob Agents Chemother* 2001, **45:**2397-2399.
39. Haynes RK, Chan WC, Lung CM, Uhlemann AC, Eckstein U, Taramelli D, Parapini S, Monti D, Krishna S: **The Fe2+-mediated decomposition, PfATP6 binding, and antimalarial activities of artemisone and other artemisinins: the unlikelihood of C-centered radicals as bioactive intermediates.** *ChemMedChem* 2007, **2:**1480-1497.
40. Eckstein-Ludwig U, Webb RJ, Van Goethem ID, East JM, Lee AG, Kimura M, O'Neill PM, Bray PG, Ward SA, Krishna S: **Artemisinins target the SERCA of Plasmodium falciparum.** *Nature* 2003, **424:**957-961.
41. Krishna S, Uhlemann AC, Haynes RK: **Artemisinins: mechanisms of action and potential for resistance.** *Drug Resist Updat* 2004, **7:**233-244.

42. Golenser J, Waknine JH, Krugliak M, Hunt NH, Grau GE: **Current perspectives on the mechanism of action of artemisinins.** *Int J Parasitol* 2006, **36:**1427-1441.
43. Li W, Mo W, Shen D, Sun L, Wang J, Lu S, Gitschier JM, Zhou B: **Yeast model uncovers dual roles of mitochondria in action of artemisinin.** *PLoS Genet* 2005, **1:**e36.
44. **Containment of Malaria Multi-Drug Resistance on the Cambodia-Thailand Border.** Geneva: World Health Organization; 2007.
45. Bruce-Chwatt LJ: **Malaria vaccine trials: a guided step into the unknown.** *Ann Soc Belg Med Trop* 1986, **66:**5-13.
46. **Global report on antimalarial drug efficacy and drug resistance: 2000-2010.** Geneva: World Health Organization; 2010.
47. Boudreau EF, Webster HK, Pavanand K, Thosingha L: **Type II mefloquine resistance in Thailand.** *Lancet* 1982, **2:**1335.
48. Lopes D, Rungsihirunrat K, Nogueira F, Seugorn A, Gil JP, do Rosario VE, Cravo P: **Molecular characterisation of drug-resistant Plasmodium falciparum from Thailand.** *Malar J* 2002, **1:**12.
49. Rathod PK, McErlean T, Lee PC: **Variations in frequencies of drug resistance in Plasmodium falciparum.** *Proc Natl Acad Sci U S A* 1997, **94:**9389-9393.
50. Sidhu AB, Verdier-Pinard D, Fidock DA: **Chloroquine resistance in Plasmodium falciparum malaria parasites conferred by pfcrt mutations.** *Science* 2002, **298:**210-213.
51. Djimde A, Doumbo OK, Cortese JF, Kayentao K, Doumbo S, Diourte Y, Coulibaly D, Dicko A, Su XZ, Nomura T, et al: **A molecular marker for chloroquine-resistant falciparum malaria.** *N Engl J Med* 2001, **344:**257-263.
52. Reed MB, Saliba KJ, Caruana SR, Kirk K, Cowman AF: **Pgh1 modulates sensitivity and resistance to multiple antimalarials in Plasmodium falciparum.** *Nature* 2000, **403:**906-909.
53. Naude B, Brzostowski JA, Kimmel AR, Wellems TE: **Dictyostelium discoideum expresses a malaria chloroquine resistance mechanism upon transfection with mutant, but not wild-type, Plasmodium falciparum transporter PfCRT.** *J Biol Chem* 2005, **280:**25596-25603.
54. Lehane AM, Kirk K: **Chloroquine Resistance-Conferring Mutations in pfcrt Give Rise to a Chloroquine-Associated H+ Leak from the Malaria Parasite's Digestive Vacuole.** *Antimicrob Agents Chemother* 2008, **52:**4374-4380.
55. Price RN, Uhlemann AC, Brockman A, McGready R, Ashley E, Phaipun L, Patel R, Laing K, Looareesuwan S, White NJ, et al: **Mefloquine resistance in Plasmodium falciparum and increased pfmdr1 gene copy number.** *Lancet* 2004, **364:**438-447.
56. Cravo PV, Carlton JM, Hunt P, Bisoni L, Padua RA, Walliker D: **Genetics of mefloquine resistance in the rodent malaria parasite Plasmodium chabaudi.** *Antimicrob Agents Chemother* 2003, **47:**709-718.
57. Cowman AF, Morry MJ, Biggs BA, Cross GA, Foote SJ: **Amino acid changes linked to pyrimethamine resistance in the dihydrofolate reductase-thymidylate synthase gene of Plasmodium falciparum.** *Proc Natl Acad Sci U S A* 1988, **85:**9109-9113.
58. Peterson DS, Walliker D, Wellems TE: **Evidence that a point mutation in dihydrofolate reductase-thymidylate synthase confers resistance to pyrimethamine in falciparum malaria.** *Proc Natl Acad Sci U S A* 1988, **85:**9114-9118.
59. Sibley CH, Hyde JE, Sims PF, Plowe CV, Kublin JG, Mberu EK, Cowman AF, Winstanley PA, Watkins WM, Nzila AM: **Pyrimethamine-sulfadoxine resistance in Plasmodium falciparum: what next?** *Trends Parasitol* 2001, **17:**582-588.
60. Brooks DR, Wang P, Read M, Watkins WM, Sims PF, Hyde JE: **Sequence variation of the hydroxymethyldihydropterin pyrophosphokinase: dihydropteroate synthase**

gene in lines of the human malaria parasite, Plasmodium falciparum, with differing resistance to sulfadoxine. *Eur J Biochem* 1994, **224:**397-405.

61. Wang P, Read M, Sims PF, Hyde JE: **Sulfadoxine resistance in the human malaria parasite Plasmodium falciparum is determined by mutations in dihydropteroate synthetase and an additional factor associated with folate utilization.** *Mol Microbiol* 1997, **23:**979-986.
62. Triglia T, Wang P, Sims PF, Hyde JE, Cowman AF: **Allelic exchange at the endogenous genomic locus in Plasmodium falciparum proves the role of dihydropteroate synthase in sulfadoxine-resistant malaria.** *Embo J* 1998, **17:**3807-3815.
63. White NJ: **Antimalarial drug resistance.** *J Clin Invest* 2004, **113:**1084-1092.
64. L von Seidlein MJ, R Coleman, T Doherty, G Walraven, G Targett **Parasitaemia and gametocytaemia after treatment with chloroquine, pyrimethamine/sulfadoxine, and pyrimethamine/sulfadoxine combined with artesunate in young Gambians with uncomplicated malaria.** *Trop Med Int Health* 2001, **2:**8.
65. Noedl H: **Artemisinin resistance: how can we find it?** *Trends Parasitol* 2005, **21:**404-405.
66. Dondorp AM, Nosten F, Yi P, Das D, Phyo AP, Tarning J, Lwin KM, Ariey F, Hanpithakpong W, Lee SJ, et al: **Artemisinin resistance in Plasmodium falciparum malaria.** *N Engl J Med* 2009, **361:**455-467.
67. White NJ: **The parasite clearance curve.** *Malar J* 2011, **10:**278.
68. Luxemburger C, Brockman A, Silamut K, Nosten F, van Vugt M, Gimenez F, Chongsuphajaisiddhi T, White NJ: **Two patients with falciparum malaria and poor in vivo responses to artesunate.** *Trans R Soc Trop Med Hyg* 1998, **92:**668-669.
69. Gogtay NJ, Kadam VS, Karnad DR, Kanbur A, Kamtekar KD, Kshirsagar NA: **Probable resistance to parental artemether in Plasmodium falciparum: Case reports from Mumbai (Bombay), India.** *Ann Trop Med Parasitol* 2000, **94:**519-520.
70. Sahr F, Willoughby VR, Gbakima AA, Bockarie MJ: **Apparent drug failure following artesunate treatment of Plasmodium falciparum malaria in Freetown, Sierra Leone: four case reports.** *Ann Trop Med Parasitol* 2001, **95:**445-449.
71. Huong NM, Hewitt S, Davis TM, Dao LD, Toan TQ, Kim TB, Hanh NT, Phuong VN, Nhan DH, Cong LD: **Resistance of Plasmodium falciparum to antimalarial drugs in a highly endemic area of southern Viet Nam: a study in vivo and in vitro.** *Trans R Soc Trop Med Hyg* 2001, **95:**325-329.
72. Menard D, Matsika-Claquin MD, Djalle D, Yapou F, Manirakiza A, Dolmazon V, Sarda J, Talarmin A: **Association of failures of seven-day courses of artesunate in a non-immune population in Bangui, Central African Republic with decreased sensitivity of Plasmodium falciparum.** *Am J Trop Med Hyg* 2005, **73:**616-621.
73. **Global malaria control and elimination : report of a meeting on containment of artemisinin tolerance.** Geneva: World Health Organization; 2008.
74. Yeung S, Pongtavornpinyo W, Hastings IM, Mills AJ, White NJ: **Antimalarial drug resistance, artemisinin-based combination therapy, and the contribution of modeling to elucidating policy choices.** *Am J Trop Med Hyg* 2004, **71:**179-186.
75. Uhlemann AC, Cameron A, Eckstein-Ludwig U, Fischbarg J, Iserovich P, Zuniga FA, East M, Lee A, Brady L, Haynes RK, Krishna S: **A single amino acid residue can determine the sensitivity of SERCAs to artemisinins.** *Nat Struct Mol Biol* 2005, **12:**628-629.
76. Jambou R, Legrand E, Niang M, Khim N, Lim P, Volney B, Ekala MT, Bouchier C, Esterre P, Fandeur T, Mercereau-Puijalon O: **Resistance of Plasmodium falciparum field isolates to in-vitro artemether and point mutations of the SERCA-type PfATPase6.** *Lancet* 2005, **366:**1960-1963.

77. Ferrer-Rodriguez I, Perez-Rosado J, Gervais GW, Peters W, Robinson BL, Serrano AE: **Plasmodium yoelii: identification and partial characterization of an MDR1 gene in an artemisinin-resistant line.** *J Parasitol* 2004, **90:**152-160.
78. Price RN, Cassar C, Brockman A, Duraisingh M, van Vugt M, White NJ, Nosten F, Krishna S: **The pfmdr1 gene is associated with a multidrug-resistant phenotype in Plasmodium falciparum from the western border of Thailand.** *Antimicrob Agents Chemother* 1999, **43:**2943-2949.
79. Walker DJ, Pitsch JL, Peng MM, Robinson BL, Peters W, Bhisutthibhan J, Meshnick SR: **Mechanisms of artemisinin resistance in the rodent malaria pathogen Plasmodium yoelii.** *Antimicrob Agents Chemother* 2000, **44:**344-347.
80. Peters W, Robinson BL: **The chemotherapy of rodent malaria. LVI. Studies on the development of resistance to natural and synthetic endoperoxides.** *Ann Trop Med Parasitol* 1999, **93:**325-329.
81. Hunt P, Afonso A, Creasey A, Culleton R, Sidhu AB, Logan J, Valderramos SG, McNae I, Cheesman S, do Rosario V, et al: **Gene encoding a deubiquitinating enzyme is mutated in artesunate- and chloroquine-resistant rodent malaria parasites.** *Mol Microbiol* 2007, **65:**27-40.
82. Afonso A, Hunt P, Cheesman S, Alves AC, Cunha CV, do Rosario V, Cravo P: **Malaria parasites can develop stable resistance to artemisinin but lack mutations in candidate genes atp6 (encoding the sarcoplasmic and endoplasmic reticulum Ca2+ ATPase), tctp, mdr1, and cg10.** *Antimicrob Agents Chemother* 2006, **50:**480-489.
83. Muller S: **Redox and antioxidant systems of the malaria parasite Plasmodium falciparum.** *Mol Microbiol* 2004, **53:**1291-1305.
84. Kehr S, Sturm N, Rahlfs S, Przyborski JM, Becker K: **Compartmentation of redox metabolism in malaria parasites.** *PLoS Pathog* 2010, **6:**e1001242.
85. Richard D, Bartfai R, Volz J, Ralph SA, Muller S, Stunnenberg HG, Cowman AF: **A genome-wide chromatin-associated nuclear peroxiredoxin from the malaria parasite Plasmodium falciparum.** *J Biol Chem* 2011, **286:**11746-11755.
86. Foth BJ, Zhang N, Chaal BK, Sze SK, Preiser PR, Bozdech Z: **Quantitative time-course profiling of parasite and host cell proteins in the human malaria parasite Plasmodium falciparum.** *Mol Cell Proteomics* 2011.
87. Koncarevic S, Rohrbach P, Deponte M, Krohne G, Prieto JH, Yates J, 3rd, Rahlfs S, Becker K: **The malarial parasite Plasmodium falciparum imports the human protein peroxiredoxin 2 for peroxide detoxification.** *Proc Natl Acad Sci U S A* 2009, **106:**13323-13328.
88. Meierjohann S, Walter RD, Muller S: **Regulation of intracellular glutathione levels in erythrocytes infected with chloroquine-sensitive and chloroquine-resistant Plasmodium falciparum.** *Biochem J* 2002, **368:**761-768.
89. Raj DK, Mu J, Jiang H, Kabat J, Singh S, Sullivan M, Fay MP, McCutchan TF, Su XZ: **Disruption of a Plasmodium falciparum multidrug resistance-associated protein (PfMRP) alters its fitness and transport of antimalarial drugs and glutathione.** *J Biol Chem* 2009, **284:**7687-7696.
90. Gilles HM, Fletcher KA, Hendrickse RG, Lindner R, Reddy S, Allan N: **Glucose-6-phosphate-dehydrogenase deficiency, sickling, and malaria in African children in South Western Nigeria.** *Lancet* 1967, **1:**138-140.
91. Friedman MJ: **Oxidant damage mediates variant red cell resistance to malaria.** *Nature* 1979, **280:**245-247.
92. Roth EF, Jr., Raventos-Suarez C, Rinaldi A, Nagel RL: **Glucose-6-phosphate dehydrogenase deficiency inhibits in vitro growth of Plasmodium falciparum.** *Proc Natl Acad Sci U S A* 1983, **80:**298-299.

93. Luzzatto L, Usanga FA, Reddy S: **Glucose-6-phosphate dehydrogenase deficient red cells: resistance to infection by malarial parasites.** *Science* 1969, **164:**839-842.
94. Guindo A, Fairhurst RM, Doumbo OK, Wellems TE, Diallo DA: **X-linked G6PD deficiency protects hemizygous males but not heterozygous females against severe malaria.** *PLoS medicine* 2007, **4:**e66.
95. Bienzle U, Ayeni O, Lucas AO, Luzzatto L: **Glucose-6-phosphate dehydrogenase and malaria. Greater resistance of females heterozygous for enzyme deficiency and of males with non-deficient variant.** *Lancet* 1972, **1:**107-110.
96. Bozdech Z, Llinas M, Pulliam BL, Wong ED, Zhu J, DeRisi JL: **The transcriptome of the intraerythrocytic developmental cycle of Plasmodium falciparum.** *PLoS Biol* 2003, **1:**E5.
97. Llinas M, Bozdech Z, Wong ED, Adai AT, DeRisi JL: **Comparative whole genome transcriptome analysis of three Plasmodium falciparum strains.** *Nucleic Acids Res* 2006, **34:**1166-1173.
98. Gonzales JM, Patel JJ, Ponmee N, Jiang L, Tan A, Maher SP, Wuchty S, Rathod PK, Ferdig MT: **Regulatory hotspots in the malaria parasite genome dictate transcriptional variation.** *PLoS Biol* 2008, **6:**e238.
99. Daily JP, Scanfeld D, Pochet N, Le Roch K, Plouffe D, Kamal M, Sarr O, Mboup S, Ndir O, Wypij D, et al: **Distinct physiological states of Plasmodium falciparum in malaria-infected patients.** *Nature* 2007, **450:**1091-1095.
100. Waller RF, Ralph SA, Reed MB, Su V, Douglas JD, Minnikin DE, Cowman AF, Besra GS, McFadden GI: **A type II pathway for fatty acid biosynthesis presents drug targets in Plasmodium falciparum.** *Antimicrob Agents Chemother* 2003, **47:**297-301.
101. Lemieux JE, Gomez-Escobar N, Feller A, Carret C, Amambua-Ngwa A, Pinches R, Day F, Kyes SA, Conway DJ, Holmes CC, Newbold CI: **Statistical estimation of cell-cycle progression and lineage commitment in Plasmodium falciparum reveals a homogeneous pattern of transcription in ex vivo culture.** *Proc Natl Acad Sci U S A* 2009, **106:**7559-7564.
102. Wirth D, Daily J, Winzeler E, Mesirov JP, Regev A: **In vivo profiles in malaria are consistent with a novel physiological state.** *Proc Natl Acad Sci U S A* 2009, **106:**E70; author reply E71-72.
103. Milner DA, Jr., Pochet N, Krupka M, Williams C, Seydel K, Taylor TE, Van de Peer Y, Regev A, Wirth D, Daily JP, Mesirov JP: **Transcriptional profiling of Plasmodium falciparum parasites from patients with severe malaria identifies distinct low vs. high parasitemic clusters.** *PLoS One* 2012, **7:**e40739.
104. Lambros C, Vanderberg JP: **Synchronization of Plasmodium falciparum erythrocytic stages in culture.** *J Parasitol* 1979, **65:**418-420.
105. Rosario V: **Cloning of naturally occurring mixed infections of malaria parasites.** *Science* 1981, **212:**1037-1038.
106. Chenchik A, Zhu, Y. Y., Diatchenko, L., Li, R., Hill, J. & Siebert, P. D. : **Generation and use of high-quality cDNA from small amounts of total RNA by SMART PCR.** In *Gene Cloning and Analysis by RT-PCR* Edited by Siebert PD, Larrick JW. Natick, MA: BioTechniques Books; 1998: 305-319: *BioTechniques molecular laboratory methods series*].
107. MR4/ATCC: **Methods in Malaria Research.** (Ljungström I, Perlmann H, Schlichtherle M, Scherf A, Wahlgren M eds.), vol. 4th Edition: Malaria Research and Reference Reagent Resource Center (MR4); 2004.
108. Hu G, Llinas M, Li J, Preiser PR, Bozdech Z: **Selection of long oligonucleotides for gene expression microarrays using weighted rank-sum strategy.** *BMC Bioinformatics* 2007, **8:**350.

109. Edgar R, Domrachev M, Lash AE: **Gene Expression Omnibus: NCBI gene expression and hybridization array data repository.** *Nucleic Acids Res* 2002, **30:**207-210.
110. Subramanian A, Tamayo P, Mootha VK, Mukherjee S, Ebert BL, Gillette MA, Paulovich A, Pomeroy SL, Golub TR, Lander ES, Mesirov JP: **Gene set enrichment analysis: a knowledge-based approach for interpreting genome-wide expression profiles.** *Proc Natl Acad Sci U S A* 2005, **102:**15545-15550.
111. Kanehisa M, Goto S, Kawashima S, Okuno Y, Hattori M: **The KEGG resource for deciphering the genome.** *Nucleic Acids Res* 2004, **32:**D277-280.
112. **Malaria Parasite Metabolic Pathways** [http://sites.huji.ac.il/malaria/]
113. Le Roch KG, Zhou Y, Blair PL, Grainger M, Moch JK, Haynes JD, De La Vega P, Holder AA, Batalov S, Carucci DJ, Winzeler EA: **Discovery of gene function by expression profiling of the malaria parasite life cycle.** *Science* 2003, **301:**1503-1508.
114. Ashburner M, Ball CA, Blake JA, Botstein D, Butler H, Cherry JM, Davis AP, Dolinski K, Dwight SS, Eppig JT, et al: **Gene ontology: tool for the unification of biology. The Gene Ontology Consortium.** *Nat Genet* 2000, **25:**25-29.
115. Mackinnon MJ, Li J, Mok S, Kortok MM, Marsh K, Preiser PR, Bozdech Z: **Comparative transcriptional and genomic analysis of Plasmodium falciparum field isolates.** *PLoS Pathog* 2009, **5:**e1000644.
116. Pique-Regi R, Ortega A, Asgharzadeh S: **Joint estimation of copy number variation and reference intensities on multiple DNA arrays using GADA.** *Bioinformatics* 2009, **25:**1223-1230.
117. Hall TA: **BioEdit: a user-friendly biological sequence alignment editor and analysis program for Windows 95/98/NT.** *Nucleic Acids Symp Ser* 1999, **41:**95-98.
118. Snounou G: **Genotyping of Plasmodium spp. Nested PCR.** *Methods Mol Med* 2002, **72:**103-116.
119. Snounou G, Zhu X, Siripoon N, Jarra W, Thaithong S, Brown KN, Viriyakosol S: **Biased distribution of msp1 and msp2 allelic variants in Plasmodium falciparum populations in Thailand.** *Trans R Soc Trop Med Hyg* 1999, **93:**369-374.
120. Ponnudurai T, Leeuwenberg AD, Meuwissen JH: **Chloroquine sensitivity of isolates of Plasmodium falciparum adapted to in vitro culture.** *Trop Geogr Med* 1981, **33:**50-54.
121. Delemarre BJ, van der Kaay HJ: **[Tropical malaria contracted the natural way in the Netherlands].** *Nederlands tijdschrift voor geneeskunde* 1979, **123:**1981-1982.
122. Walliker D, Quakyi IA, Wellems TE, McCutchan TF, Szarfman A, London WT, Corcoran LM, Burkot TR, Carter R: **Genetic analysis of the human malaria parasite Plasmodium falciparum.** *Science* 1987, **236:**1661-1666.
123. Crameri A, Marfurt J, Mugittu K, Maire N, Regos A, Coppee JY, Sismeiro O, Burki R, Huber E, Laubscher D, et al: **Rapid microarray-based method for monitoring of all currently known single-nucleotide polymorphisms associated with parasite resistance to antimalaria drugs.** *J Clin Microbiol* 2007, **45:**3685-3691.
124. Scherf A, Lopez-Rubio JJ, Riviere L: **Antigenic variation in Plasmodium falciparum.** *Annu Rev Microbiol* 2008, **62:**445-470.
125. Lavstsen T, Salanti A, Jensen AT, Arnot DE, Theander TG: **Sub-grouping of Plasmodium falciparum 3D7 var genes based on sequence analysis of coding and non-coding regions.** *Malar J* 2003, **2:**27.
126. Kraemer SM, Kyes SA, Aggarwal G, Springer AL, Nelson SO, Christodoulou Z, Smith LM, Wang W, Levin E, Newbold CI, et al: **Patterns of gene recombination shape var gene repertoires in Plasmodium falciparum: comparisons of geographically diverse isolates.** *BMC Genomics* 2007, **8:**45.
127. Claessens A, Ghumra A, Gupta AP, Mok S, Bozdech Z, Rowe JA: **Design of a variant surface antigen-supplemented microarray chip for whole transcriptome analysis of**

multiple Plasmodium falciparum cytoadherent strains, and identification of strain-transcendent rif and stevor genes. *Malar J* 2011, **10:**180.

128. Mok BW, Ribacke U, Winter G, Yip BH, Tan CS, Fernandez V, Chen Q, Nilsson P, Wahlgren M: **Comparative transcriptomal analysis of isogenic Plasmodium falciparum clones of distinct antigenic and adhesive phenotypes.** *Mol Biochem Parasitol* 2007, **151:**184-192.
129. Rovira-Graells N, Gupta AP, Planet E, Crowley VM, Mok S, Ribas de Pouplana L, Preiser PR, Bozdech Z, Cortes A: **Transcriptional variation in the malaria parasite Plasmodium falciparum.** *Genome Res* 2012.
130. Cortes A, Carret C, Kaneko O, Yim Lim BY, Ivens A, Holder AA: **Epigenetic silencing of Plasmodium falciparum genes linked to erythrocyte invasion.** *PLoS Pathog* 2007, **3:**e107.
131. Lopez-Rubio JJ, Mancio-Silva L, Scherf A: **Genome-wide analysis of heterochromatin associates clonally variant gene regulation with perinuclear repressive centers in malaria parasites.** *Cell Host Microbe* 2009, **5:**179-190.
132. Jiang L, Lopez-Barragan MJ, Jiang H, Mu J, Gaur D, Zhao K, Felsenfeld G, Miller LH: **Epigenetic control of the variable expression of a Plasmodium falciparum receptor protein for erythrocyte invasion.** *Proc Natl Acad Sci U S A* 2010, **107:**2224-2229.
133. Crowley VM, Rovira-Graells N, Ribas de Pouplana L, Cortes A: **Heterochromatin formation in bistable chromatin domains controls the epigenetic repression of clonally variant Plasmodium falciparum genes linked to erythrocyte invasion.** *Mol Microbiol* 2011, **80:**391-406.
134. Salcedo-Amaya AM, van Driel MA, Alako BT, Trelle MB, van den Elzen AM, Cohen AM, Janssen-Megens EM, van de Vegte-Bolmer M, Selzer RR, Iniguez AL, et al: **Dynamic histone H3 epigenome marking during the intraerythrocytic cycle of Plasmodium falciparum.** *Proc Natl Acad Sci U S A* 2009, **106:**9655-9660.
135. Bartfai R, Hoeijmakers WA, Salcedo-Amaya AM, Smits AH, Janssen-Megens E, Kaan A, Treeck M, Gilberger TW, Francoijs KJ, Stunnenberg HG: **H2A.Z demarcates intergenic regions of the plasmodium falciparum epigenome that are dynamically marked by H3K9ac and H3K4me3.** *PLoS Pathog* 2010, **6:**e1001223.
136. Lopez-Rubio JJ, Gontijo AM, Nunes MC, Issar N, Hernandez Rivas R, Scherf A: **5' flanking region of var genes nucleate histone modification patterns linked to phenotypic inheritance of virulence traits in malaria parasites.** *Mol Microbiol* 2007, **66:**1296-1305.
137. Voss TS, Healer J, Marty AJ, Duffy MF, Thompson JK, Beeson JG, Reeder JC, Crabb BS, Cowman AF: **A var gene promoter controls allelic exclusion of virulence genes in Plasmodium falciparum malaria.** *Nature* 2006, **439:**1004-1008.
138. Swamy L, Amulic B, Deitsch KW: **Plasmodium falciparum var gene silencing is determined by cis DNA elements that form stable and heritable interactions.** *Eukaryot Cell* 2011, **10:**530-539.
139. Calderwood MS, Gannoun-Zaki L, Wellems TE, Deitsch KW: **Plasmodium falciparum var genes are regulated by two regions with separate promoters, one upstream of the coding region and a second within the intron.** *J Biol Chem* 2003, **278:**34125-34132.
140. Frank M, Dzikowski R, Costantini D, Amulic B, Berdougo E, Deitsch K: **Strict pairing of var promoters and introns is required for var gene silencing in the malaria parasite Plasmodium falciparum.** *J Biol Chem* 2006, **281:**9942-9952.
141. Tonkin CJ, Carret CK, Duraisingh MT, Voss TS, Ralph SA, Hommel M, Duffy MF, Silva LM, Scherf A, Ivens A, et al: **Sir2 paralogues cooperate to regulate virulence genes and antigenic variation in Plasmodium falciparum.** *PLoS Biol* 2009, **7:**e84.

142. Zhang Q, Huang Y, Zhang Y, Fang X, Claes A, Duchateau M, Namane A, Lopez-Rubio JJ, Pan W, Scherf A: **A critical role of perinuclear filamentous actin in spatial repositioning and mutually exclusive expression of virulence genes in malaria parasites.** *Cell Host Microbe* 2011, **10:**451-463.
143. Duraisingh MT, Voss TS, Marty AJ, Duffy MF, Good RT, Thompson JK, Freitas-Junior LH, Scherf A, Crabb BS, Cowman AF: **Heterochromatin silencing and locus repositioning linked to regulation of virulence genes in Plasmodium falciparum.** *Cell* 2005, **121:**13-24.
144. Petter M, Lee CC, Byrne TJ, Boysen KE, Volz J, Ralph SA, Cowman AF, Brown GV, Duffy MF: **Expression of P. falciparum var genes involves exchange of the histone variant H2A.Z at the promoter.** *PLoS Pathog* 2011, **7:**e1001292.
145. Volz JC, Bartfai R, Petter M, Langer C, Josling GA, Tsuboi T, Schwach F, Baum J, Rayner JC, Stunnenberg HG, et al: **PfSET10, a Plasmodium falciparum Methyltransferase, Maintains the Active var Gene in a Poised State during Parasite Division.** *Cell Host Microbe* 2012, **11:**7-18.
146. Flueck C, Bartfai R, Volz J, Niederwieser I, Salcedo-Amaya AM, Alako BT, Ehlgen F, Ralph SA, Cowman AF, Bozdech Z, et al: **Plasmodium falciparum heterochromatin protein 1 marks genomic loci linked to phenotypic variation of exported virulence factors.** *PLoS Pathog* 2009, **5:**e1000569.
147. Perez-Toledo K, Rojas-Meza AP, Mancio-Silva L, Hernandez-Cuevas NA, Delgadillo DM, Vargas M, Martinez-Calvillo S, Scherf A, Hernandez-Rivas R: **Plasmodium falciparum heterochromatin protein 1 binds to tri-methylated histone 3 lysine 9 and is linked to mutually exclusive expression of var genes.** *Nucleic Acids Res* 2009, **37:**2596-2606.
148. Bozdech Z, Zhu J, Joachimiak MP, Cohen FE, Pulliam B, DeRisi JL: **Expression profiling of the schizont and trophozoite stages of Plasmodium falciparum with a long-oligonucleotide microarray.** *Genome Biol* 2003, **4:**R9.
149. Young JA, Fivelman QL, Blair PL, de la Vega P, Le Roch KG, Zhou Y, Carucci DJ, Baker DA, Winzeler EA: **The Plasmodium falciparum sexual development transcriptome: a microarray analysis using ontology-based pattern identification.** *Mol Biochem Parasitol* 2005, **143:**67-79.
150. Gissot M, Refour P, Briquet S, Boschet C, Coupe S, Mazier D, Vaquero C: **Transcriptome of 3D7 and its gametocyte-less derivative F12 Plasmodium falciparum clones during erythrocytic development using a gene-specific microarray assigned to gene regulation, cell cycle and transcription factors.** *Gene* 2004, **341:**267-277.
151. Oakley MS, Kumar S, Anantharaman V, Zheng H, Mahajan B, Haynes JD, Moch JK, Fairhurst R, McCutchan TF, Aravind L: **Molecular factors and biochemical pathways induced by febrile temperature in intraerythrocytic Plasmodium falciparum parasites.** *Infect Immun* 2007, **75:**2012-2025.
152. Hu G, Cabrera A, Kono M, Mok S, Chaal BK, Haase S, Engelberg K, Cheemadan S, Spielmann T, Preiser PR, et al: **Transcriptional profiling of growth perturbations of the human malaria parasite Plasmodium falciparum.** *Nat Biotechnol* 2010, **28:**91-98.
153. Natalang O, Bischoff E, Deplaine G, Proux C, Dillies MA, Sismeiro O, Guigon G, Bonnefoy S, Patarapotikul J, Mercereau-Puijalon O, et al: **Dynamic RNA profiling in Plasmodium falciparum synchronized blood stages exposed to lethal doses of artesunate.** *BMC Genomics* 2008, **9:**388.
154. Kritsiriwuthinan K, Chaotheing S, Shaw PJ, Wongsombat C, Chavalitshewinkoon-Petmitr P, Kamchonwongpaisan S: **Global gene expression profiling of Plasmodium falciparum in response to the anti-malarial drug pyronaridine.** *Malar J* 2011, **10:**242.

155. Becker JV, Mtwisha L, Crampton BG, Stoychev S, van Brummelen AC, Reeksting S, Louw AI, Birkholtz LM, Mancama DT: **Plasmodium falciparum spermidine synthase inhibition results in unique perturbation-specific effects observed on transcript, protein and metabolite levels.** *BMC Genomics* 2010, **11:**235.
156. Mok S, Imwong M, Mackinnon MJ, Sim J, Ramadoss R, Yi P, Mayxay M, Chotivanich K, Liong KY, Russell B, et al: **Artemisinin resistance in Plasmodium falciparum is associated with an altered temporal pattern of transcription.** *BMC Genomics* 2011, **12:**391.
157. Daily JP, Le Roch KG, Sarr O, Ndiaye D, Lukens A, Zhou Y, Ndir O, Mboup S, Sultan A, Winzeler EA, Wirth DF: **In vivo transcriptome of Plasmodium falciparum reveals overexpression of transcripts that encode surface proteins.** *J Infect Dis* 2005, **191:**1196-1203.
158. Zhang Q, Zhang Y, Huang Y, Xue X, Yan H, Sun X, Wang J, McCutchan TF, Pan W: **From in vivo to in vitro: dynamic analysis of Plasmodium falciparum var gene expression patterns of patient isolates during adaptation to culture.** *PLoS One* 2011, **6:**e20591.
159. Peters JM, Fowler EV, Krause DR, Cheng Q, Gatton ML: **Differential changes in Plasmodium falciparum var transcription during adaptation to culture.** *J Infect Dis* 2007, **195:**748-755.
160. Bachmann A, Predehl S, May J, Harder S, Burchard GD, Gilberger TW, Tannich E, Bruchhaus I: **Highly co-ordinated var gene expression and switching in clinical Plasmodium falciparum isolates from non-immune malaria patients.** *Cell Microbiol* 2011, **13:**1397-1409.
161. Ward P, Equinet L, Packer J, Doerig C: **Protein kinases of the human malaria parasite Plasmodium falciparum: the kinome of a divergent eukaryote.** *BMC Genomics* 2004, **5:**79.
162. Nunes MC, Okada M, Scheidig-Benatar C, Cooke BM, Scherf A: **Plasmodium falciparum FIKK kinase members target distinct components of the erythrocyte membrane.** *PLoS One* 2010, **5:**e11747.
163. Tewari R, Straschil U, Bateman A, Bohme U, Cherevach I, Gong P, Pain A, Billker O: **The systematic functional analysis of Plasmodium protein kinases identifies essential regulators of mosquito transmission.** *Cell Host Microbe* 2010, **8:**377-387.
164. Lavazec C, Sanyal S, Templeton TJ: **Expression switching in the stevor and Pfmc-2TM superfamilies in Plasmodium falciparum.** *Mol Microbiol* 2007, **64:**1621-1634.
165. McRobert L, Preiser P, Sharp S, Jarra W, Kaviratne M, Taylor MC, Renia L, Sutherland CJ: **Distinct trafficking and localization of STEVOR proteins in three stages of the Plasmodium falciparum life cycle.** *Infect Immun* 2004, **72:**6597-6602.
166. Blythe JE, Yam XY, Kuss C, Bozdech Z, Holder AA, Marsh K, Langhorne J, Preiser PR: **Plasmodium falciparum STEVOR proteins are highly expressed in patient isolates and located in the surface membranes of infected red blood cells and the apical tips of merozoites.** *Infect Immun* 2008, **76:**3329-3336.
167. Kyes SA, Rowe JA, Kriek N, Newbold CI: **Rifins: a second family of clonally variant proteins expressed on the surface of red cells infected with Plasmodium falciparum.** *Proc Natl Acad Sci U S A* 1999, **96:**9333-9338.
168. Khattab A, Meri S: **Exposure of the Plasmodium falciparum clonally variant STEVOR proteins on the merozoite surface.** *Malar J* 2011, **10:**58.
169. Niang M, Yan Yam X, Preiser PR: **The Plasmodium falciparum STEVOR multigene family mediates antigenic variation of the infected erythrocyte.** *PLoS Pathog* 2009, **5:**e1000307.
170. Sharp S, Lavstsen T, Fivelman QL, Saeed M, McRobert L, Templeton TJ, Jensen AT, Baker DA, Theander TG, Sutherland CJ: **Programmed transcription of the var gene**

family, but not of stevor, in Plasmodium falciparum gametocytes. *Eukaryot Cell* 2006, **5:**1206-1214.
171. Sanyal S, Egee S, Bouyer G, Perrot S, Safeukui I, Bischoff E, Buffet P, Deitsch KW, Mercereau-Puijalon O, David PH, et al: **Plasmodium falciparum STEVOR proteins impact erythrocyte mechanical properties.** *Blood* 2012, **119:**e1-8.
172. Frank M, Dzikowski R, Amulic B, Deitsch K: **Variable switching rates of malaria virulence genes are associated with chromosomal position.** *Mol Microbiol* 2007, **64:**1486-1498.
173. Mok BW, Ribacke U, Rasti N, Kironde F, Chen Q, Nilsson P, Wahlgren M: **Default Pathway of var2csa switching and translational repression in Plasmodium falciparum.** *PLoS One* 2008, **3:**e1982.
174. Srivastava A, Gangnard S, Round A, Dechavanne S, Juillerat A, Raynal B, Faure G, Baron B, Ramboarina S, Singh SK, et al: **Full-length extracellular region of the var2CSA variant of PfEMP1 is required for specific, high-affinity binding to CSA.** *Proc Natl Acad Sci U S A* 2010, **107:**4884-4889.
175. Oleinikov AV, Voronkova VV, Frye IT, Amos E, Morrison R, Fried M, Duffy PE: **A Plasma Survey Using 38 PfEMP1 Domains Reveals Frequent Recognition of the Plasmodium falciparum Antigen VAR2CSA among Young Tanzanian Children.** *PLoS One* 2012, **7:**e31011.
176. Kraemer SM, Gupta L, Smith JD: **New tools to identify var sequence tags and clone full-length genes using type-specific primers to Duffy binding-like domains.** *Mol Biochem Parasitol* 2003, **129:**91-102.
177. Misteli T, Soutoglou E: **The emerging role of nuclear architecture in DNA repair and genome maintenance.** *Nat Rev Mol Cell Biol* 2009, **10:**243-254.
178. Kidgell C, Volkman SK, Daily J, Borevitz JO, Plouffe D, Zhou Y, Johnson JR, Le Roch K, Sarr O, Ndir O, et al: **A systematic map of genetic variation in Plasmodium falciparum.** *PLoS Pathog* 2006, **2:**e57.
179. Kim A, Murphy MP, Oberley TD: **Mitochondrial redox state regulates transcription of the nuclear-encoded mitochondrial protein manganese superoxide dismutase: a proposed adaptive response to mitochondrial redox imbalance.** *Free Radic Biol Med* 2005, **38:**644-654.
180. Kim A, Joseph S, Khan A, Epstein CJ, Sobel R, Huang TT: **Enhanced expression of mitochondrial superoxide dismutase leads to prolonged in vivo cell cycle progression and up-regulation of mitochondrial thioredoxin.** *Free Radic Biol Med* 2010, **48:**1501-1512.
181. Skopelitis DS, Paranychianakis NV, Paschalidis KA, Pliakonis ED, Delis ID, Yakoumakis DI, Kouvarakis A, Papadakis AK, Stephanou EG, Roubelakis-Angelakis KA: **Abiotic stress generates ROS that signal expression of anionic glutamate dehydrogenases to form glutamate for proline synthesis in tobacco and grapevine.** *Plant Cell* 2006, **18:**2767-2781.
182. Young JA, Johnson JR, Benner C, Yan SF, Chen K, Le Roch KG, Zhou Y, Winzeler EA: **In silico discovery of transcription regulatory elements in Plasmodium falciparum.** *BMC Genomics* 2008, **9:**70.
183. Rosenberg E, Ben-Shmuel A, Shalev O, Sinay R, Cowman A, Pollack Y: **Differential, positional-dependent transcriptional response of antigenic variation (var) genes to biological stress in Plasmodium falciparum.** *PLoS One* 2009, **4:**e6991.
184. Reilly HB, Wang H, Steuter JA, Marx AM, Ferdig MT: **Quantitative dissection of clone-specific growth rates in cultured malaria parasites.** *Int J Parasitol* 2007, **37:**1599-1607.
185. Carrara VI, Zwang J, Ashley EA, Price RN, Stepniewska K, Barends M, Brockman A, Anderson T, McGready R, Phaiphun L, et al: **Changes in the treatment responses to**

artesunate-mefloquine on the northwestern border of Thailand during 13 years of continuous deployment. *PLoS One* 2009, **4:**e4551.
186. Bozdech Z, Mok S, Hu G, Imwong M, Jaidee A, Russell B, Ginsburg H, Nosten F, Day NP, White NJ, et al: **The transcriptome of Plasmodium vivax reveals divergence and diversity of transcriptional regulation in malaria parasites.** *Proc Natl Acad Sci U S A* 2008, **105:**16290-16295.
187. Mendis K, Rietveld A, Warsame M, Bosman A, Greenwood B, Wernsdorfer WH: **From malaria control to eradication: The WHO perspective.** *Trop Med Int Health* 2009, **14:**802-809.
188. Bruce-Chwatt LJ: **Malaria and its control: present situation and future prospects.** *Annu Rev Public Health* 1987, **8:**75-110.
189. Wellems TE: **Transporter of a malaria catastrophe.** *Nat Med* 2004, **10:**1169-1171.
190. Wellems TE, Hayton K, Fairhurst RM: **The impact of malaria parasitism: from corpuscles to communities.** *J Clin Invest* 2009, **119:**2496-2505.
191. Wongsrichanalai C, Pickard AL, Wernsdorfer WH, Meshnick SR: **Epidemiology of drug-resistant malaria.** *Lancet Infect Dis* 2002, **2:**209-218.
192. Kachur SP, MacArthur JR, Slutsker L: **A call to action: addressing the challenge of artemisinin-resistant malaria.** *Expert Rev Anti Infect Ther* 2010, **8:**365-366.
193. Noedl H, Se Y, Schaecher K, Smith BL, Socheat D, Fukuda MM: **Evidence of artemisinin-resistant malaria in western Cambodia.** *N Engl J Med* 2008, **359:**2619-2620.
194. Alker AP, Lim P, Sem R, Shah NK, Yi P, Bouth DM, Tsuyuoka R, Maguire JD, Fandeur T, Ariey F, et al: **Pfmdr1 and in vivo resistance to artesunate-mefloquine in falciparum malaria on the Cambodian-Thai border.** *Am J Trop Med Hyg* 2007, **76:**641-647.
195. Lim P, Alker AP, Khim N, Shah NK, Incardona S, Doung S, Yi P, Bouth DM, Bouchier C, Puijalon OM, et al: **Pfmdr1 copy number and arteminisin derivatives combination therapy failure in falciparum malaria in Cambodia.** *Malar J* 2009, **8:**11.
196. Saralamba S, Pan-Ngum W, Maude RJ, Lee SJ, Tarning J, Lindegardh N, Chotivanich K, Nosten F, Day NP, Socheat D, et al: **Intrahost modeling of artemisinin resistance in Plasmodium falciparum.** *Proc Natl Acad Sci U S A* 2011, **108:**397-402.
197. Witkowski B, Lelievre J, Lopez Barragan MJ, Laurent V, Su XZ, Berry A, Benoit-Vical F: **Increased tolerance to artemisinin in Plasmodium falciparum is mediated by a quiescence mechanism.** *Antimicrob Agents Chemother* 2010.
198. Teuscher F, Gatton ML, Chen N, Peters J, Kyle DE, Cheng Q: **Artemisinin-induced dormancy in plasmodium falciparum: duration, recovery rates, and implications in treatment failure.** *J Infect Dis* 2010, **202:**1362-1368.
199. Nosten F: **Waking the sleeping beauty.** *J Infect Dis* 2010, **202:**1300-1301.
200. Anderson TJ, Nair S, Nkhoma S, Williams JT, Imwong M, Yi P, Socheat D, Das D, Chotivanich K, Day NP, et al: **High heritability of malaria parasite clearance rate indicates a genetic basis for artemisinin resistance in western Cambodia.** *J Infect Dis* 2010, **201:**1326-1330.
201. Chaal BK, Gupta AP, Wastuwidyaningtyas BD, Luah YH, Bozdech Z: **Histone deacetylases play a major role in the transcriptional regulation of the Plasmodium falciparum life cycle.** *PLoS Pathog* 2010, **6:**e1000737.
202. Halbert J, Ayong L, Equinet L, Le Roch K, Hardy M, Goldring D, Reininger L, Waters N, Chakrabarti D, Doerig C: **A Plasmodium falciparum transcriptional cyclin-dependent kinase-related kinase with a crucial role in parasite proliferation associates with histone deacetylase activity.** *Eukaryot Cell* 2010, **9:**952-959.
203. Cheeseman IH, Gomez-Escobar N, Carret CK, Ivens A, Stewart LB, Tetteh KK, Conway DJ: **Gene copy number variation throughout the Plasmodium falciparum genome.** *BMC Genomics* 2009, **10:**353.

204. Jiang H, Yi M, Mu J, Zhang L, Ivens A, Klimczak LJ, Huyen Y, Stephens RM, Su X-z: **Detection of genome-wide polymorphisms in the AT-rich Plasmodium falciparum genome using a high-density microarray.** *BMC Genomics* 2008, **9:**398.
205. Ribacke U, Mok BW, Wirta V, Normark J, Lundeberg J, Kironde F, Egwang TG, Nilsson P, Wahlgren M: **Genome wide gene amplifications and deletions in Plasmodium falciparum.** *Mol Biochem Parasitol* 2007, **155:**33-44.
206. Uhlemann AC, McGready R, Ashley EA, Brockman A, Singhasivanon P, Krishna S, White NJ, Nosten F, Price RN: **Intrahost selection of Plasmodium falciparum pfmdr1 alleles after antimalarial treatment on the northwestern border of Thailand.** *J Infect Dis* 2007, **195:**134-141.
207. Dharia NV, Sidhu AB, Cassera MB, Westenberger SJ, Bopp SE, Eastman RT, Plouffe D, Batalov S, Park DJ, Volkman SK, et al: **Use of high-density tiling microarrays to identify mutations globally and elucidate mechanisms of drug resistance in Plasmodium falciparum.** *Genome Biol* 2009, **10:**R21.
208. Nair S, Miller B, Barends M, Jaidee A, Patel J, Mayxay M, Newton P, Nosten F, Ferdig MT, Anderson TJ: **Adaptive copy number evolution in malaria parasites.** *PLoS Genet* 2008, **4:**e1000243.
209. Mita T, Kaneko A, Hombhanje F, Hwaihwanje I, Takahashi N, Osawa H, Tsukahara T, Masta A, Lum JK, Kobayakawa T, et al: **Role of pfmdr1 mutations on chloroquine resistance in Plasmodium falciparum isolates with pfcrt K76T from Papua New Guinea.** *Acta Trop* 2006, **98:**137-144.
210. Enosse S, Magnussen P, Abacassamo F, Gomez-Olive X, Ronn AM, Thompson R, Alifrangis M: **Rapid increase of Plasmodium falciparum dhfr/dhps resistant haplotypes, after the adoption of sulphadoxine-pyrimethamine as first line treatment in 2002, in southern Mozambique.** *Malar J* 2008, **7:**115.
211. Babiker HA, Al-Saai S, Kheir A, Abdel-Muhsin AMA, Al-Ghazali A, Nwakanma D, Swedberg G: **Distinct haplotypes of dhfr and dhps among Plasmodium falciparum isolates in an area of high level of sulfadoxine-pyrimethamine (SP) resistance in eastern Sudan.** *Infect Genet Evol* 2009, **9:**778-783.
212. Imwong M, Dondorp AM, Nosten F, Yi P, Mungthin M, Hanchana S, Das D, Phyo AP, Lwin KM, Pukrittayakamee S, et al: **Exploring the contribution of candidate genes to artemisinin resistance in Plasmodium falciparum.** *Antimicrob Agents Chemother* 2010, **54:**2886-2892.
213. Chen N, Chavchich M, Peters JM, Kyle DE, Gatton ML, Cheng Q: **Deamplification of pfmdr1-Containing Amplicon on Chromosome 5 in Plasmodium falciparum Is Associated with Reduced Resistance to Artelinic Acid In Vitro.** *Antimicrob Agents Chemother* 2010, **54:**3395-3401.
214. Hunt P, Martinelli A, Modrzynska K, Borges S, Creasey A, Rodrigues L, Beraldi D, Loewe L, Fawcett R, Kumar S, et al: **Experimental evolution, genetic analysis and genome re-sequencing reveal the mutation conferring artemisinin resistance in an isogenic lineage of malaria parasites.** *BMC Genomics* 2010, **11:**499.
215. Klonis N, Crespo-Ortiz MP, Bottova I, Abu-Bakar N, Kenny S, Rosenthal PJ, Tilley L: **Artemisinin activity against Plasmodium falciparum requires hemoglobin uptake and digestion.** *Proc Natl Acad Sci U S A* 2011, **108:**11405-11410.
216. Flint J, Harding RM, Boyce AJ, Clegg JB: **The population genetics of the haemoglobinopathies.** *Baillieres Clin Haematol* 1998, **11:**1-51.
217. Wiwanitkit V: **Genetic disorders and malaria in Indo-China region.** *J Vector Borne Dis* 2008, **45:**98-104.
218. Meshnick SR, Taylor TE, Kamchonwongpaisan S: **Artemisinin and the antimalarial endoperoxides: from herbal remedy to targeted chemotherapy.** *Microbiol Rev* 1996, **60:**301-315.

219. Robert A, Bonduelle C, Laurent SAL, Meunier B: **Heme alkylation by artemisinin and trioxaquines.** *J Phys Org Chem* 2006, **19:**562-569.
220. Campbell TL, De Silva EK, Olszewski KL, Elemento O, Llinas M: **Identification and Genome-Wide Prediction of DNA Binding Specificities for the ApiAP2 Family of Regulators from the Malaria Parasite.** *PLoS Pathog* 2010, **6:**e1001165.
221. Kim UJ, Han M, Kayne P, Grunstein M: **Effects of histone H4 depletion on the cell cycle and transcription of Saccharomyces cerevisiae.** *EMBO J* 1988, **7:**2211-2219.
222. Prado F, Aguilera A: **Partial depletion of histone H4 increases homologous recombination-mediated genetic instability.** *Mol Cell Biol* 2005, **25:**1526-1536.
223. Mu J, Myers RA, Jiang H, Liu S, Ricklefs S, Waisberg M, Chotivanich K, Wilairatana P, Krudsood S, White NJ, et al: **Plasmodium falciparum genome-wide scans for positive selection, recombination hot spots and resistance to antimalarial drugs.** *Nat Genet* 2010, **42:**268-271.
224. Jones PM, George AM: **Multidrug resistance in parasites: ABC transporters, P-glycoproteins and molecular modelling.** *Int J Parasitol* 2005, **35:**555-566.
225. Dahlstrom S, Veiga MI, Martensson A, Bjorkman A, Gil JP: **Polymorphism in PfMRP1 (Plasmodium falciparum multidrug resistance protein 1) amino acid 1466 associated with resistance to sulfadoxine-pyrimethamine treatment.** *Antimicrob Agents Chemother* 2009, **53:**2553-2556.
226. Dahlstrom S, Ferreira PE, Veiga MI, Sedighi N, Wiklund L, Martensson A, Farnert A, Sisowath C, Osorio L, Darban H, et al: **Plasmodium falciparum multidrug resistance protein 1 and artemisinin-based combination therapy in Africa.** *J Infect Dis* 2009, **200:**1456-1464.
227. Veiga MI, Ferreira PE, Jornhagen L, Malmberg M, Kone A, Schmidt BA, Petzold M, Bjorkman A, Nosten F, Gil JP: **Novel polymorphisms in Plasmodium falciparum ABC transporter genes are associated with major ACT antimalarial drug resistance.** *PLoS One* 2011, **6:**e20212.
228. Kavishe RA, van den Heuvel JM, van de Vegte-Bolmer M, Luty AJ, Russel FG, Koenderink JB: **Localization of the ATP-binding cassette (ABC) transport proteins PfMRP1, PfMRP2, and PfMDR5 at the Plasmodium falciparum plasma membrane.** *Malar J* 2009, **8:**205.
229. Klokouzas A, Tiffert T, van Schalkwyk D, Wu CP, van Veen HW, Barrand MA, Hladky SB: **Plasmodium falciparum expresses a multidrug resistance-associated protein.** *Biochem Biophys Res Commun* 2004, **321:**197-201.
230. Zaman GJ, Flens MJ, van Leusden MR, de Haas M, Mulder HS, Lankelma J, Pinedo HM, Scheper RJ, Baas F, Broxterman HJ, et al.: **The human multidrug resistance-associated protein MRP is a plasma membrane drug-efflux pump.** *Proc Natl Acad Sci U S A* 1994, **91:**8822-8826.
231. Rajagopal A, Simon SM: **Subcellular localization and activity of multidrug resistance proteins.** *Mol Biol Cell* 2003, **14:**3389-3399.
232. Eilers M, Roy U, Mondal D: **MRP (ABCC) transporters-mediated efflux of anti-HIV drugs, saquinavir and zidovudine, from human endothelial cells.** *Exp Biol Med (Maywood)* 2008, **233:**1149-1160.
233. Zhou SF, Wang LL, Di YM, Xue CC, Duan W, Li CG, Li Y: **Substrates and inhibitors of human multidrug resistance associated proteins and the implications in drug development.** *Curr Med Chem* 2008, **15:**1981-2039.
234. Konig J, Nies AT, Cui Y, Leier I, Keppler D: **Conjugate export pumps of the multidrug resistance protein (MRP) family: localization, substrate specificity, and MRP2-mediated drug resistance.** *Biochim Biophys Acta* 1999, **1461:**377-394.
235. Robinson T, Campino SG, Auburn S, Assefa SA, Polley SD, Manske M, MacInnis B, Rockett KA, Maslen GL, Sanders M, et al: **Drug-resistant genotypes and multi-**

clonality in Plasmodium falciparum analysed by direct genome sequencing from peripheral blood of malaria patients. *PLoS One* 2011, **6:**e23204.
236. Mu J, Ferdig MT, Feng X, Joy DA, Duan J, Furuya T, Subramanian G, Aravind L, Cooper RA, Wootton JC, et al: **Multiple transporters associated with malaria parasite responses to chloroquine and quinine.** *Mol Microbiol* 2003, **49:**977-989.
237. Martin RE, Marchetti RV, Cowan AI, Howitt SM, Broer S, Kirk K: **Chloroquine transport via the malaria parasite's chloroquine resistance transporter.** *Science* 2009, **325:**1680-1682.
238. Setthaudom C, Tan-ariya P, Sitthichot N, Khositnithikul R, Suwandittakul N, Leelayoova S, Mungthin M: **Role of Plasmodium falciparum chloroquine resistance transporter and multidrug resistance 1 genes on in vitro chloroquine resistance in isolates of Plasmodium falciparum from Thailand.** *Am J Trop Med Hyg* 2011, **85:**606-611.
239. Fidock DA, Nomura T, Talley AK, Cooper RA, Dzekunov SM, Ferdig MT, Ursos LM, Sidhu AB, Naude B, Deitsch KW, et al: **Mutations in the P. falciparum digestive vacuole transmembrane protein PfCRT and evidence for their role in chloroquine resistance.** *Mol Cell* 2000, **6:**861-871.
240. Anderson TJ, Nair S, Qin H, Singlam S, Brockman A, Paiphun L, Nosten F: **Are transporter genes other than the chloroquine resistance locus (pfcrt) and multidrug resistance gene (pfmdr) associated with antimalarial drug resistance?** *Antimicrob Agents Chemother* 2005, **49:**2180-2188.
241. Lehane AM, van Schalkwyk DA, Valderramos SG, Fidock DA, Kirk K: **Differential drug efflux or accumulation does not explain variation in the chloroquine response of Plasmodium falciparum strains expressing the same isoform of mutant PfCRT.** *Antimicrob Agents Chemother* 2011, **55:**2310-2318.
242. Valderramos SG, Valderramos JC, Musset L, Purcell LA, Mercereau-Puijalon O, Legrand E, Fidock DA: **Identification of a mutant PfCRT-mediated chloroquine tolerance phenotype in Plasmodium falciparum.** *PLoS Pathog* 2010, **6:**e1000887.
243. Cojean S, Noel A, Garnier D, Hubert V, Le Bras J, Durand R: **Lack of association between putative transporter gene polymorphisms in Plasmodium falciparum and chloroquine resistance in imported malaria isolates from Africa.** *Malar J* 2006, **5:**24.
244. Bozdech Z, Ginsburg H: **Antioxidant defense in Plasmodium falciparum--data mining of the transcriptome.** *Malar J* 2004, **3:**23.
245. Shuman S, Glickman MS: **Bacterial DNA repair by non-homologous end joining.** *Nat Rev Microbiol* 2007, **5:**852-861.
246. McVey M, Lee SE: **MMEJ repair of double-strand breaks (director's cut): deleted sequences and alternative endings.** *Trends Genet* 2008, **24:**529-538.
247. Corcoran LM, Thompson JK, Walliker D, Kemp DJ: **Homologous recombination within subtelomeric repeat sequences generates chromosome size polymorphisms in P. falciparum.** *Cell* 1988, **53:**807-813.
248. Elemento O, Slonim N, Tavazoie S: **A universal framework for regulatory element discovery across all genomes and data types.** *Mol Cell* 2007, **28:**337-350.
249. Gonzalez-Pons M, Szeto AC, Gonzalez-Mendez R, Serrano AE: **Identification and bioinformatic characterization of a multidrug resistance associated protein (ABCC) gene in Plasmodium berghei.** *Malar J* 2009, **8:**1.
250. Becker K, Tilley L, Vennerstrom JL, Roberts D, Rogerson S, Ginsburg H: **Oxidative stress in malaria parasite-infected erythrocytes: host-parasite interactions.** *Int J Parasitol* 2004, **34:**163-189.
251. Sullivan DJ, Jr., Matile H, Ridley RG, Goldberg DE: **A common mechanism for blockade of heme polymerization by antimalarial quinolines.** *J Biol Chem* 1998, **273:**31103-31107.

252. He Z, Chen L, You J, Qin L, Chen X: **Antiretroviral protease inhibitors potentiate chloroquine antimalarial activity in malaria parasites by regulating intracellular glutathione metabolism.** *Exp Parasitol* 2009, **123:**122-127.
253. Ginsburg H, Golenser J: **Glutathione is involved in the antimalarial action of chloroquine and its modulation affects drug sensitivity of human and murine species of Plasmodium.** *Redox Rep* 2003, **8:**276-279.
254. Ginsburg H: **Progress in in silico functional genomics: the malaria Metabolic Pathways database.** *Trends Parasitol* 2006, **22:**238-240.